

# Important Notice

This copy may be used only for the purposes of research and private study, and any use of the copy for a purpose other than research or private study may require the authorization of the copyright owner of the work in question. Responsibility regarding questions of copyright that may arise in the use of this copy is assumed by the recipient.

THE UNIVERSITY OF CALGARY

**Multicomponent seismology: Elastic-wave sources,  
composite media, anisotropy, and modeling**

by

Donald T. Easley

A THESIS

SUBMITTED TO THE FACULTY OF GRADUATE STUDIES  
IN PARTIAL FULFILLMENT OF THE REQUIREMENTS FOR THE  
DEGREE OF DOCTOR OF PHILOSOPHY

DEPARTMENT OF GEOLOGY AND GEOPHYSICS

CALGARY, ALBERTA

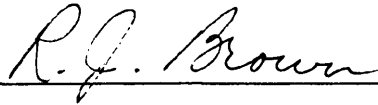
DECEMBER, 1995

© Donald T. Easley 1995

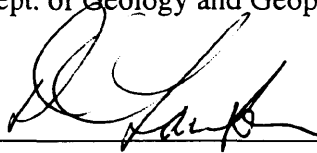
THE UNIVERSITY OF CALGARY

FACULTY OF GRADUATE STUDIES

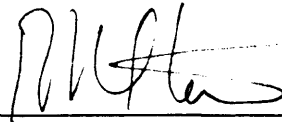
The undersigned certify that they have read, and recommend to the Faculty of Graduate Studies for acceptance, a dissertation entitled "Multicomponent seismology: Elastic-wave sources, composite media, anisotropy, and modeling" submitted by Donald Thomas Easley in partial fulfillment of the requirements of the degree of Doctor of Philosophy.



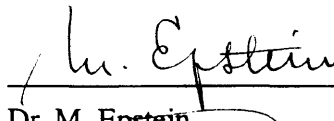
Supervisor, Dr. R. J. Brown,  
Dept. of Geology and Geophysics



Dr. D. C. Lawton,  
Dept. of Geology and Geophysics



Dr. R. R. Stewart,  
Dept. of Geology and Geophysics



Dr. M. Epstein,  
Dept. of Mechanical Engineering



External Examiner, Dr. Z. Hajnal,  
University of Saskatchewan

1996-01-31

Date

## **Abstract**

Four distinct topics are covered in this dissertation. These topics can be grouped under the general heading of multicomponent seismology.

The first topic, deals with the generation of shear waves using vertical vibrators. Two methods were used to investigate this experimentally proven phenomenon. The first involves assuming the surface sources at some point can be modeled as vibrators with displacements in counterphase. The resulting far-field radiation pattern is then calculated. This shows the potential for strong vertically incident shear waves. The second method is based on simple mechanical models for vibrators that are allowed to interact over an elastic half-space. The theory for this method is developed fully and ready for numerical implementation.

The second topic deals with describing the composite earth as a generalized continuum. The method of Backus averaging, for a stack of finely layered media, is generalized to develop a new generalized continuum description. This development extends the averaging method to non-zero frequencies. The possibility of plane waves within this medium is investigated. This investigation show the plane waves in this type of media have the kinematic properties of waves in an elastic medium, but dynamic effects of absorption and dispersion are present.

The third topic, involves a statistical method for finding the preferred frame of reference of an elastic tensor. The method is tested for the case of cubic symmetry and the preferred frame was extracted from a cubic elastic tensor represented in an arbitrary frame. Methods to extend the method to cases where the symmetry is unknown are presented.

The last topic, is concerned with a novel method of generating P- and S-wave synthetic seismograms using the state-space approach with coupled Goupillaud models. The method is implemented and synthetic seismograms generated showing good kinematic agreement to what is expected from the input model.

## Acknowledgments

There are so many people who have helped and inspired me during my research, that I find it a daunting task to adequately thank them all. Therefore, I shall give a heartfelt " THANK YOU " to all those who have helped directly or indirectly in my research.

I must thank Dr. Jim Brown for all the support he has given me in my years of study. If this thesis is at all readable, it is in no small part due to the efforts of Dr. Brown. The CREWES project, in many ways, made this thesis a more enjoyable effort; for this I wish to thank, Dr. Rob Stewart, Dr. Don Lawton and Dr. Jim Brown for keeping the project going. Special thanks to Darren Foltinek, who was not only a great help in matters relating to the computer, but also a great colleague in our modest collaboration. The rest of the staff were each and every one important, even at times crucial to the running of the project. In order not to miss anyone, I thank you all. Special mention for all the sponsors of the CREWES project, for providing the fuel that runs this project. The student body, of which I had the privilege of being a part, was an endless source of adventures, some of which even directly affected my research. Courses I took also effected the direction of thought as well as methodology I employed. One course in particular, on continuum mechanics, given by Dr. M. Epstein was very useful. All these people enriched my experience at The University of Calgary. I hope I was able to reciprocate in some fashion.

These were rather troubled times on the home front. Through it all, my family helped me get through it and allowed me the freedom to pursue my studies. For this chance I am grateful.

# Table of Contents

<b>Abstract</b> .....	<b>iii</b>
<b>Acknowledgments</b> .....	<b>iv</b>
<b>Contents</b> .....	<b>v</b>
<b>List of Tables</b> .....	<b>x</b>
<b>List of Figures</b> .....	<b>xi</b>
<b>0: Introduction</b> .....	<b>1</b>
0.1: Historical review .....	1
0.2: Structure of thesis .....	2
0.2.1: Shear waves from vertical vibrators .....	2
0.2.2: Composite media as generalized continua .....	3
0.2.3: Elastic tensors and their preferred frames of reference .....	3
0.2.4: Goupillaud P- and S-wave synthetic seismograms .....	4
0.2.4: Appendices .....	4
<b>1: Shear Waves from Vertical Vibrators</b> .....	<b>5</b>
1.1: Introduction .....	5
1.1.a: Overview of experimental evidence .....	5
1.1.b: Overview of theoretical development .....	6
1.2: Displacement in counterphase .....	9
1.3.1: Fabricating the mechanical model of a vertical vibrator .....	39
1.3.2: Getting the elastic half-space involved .....	52

1.3.3: Procedure to solve the idealized interacting-vibrator problem .....	55
<b>2: Composite media as generalized continua .....</b>	<b>58</b>
2.1: The composite earth .....	58
2.1.1: Where others have gone before and where I have wandered .....	58
2.2: A perturbation to Backus's averaging method .....	59
2.2.1: Defining the averaging technique .....	60
2.2.2: Application to linear elasticity .....	62
2.2.3: A plane-wave solution .....	64
2.3: Other possible directions for investigation .....	66
<b>3: Elastic tensors and their preferred frames of reference.....</b>	<b>71</b>
3.1: A brief review .....	71
3.1.1: Preliminary mathematical considerations .....	72
3.2: Statistical determination of elastic tensor's preferred frame .....	73
3.3: The proof of the pudding ( the numerical trial ) .....	76
<b>4: Synthetic seismograms for P and S waves using the Goupillaud     model .....</b>	<b>79</b>
4.1: A brief review .....	79
4.2: A bit of the theory .....	80
4.2.1: Traditional nonnormally incident Goupillaud model .....	80
4.2.2: Coupled P- and S-wave Goupillaud models .....	83
4.3: Synthetic seismogram examples .....	86
4.3.1: The pictures that are worth a 1000 words .....	86

4.3.2: At what cost ? (Run time Considerations) .....	87
4.4: Always more to do. Possible enhancements .....	87
<b>5: Conclusions .....</b>	<b>88</b>
5.1: Shear waves from vertical vibrators .....	88
5.2: Composite media as generalized continua .....	89
5.3: Elastic tensors and their preferred frames of reference .....	89
5.4: Synthetic seismograms for P and S waves using the Goupillaud model .....	90
<b>A: Radiation Field of a Vertical Vibrator Over a Half Space.....</b>	<b>91</b>
A.1: Introduction .....	91
A.2: Equations of Motion.....	92
A.3: Solving for Dilatation $\Delta$ and Circulation $\omega_\varphi$ .....	96
A.4: Matching Boundary Conditions .....	102
E5: Branch cuts and poles of Rayleigh's function.....	108
A.5.1: Branch Cuts .....	108
A.5.2: Zeros of Rayleigh's Function .....	121
A.6: The Integral Equations of Motion and the Field at Infinity .....	131
<b>B: Review of the Theory of an Elastic Continuum .....</b>	<b>156</b>
B.1: Conservation laws .....	156
Differential form of the conservation laws .....	158
Conservation of mass .....	158
Conservation of momentum .....	159

Conservation of moment of momentum .....	160
Conservation of energy .....	160
B.2: Constitutive relationships .....	160
B.3: Linearization .....	164
Internal Energy .....	164
Displacement .....	165
Linearized equation of motion and isotropy .....	169
B.4: Equations of linear elasticity in orthogonal Cartesian and cylindrical coordinates .....	173
Cartesian orthogonal coordinates .....	173
Cylindrical coordinates .....	175
<b>C: Cosserat media .....</b>	<b>188</b>
C.1: Introduction .....	188
C.2: Force and Couple Stresses in Elasticity (Cosserat Equations) .....	188
C.3: Toupin's constitutive relations .....	200
C.4: Linearization .....	204
C.5: Wave motion .....	207
<b>D: Method of Steepest Descent .....</b>	<b>210</b>
D.1: Introduction .....	210
D.2: Watson's lemma .....	211
D.2.a: Case 1 ( Equation (D.1-2a) ) .....	211
D.2.b: Case 2 ( Equation (D.1-2b) ) .....	217

D.3: Steepest-descent or saddle-point method .....	223
<b>E: The Cauchy Tetrahedron Argument .....</b>	<b>236</b>
<b>Bibliography .....</b>	<b>239</b>

## List of Tables

<b>Table 0.1-1:</b>	Historical development of multicomponent seismology. ....	1
<b>Table 1.2-1:</b>	Relationships between spherical and rectangular Cartesian coordinates. ....	18
<b>Table 1.2-2:</b>	Matrix elements for the matrix $\frac{\partial \tilde{\mathbf{A}}}{\partial \xi}$ for the cases where $\xi = x$ and $\xi = z$ ...	21
<b>Table 1.2-3:</b>	Displacements due to different source types. ....	27

## List of Figures

<b>Fig. 1.1.a-1.</b>	Shear wave shot records as recorded from two in-line vertical vibrators in counterphase. ....	5
<b>Fig. 1.1.b-1.</b>	Horizontal displacement produced by two vertical vibrators in counterphase. ....	6
<b>Fig. 1.1.b-2.</b>	Radiation characteristics of two vibrators in counterphase (a) Far-field response. (b) Near-field response. ....	8
<b>Fig. 1.2-1.</b>	(a) A volumetric potato representing the volume over which sources are integrated to obtain the total displacement. (b) A cut is introduced half way into the potato to create surfaces $\Sigma^+$ , $\Sigma^-$ and $\epsilon$ . ....	11
<b>Fig. 1.2-2.</b>	Graphical representation of point displacements embedded in surfaces $\Sigma^+$ and $\Sigma^-$ . ....	12
<b>Fig 1.2-3a.</b>	Single couple corresponding in the limit as $\epsilon \rightarrow 0$ to the response $G_{3n,1}$ . ....	15
<b>Fig 1.2-3b.</b>	Single couple corresponding in the limit as $\epsilon \rightarrow 0$ to the response $G_{1n,3}$ . ....	15
<b>Fig 1.2-4.</b>	Radiation pattern for a double-couple source in the plane containing both sources. ....	16
<b>Fig 1.2-4.</b>	Relationship between spherical and rectangular Cartesian coordinates. ....	19
<b>Fig. 1.2-5a.</b>	P-wave radiation pattern for a vertical point force. ....	29
<b>Fig. 1.2-5b.</b>	S-wave radiation pattern for a vertical point force. ....	30
<b>Fig. 1.2-6a.</b>	P-wave radiation pattern for a horizontal point force. ....	31
<b>Fig. 1.2-6b.</b>	S-wave radiation pattern for a horizontal point force. ....	32
<b>Fig. 1.2-7a.</b>	P-wave radiation pattern for a vertical couple. ....	33
<b>Fig. 1.2-7b.</b>	S-wave radiation pattern for a vertical couple. ....	34
<b>Fig. 1.2-8a.</b>	P-wave radiation pattern for a horizontal couple. ....	35
<b>Fig. 1.2-8b.</b>	S-wave radiation pattern for a horizontal couple. ....	36
<b>Fig. 1.2-9a.</b>	P-wave radiation pattern for a double couple. ....	37
<b>Fig. 1.2-9b.</b>	S-wave radiation pattern for a double couple. ....	38
<b>Fig. 1.3.1-1.</b>	Coupled spring, dash pot and mass model of a vertical vibrator. ....	40
<b>Fig. 1.3.2-2.</b>	Source volume in elastic half-space. ....	54
<b>Fig. 1.3.3-1.</b>	Flow-chart showing how to solve the coupled system of equations. ....	57

<b>Fig. 3.2-1.</b>	Flowchart for a method to determine the preferred frame of reference of the elastic tensor (cubic example).	76
<b>Fig. 4.2.1-1.</b>	Particle displacement notation.	80
<b>Fig.4.2.1-2.</b>	Partitioning of waves at interfaces.	82
<b>Fig 4.2.2-2.</b>	Transformation of depth model to P- and S-wave Goupillaud time models.	83
<b>Fig 4.3-3.</b>	Vertical and horizontal VSP sections.	86
<b>Fig. A.1-1.</b>	Vibrating circular disk over an elastic half-space.	88
<b>Fig. A.1-2.</b>	Cylindrical coordinates for vibrating disk problem.	89
<b>Fig. A.4-1.</b>	Disk on a free surface driven by a vertical force $f_z(t)$ .	100
<b>Fig. A.5.1-1.</b>	Polar coordinate transformation.	106
<b>Fig. A.5.1-2.</b>	Mapping of a point in the $\xi$ plane into points in the $w$ plane, as determined by the function $w = \sqrt{(\xi - \kappa)}$ .	107
<b>Fig. A.5.1-3.</b>	A particular branch cut of the function $w = \sqrt{(\xi - \kappa)}$ and the mapping of the resultant $\xi$ plane into the reduced $w$ plane as shown in grey.	108
<b>Fig. A.5.1-4.</b>	Riemann sheets in the $\xi$ plane and its corresponding image in the $w$ plane as determined by the function $w = \sqrt{(\xi - \kappa)}$ .	109
<b>Fig. A.5.1-5.</b>	Shifted polar coordinates for the function $W = \sqrt{\xi - \kappa_1} \sqrt{\xi - \kappa_2}$ .	110
<b>Fig. A.5.1-6.</b>	A possible branch cut and domain of the function $W = \sqrt{\xi - \kappa_1} \sqrt{\xi - \kappa_2}$ .	110
<b>Fig. A.5.1-7.</b>	Another equally good branch cut and domain of the function $W = \sqrt{\xi - \kappa_1} \sqrt{\xi - \kappa_2}$ .	111
<b>Fig. A.5.1-8.</b>	Final branch cut and domain of definition for the function $W = \sqrt{\xi - \kappa_1} \sqrt{\xi - \kappa_2}$ .	112
<b>Fig. A.5.1-9.</b>	Behavior of $W = \sqrt{\xi - \kappa_1} \sqrt{\xi - \kappa_2}$ around branch cut.	112
<b>Fig. A.5.1-10.</b>	Mapping between $\xi$ and $w$ planes due to the function $w = \sqrt{\xi - \kappa_1} \sqrt{\xi - \kappa_2}$ .	113
<b>Fig. A.5.1-11.</b>	Riemann sheets for the function $W = \sqrt{\xi - \kappa_1} \sqrt{\xi - \kappa_2}$ .	116
<b>Fig. A.5.1-12.</b>	Branch cuts and domain of definition for the function $w = (\sqrt{(\xi - \kappa_1)} \sqrt{(\xi - \kappa_2)}) (\sqrt{(\xi + \kappa_1)} \sqrt{(\xi + \kappa_2)})$ .	117
<b>Fig. A.5.1-13.</b>	Riemann sheets for the function $w = (\sqrt{(\xi - \kappa_1)} \sqrt{(\xi - \kappa_2)}) (\sqrt{(\xi + \kappa_1)} \sqrt{(\xi + \kappa_2)})$ .	118
<b>Fig. A.5.2-1.</b>	Contour of integration to find numbers of zeros of Rayleigh's function.	121

<b>Fig. A.5.2-2.</b>	One branch cut of Rayleigh's function and path of integration $C_3$ .....	122
<b>Fig. A.5.2-3.</b>	Mapping of path $C_3$ in the $\xi$ plane onto path $C_3^{\zeta}$ in the $\zeta$ plane, for the case where $m = 2$ . .....	123
<b>Fig. A.5.2-4a.</b>	First root of the rationalized Rayleigh's equation .....	127
<b>Fig. A.5.2-4b.</b>	Second root of the rationalized Rayleigh's equation .....	128
<b>Fig. A.5.2-4c.</b>	Third root of the rationalized Rayleigh's equation .....	129
<b>Fig. A.6-1.</b>	Multiplicative factors in the perturbation equation .....	135
<b>Fig. A.6-2.</b>	A possible contour of integration for the integral equations of motion .....	136
<b>Fig. A.6-3a.</b>	Polar coordinate transformation .....	138
<b>Fig. A.6-3b.</b>	Pictorial representation of the solution to equation (A.6-15b) .....	139
<b>Fig. A.6-4.</b>	Path of steepest descent .....	145
<b>Fig. A.6-5.</b>	Path of steepest descent including Rayleigh pole outside of main path .....	147
<b>Fig. A.6-6.</b>	Path of integration when $\theta$ approaches $\frac{\pi}{2}$ .....	148
<b>Fig. A.6.b-1.</b>	Steepest descent path for $C_3$ .....	151
<b>Fig. B.1-1.</b>	Forces acting on a material volume .....	154
<b>Fig. B.3-1.</b>	Frames of reference and motion .....	164
<b>Fig. B.4-1.</b>	Cylindrical coordinates .....	173
<b>Fig. C.2-1.</b>	Forces and couples acting on a volume of material .....	187
<b>Fig. D.3-1.</b>	Surface of $\varphi(x,y)$ around a saddle point where $d\varphi = 0$ .....	222
<b>Fig. D.3-2.</b>	Direction of the path of steepest descent .....	224
<b>Fig. D.3-3a.</b>	A paraboloid .....	226
<b>Fig. D.3-3b.</b>	An ellipsoid .....	227
<b>Fig. D.3-3.</b>	A saddle .....	227
<b>Fig. E-1.</b>	Cauchy's elemental tetrahedron .....	235

## 0: Introduction

### 0.1: Historical review

Seismology, without need of much evidence, could probably be traced to the first sentient being that felt the physical earth move under his/her feet. A more quantitative approach can still be traced back to ancient China, during the Han dynasty (AD 132), a rudimentary seismograph was constructed by Chang Heng (Encyclopaedia Britannica, 1981). But, it was not till the early 1800s that quantitative seismology, in which modern seismology has its roots, can actually be said to begin. The topic of exploration multicomponent seismology, has its inception as recently as the 1940s. A good brief overview of the history of multicomponent seismology can be obtained by examining table 0.1-1, adapted from Tatham and McCormack (1991).

<b>Table 0.1-1: Historical development of multicomponent seismology</b>	
<b>Era</b>	<b>Development</b>
1800s	Use of multicomponent recording, especially horizontal seismometers. Earthquake Seismology
1940s	Observation of S-wave arrivals in routine check-shot survey. Horton (1943)
1950s	Use of multicomponent geophones in observational studies of fundamental seismic wave propagation. Jolly (1956), White, Heaps and Lawrence. (1956), Press and Dobrin (1956).
1960s	Use of horizontally polarized Vibroseis sources and geophones for S-wave reflection observations. Cherry and Waters (1968), Erickson, Miller and Waters (1968).

1970s	Use of improved horizontal Vibroseis sources and conventional Vibroseis for P- and S-wave reflection studies over a large number of known fields. Conoco Group Shoot (1977-1978).
1980s	<p>Observation of S-wave reflection in marine environments.</p> <p>Tatham and Stoffa (1976), Tatham, Goolsbee, Massell and Nelson (1983), Tatham and Goolsbee, (1984).</p> <p>Nine component recording- multicomponent recording, anisotropy and shear-wave splitting reported a improving shear-wave data quality and mapping fractures. Alford (1986), Johnston (1986):</p>
( After Tatham and McCormack, 1991 )	

Multicomponent seismology has been a very rich source of research topics and this thesis is comprised of a few topics under this heading.

## **0.2: Structure of thesis**

This thesis examines several very different topics under the framework of multicomponent seismology. I have attempted to make this thesis self-contained so there is quite an extensive appendix section; the subject is so broad, however, I was only partially successful in this endeavor. Even though much of the material in the appendices is review, I have included original developments and analysis in appendix A. The following is a chapter-by-chapter preface to the thesis.

### **0.2.1: Shear waves from vertical vibrators**

It is rather fitting to start this thesis on multicomponent seismology by considering seismic sources. Chapter 1 deals with the generation of shear-waves using vertical vibrators. Experimental evidence of shear-waves generated by vertical vibrators in counterphase was collected by Edelmann (1981). The theoretical explanation of this near-vertically incident shear-wave was not readily available. Dankbaar (1983) and Tan

(1985) analyzed the situation theoretically and found no evidence for vertically incident shear-waves.

I have taken the works of Dankbaar (1983) and Tan (1985) and generalized them. In this way, I am able to show the potential of shear-wave generation in the near-vertical direction from interacting vibrators.

### **0.2.2: Composite media as generalized continua**

After looking at sources, it is appropriate to look in more detail at the medium in which we are placing our sources. Chapter 2 is concerned with composite materials and how we may be able to better describe them by treating them as generalized continua.

Backus (1962) showed that a stack of finely layered isotropic or transversely isotropic media can, in the case of long wavelengths, be approximated by a homogeneous transversely isotropic media. I have generalized this method to indicate how we may approximate the composite under conditions of shorter wavelengths. I have also suggested other avenues to pursue this topic.

### **0.2.3: Elastic tensors and their preferred frames of reference**

Elastic tensors, having many intrinsic symmetries, still possess 21 constants in an arbitrary frame of reference, though they may not all be independent. Given an arbitrary elastic tensor, it is difficult to determine what symmetries may exist for the elastic tensor. Backus (1970) proposed a method to decompose an arbitrary elastic tensor into vector bouquets; by examining the symmetries of these bouquets one can determine the underlying symmetry. Baerheim (1993) proposed a more direct method to find the underlying symmetry, but it is not applicable for all symmetries.

These existing methods are good methods with some drawbacks. The method of Backus requires visual inspection while Baerheim's method is not universally applicable. Both methods are analytic and depend on the eigenstructure of tensors related to the elastic tensor, which may not be stable under small perturbations of the constants. I propose a statistical method that should be universal and, by its statistical nature, not sensitive to small perturbations. The statistical method was tried on an elastic tensor with cubic symmetry. The results from the trial confirmed the viability of the method.

### **0.2.4: Goupillaud P- and S-wave synthetic seismograms**

Mendel, Nahi and Chan (1979) showed how to use a state-space approach to generate plane-wave synthetic seismograms within a Goupillaud model. Because of the differing P- and S-wave velocities, their method was only applicable for a single wave type. They did, however, have a complete elastic plane-wave modeling method that is not based on the Goupillaud model that is both memory- and speed- intensive as compared to one based on the Goupillaud model.

Because of the speed and memory benefits of the Goupillaud model, I devised a method to generate synthetic seismograms for both P- and S-waves using two parallel Goupillaud models. This method was implemented and found to be fast and memory-efficient. Many additional enhancements that already exist for the state-space Goupillaud model can directly applied to the dual Goupillaud model case.

### **0.2.4: Appendices**

Appendix A deals with the wavefield of a vertically vibrating disk on an elastic half-space (Miller and Pursey, 1953). This treatment of Miller and Pursey's (1953) work is quite different from their paper. The treatment here is more general and there are a few points of analysis that are quite different. The results of this appendix are central to the developments in chapter 1.

Appendix B is a review, from a few different sources, of the theory of an elastic continuum. The results are used throughout this thesis. Appendix C is meant to mirror Appendix B, but for the special case of a Cosserat continuum. This type of continuum is the prototype of generalized continua, which is the topic of chapter 2. Appendix D develops the method of steepest descent and appendix E develops Cauchy's tetrahedron argument; both of these are used in other appendices.

## 1: Shear Waves from Vertical Vibrators

### 1.1: Introduction

#### 1.1.a: Overview of experimental evidence

The possibility of generating shear waves in the near-vertical direction by using vertical or P-wave vibrators was first considered by Edelman (1981). He showed in his (1981) paper that it was possible to collect in-line shear-wave data by using two in-line vertical vibrators in counterphase ( $180^\circ$  out of phase) as the source. Since the early experiments by Edelman other field experiments (Sun and Jones, 1993) and some very preliminary physical modeling experiments at the University of Calgary also support this observation. I have reproduced the figure in Edelman's (1981) paper as figure 1.1.a-1, which shows in-line particle motion due to in-line counterphase vertical vibrators.

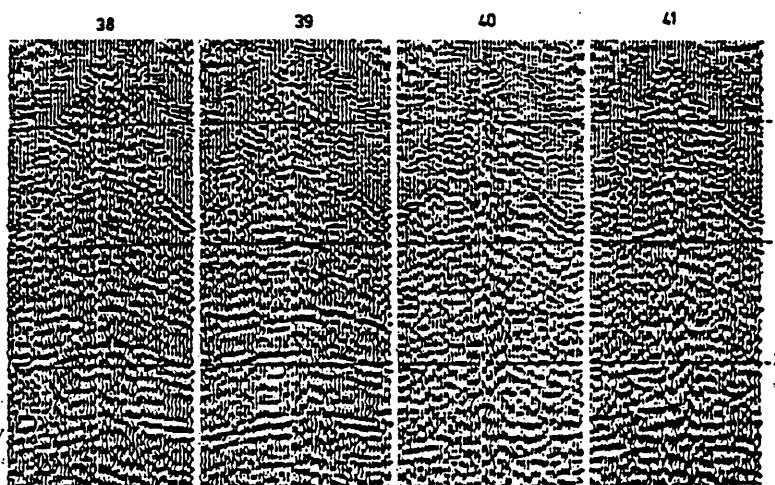


**Fig. 1.1.a-1.** Shear wave shot records as recorded from two in-line vertical vibrators in counterphase.  
(From Edelman, 1981, Figure 8)

The acquisition geometry is shown in figure 1.1.b-1. The important feature is the coherent energy on the inside traces, even at a time of over three seconds. This energy, I

surmise, must come from a takeoff angle extremely close to the vertical. Edelman's paper does not give the exact shooting geometry, so an accurate estimate of the takeoff angle is not available.

The support for the observed shear waves in the near vertical direction has not had as much support theoretically as it has experimentally.

### 1.1.b: Overview of theoretical development

From my survey of the literature, a few authors have given the subject some thought but have not come up with a satisfactory explanation of the observed phenomenon. Edelman (1981) conjectured that since a disk vibrating vertically on a free surface produces strong shear waves around  $37^\circ$  from the vertical, as developed in appendix A as well as by Miller and Pursey (1953), then the two vibrators running in counterphase would produce a strong uncompensated shear-wave between the two vibrators. This situation, as represented by figure 1.1.b-1, is certainly true for a region  $37^\circ$  between the two vibrators but this is necessarily a near-field phenomenon so does not explain the deeper near-offset shear-wave energy which we observed in figure 1.1.a-1.

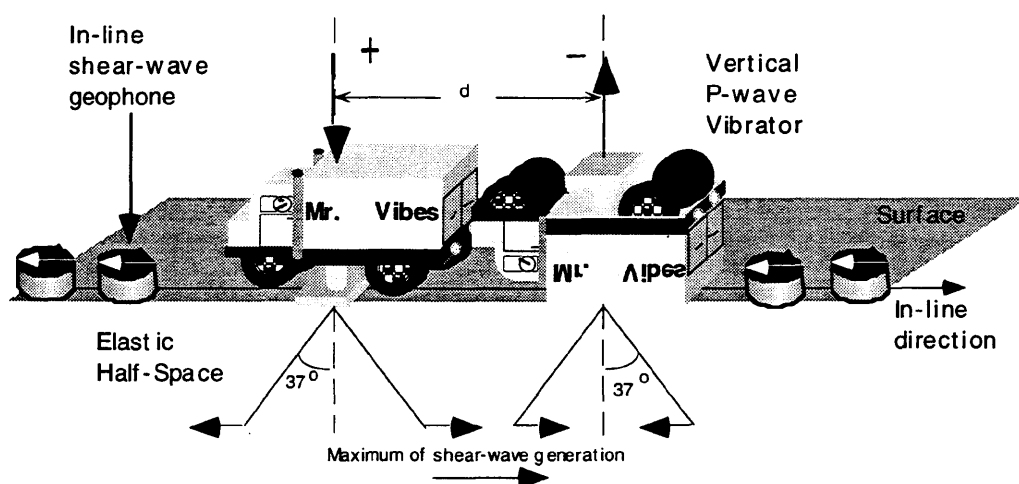


**Fig. 1.1.b-1.** Horizontal displacement produced by two vertical vibrators in counterphase.

(Adapted from Edelman, 1981, Figure 6)

Dankbaar (1983) placed the ideas of Edelman on good theoretical ground. I will here give a brief summary of Dankbaar's contribution. He used the far-field displacement

of what is essentially the response of a vertical point source on a free surface, as given by equations (A.6-24a) and (A.6-24b) in appendix A or equations (116) and (117) in Miller and Pursey's (1953) paper, and constructed the resultant wavefield that would be observed if there were two of these sources separated by a small distance with forces acting in opposite directions. To develop the previous discussion mathematically I will begin by defining the point-source response. I will follow the convention of Aki and Richards (1980) by calling this response

$$G_{il}^{\text{free}}(\mathbf{x}, t; \boldsymbol{\xi}, \tau), \quad (1.1.b-1)$$

which is the elastodynamic Green's function, representing the  $i$ th component of displacement at the point  $\mathbf{x}$  and time  $t$  resulting from a point impulsive source in the  $l$ -direction (which is vertically downwards in the present discussion) located on the free surface at point  $\boldsymbol{\xi}$  and detonated at time  $\tau$ . Dankbaar then used a Taylor-series to get the response of a source displaced from  $\boldsymbol{\xi}$  in the direction of unit vector  $\Delta$  for a distance  $D$  as follows:

$$G_{in}^{\text{free}}(\mathbf{x}; \boldsymbol{\xi} + D\Delta) = G_{in}^{\text{free}}(\mathbf{x}; \boldsymbol{\xi}) + \left[ \frac{\partial G_{in}^{\text{free}}(\mathbf{x}; \boldsymbol{\xi})}{\partial \xi^j} \Delta^j \right] D + \frac{1}{2} \left[ \frac{\partial^2 G_{in}^{\text{free}}(\mathbf{x}; \boldsymbol{\xi})}{\partial \xi^j \partial \xi^k} \Delta^j \Delta^k \right] D^2 + \dots \quad (1.1.b-2)$$

where  $n = 1$  and Einstein summation notation is in effect for repeated indices. By taking the appropriate derivatives of equation (1.1.b-1) and using displacements of  $D$  and  $-D$  in conjunction with equation (1.1.b-2) Dankbaar showed that the combined effect of these two sources added together can be represented by:

$$G_{mn}^{\text{free}}(\mathbf{x}; \boldsymbol{\xi} + D\Delta) - G_{mn}^{\text{free}}(\mathbf{x}; \boldsymbol{\xi} - D\Delta) = 2 \left[ \frac{\partial G_{mn}^{\text{free}}(\mathbf{x}; \boldsymbol{\xi})}{\partial \xi^i} \Delta^i \right] D + \frac{1}{3} \left[ \frac{\partial^3 G_{mn}^{\text{free}}(\mathbf{x}; \boldsymbol{\xi})}{\partial \xi^i \partial \xi^j \partial \xi^k} \Delta^i \Delta^j \Delta^k \right] D^3 + \dots \quad (1.1.b-3)$$

Equation (1.1.b-3) is just the response of the elastic half-space to a simple couple (Symon, 1971, p. 231 ff), a couple or torque being a system of forces the sum of which is zero. However, except as a trivial case, the system of forces will have a resultant nonzero

torque. An example of a couple is a system consisting of two forces of equal magnitude acting in opposite directions and not collinear; thus a torque is produced. It is interesting to note that for rigid bodies any system of forces can be reduced to a single resultant force plus a couple. Now back to the topic at hand. Since Dankbaar assumes  $D$  to be small, he only uses the first term of the expansion given by equation (1.1.b-3). Actual analytic expressions for equation (1.1.b-3) will be derived as an intermediate result in the development in the next section, §1.2 [equations (1.2-31a), (1.2-31b) and (1.2-31c)], so will be omitted here. With this description Dankbaar (1983) was able to show that at an angle greater than five to ten degrees, shear-wave energy dominates over compressional-wave energy. This can be seen on figure 1.1.b-2a which shows the radiation characteristics of two vibrators in counterphase. Dankbaar (1983) was also able to show the effect described by Edelman (1981) as a near-field effect which can also be seen in figure 1.1.b-2.

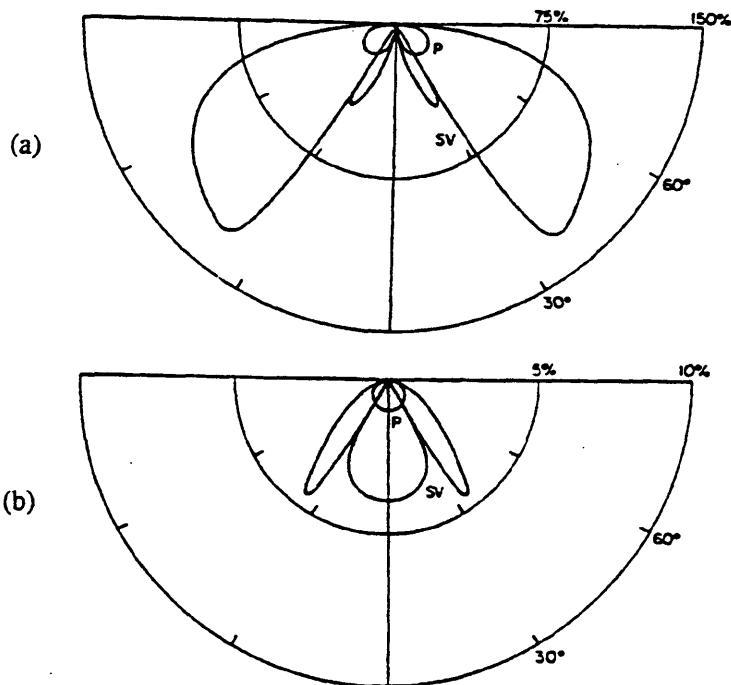


**Fig. 1.1.b-2.** Radiation characteristics of two vibrators in counterphase.

(a) Far-field response. (b) Near-field response.

(From Dankbaar, 1983, Figure 5)

Dankbaar's development basically assumes that the two vibrators do not interact with each other and that, as a matter of fact the two vibrators could have been run separately and the result summed in the computer later to achieve the same result. This situation of

non-interacting vibrators is a rather unrealistic case, especially since the vibrators are assumed to be close to each other.

Tan's (1985) approach is far more general. Tan assumed a simple mechanical vibrator system, which was two-dimensional (2-D) thus representing a line source. A series of these theoretical 2-D vibrators were then placed parallel to each other on a frictionless free surface of an elastic half-space. Since the mechanics of both the vibrators, which were coupled through the half-space, and the elastic half-space itself were known, Tan was able to calculate numerically the resulting wavefield within the half-space after the vibrators were set into a prescribed sequence of gyrations. The radiation patterns calculated by Tan also failed to show the existence of normally incident shear-waves. I believe one of the reasons Tan's (1985) radiation patterns fail to show normally incident shear waves is due to the frictionless-surface assumption that was made. In §1.3 I will develop the theory which relaxes two of the assumptions present in Tan's paper, namely the 2-D assumption and the assumption of a frictionless free surface. Since much of the details of this method will be elaborated on there, I will not go into anymore detail here.

The review so far has not shown a theoretical framework that supports the observed experimental data. In an attempt to bridge this gap, I have tried to generalize the work of Dankbaar (1983) and Tan (1985). The preliminary results were published in the CREWES Project research report (Easley, 1992a and 1993a). Those results and extensions are the subjects of the next two sections. §1.2 concerns extension to Dankbaar's ideas whereas §1.3 deals with Tan's work. Work can be done to flesh out the material in section §1.3, in terms of numerical solutions, but lack of available time means that this must wait for a future date. The theory developed, however, is, in my opinion, complete.

## **1.2: Displacement in counterphase**

The description of two vibrators in counterphase given by Dankbaar (1983) is one which assumes that the two vibrators do not interact with each other and there is no self-interaction of the vibrators. Under these severe restrictions it is not surprising that no shear-wave energy was predicted to exist in the normal direction between the two vibrators. One of the major features of Dankbaar's development is the assumption that the

stress imparted to the elastic half-space is exactly the sum of stresses generated by the vibrators individually. This assumption, of course, precluded any interaction of adjacent vibrators. If we were to allow interactions among the vibrators, there could be situations where counterphase stresses may not provide a good description. I made the assumption (Easley, 1992a) that under certain circumstances the vibrators could be modeled as displacements in counterphase. Under this assumption, and prompted by results from earthquake seismology (Aki and Richards, 1980, p. 43-84), I was able to show that normal-incidence shear-waves are a possibility from interacting vertical vibrators. To begin we need a relationship between the displacements at the free surface and the resultant displacement field in the elastic half-space. The representation theorem as given by Aki and Richards (1981, p. 29) is exactly such a relationship; this theorem is embodied in the following equation:

$$\begin{aligned}
 u_n(\mathbf{x}, t) = & \int_{-\infty}^{\infty} d\tau \int_V f_m(\boldsymbol{\xi}, \tau) G_{nm}(\mathbf{x}, t-\tau; \boldsymbol{\xi}, 0) dV(\boldsymbol{\xi}) + \\
 & \int_{-\infty}^{\infty} d\tau \int_S T_m(\mathbf{u}(\boldsymbol{\xi}, \tau), \mathbf{n}) G_{nm}(\mathbf{x}, t-\tau; \boldsymbol{\xi}, 0) dS(\boldsymbol{\xi}) + \\
 & \int_{-\infty}^{\infty} d\tau \int_S u_m(\boldsymbol{\xi}, \tau) c_{mjkl}(\boldsymbol{\xi}) n_j G_{nk,l}(\mathbf{x}, t-\tau; \boldsymbol{\xi}, 0) dS(\boldsymbol{\xi})
 \end{aligned} \tag{1.2-1}$$

where	$\mathbf{u}$	$\equiv$	displacement vector,
	$\mathbf{x}$	$\equiv$	observation point vector,
	$\boldsymbol{\xi}$	$\equiv$	source point vector,
	$G_{nm}(\mathbf{x}, t-\tau; \boldsymbol{\xi}, 0)$	$\equiv$	$n$ th component of the elastodynamic Green's function with unit impulse applied at $\boldsymbol{\xi}$ and time $\tau$ ,
	$G_{nk,l}$	$\equiv$	partial derivative of the Green's function with respect to source coordinate $\xi_l$ ,
	$V$	$\equiv$	volume of integration containing source mechanisms,
	$S$	$\equiv$	closed orientable surface containing $V$ ,
	$\mathbf{n}$	$\equiv$	unit outward normal of surface $S$ ,
	$f_m$	$\equiv$	$m$ th component of body force vector,

$T_m(\mathbf{u}(\xi, \tau), \mathbf{n}) \equiv m\text{th component of traction vector consistent with displacement } \mathbf{u} \text{ on surface element with unit normal } \mathbf{n}$   
 and  $c_{mjkl}(\xi) \equiv \text{elastic tensor at source location } \xi.$

Equation (1.2-1) describes the displacement due to the existence of sources within the volume  $V$  and on the surface  $S$ . As I wish to investigate the dynamic properties of a counterphase displacement source embedded on the free surface of an elastic half-space, we will not need to consider the effects due to body forces within  $V$ , nor do we need to consider any surface tractions upon  $S$ . With this in mind we can see that only the third integral in equation (1.2-1) needs to be retained. The resulting integral becomes:

$$u_n(\mathbf{x}, t) = \int_{-\infty}^{\infty} d\tau \int_S u_m(\xi, \tau) c_{mjkl}(\xi) n_j G_{nk,l}(\mathbf{x}, t-\tau; \xi, 0) dS(\xi). \quad (1.2-2)$$

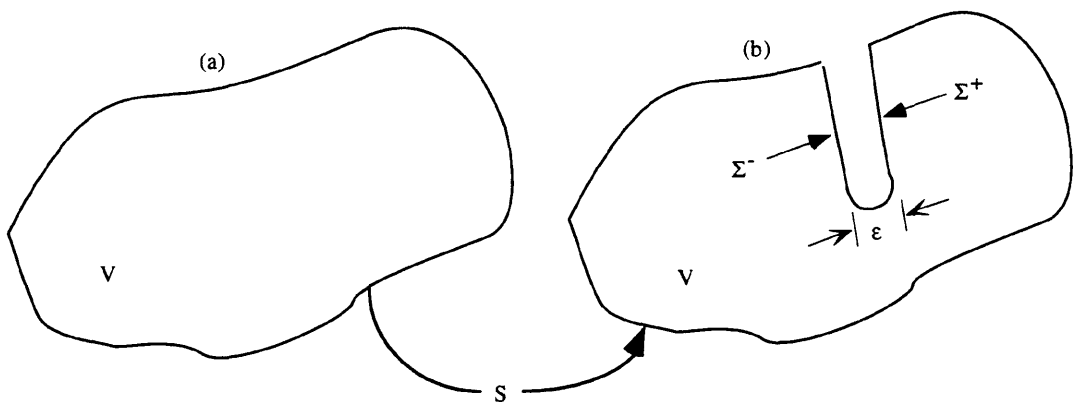


**Fig. 1.2-1.** (a) A volumetric potato representing the volume over which sources are integrated to obtain the total displacement.  
 (b) A cut is introduced half way into the potato to create surfaces  $\Sigma^+$ ,  $\Sigma^-$  and  $\epsilon$ .

To follow the development of Aki and Richards we shall first consider a volume  $V$  embedded within a homogeneous medium. This abstract volume is represented in figure 1.2-1a. We will augment the surface  $S$  as shown in figure 1.2-1b, which is the same volume with an indentation creating new surfaces  $\Sigma^+$  and  $\Sigma^-$  separated by  $\epsilon$ .

We now embed the displacement discontinuity within the two newly created surfaces and introduce a coordinate system as shown in figure 1.2-2.

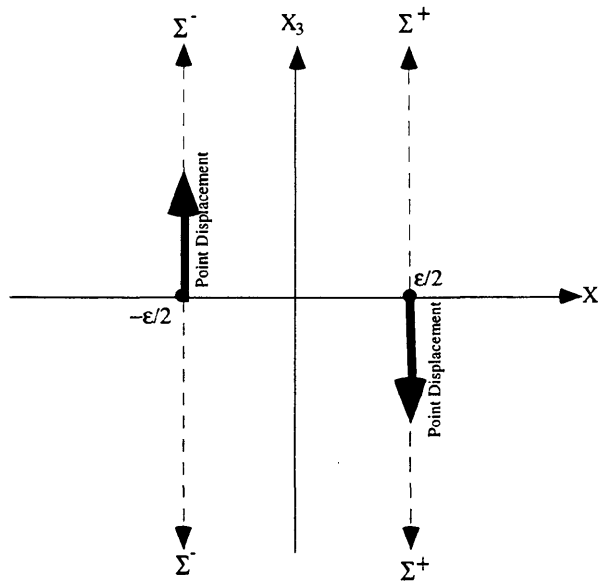


**Fig. 1.2-2.** Graphical representation of point displacements embedded in surfaces  $\Sigma^+$  and  $\Sigma^-$ .

The assumption of isotropy allows the elastic tensor to be expressed in the following manner:

$$c_{ijkl} = \lambda \delta_{ij} \delta_{kl} + \mu (\delta_{ik} \delta_{jl} + \delta_{il} \delta_{jk}), \quad (1.2-3)$$

where  $\lambda$  and  $\mu$   $\equiv$  Lamé constants,  
and  $\delta_{ij}$   $\equiv$  Kronecker delta .

Substitution of equation (1.2-3) into equation (1.2-2) results in

$$u_n(x, t) = \int_{-\infty}^{\infty} d\tau \int_S \lambda u_j n_j G_{nl,l} + \mu (u_k n_l G_{nk,l} + u_l n_k G_{nk,l}) dS. \quad (1.2-4)$$

On surface  $\Sigma^+$ ,  $n_i = \delta_{i1}$  and on surface  $\Sigma^-$ ,  $n_i = -\delta_{i1}$ . All other surfaces of S have no displacement sources so we will not need to consider the normal vectors there. With this in mind equation (1.2-4) becomes

$$\begin{aligned}
 u_n(\mathbf{x}, t) = & - \int_{-\infty}^{\infty} d\tau \int_{\Sigma^+} u_m [G_{mn,1} + G_{1n,m}] \mu dS + \\
 & + \int_{-\infty}^{\infty} d\tau \int_{\Sigma^-} u_m [G_{mn,1} + G_{1n,m}] \mu dS .
 \end{aligned}
 \tag{1.2-5}$$

Since the displacement sources have displacements only in the 3-direction, and assuming the displacements are localized in time and space, we can represent them as:

$$u_m(\xi, \tau) = \delta_{m3} \delta(\tau) \left[ \delta\left(\left|\xi + \frac{\epsilon}{2}\mathbf{x}_1\right|\right) - \delta\left(\left|\xi - \frac{\epsilon}{2}\mathbf{x}_1\right|\right) \right]
 \tag{1.2-6}$$

where

$|\cdot| \equiv$  magnitude of the argument,

$\delta(\tau) \equiv$  Dirac delta function (distribution),

and  $\mathbf{x}_1 \equiv$  unit vector in the positive 1-direction.

Substitution of the relations above to equation (1.2-5) results in

$$\begin{aligned}
 u_n(\mathbf{x}, t) = & \int_{-\infty}^{\infty} d\tau \int_{\Sigma^+} \delta(\tau) \delta\left(\left|\xi - \frac{\epsilon}{2}\mathbf{x}_1\right|\right) [G_{3n,1} + G_{1n,3}] \mu dS + \\
 & + \int_{-\infty}^{\infty} d\tau \int_{\Sigma^-} \delta(\tau) \left[ \delta\left(\left|\xi + \frac{\epsilon}{2}\mathbf{x}_1\right|\right) \right] [G_{3n,1} + G_{1n,3}] \mu dS .
 \end{aligned}
 \tag{1.2-7}$$

I have not evaluated the Dirac delta functions in equation (1.2-7) so that the following steps will hopefully be clearer. If  $\epsilon$  is allowed to approach zero then the surfaces  $\Sigma^+$  and

$\Sigma^-$  will approach a single surface  $\Sigma$  which is located on the 2-3 plane in this instance.

This will transform equation (1.2-7) into:

$$u_n(\mathbf{x}, t) = 2 \int_{-\infty}^{\infty} d\tau \int_{\Sigma} \delta(\tau) \delta(|\xi|) [G_{3n,1} + G_{1n,3}] \mu dS. \quad (1.2-8)$$

Evaluation of equation (1.2-8) results in:

$$u_n(\mathbf{x}, t) = 2 \mu [G_{3n,1}(\mathbf{x}, t, \xi, 0) + G_{1n,3}(\mathbf{x}, t, \xi, 0)]_{(\xi=0)}. \quad (1.2-9)$$

To see that equation (1.2-9) represents the response to the sum of two single couples, we shall show that each term within the square brackets represents the wavefield of a single couple. To do this we need only to write out the operational definition of the partial derivatives within the square bracket as:

$$\begin{aligned} G_{3n,1}(\mathbf{x}, t, \xi, 0) &= \frac{\partial G_{3n}}{\partial \xi_1} = \\ &= \lim_{\varepsilon \rightarrow 0} \left( \frac{G_{3n}(\mathbf{x}, t, \xi - \varepsilon \xi_1, 0) - G_{3n}(\mathbf{x}, t, \xi + \varepsilon \xi_1, 0)}{2\varepsilon} \right). \end{aligned} \quad (1.2-10a)$$

The term 
$$\frac{G_{3n}(\mathbf{x}, t, \xi - \varepsilon \xi_1, 0) - G_{3n}(\mathbf{x}, t, \xi + \varepsilon \xi_1, 0)}{2\varepsilon}, \quad (1.2-10b)$$

is just the response of a single couple as shown in figure (1.2-3a). The second term in equation (1.2-10b) represents the response in the limit of a couple as shown in figure 1.2-3b.

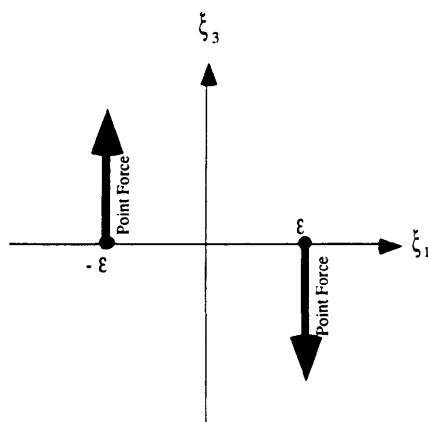


**Fig 1.2-3a.** Single couple corresponding in the limit as  $\epsilon \rightarrow 0$  to the response  $G_{3n,1}$ .

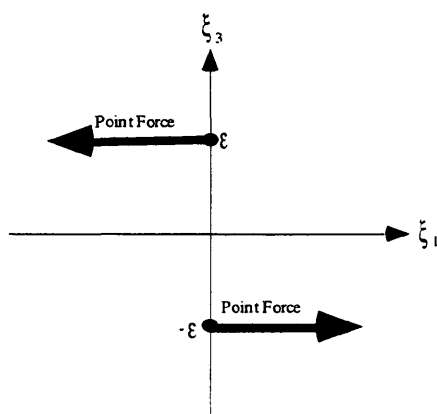


**Fig. 1.2-3b.** Single couple corresponding in the limit as  $\epsilon \rightarrow 0$  to the response  $G_{1n,3}$ .

The Green's function for a point force in an unbounded, homogeneous, isotropic and elastic medium is known. The far-field displacement is given by Aki and Richards [1980, p. 74, equations (4.24) and (4.25)]. The double-couple response in this situation is also known (Aki and Richards, 1980, p. 81) and, since we will be deriving the double-couple response for a source on the free surface of an elastic half-space, I will not derive these equations here; however, even at this preliminary stage, we can see by the radiation patterns for a double-couple source in an unbounded, homogeneous, isotropic and elastic space (figure 1.2-4) that, as compared to the radiation of a single couple, here the shear-wave radiation pattern contains a shear-wave lobe in the vertical direction.

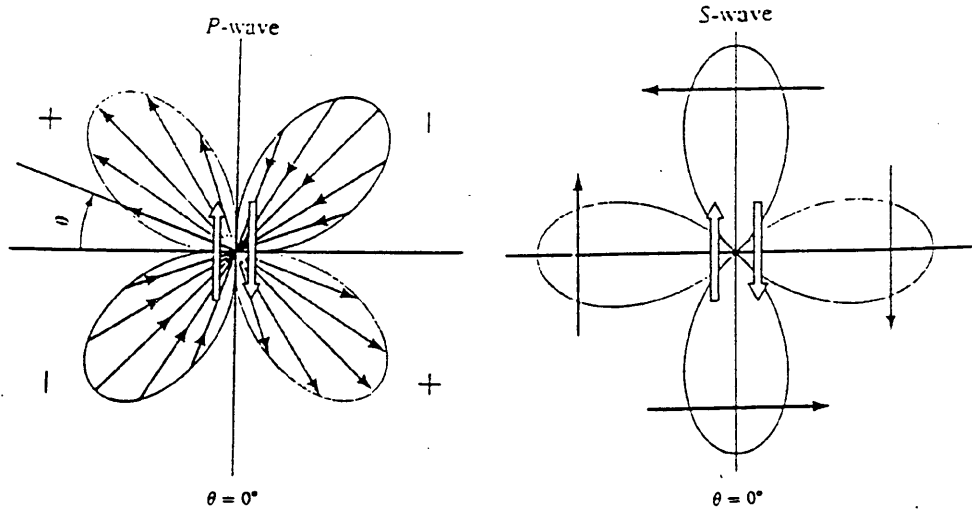


**Fig. 1.2-4.** Radiation pattern for a double-couple source in the plane containing both sources.

(adapted from Aki and Richards, 1980, p. 82-83, figure 4.5 and 4.6)

As I have already mentioned, the results so far have been for double-couple sources within an unbounded space. The next step is to find the radiation pattern for a double-couple source on a free surface.

The first things we need are the far-field responses of vertical and horizontal point forces on a free surface. The responses we will be using are the far-field body wave responses due to a disk of radius  $a$  and strength  $M$ . This, however, is not a problem since as stated by Cherry (1962, p. 32), "If  $Ma^2$  remains finite as  $a$  approaches zero, then a point force is obtained at the origin of coordinates.". The response for a vertical force on the free surface is derived in appendix A and given by equations (A.6-24a) and (A.6-24b) which are equivalent to equations (116) and (117) in Miller and Pursey's paper (1953). These formulas are reproduced here as:

$$u_R^V = -S \frac{e^{-iR}}{R} \frac{\cos \theta (m^2 - 2 \sin^2 \theta)}{2 F_0(-\sin \theta)}, \quad (1.2-11a)$$

$$u_\theta^V = -i S m^3 \frac{e^{-imR}}{R} \frac{\sin 2\theta \sqrt{m^2 \sin^2 \theta - 1}}{2 F_0(-m \sin \theta)} \quad (1.2-11b)$$

and

$$u_{\phi}^V = 0 \quad (1.2-11c)$$

where

$$F_0(\xi) = (2\xi^2 - m^2)^2 - 4\xi^2 \sqrt{\xi^2 - 1} \sqrt{\xi^2 - m^2} \quad (1.2-11d)$$

is Rayleigh's function and I have placed all source-related terms and similar constants under the constant  $S$  to simplify future developments. Note that I have removed the superscript indicating Fourier transforms and replaced it with the letter V to indicate its relationship to a vertical point force. The removal of the Fourier transform can be justified by assuming an impulsive source which should not cause any problems, since this will not affect the radiation patterns of concern to us. Now we need to consider a horizontal point force.

The equivalent formulas for radiation patterns associated with a horizontal force are derived in Cherry's [1962, p. 31, equations (29), (30) and (31)] paper. In order to have a consistent notation, I will transcribe these equations here as

$$u_R^H = S \frac{e^{-iR}}{R} \frac{\sin 2\theta \sqrt{m^2 - \sin^2 \theta}}{F_0(-\sin \theta)} \sin \phi, \quad (1.2-12a)$$

$$u_{\theta}^H = -S \frac{e^{-imR}}{R} \frac{\cos \theta (1 - 2 \sin^2 \theta)}{F_0(-m \sin \theta)} \sin \phi \quad (1.2-12b)$$

and

$$u_{\phi}^H = S \frac{e^{-imR}}{R} \cos \phi \quad (1.2-12c)$$

where the superscript H is used to indicate the connection to a horizontal point force. Before we continue we need to make a correspondence. The Green's function,  $G_{mn}$ , represents the displacement in the  $n$ -direction due to a point force in the  $m$ -direction. Therefore,  $G_{3n}$  is directly related to equations (1.2-11a), (1.2-11b) and (1.2-11c), whereas  $G_{1n}$  is related to equations (1.2-12a), (1.2-12b) and (1.2-12c). I will use matrix notation to simplify the equations. Let a bold symbol capped with  $\sim$  represent a matrix and a bold symbol capped with  $\wedge$  be a unit vector. Since we will be dealing with both spherical polar

coordinates as well as rectangular Cartesian coordinates, as shown in figure 1.2-4, we shall define the following column matrices

$$\tilde{\mathbf{r}} = \begin{bmatrix} \hat{\mathbf{r}} \\ \hat{\boldsymbol{\theta}} \\ \hat{\boldsymbol{\phi}} \end{bmatrix} \text{ and } \tilde{\mathbf{x}} = \begin{bmatrix} \hat{\mathbf{x}} \\ \hat{\mathbf{y}} \\ \hat{\mathbf{z}} \end{bmatrix}. \quad (1.2-13)$$

We will also place all the displacement components within a column matrix without appending the superscript; this is to mean whatever relationship written in this fashion will apply to both vertical, V, and horizontal, H, cases. With this in mind we shall write:

$$\tilde{\mathbf{u}} = \begin{bmatrix} u_R \\ u_\theta \\ u_\phi \end{bmatrix}. \quad (1.2-14)$$

With the matrices defined in equation (1.2-13) and (1.2-14) we can now write the total displacement vector  $\mathbf{u}$  as the matrix product

$$\mathbf{u} = \tilde{\mathbf{u}} \tilde{\mathbf{r}}^T = u_R \hat{\mathbf{r}} + u_\theta \hat{\boldsymbol{\theta}} + u_\phi \hat{\boldsymbol{\phi}}, \quad (1.2-15)$$

where the superscript T means matrix transpose. The relationships between spherical and rectangular Cartesian coordinates are well known and summarized in table 1.2-1. These relationships can be easily derived from figure 1.2-4. More importantly, these relationships allow us to relate derivatives from one coordinate system to the other.

Table 1.2-1: Relationships between spherical and rectangular Cartesian coordinates.	
Rectangular to Spherical	Spherical to Rectangular
$x = R \sin \theta \cos \phi$ (1.2-16a)	$R = \sqrt{x^2 + y^2 + z^2}$ (1.2-16d)
$y = R \sin \theta \sin \phi$ (1.2-16b)	$\theta = \arccos \left( \frac{z}{R} \right)$ (1.2-16e)
$z = R \cos \theta$ (1.2-16c)	$\phi = \arctan \left( \frac{y}{x} \right)$ (1.2-16f)



$$\tilde{\mathbf{A}} = \begin{bmatrix} \sin \theta \cos \varphi, & \sin \theta \sin \varphi, & \cos \theta \\ \cos \theta \cos \varphi, & \cos \theta \sin \varphi, & -\sin \theta \\ -\sin \theta, & \cos \theta, & 0 \end{bmatrix}. \quad (1.2-18b)$$

Since  $\tilde{\mathbf{A}}$  is an orthogonal matrix, which means  $\tilde{\mathbf{A}}^{-1} = \tilde{\mathbf{A}}^T$ , we can also state that

$$\tilde{\mathbf{x}}^T = \tilde{\mathbf{A}}^T \tilde{\mathbf{r}}^T. \quad (1.2-19)$$

Therefore, differentiation of equation (1.2-18a) results in:

$$\begin{aligned} \frac{\partial \tilde{\mathbf{r}}^T}{\partial \xi} &= \frac{\partial \tilde{\mathbf{A}}}{\partial \xi} \tilde{\mathbf{x}}^T + \tilde{\mathbf{A}} \frac{\partial \tilde{\mathbf{x}}^T}{\partial \xi} = \frac{\partial \tilde{\mathbf{A}}}{\partial \xi} \tilde{\mathbf{x}}^T \\ &= \frac{\partial \tilde{\mathbf{A}}}{\partial \xi} \tilde{\mathbf{A}}^T \tilde{\mathbf{r}}^T, \end{aligned} \quad (1.2-20a)$$

where I have used the fact that  $\tilde{\mathbf{x}}$  is a row matrix of constant unit vectors to go from the first equality to the second, while going from the second to the third just involves substitution from equation (1.2-19). Now, if we use the coordinate system relationships in table 1.2-1 and equation (1.2-18b), we can state explicitly

$$\frac{\partial \tilde{\mathbf{A}}}{\partial \xi} = \frac{1}{R} [a^i]_{i,j=1}^3, \quad (1.2-20b)$$

where  $i$  is the row counter, and  $j$  is the column counter, and the elements of the matrix are tabulated in table 1.2-2.

Table 1.2-2: Matrix elements for the matrix $\frac{\partial \tilde{A}}{\partial \xi}$ for the cases where $\xi = x$ and $\xi = z$ .		
elements	$\xi = x$	$\xi = z$
$a_1^1$	$\cos^2\theta \cos^2\varphi + \sin^2\theta$	$-\cos\varphi \cos\theta \sin\theta$
$a_2^1$	$-\cos\varphi \sin\varphi \sin^2\theta$	$-\cos\theta \sin\theta \sin\varphi$
$a_3^1$	$-\cos\varphi \sin\theta \cos\varphi$	$\sin^2\theta$
$a_1^2$	$[\sin^2\varphi - \cos^2\varphi \sin^2\theta] \cot\theta$	$\cos\varphi \sin^2\theta$
$a_2^2$	$-\sin^2\theta + 1 \sin\varphi \cos\varphi \cot\theta$	$\sin\varphi \sin^2\theta$
$a_3^2$	$-\cos\varphi \cos^2\theta$	$\cos\theta \sin\theta$
$a_1^3$	$\frac{\cos\varphi \sin\varphi}{\sin\theta}$	0
$a_2^3$	$\frac{\sin^2\varphi}{\sin\theta}$	0
$a_3^3$	0	0

We will now define another matrix:

$$\tilde{B}_\xi = \frac{\partial \tilde{A}}{\partial \xi} \tilde{A}^T, \quad (1.2-21a)$$

where, from equations (1.2-20b) and (1.2-17b), we have for  $\xi = x$ :

$$\tilde{B}_x = \frac{1}{R} \begin{bmatrix} 0, & \cos\varphi \cos\theta, & -\sin\varphi \\ -\cos\varphi \cos\theta, & 0, & -\frac{\cos\theta \sin\varphi}{\sin\theta} \\ \sin\theta, & \frac{\cos\theta \sin\varphi}{\sin\theta}, & 0 \end{bmatrix}, \quad (1.2-21b)$$

and for  $\xi = z$ :

$$\tilde{\mathbf{B}}_z = \frac{1}{R} \begin{bmatrix} 0, & -\sin \varphi, & 0 \\ \sin \varphi, & 0, & 0 \\ 0, & 0, & 0 \end{bmatrix}. \quad (1.2-21c)$$

Finally, using equations (1.2-21a) and (1.2-20a), we can rewrite equation (1.2-17) in the form:

$$\frac{\partial \mathbf{u}}{\partial \xi} = \left[ \frac{\partial \tilde{\mathbf{u}}}{\partial \xi} + \tilde{\mathbf{u}} \tilde{\mathbf{B}}_\xi \right] \tilde{\mathbf{r}}^T. \quad (1.2-22)$$

The only term in the equation above for which we do not have explicit formulas is  $\frac{\partial \tilde{\mathbf{u}}}{\partial \xi}$ , which can be derived from equations (1.2-11a), (1.2-11b), (1.2-11c), (1.2-12a), (1.2-12b) and (1.2-12c). The actual derivations of these formulas are rather cumbersome involving many terms, so I used a symbolic manipulator to help me out. The product I used is Theorist<sup>®</sup> on a Mac<sup>®</sup> IIsi computer. First I shall tabulate the results for the case where  $\xi = x$  and the force is in the  $z$  direction, which means from equation (1.2-14):

$$\frac{\partial \tilde{\mathbf{u}}}{\partial \xi} = \frac{\partial \tilde{\mathbf{u}}^V}{\partial \xi} = \left[ \frac{\partial u_R^V}{\partial \xi}, \frac{\partial u_\theta^V}{\partial \xi}, \frac{\partial u_\varphi^V}{\partial \xi} \right]^T, \quad (1.2-23)$$

such that the first term on the right-hand side is given by:

$$\frac{\partial u_R^V}{\partial x} = \frac{S e^{iR} \alpha_R^V(\theta, \varphi)}{R^2 F_0(-\sin \theta)} + \frac{S i e^{iR} \beta_R^V(\theta, \varphi)}{R F_0(-\sin \theta)}, \quad (1.2-24a)$$

where

$$\alpha_R^V = \frac{([\sin^2 2\theta - 2 m^2 \cos^2 \theta] G(\sin \theta) + 2 [6 \sin^2 \theta - m^2 - 4] \sin \theta) \sin \varphi}{2 \sin \theta} + \frac{(m^2 - 2 \sin^2 \theta)}{2}, \quad (1.2-24b)$$

$$\beta_R^V = \frac{(2 \sin^2 \theta - m^2) \cos \varphi \sin 2\theta}{2}, \quad (1.2-24c)$$

$$G(\zeta) = \frac{P(\zeta)}{F_0(\zeta)}, \quad (1.2-24d)$$

and

$$P(\zeta) = -4 \frac{(2\zeta^2 - m^2 - 1)\zeta^3}{\sqrt{\zeta^2 - 1} \sqrt{\zeta^2 - m^2}} + 8\zeta(2\zeta^2 - m^2 - \sqrt{\zeta^2 - 1} \sqrt{\zeta^2 - m^2}); \quad (1.2-24e)$$

the second term is given by:

$$\frac{\partial u_\theta^V}{\partial x} = \frac{S i m^3 e^{i m R} \alpha_\theta^V(\theta, \varphi)}{R^2 F_0(-m \sin \theta)} + \frac{S m^3 e^{i m R} \beta_\theta^V(\theta, \varphi)}{R F_0(-m \sin \theta)}, \quad (1.2-25a)$$

where

$$\alpha_\theta^V = g(\theta) \cos \varphi + f(\theta) \sin \varphi, \quad (1.2-25b)$$

$$g(\theta) = \sin \theta \sin 2\theta \sqrt{m^2 \sin^2 \theta - 1}, \quad (1.2-25c)$$

$$f(\theta) = \frac{(4 \cos 2\theta - 2 m G(m \sin \theta) \cos \theta \sin 2\theta)(m^2 \sin^2 \theta - 1) + m^2 \sin^2 2\theta}{2 \sin \theta \sqrt{m^2 \sin^2 \theta - 1}}, \quad (1.2-25d)$$

and

$$\beta_\theta^V = \sin \theta \sin 2\theta \sqrt{m^2 - 1} \cos \varphi; \quad (1.2-25e)$$

and the third and final term in this group is:

$$\frac{\partial u_\varphi^V}{\partial x} = 0. \quad (1.2-26)$$

Second, I shall tabulate the results for the case where  $\xi = z$  and the force is in the  $x$ -direction, which means, from equation (1.2-14),

$$\frac{\partial \tilde{\mathbf{u}}}{\partial \xi} = \frac{\partial \tilde{\mathbf{u}}^H}{\partial \xi} = \left[ \frac{\partial u_R^H}{\partial \xi}, \frac{\partial u_\theta^H}{\partial \xi}, \frac{\partial u_\phi^H}{\partial \xi} \right]^T, \quad (1.2-27)$$

such that the first term is given by:

$$\frac{\partial u_R^H}{\partial z} = \frac{S e^{iR} \alpha_R^H(\theta) \sin \varphi}{2 R^2 F_0(-\sin \theta)} + \frac{S i e^{iR} \beta_R^H(\theta) \sin \varphi}{2 R F_0(-\sin \theta)}, \quad (1.2-28a)$$

where

$$\alpha_R^H(\theta) = \frac{2 [(6 m^2 - 2) \sin^2 \theta + 2 \sin^2 2\theta - 4 m^2] \sin \theta}{\sqrt{m^2 - \sin^2 \theta} - G(-\sin \theta) \sin^2 2\theta \sqrt{m^2 - \sin^2 \theta}}, \quad (1.2-28b)$$

and

$$\beta_R^H(\theta) = \frac{(\sin^2 2\theta - 4 m^2 \cos^2 \theta) \sin \theta}{\sqrt{m^2 - \sin^2 \theta}}, \quad (1.2-28c)$$

and  $G(\zeta)$  has been defined in equation (1.2-24d). The second term has the form:

$$\frac{\partial u_\theta^H}{\partial z} = \frac{S m^4 e^{-imR} \alpha_\theta^H(\theta) \sin \varphi}{4 R^2 F_0(-m \sin \theta)} + \frac{S i m^4 e^{-imR} \beta_\theta^H(\theta) \sin \varphi}{4 R F_0(-m \sin \theta)}, \quad (1.2-29a)$$

where

$$\alpha_\theta^H(\theta) = 4 (3 \sin^2 2\theta - 1) - m G(-m \sin \theta) \cos \theta \sin 4\theta, \quad (1.2-29b)$$

and

$$\beta_\theta^H(\theta) = 4 m (\sin^2 2\theta - \cos^2 \theta); \quad (1.2-29c)$$

and finally the third term,

$$\frac{\partial u_{\varphi}^H}{\partial z} = -\frac{S e^{-imR} \cos \theta \cos \varphi}{R^2} - \frac{S i m e^{-imR} \cos \theta \cos \varphi}{R}. \quad (1.2-30)$$

We should notice that equations (1.2-24a), (1.2-25a), (1.2-26), (1.2-28a), (1.2-29a) and (1.2-30) are all comprised of two parts, a far-field portion with the factor  $R$  in the denominator and a near-field portion with the factor  $R^2$  in the denominator. Since our derivations for displacements only consider the far field, we would be justified in dropping all the near-field terms; but to be complete I have included both terms. We now have all the terms in equation (1.2-22) defined explicitly and, since this equation represents the displacement field due to the two couples of concern, we have the radiation pattern for both the single-couple case, as considered by Dankbaar (1983), or, by combining the other couple as required in equation (1.2-9), we have the radiation from a double couple on a free surface over an elastic half-space. To complete the picture, we will write down the expressions for all the new types of sources we have considered, namely, the vertical couple, horizontal couple and the double couple on the free surface of an elastic half-space. The displacement equations of a single vertical couple on a free surface of an elastic half-space are:

$$u_R^{VC} = \frac{\partial u_R^V}{\partial x} - u_{\theta}^V \frac{\cos \varphi \cos \theta}{R} + u_{\varphi}^V \frac{\sin \varphi}{R}, \quad (1.2-31a)$$

$$u_{\theta}^{VC} = \frac{\partial u_{\theta}^V}{\partial x} + u_{\varphi}^V \frac{\sin \varphi \cos \theta}{R \sin \theta} + u_R^V \frac{\cos \varphi \cos \theta}{R}, \quad (1.2-31b)$$

and

$$u_{\varphi}^{VC} = \frac{\partial u_{\varphi}^V}{\partial x} - u_R^V \frac{\sin \varphi}{R} + u_{\theta}^V \frac{\sin \varphi \cos \theta}{R \sin \theta}, \quad (1.2-31c)$$

where all the terms above are explicitly expressed in equations (1.2-11), (1.2-24a), (1.2-25a) and (1.2-26) and I have used the superscript VC to indicate displacements due to a vertical couple. The displacement equations of a single horizontal couple on a free surface of an elastic half-space are:

$$u_R^{HC} = \frac{\partial u_R^H}{\partial z} + u_\theta^H \frac{\sin \theta}{R}, \quad (1.2-32a)$$

$$u_\theta^{HC} = \frac{\partial u_\theta^H}{\partial z} - u_R^H \frac{\sin \theta}{R}, \quad (1.2-32b)$$

and

$$u_\phi^{HC} = \frac{\partial u_\phi^H}{\partial z}, \quad (1.2-32c)$$

where all the terms above are explicitly expressed in equations (1.2-12), (1.2-28a), (1.2-29a) and (1.2-30) and I have used the superscript HC to indicate displacements due to a horizontal couple. Finally we can combine the equations above using equation (1.2-9) to give the equation of motion due to a double couple on the free surface of an elastic half-space. These equations are:

$$u_\phi^{DC} = 2\mu \left[ u_R^{VC} + u_R^{HC} \right], \quad (1.2-33a)$$

$$u_\theta^{DC} = 2\mu \left[ u_\theta^{VC} + u_\theta^{HC} \right], \quad (1.2-33b)$$

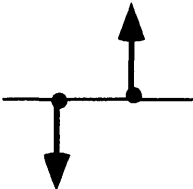
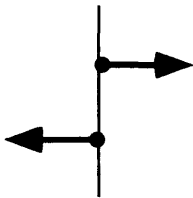
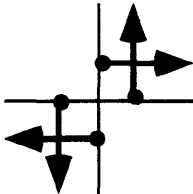
and

$$u_\phi^{DC} = 2\mu \left[ u_\phi^{VC} + u_\phi^{HC} \right], \quad (1.2-33c)$$

where all the terms above are explicitly expressed in equations (1.2-32) and (1.2-31) and I have used the superscript DC to indicate displacements due to a double couple.

We can summarize all the displacement equations we have dealt with in the following table 1.2-3.

**Table 1.2-3:** Displacements due to different source types.

Source Type	Diagrammatic Representation	Displacements			
		$u$	Wave Type	Equation Number	Figure Number
Vertical Point Force		$u_R^V$	P-wave	1.2-11a	1.2-5a
		$u_\theta^V$	SV-wave	1.2-11b	
		$u_\phi^V$	SH-wave	1.2-11c	
Horizontal Point Force		$u_R^H$	P-wave	1.2-12a	1.2-6a
		$u_\theta^H$	SV-wave	1.2-12b	
		$u_\phi^H$	SH-wave	1.2-12c	
Vertical Couple		$u_R^{VC}$	P-wave	1.2-31a	1.2-7a
		$u_\theta^{VC}$	SV-wave	1.2-31b	
		$u_\phi^{VC}$	SH-wave	1.2-31c	
Horizontal Couple		$u_R^{HC}$	P-wave	1.2-32a	1.2-8a
		$u_\theta^{HC}$	SV-wave	1.2-32b	
		$u_\phi^{HC}$	SH-wave	1.2-32c	
Double Couple		$u_R^{DC}$	P-wave	1.2-33a	1.2-9a
		$u_\theta^{DC}$	SV-wave	1.2-33b	
		$u_\phi^{DC}$	SH-wave	1.2-33c	

Since the sear-wave displacements have been separated into their components in the  $\theta$  and  $\varphi$  directions I should state for completeness that the magnitude of sear-wave displacement should be given by

$$u^S = \sqrt{(u_\theta)^2 + (u_\varphi)^2}. \quad (1.2-34)$$

Keeping this in mind, we shall plot the far-field radiation patterns for P and S waves. The source types and their associated figure numbers are given in table 1.2-3, the actual figures are at the end of this section. All the figures assumes the source strength  $S = 1$ .

This ends our discussion of both stresses and displacements in counterphase. Both of these assumptions are rather unrealistic impositions on vibrators and serve only to indicate the possible range of phenomena that can be expected. One outcome of the development of double-couple sources is that shear-wave generation in the vertical direction is not such a strange phenomenon. In the next section we will explore a more reasonable method to investigate the wavefield produced by interacting vibrators.

# P-Wave Radiation Pattern for a Vertical Point Force

Fig. 1.2-5a

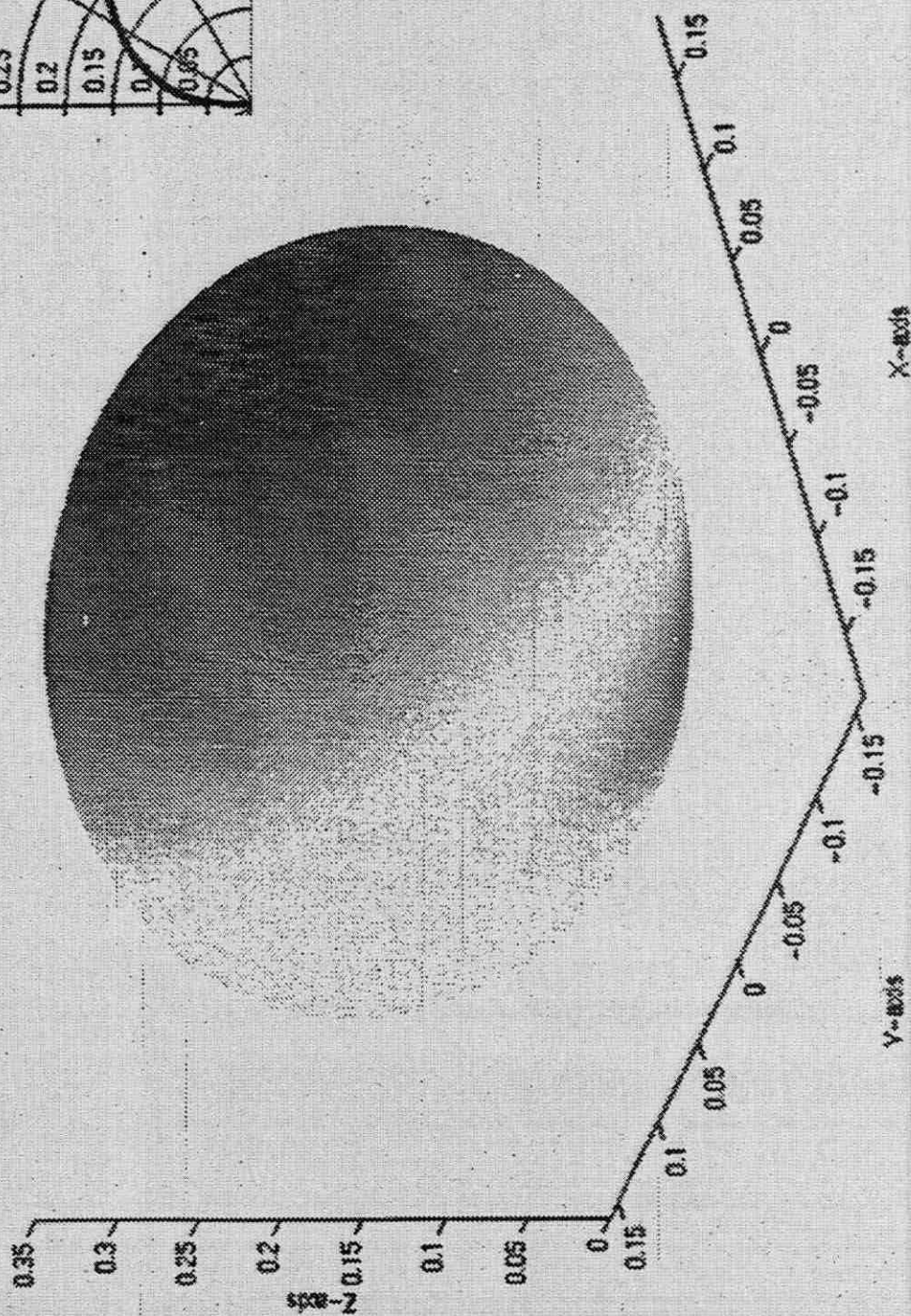
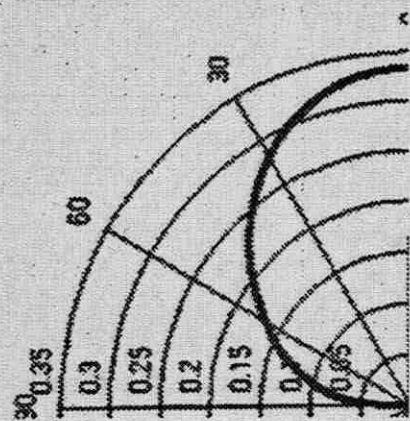


Fig. 1.2-5b S-Wave Radiation Pattern for a Vertical Point Force

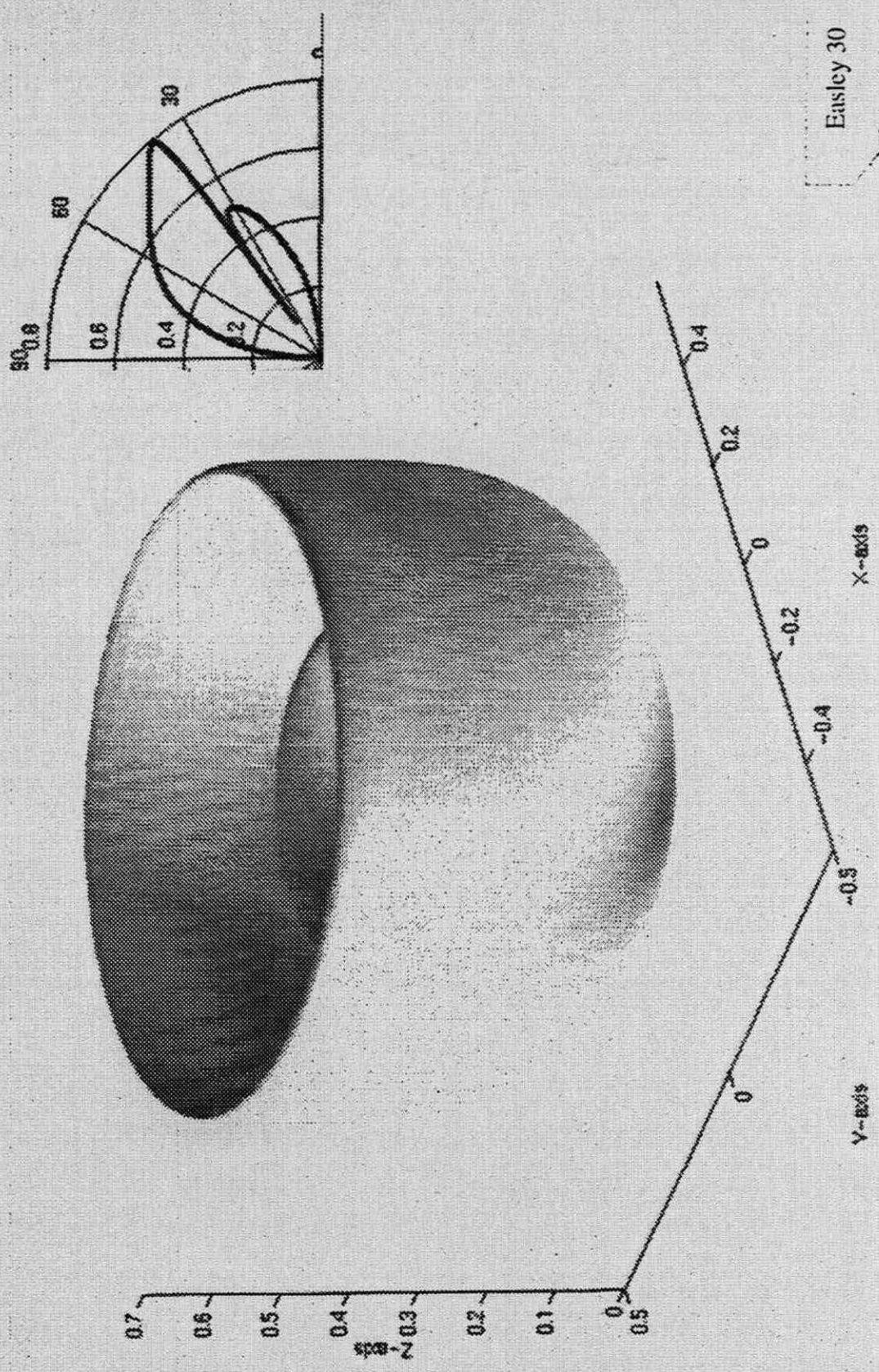


Fig. 1.2-6a P-Wave Radiation Pattern for a Horizontal Point Force

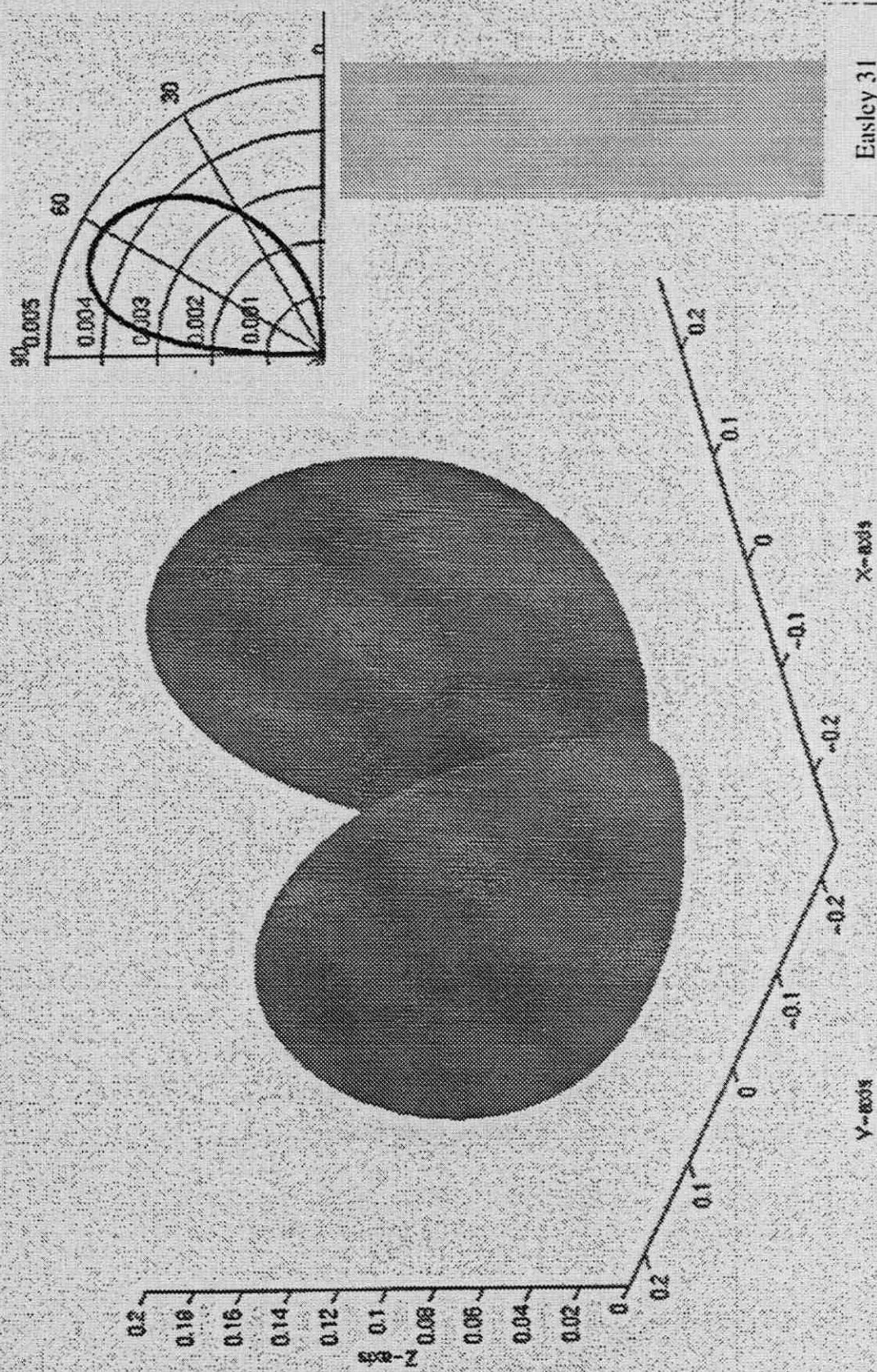


Fig. 1.2-6b

S-Wave Radiation Pattern for a Horizontal Point Force

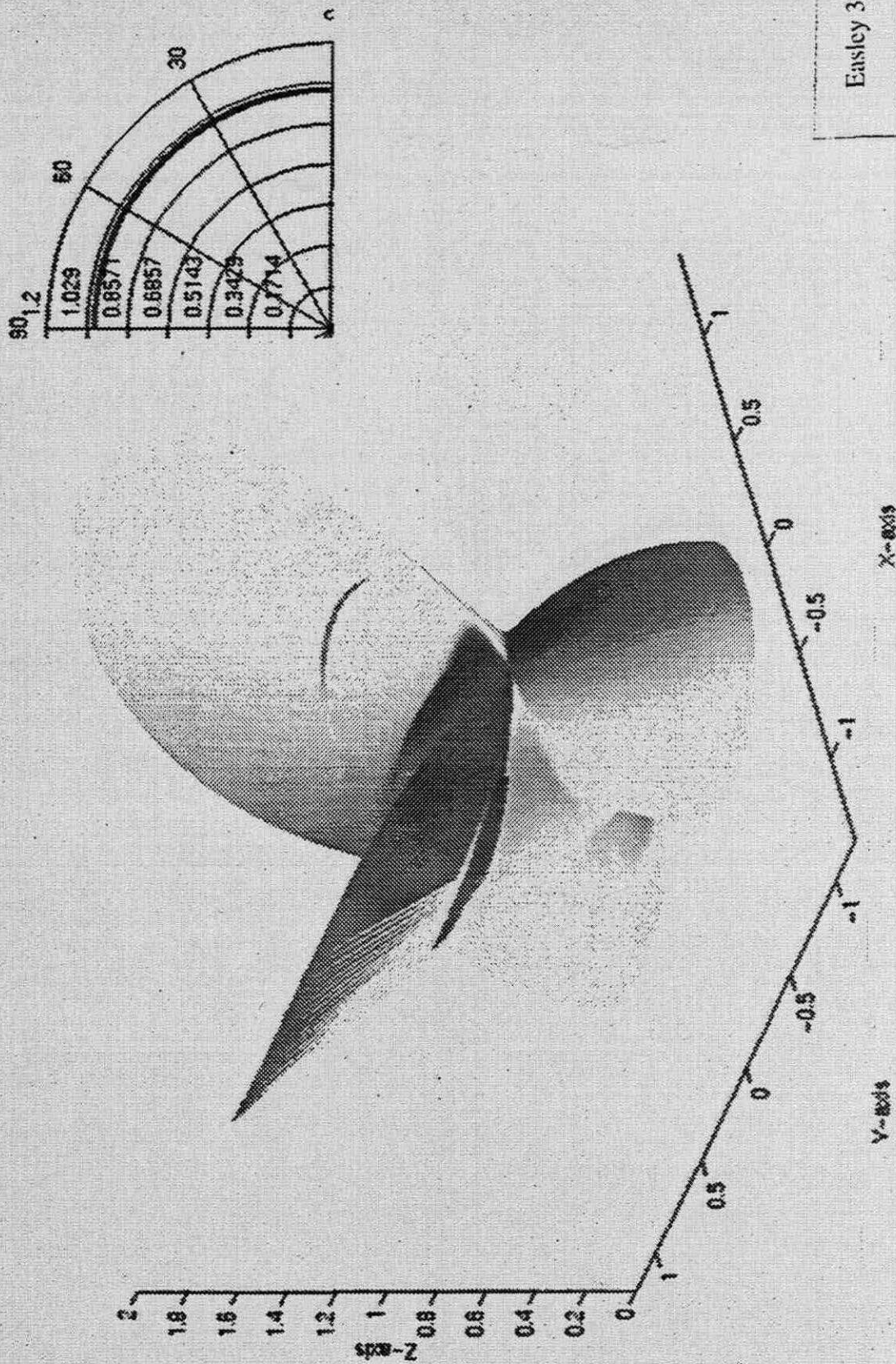


Fig. 1.2-7a

P-Wave Radiation Pattern for a Vertical Couple

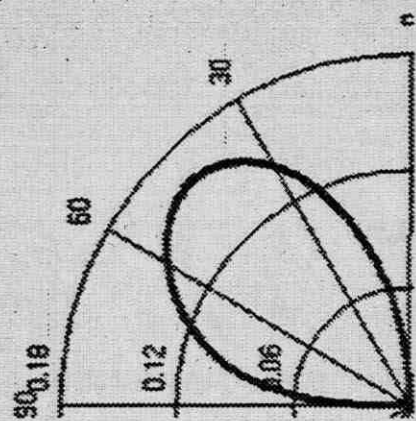
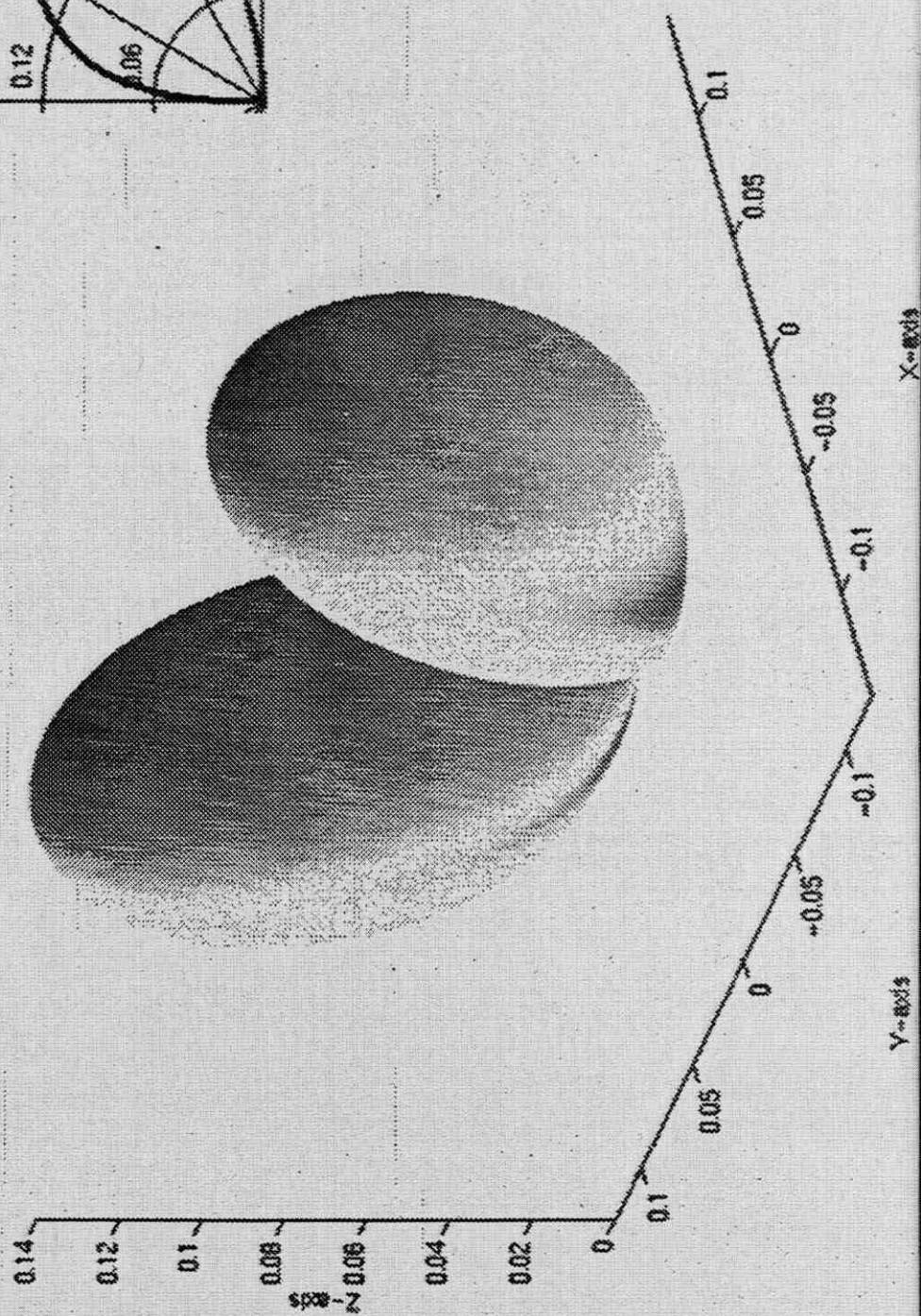


Fig. 1.2-7b

S-wave Radiation Pattern for a Vertical Couple

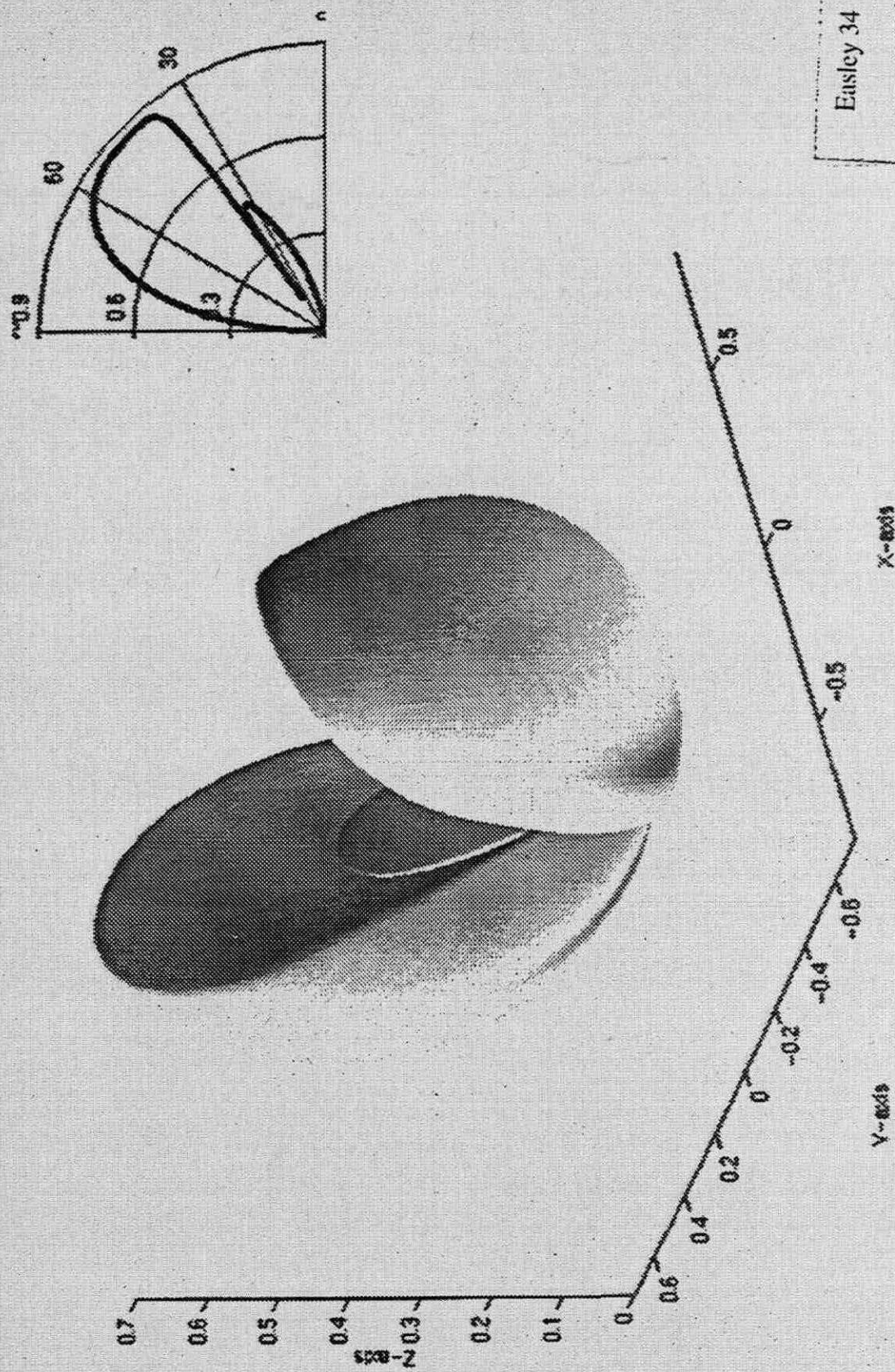


Fig. 1.2-8a | P-Wave Radiation Pattern for a Horizontal Couple

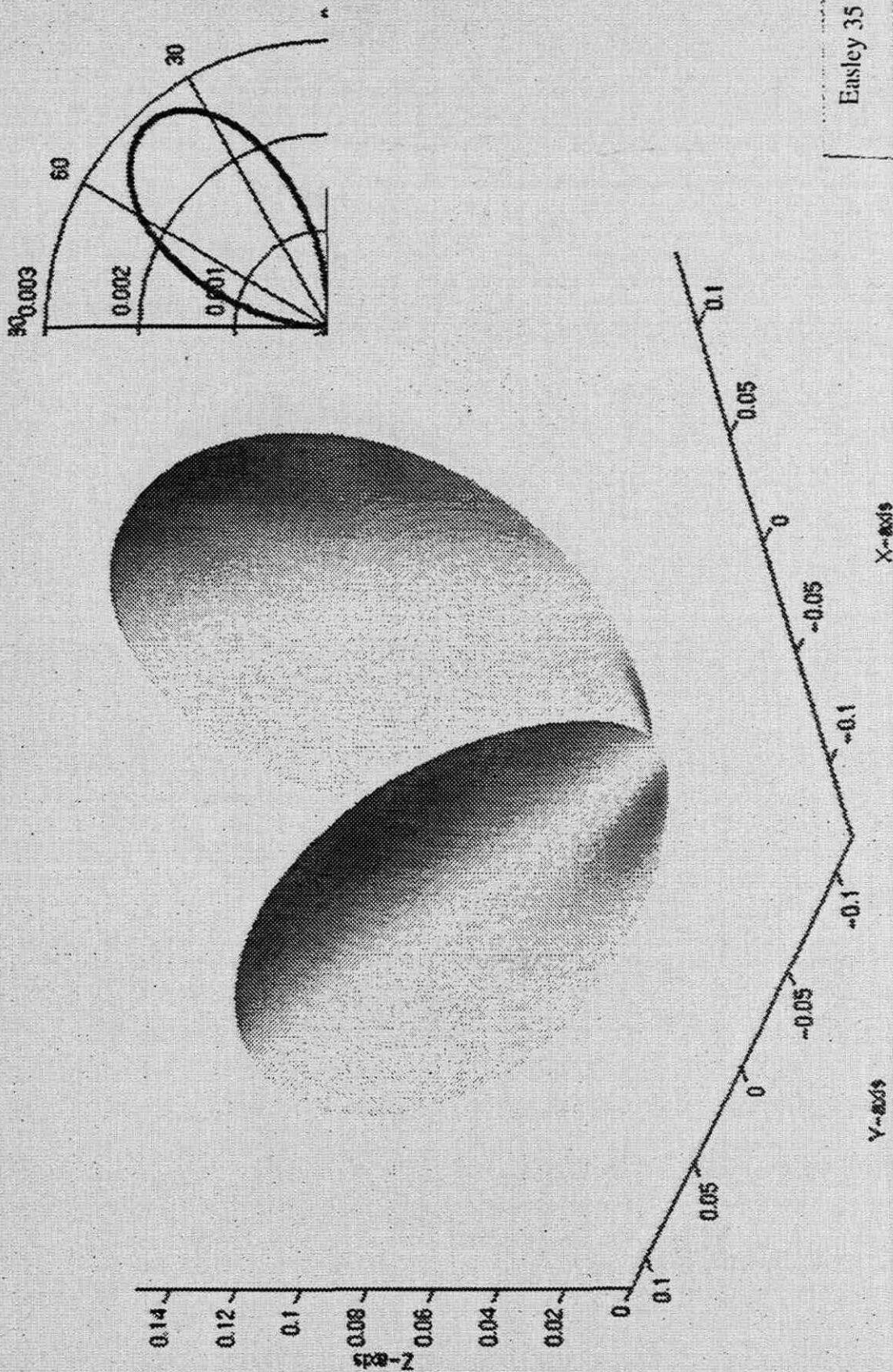


Fig. 1.2-8b

S-Wave Radiation Pattern for a Horizontal Couple

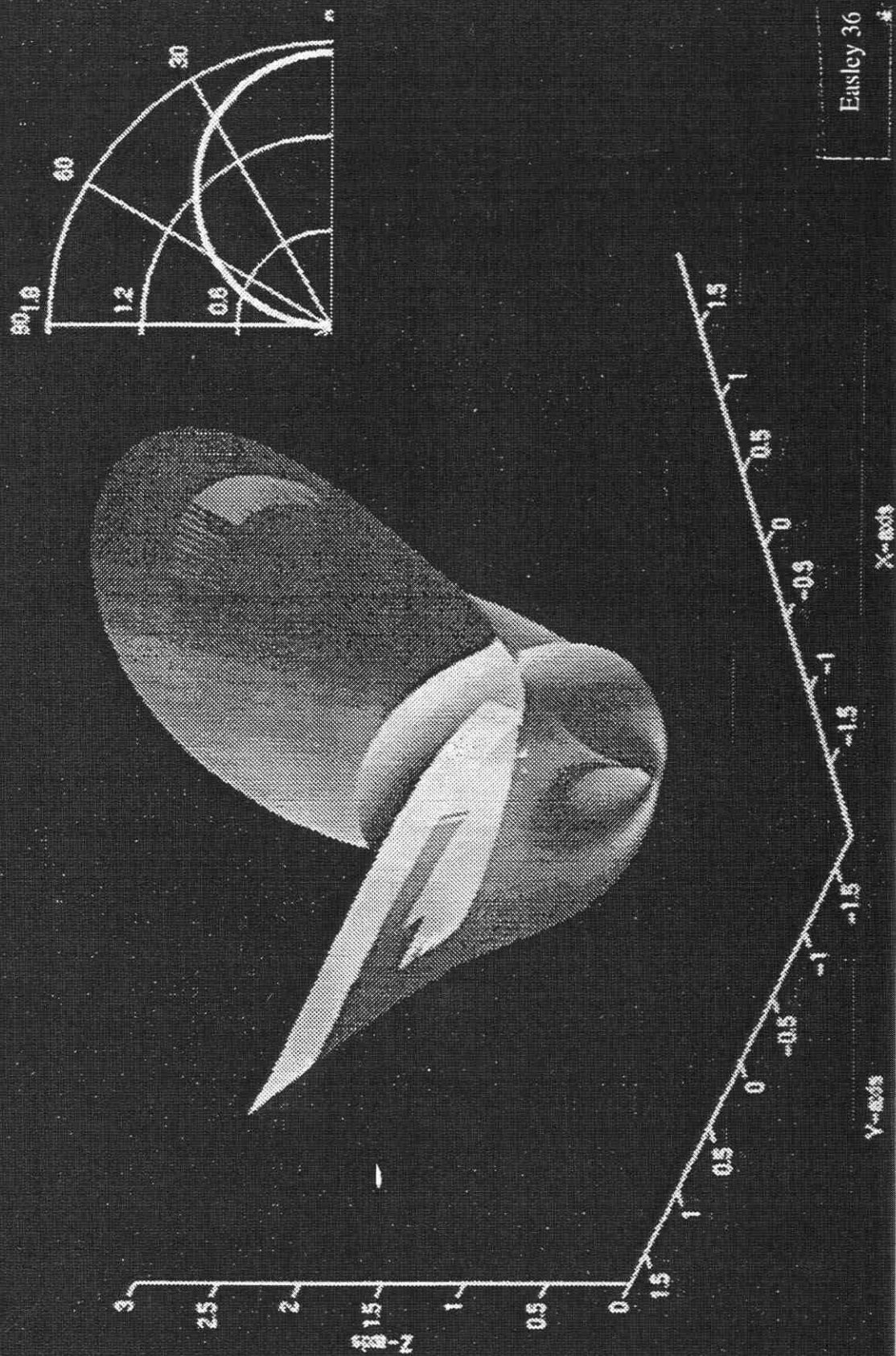


Fig. 1.2-9a

P-Wave Radiation Pattern for a Double Couple

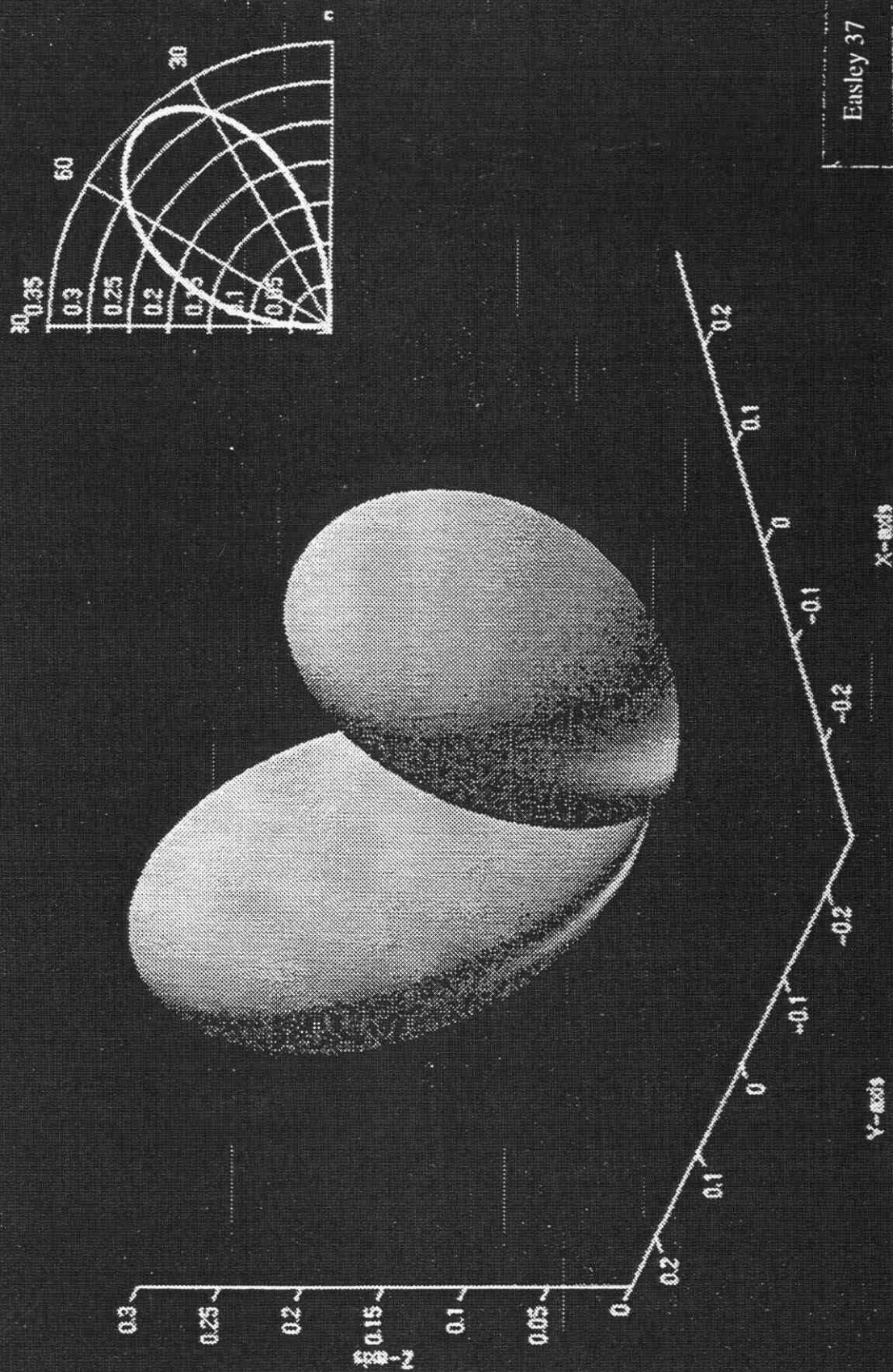
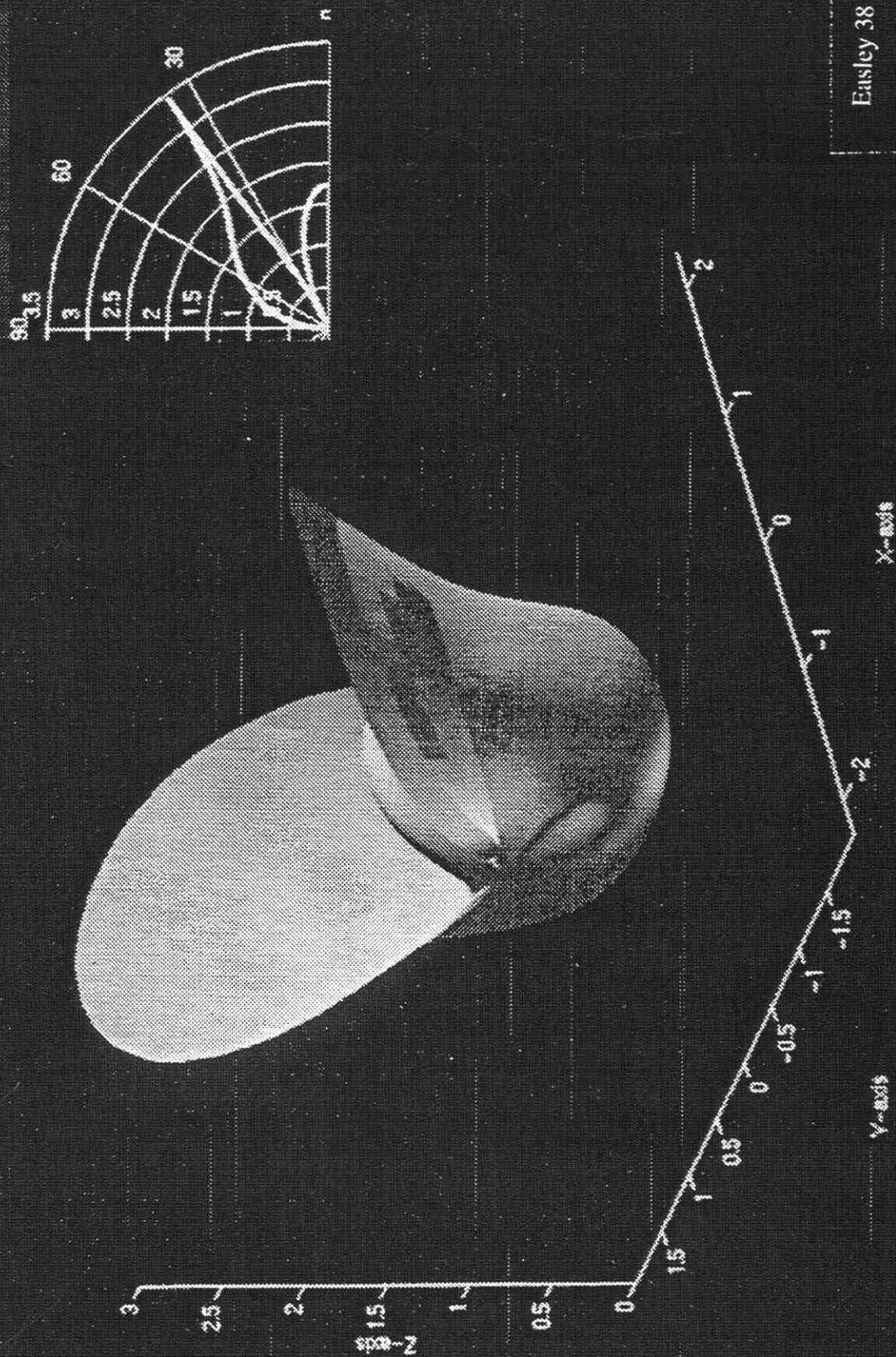


Fig. 1.2-9b

S-Wave Radiation Pattern for a Double Couple



### 1.3 Mixed-phase coupled vibrators

In section 1.2 we made assumptions as to how a pair of vibrators can interact on a free surface. This, as already mentioned, is at best a very crude estimate. In this section I will expand upon a method originated by Tan (1985). As stated in the introduction to this chapter, Tan's (1985) approach consists of fabrication of simple two-dimensional (2-D) mechanical models which are meant to mimic 2-D vibrators. These simple vibrator models are placed parallel to each other on a frictionless surface of an elastic half-space. The coupled system of equations is then solved to find the radiation pattern of the system consisting of the vibrators and the elastic half-space. The radiation patterns calculated by Tan, as with Dankbaar's (1983) analysis, also fail to show the existence of normally incident shear waves. I believe the lack of shear waves in the vertical direction is in part due to the frictionless surface assumption.

I have used a methodology similar to Tan's and derived the coupled equations for a simple vibrator model over an elastic half-space, allowing interactions in all three orthogonal spatial directions. I have made the assumption that plate rotation is negligible and that the vibrators are in welded contact with the surface. With these assumptions, a set of coupled equations is derived that allows the modeling of the wavefield within the elastic half space along with the dynamics of the vibrators.

#### 1.3.1: Fabricating the mechanical model of a vertical vibrator

I will be going into some detail in this section. If the reader only wants the results, it is only necessary to go through the next paragraph and diagram and then proceed to the final equations (1.3.1-30a) - (1.3.1-30c), noting that the displacements of the center of mass of the base plates are, from equilibrium, as defined in equation (1.3.1-3b).

Since I wish to have a mechanical system that is quite simple yet has enough complexity to approximate a real vibrator, I will utilize a spring-mass-dash pot system. Figure 1.3.1-1 represents the system we will be using, with displacements and forces only in the vertical direction shown. Properties in this direction will be denoted by the subscript 3.

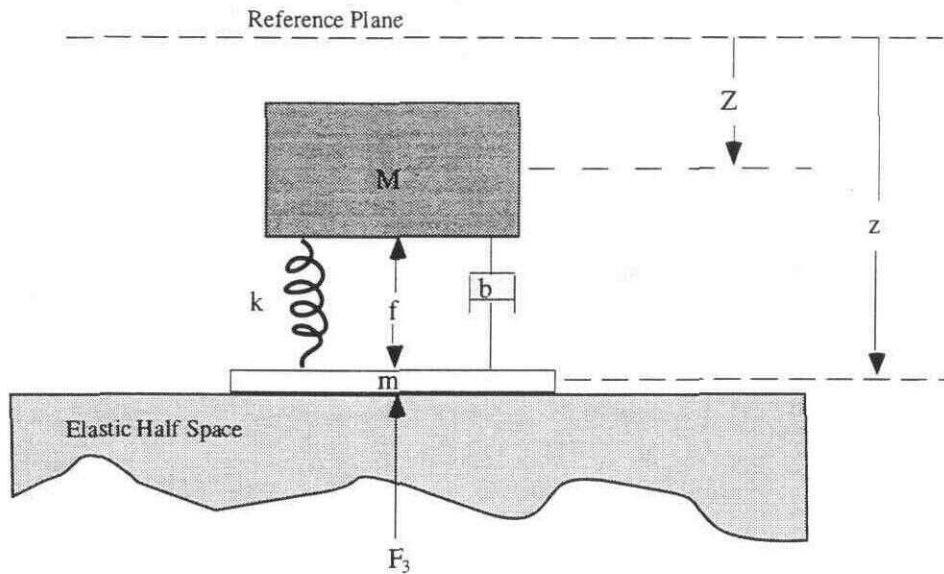


**Fig. 1.3.1-1.** Coupled spring, dashpot and mass model of a vertical vibrator.

In figure 1.3.1-1 we have defined the following symbols as follows:

$M \equiv$  hold-down mass,

$m \equiv$  mass of vibrator plate,

$k \equiv$  spring constant,

$b \equiv$  damping constant of dashpot,

$f \equiv$  force acting between the hold-down mass and the plate,

$F_3 \equiv$  force exerted on the plate by the elastic half-space,

$Z \equiv$  instantaneous position of center of mass of hold-down mass,

$z \equiv$  instantaneous position of center of mass of plate,

$Z^0 \equiv$  equilibrium position of center of mass of hold-down mass,

and  $z^0 \equiv$  equilibrium position of center of mass of plate.

When we first place our lovely vibrator upon the elastic half-space, there is bound to be some initial transient motion on the elastic half-space. This transient motion is

assumed to eventually die out and everything would come to rest unless some other force were applied to the system. When the system has reached this rest state, we will say the system is in equilibrium. In the equilibrium state the centers of mass of the hold-down mass and the plate are in positions  $Z^0$  and  $z^0$ , respectively, from the reference plane as shown in figure 1.2.1. I will assume the system has reached the equilibrium state prior to  $t = 0$ . Since in equilibrium there is no net force acting on the system, the gravitational force due to the hold-down mass and plate must be equal but opposite in direction to the vertical reaction force of the elastic half-space. Let the vertical force supplied by the half-space be  $F_3^0$  when the system is in equilibrium. This means that

$$(M + m)g = -F_3^0, \quad (1.3.1-1a)$$

which is a restatement of the equilibrium condition of this system. The forces in any other two perpendicular directions are assumed to be zero at equilibrium. Symbolically this can be written as:

$$F_1^0 = F_2^0 = 0, \quad (1.3.1-1b)$$

where we have taken the two horizontal directions to be represented by subscripts 1 and 2. The 1, 2, and 3 axes are assumed to form a right-handed rectangular coordinate system. Another relation of the equilibrium state comes from considering the hold-down mass being solely supported by the spring, this means :

$$k(z^0 - Z^0 - L) = -Mg, \quad (1.3.1-2)$$

where  $L$  is the length of the unstressed spring. The equilibrium equations provide a means of testing the dynamic equations that we will develop. When a dynamic force  $f(t)$  is applied between the hold-down mass and plate, the two masses will in general move from their equilibrium positions. Let the vertical displacements from equilibrium of the center of mass of the hold-down mass and of the plate be respectively:

$$U_3 = Z - Z^0, \quad (1.3.1-3a)$$

and

$$u_3 = z - z^0. \quad (1.3.1-3b)$$

As the masses are displaced, the distance between them can change. The change in this distance can be written as:

$$z - Z = u_3 - U_3 + (z^0 - Z^0). \quad (1.3.1-4)$$

Substitution of equation (1.3.1-2) into equation (1.3.1-4) results in:

$$z - Z = u_3 - U_3 - \frac{Mg}{k} + L. \quad (1.3.1-5)$$

As a first step towards developing the coupled system of equations of motion for the two masses, we will consider all the forces acting on each mass individually. The forces acting on the plate are:

$$mg = \text{gravitational force}, \quad (1.3.1-6a)$$

$$-k(z - Z - L) = \text{force due to the spring}, \quad (1.3.1-6b')$$

$$-b(\dot{z} - \dot{Z}) = \text{frictional damping force from the dashpot}, \quad (1.3.1-6c')$$

$$f(t) = \text{applied force between the masses}, \quad (1.3.1-6d)$$

and

$$F_3(t) = \text{force due to the elastic half-space}. \quad (1.3.1-6e)$$

By using equation (1.3.1-5), forces (1.3.1-6b') and (1.3.1-6c') can be put in terms of displacement as:

$$-k(z - Z - L) \rightarrow -k(u_3 - U_3) + Mg, \quad (1.3.1-6b)$$

and

$$-b(\dot{z} - \dot{Z}) \rightarrow -b(\dot{u}_3 - \dot{U}_3). \quad (1.3.1-6c)$$

The corresponding forces acting on the hold-down mass are

$$Mg = \text{gravitational force}, \quad (1.3.1-7a)$$

$$-f(t) = \text{applied force acting between the masses}, \quad (1.3.1-7b)$$

$$k(u_3 - U_3) - Mg = \text{force due to the spring}, \quad (1.3.1-7c)$$

and

$$b(\dot{u}_3 - \dot{U}_3) = \text{frictional damping force from the dashpot}. \quad (1.3.1-7d)$$

Forces (1.3.1-6a) - (1.3.1-6e) and (1.3.1-7a) - (1.3.1-7d), along with Newton's second law, can be used to obtain the equations of motion in the vertical direction for the plate and hold-down mass, respectively, as:

$$\ddot{u}_3 m = (m + M)g + f + F_3 - k(u_3 - U_3) - b(\dot{u}_3 - \dot{U}_3), \quad (1.3.1-8a)$$

and

$$\ddot{U}_3 M = -f + k(u_3 - U_3) + b(\dot{u}_3 - \dot{U}_3). \quad (1.3.1-8b)$$

These dynamic equations reduce to equation (1.3.1-1a) in the static situation, which is a nice check for correctness. The only forces acting in the two horizontal directions are assumed to arise solely from the elastic half space. Let the forces in the 1 and 2 directions from the elastic half-space be respectively  $F_1$  and  $F_2$ . By assuming that the vibrator acts as a solid unit to forces in these directions, which means  $u_1 = U_1$  and  $u_2 = U_2$ , Newton's second law in these directions takes the form:

$$(M + m) \ddot{u}_1 = F_1, \quad (1.3.1-8c)$$

and

$$(M + m) \ddot{u}_2 = F_2. \quad (1.3.1-8d)$$

We have assumed that the vibrator remains vertical throughout the experiment. Taking  $m$  times equation (1.3.1-8b), subtracting  $M$  times equation (1.3.1-8a), and substituting a few variables, we arrive at the following equation:

$$\dot{v} \mu + v b + v k = \Pi, \quad (1.3.1-9)$$

where

$$v = u_3 - U_3,$$

$$\mu = \frac{mM}{m+M},$$

and

$$\Pi = f + \frac{\mu}{m} F_3 + Mg.$$

Equation (1.3.1-9) represents a damped harmonic oscillator with displacement  $v$  and forcing term  $\Pi$ . The first step we take in solving equation (1.3.1-9) is to consider the homogeneous case. The solution of the homogeneous ( $\Pi = 0$ ) form of equation (1.3.1-9) (Symon, 1971) is:

$$v = A e^{-\gamma t} \cos(\omega_1 t + \theta), \quad (1.3.1-10)$$

where  $A$  and  $\theta$  are constants of integration which are to be determined by boundary conditions and  $\omega_1 = \sqrt{\omega_0^2 - \gamma^2}$  in which  $\omega_0 = \sqrt{\frac{k}{\mu}}$  and  $\gamma = \frac{b}{2\mu}$ .

As a second step towards the solution of equation (1.3.1-9), we will find the Green's function  $v_G$  associated with it. The causal Green's function is defined to be the solution of the following problem:

$$\ddot{v}_G \mu + \dot{v}_G b + v_G k = \delta(t - \tau), \quad (1.3.1-11a)$$

such that:

$$-\infty < t, \tau < \infty.$$

By causal, I mean there will be no response until the impulse at  $t = \tau$ . The initial value problem given by equation (1.3.1-11a) can be cast in another form incorporating a jump condition as:

$$\dot{v}_G \mu + \dot{v}_G b + v_G k = 0. \quad (1.3.1-11b)$$

when  $t$  is in the ranges:

$$-\infty < t < \tau, \quad \tau < t < \infty,$$

with the following additional conditions:

$$v_G \text{ continuous at } t = \tau,$$

and

$$\lim_{\varepsilon \rightarrow 0} \dot{v}_G(\tau + \varepsilon) - \dot{v}_G(\tau - \varepsilon) = \frac{1}{\mu}.$$

The causality condition is still enforced. The Green's function for equations (1.3.1-11a) and (1.3.1-11b) (Stakgold, 1979) is:

$$v_G(t, \tau) = H(t - \tau) \frac{e^{-\gamma t}}{\omega_1 \mu} \sin(\omega_1 [t - \tau]) = v_G(t - \tau), \quad (1.3.1-12)$$

where the Heaviside function,  $H(t)$ , is defined to be:

$$H(t) = \begin{cases} 1 & : t > 0 \\ 0 & : t < 0 \end{cases}.$$

Before proceeding to writing down the solution for equation (1.3.1-9) it is necessary to state the following. Equation (1.3.1-9) can be broken into two equations, namely:

$$\dot{v}_1\mu + \dot{v}_1b + v_1k = \pi_1(t) , \quad (1.3.1-13a)$$

and

$$\dot{v}_2\mu + \dot{v}_2b + v_2k = \pi_2 , \quad (1.3.1-13b)$$

with:

$$\pi_1(t) = \frac{\mu}{m} \Delta F_3(t) + f(t) ,$$

and

$$\pi_2 = \frac{\mu}{m} F_3^0 + Mg ,$$

where the force due to the elastic half space  $F_3(t)$  is partitioned into a constant equilibrium restoring force term  $F_3^0$  and a term  $\Delta F_3(t)$  representing a perturbation from equilibrium. This can be represented by:

$$F_3(t) = F_3^0 + \Delta F_3(t) ; \quad (1.3.1-13c)$$

Note that  $F_3^0$  has been defined in equation (1.3.1-1a). Due to the linearity of equation (1.3.1-9) its solution can be written as:

$$v = v_1 + v_2 . \quad (1.3.1-14)$$

By direct substitution of equation (1.3.1-1a) into the definition of  $\pi_2$  in equation (1.3.1-13b) we can see that  $\pi_2$  is identically zero. Since the unique solution of the homogeneous problem with homogeneous initial conditions is the trivial solution, we have:

$$v_2 = 0 . \quad (1.3.1-15)$$

We will use the Green's function of equation (1.3.1-12) to obtain a particular solution of equation (1.3.1-13a). The form of this solution is:

$$v_1(t) = \int_{-\infty}^{\infty} v_G(t - \tau) \pi_1(\tau) dt. \quad (1.3.1-16)$$

If we assume, with no loss of generality, that  $\pi_1$  is zero before  $t = 0$ , we can rewrite equation (1.3.1-16) in the following manner:

$$v_1(t) = \int_0^t \frac{e^{-\gamma[t-\tau]}}{\omega_1 \mu} \sin(\omega_1 [t - \tau]) \pi_1(\tau) dt. \quad (1.3.1-17)$$

Now that we have particular solutions to equations (1.3.1-13a) and (1.3.1-13b), we can use equation (1.3.1-14) to obtain a particular solution to equation (1.3.1-9), then add the solution of the homogeneous equation given by equation (1.3.1-10) to get the general solution of equation (1.3.1-9). The general solution would then be given by:

$$v(t) = \int_0^t \frac{e^{-\gamma[t-\tau]}}{\omega_1 \mu} \sin(\omega_1 [t - \tau]) \pi_1(\tau) d\tau + A e^{-\gamma t} \cos(\omega_1 t + \theta), \quad (1.3.1-18)$$

where  $A$  and  $\theta$  are arbitrary constants to be determined from boundary conditions.

Following the technique above, we shall solve another intermediate problem. By adding equations (1.3.1-8a) and (1.3.1-8b) and defining a few new variables we get:

$$\dot{w} = \lambda(t), \quad (1.3.1-19)$$

where

$$w = u_3 m + U_3 M,$$

and

$$\lambda(t) = (m + M) g + F_3(t).$$

As in the previous differential equation, we begin by solving two related problems. First we solve the associated homogeneous problem given by:

$$\dot{w}_0 = 0; \quad (1.3.1-20)$$

secondly we solve the associated causal Green's problem below:

$$\ddot{w}_G = \delta(t - \tau), \quad (1.3.1-21)$$

such that

$$-\infty < t, \tau < \infty.$$

The general solutions of differential equations (1.3.1-20) and (1.3.1-21) are respectively:

$$w_0 = At + B, \quad (1.3.1-22)$$

and:

$$w_G = H(t - \tau) (t - \tau), \quad (1.3.1-23)$$

where  $H(t)$  is the Heaviside function previously defined, with  $A$  and  $B$  being constants to be determined by boundary conditions. As before, we will now split equation (1.3.1-19) into two separate expressions whose sum, due to the linearity of the equation, is the solution of equation (1.3.1-19). The two expressions are:

$$\ddot{w}_1 = \frac{\lambda_1}{2}, \quad (1.3.1-24a)$$

and

$$\ddot{w}_2 = \lambda_2(t), \quad (1.3.1-24b)$$

where

$$w = w_1 + w_2 \quad \text{and} \quad \lambda(t) = \lambda_1 + \lambda_2(t),$$

such that

$$\lambda_1 = (m + M)g + F_3^0 \quad \text{and} \quad \lambda_2(t) = \Delta F_3(t).$$

Noting that  $\lambda_1$  is identically zero, by equation (1.3.1-1a), particular solutions of equations (1.3.1-24a) and (1.3.1-24b) are respectively:

$$w_1(t) = 0, \tag{1.3.1-25a}$$

and

$$w_2(t) = \int_0^t (t - \tau) \lambda_2(\tau) d\tau. \tag{1.3.1-25b}$$

Equation (1.3.1-25a) can be obtained by inspection of differential equation (1.3.1-24a), while equation (1.3.1-25b) was obtained by using the Green's function of equation (1.3.1-23) in equation (1.3.1-24b). Since  $w = w_1 + w_2$ , we can construct the general solution of equation (1.3.1-19) by adding the general solution of the homogeneous equation,  $w_0(t)$ , to the particular solutions  $w_1(t)$  and  $w_2(t)$ , giving:

$$w(t) = w_2(t) + w_1(t) + w_0(t),$$

or

$$w(t) = \int_0^t (t - \tau) \lambda_2(\tau) d\tau + At + B, \tag{1.3.1-26}$$

where  $A$  and  $B$  are again constants to be determined from boundary conditions. By manipulating the definitions of  $w$  and  $v$  in equations (1.3.1-9) and (1.3.1-19) we can obtain:

$$u_3(t) = \frac{\mu}{m} \left[ \frac{w(t)}{M} + v(t) \right], \tag{1.3.1-27a}$$

and

$$U_3(t) = \frac{\mu}{M} \left[ \frac{w(t)}{m} + v(t) \right]. \quad (1.3.1-27b)$$

Assuming the relatively reasonable initial conditions of  $U_3(0) = u_3(0) = 0$  and  $\dot{U}_3(0) = \dot{u}_3(0) = 0$ , then using equations (1.3.1-18) and (1.3.1-26), we can expand equations (1.3.1-27a) and (1.3.1-27b) to their final forms:

$$u_3(t) = \frac{\mu}{m} \int_0^t \frac{(t-\tau) \lambda_2(\tau)}{M} + \frac{e^{-\gamma[t-\tau]}}{\omega_1 \mu} \sin(\omega_1 [t-\tau]) \pi_1(\tau) d\tau, \quad (1.3.1-28a)$$

and

$$U_3(t) = \frac{\mu}{M} \int_0^t \frac{(t-\tau) \lambda_2(\tau)}{m} + \frac{e^{-\gamma[t-\tau]}}{\omega_1 \mu} \sin(\omega_1 [t-\tau]) \pi_1(\tau) d\tau, \quad (1.3.1-28b)$$

where

$$\pi_1(t) = \frac{\mu}{m} \Delta F_3(t) + f(t),$$

$$\lambda_2(t) = \Delta F_3(t),$$

$$\omega_1 = \sqrt{\omega_0^2 - \gamma^2},$$

in which

$$\omega_0 = \sqrt{\frac{k}{\mu}}, \quad \gamma = \frac{b}{2\mu}, \quad \mu = \frac{mM}{m+M} \quad \text{and} \quad F_3(t) = F_3^0 + \Delta F_3(t).$$

By direct comparison of equations (1.3.1-8c) and (1.3.1-8d) with equation (1.3.1-19), we find that the forms are identical; so we can adapt the solution of equation (1.3.1-19),

given by equation (1.3.1-26), to equations (1.3.1-8c) and (1.3.1-8d). The solutions are respectively:

$$u_1(t) = \int_0^t (t - \tau) \frac{F_1(\tau)}{(M + m)} d\tau, \quad (1.3.1-29a)$$

and

$$u_2(t) = \int_0^t (t - \tau) \frac{F_2(\tau)}{(M + m)} d\tau, \quad (1.3.1-29b)$$

where I have made the assumption of homogeneous initial conditions. We now have a full set of equations for the motion of the vibrator as summarized below:

$$u_1(t) = \int_0^t (t - \tau) \frac{F_1(\tau)}{(M + m)} d\tau, \quad (1.3.1-30a)$$

$$u_2(t) = \int_0^t (t - \tau) \frac{F_2(\tau)}{(M + m)} d\tau; \quad (1.3.1-30b)$$

and

$$u_3(t) = \frac{\mu}{m} \int_0^t \frac{(t - \tau) \Delta F_3(\tau)}{M} + \frac{e^{-\gamma[t - \tau]}}{\omega_1 \mu} \sin(\omega_1 [t - \tau]) \left[ \frac{\mu}{m} \Delta F_3(\tau) + f(\tau) \right] d\tau, \quad (1.3.1-30c)$$

where

$$\omega_1 = \sqrt{\omega_0^2 - \gamma^2},$$

such that

$$\omega_0 = \sqrt{\frac{k}{\mu}}, \quad \gamma = \frac{b}{2\mu},$$

$$\mu = \frac{mM}{m+M},$$

and

$$F_3(t) = F_3^0 + \Delta F_3(t).$$

As can be seen from equations (1.3.1-30a), (1.3.1-30b) and (1.3.1-30c), the displacement of the vibrator plate is inextricably linked to the forces of the elastic half-space  $F_1(\tau)$ ,  $F_2(\tau)$ , and  $F_3(\tau)$ . In order to complete the characterization we must have a description of the deformation and stresses within the elastic half space due to the displacements  $u_1(t)$ ,  $u_2(t)$ , and  $u_3(t)$  of the plate. To accomplish this, we turn to the representation theorem (Aki and Richards, 1980) which can be used to relate the displacement field throughout the elastic half-space to sources within a given volume of the half-space, as well as on the surface of that volume.

### 1.3.2: Getting the elastic half-space involved

As mentioned, we now need to couple the base plates through the elastic half-space; this is the topic of this section. We begin by considering a group of  $N$  vibrators, the  $i$ th element of which has base-plate displacement characterized by:

$$u_j^i(t) : i = 1, 2, \dots, N \text{ and } j = 1, 2, 3, \quad (1.3.2-1a)$$

where subscript  $j$  indicates three orthogonal components. These base plates are situated on surface elements:

$$S_i(t) : i = 1, 2, \dots, N. \quad (1.3.2-1b)$$

It is assumed that the three displacements given by equation (1.3.2-1a) completely describe the motion of the base plate and the half-space under the base plate, with which

it is in welded contact. This rather severe restriction can be partially justified in the following manner.

By a rigid plate we have reduced the possible deformations to just a rotation and displacement. In two dimensions a rotation and translation can be written in matrix form as:

$$\begin{bmatrix} X \\ Y \end{bmatrix} = \begin{bmatrix} \cos(\theta) & -\sin(\theta) \\ \sin(\theta) & \cos(\theta) \end{bmatrix} \begin{bmatrix} x \\ y \end{bmatrix} + \begin{bmatrix} u_x \\ u_y \end{bmatrix} \quad (1.3.2-2a)$$

where  $x$  and  $y$  are the coordinates of a point before deformation while  $X$  and  $Y$  are the coordinates of the same point after a rotation by angle  $\theta$  and displacements in the  $x$  and  $y$  direction given by  $u_x$  and  $u_y$  respectively. If the rotation  $\theta$  is small compared to unity, then we can use small-angle approximations to rewrite equation (1.3.2-2a) as:

$$\begin{aligned} \begin{bmatrix} X \\ Y \end{bmatrix} &\approx \begin{bmatrix} 1 & 0 \\ 0 & 1 \end{bmatrix} \begin{bmatrix} x \\ y \end{bmatrix} + \begin{bmatrix} u_x \\ u_y \end{bmatrix} \\ &= \begin{bmatrix} x \\ y \end{bmatrix} + \begin{bmatrix} u_x \\ u_y \end{bmatrix} \end{aligned} \quad (1.3.2-2b)$$

where only the translational/displacement term has survived the approximation. This restriction, however, is not crucial to our development; it only serves to simplify developments to follow. The forces  $F_1^i$ ,  $F_2^i$  and  $F_3^i$  due to the half-space acting on the  $i$ th base plate results from the stresses set up in the elastic half-space, either by self-interaction, interaction with the other vibrators, stresses due to other external or internal sources, or any combination of these. If we represent the stress field in the elastic half-space by  $\sigma_{ij}$ , the forces acting on the individual base plates can be represented as:

$$F_j^i(t) = \int_{S_i} \sigma_{jk} n_k dS \quad (1.3.2-3)$$

where  $n_k$  is the outward normal of the surface  $S$  of which  $S_i$  is a part. The surface  $S$ , together with volume  $V$ , encompasses all sources of the half-space. Figure (1.3.2-2) shows this in two dimensions. The surface  $S$  and the volume  $V$  can be extended to cover all of the half-space.

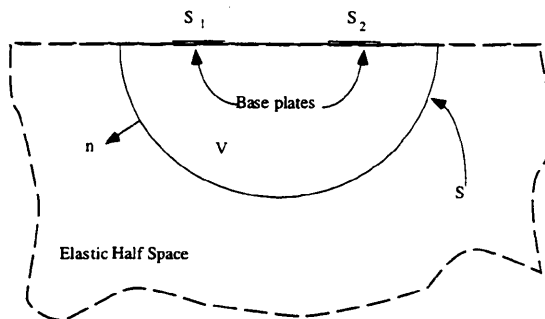


Fig. 1.3.2-2. Source volume in elastic half-space.

We will use the elastic representation theorem (Aki and Richards, 1980) to relate the displacements of the base plates to the displacements observable throughout the elastic half-space. Since the only sources are postulated to be those due to the displacements of the base plates, the appropriate form of the representation theorem would be:

$$u_n(\mathbf{x}, t) = \int_{-\infty}^{\infty} d\tau \int_S u_m(\boldsymbol{\xi}, \tau) c_{mjkl}(\boldsymbol{\xi}) n_j G_{nk,l}(\mathbf{x}, t-\tau; \boldsymbol{\xi}, 0) dS(\boldsymbol{\xi}). \quad (1.3.2-4)$$

where	$\mathbf{u}$	$\equiv$	displacement vector,
	$\mathbf{x}$	$\equiv$	observation point vector,
	$\boldsymbol{\xi}$	$\equiv$	source point vector,
	$G_{nm}(\mathbf{x}, t-\tau; \boldsymbol{\xi}, 0)$	$\equiv$	$n$ th component of the elastodynamic Green's function with unit impulse applied at $\boldsymbol{\xi}$ and time $\tau$ , subject to homogeneous boundary conditions,
	$G_{nk,l}$	$\equiv$	partial derivative of the Green's function with respect to source coordinate $\xi_l$ ,
	$V$	$\equiv$	volume of integration containing source mechanisms,
	$S$	$\equiv$	closed orientable surface containing $V$ ,
	$\mathbf{n}$	$\equiv$	unit outward normal of surface $S$ ,
and	$c_{mjkl}(\boldsymbol{\xi})$	$\equiv$	elastic tensor at source location $\boldsymbol{\xi}$ .

We will be considering only homogeneous isotropic half-spaces so the elastic tensor takes the special form:

$$c_{ijkl} = \lambda \delta_{ij} \delta_{kl} + \mu [\delta_{ik} \delta_{jl} + \delta_{il} \delta_{jk}]. \quad (1.3.2-5)$$

The final connection between the vibrators and the elastic half-space is made through the constitutive relation:

$$\sigma_{ij} = c_{ijkl} \varepsilon_{kl}, \quad (1.3.2-6)$$

where

$$\varepsilon_{kl} = \frac{1}{2} (u_{k,l} + u_{l,k}).$$

Due to the symmetries of the elastic tensor, equation (1.3.2-6) can be written in the following more convenient form:

$$\sigma_{ij} = c_{ijkl} u_{k,l}. \quad (1.3.2-7)$$

Conveniently, we have ready-made solutions for a point force on the free surface for both vertical and horizontal directions. The solutions come from the works of Miller and Pursey (1953) for vertical point forces and Cherry (1962) for horizontal forces. They were calculating the response of an elastic half-space to a vibrating circular disk where the traction under the plate is assumed to be known. They then proceeded to derive the asymptotic expansions to their integral representations. As paraphrased from Cherry (1962), if the amplitude multiplied by the radius of the disk squared remains finite as the radius of the disk approaches zero, then we have the response due to a point force on the free surface. It is just such a response that is needed in equation (1.3.2-4) for the Green's function. It should be noted that the Green's function we are considering also contain surface waves, which are perhaps the stronger agent when we are considering vibrator interactions. This completes the definitions needed to solve the complete set of coupled equations.

### 1.3.3: Procedure to solve the idealized interacting-vibrator problem

So far we have developed a complete set of equations describing the motion of the vibrators, as given by equations (1.3.1-30a) through (1.3.1-30c); however, these

equations are dependent upon the forces the half-space exerts on the vibrators. The equation describing the motion of the half-space is equation (1.3.2-4), which in turn depends on the motion the vibrators. These two sets of equations are related to each other by equations (1.3.2-3) and (1.3.2-7). If we start with the following initial conditions:

$$u_1 = u_2 = u_3 = 0 \quad (1.3.3-1a)$$

for displacements, and

$$F_1^i = F_2^i = 0 \text{ and } F_3^i = F_3^0 \quad (1.3.3-1b)$$

for forces, we can use the coupled equations to solve for all future displacements within the half-space. The actual procedure is most easily implemented by numerical integration and further simplification can be sought by transforming the equations into the frequency domain. The flow-chart in figure 1.3.3-1 shows how the variables are related to each other and indicates how an algorithm may be implemented.

In this section we have derived the set of equations which govern the evolution of a simple vibrator model consisting of a hold-down mass and a base plate joined in series by a spring and dashpot. A set of these simple vibrators were then allowed to interact upon a free surface over an elastic half-space. The equations controlling the dynamics of the elastic half-space were developed. These coupled systems of equations completely describe the wavefield that would be generated by a given set of the simple vibrators in the elastic half-space. The numerical implementation of this scheme would certainly be a wonderful addition to this work but this task is left to the future continuation of this research.

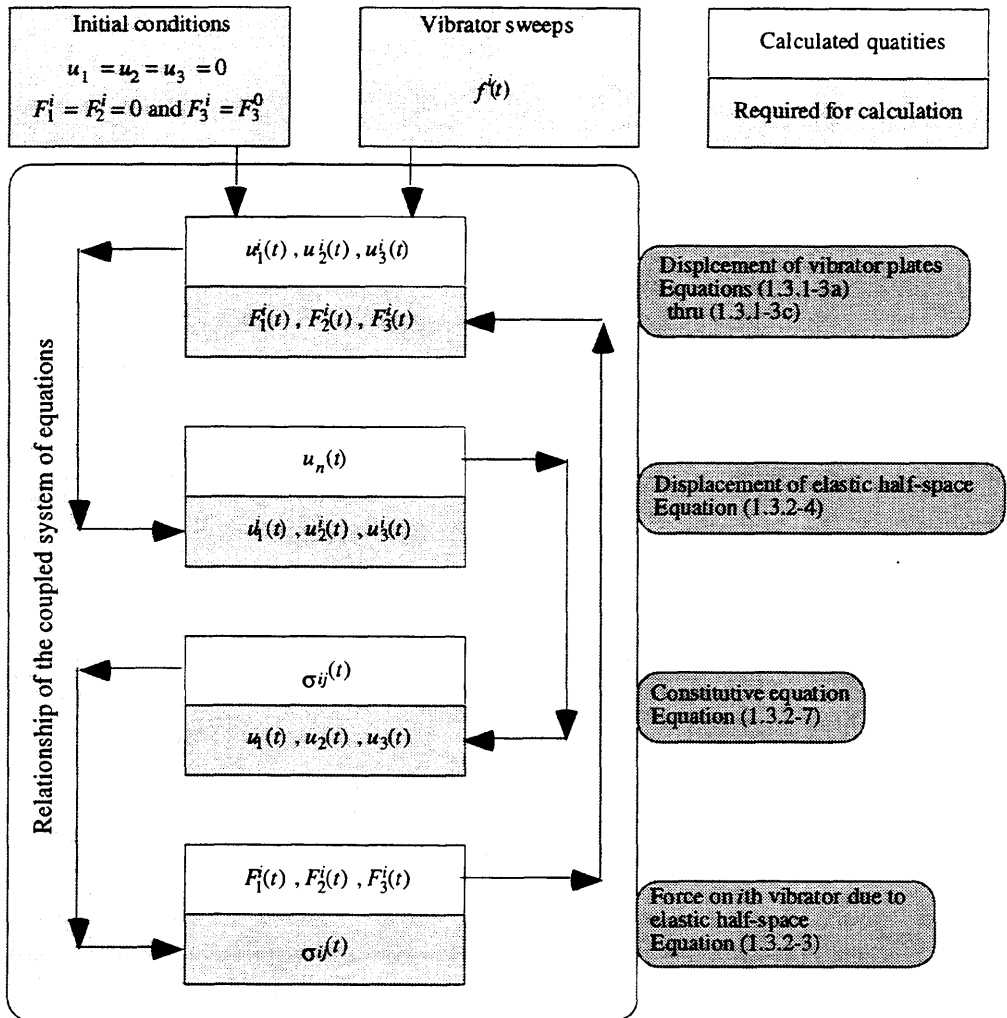


Fig. 1.3.3-1. Flowchart showing how to solve the coupled system of equations.

## **2: Composite media as generalized continua**

### **2.1: The composite earth**

There can be very little disagreement that the earth is not exactly a homogeneous elastic isotropic sphere. It can also be stated that the earth, at most scales of interest, is rather heterogeneous. But given that the earth is a rather complicated object, in particular the earth's crust must be considered to be in this category, we know that some simple mathematical descriptions actually work well as predictive tools. An example of this is the success that the elastic wave equation has had in helping us understand phenomena as diverse as earthquakes as well as seismic sources used in exploration geophysics. If we were to consider each and every detail that is a building block of the earth's crust we would very quickly throw up our hands in despair from the sheer enormity of the problem. Being pragmatic creatures, we tend to start lumping the complexity and describe the lumped object as some simple continuum, such as the simple isotropic elastic media that have already been mentioned. This process is most evident when we treat the earth's crust as a simple series of isotropic elastic layers. Even though this is a gross approximation, we are awarded a certain degree of predictive power. But we know that this is not the whole story since the dispersive nature of all seismograms, or what appear to be anisotropic effects, continuously rears their ugly heads. The subject of this chapter is aimed at finding other dynamic descriptions that take into account more of the internal complexities of the layers or lumps without abandoning the concept that there exists a relatively simple continuum that will help us come to a better understanding of the processes within the actual material that we are investigating.

#### **2.1.1: Where others have gone before and where I have wandered**

Any material that at one scale looks to be homogeneous will at some other scale appear to be heterogeneous, and even possibly discontinuous. To see this, one only needs to acknowledge the existence of molecules and atoms at some scale. Nevertheless, the continuum description has been so successful, and the alternative of describing all the

effects on all the constituent particles so daunting, that we return to the continuum description with little hesitation. Rivlin (1968) showed, through an averaging process, how a system of particles each comprised of different mass points can be described as a generalized continuum and Eringen (1968) showed how to start from a granular composite and reach the same end, which he calls a micromorphic continuum. Bedford's (1985) book showed how to use Hamilton's principle and the additional degrees of freedom of a composite to develop new generalized continuum theories. Generalized continuum theories have a long history; the prototype of this is the Cosserat continuum (Mindlin and Tiersten, 1962). A review of this type of generalized continuum can be found in appendix C. The development in appendix B follows the development of the normal elastic continuum theory as reviewed in appendix C. Both appendix B and C start from assuming knowledge of the forces acting on the medium, unlike the development using Hamilton's principle (Bedford, 1985) where the degrees of freedom in deformation are assumed to be known.

A composite, as considered here, is just a heterogeneous continuum which at some scale will also appear to be homogeneous. The behavior of such a continuum may be quite unique, differing significantly from its constituent parts, at the scale of homogeneity. Backus (1962) looked at a composite of layered isotropic and transversely isotropic media and, through averaging, was able to describe the static behavior of the composite as a transversely isotropic homogeneous medium. Schoenberg and Muir (1989) extended this idea to layers of arbitrary anisotropy by assuming the same averaging method as Backus (1962) and found the static equivalent anisotropic homogeneous medium to the finely layered composite. Others have attempted to use this basically static description to nonzero wavelengths with some success. The dynamic effects such as dispersion of the wavelet, have not been dealt with in these cases. In the next section, I will attempt to generalize Backus's (1962) averaging method, to mathematically develop a generalized continuum theory consistent with this method of averaging and hopefully relax the static or zero-frequency assumption. In §2.3 we will look at more general methods that may lead to future developments.

## **2.2: A perturbation to Backus's averaging method**

Backus (1962) showed a method of averaging a stack of finely layered isotropic or transversely isotropic media to come up with a statically (or long-wavelength)

equivalent transversely isotropic medium. I will borrow his averaging technique and try to generalize it in order to find other forms of dynamic relationships which can be used in the nonstatic cases.

### 2.2.1: Defining the averaging technique

The following averaging scheme was introduced in Backus's (1962) paper. He defined a linear averaging operator in the form:

$$\langle f \rangle(x) = \int_{-\infty}^{\infty} w(\xi - x) f(\xi) d\xi, \quad (2.2.1-1)$$

where

$$w(x) \geq 0, \quad w(\pm\infty) = 0,$$

$$\int_{-\infty}^{\infty} w(x) dx = 1, \quad \int_{-\infty}^{\infty} x w(x) dx = 0 \quad \text{and} \quad \int_{-\infty}^{\infty} x^2 w(x) dx = l^2.$$

Note that I use the notation  $\langle \cdot \rangle$  to represent the average of the quantity within the angular brackets. For functions  $f$  that are approximately constant when  $x$  is varied by no more than  $l$ , Backus used the following approximation:

$$\langle f g \rangle = f \langle g \rangle. \quad (2.2.1-2)$$

As a first step one may generalize equation (2.2.1-1) to  $n$  dimensions by letting  $\mathbf{x}$  represent an  $n$ -dimensional position vector and then recast the linear average as:

$$\langle f \rangle(\mathbf{x}) = \int_{V_{\infty}} w(\xi - \mathbf{x}) f(\xi) dV_{\xi}, \quad (2.2.1-3)$$

such that,

$$w(\mathbf{x}) \geq 0, \quad w(\pm\infty) = 0,$$

$$\int_{V_\infty} w(\mathbf{x}) dV_{\mathbf{x}} = 1, \quad \frac{1}{A_{\mathbf{t}}} \int_{-\infty}^{\infty} x w(x\mathbf{t}) dx = 0,$$

$$\frac{1}{A_{\mathbf{t}}} \int_{-\infty}^{\infty} x^2 w(x\mathbf{t}) dx = l_{\mathbf{t}}^2 \quad \text{and} \quad A_{\mathbf{t}} = \int_{-\infty}^{\infty} w(x\mathbf{t}) dx,$$

where  $\mathbf{t}$  is a unit vector, indicating the direction for which the appropriate property is calculated, and  $V_\infty$  represents the limit as a finite volume  $V_{\mathbf{x}}$  is allowed to expand and cover all space.

Now we attempt to generalize the approximation. Our assumption is, for a neighborhood around  $\mathbf{x}$ , where  $\mathbf{x}$  varies by no more than  $l_{\mathbf{t}}$  in the direction of unit vector  $\mathbf{t}$ , the function  $f$  can be represented by a Taylor's series as follows:

$$f(\mathbf{y}) = f(\mathbf{x}) + f_{,i}(\mathbf{x}) (y^i - x^i) + \frac{1}{2} f_{,ij}(\mathbf{x}) (y^i - x^i) (y^j - x^j) + \dots, \quad (2.2.1-4)$$

where  $y^i$  are the components of vector  $\mathbf{y}$ ,  $x^i$  are the components of vector  $\mathbf{x}$ ,  $f_{,i}$  represents the partial derivative of  $f$  with respect to  $x^i$ , and summation on repeated diagonal indices is enforced. We now turn our attention to the product of the function  $f$  with another function  $g$  and the average of the product:

$$\langle fg \rangle(\mathbf{x}) = \int_{V_\infty} w(\mathbf{y} - \mathbf{x}) f(\mathbf{y}) g(\mathbf{y}) dV_{\mathbf{y}} \quad (2.2.1-5)$$

$$= \int_{V_\infty} w(\mathbf{y} - \mathbf{x}) g(\mathbf{y}) \left[ f(\mathbf{x}) + f_{,i}(\mathbf{x}) (y^i - x^i) + \frac{1}{2} f_{,ij}(\mathbf{x}) (y^i - x^i) (y^j - x^j) + \dots \right] dV_{\mathbf{y}}$$

$$\begin{aligned}
&= f(\mathbf{x})\langle g(\mathbf{x}) \rangle + f_{,i}(\mathbf{x}) \left[ \langle g(\mathbf{x}) x^i \rangle - x^i \langle g(\mathbf{x}) \rangle \right] + \\
&\quad + \frac{1}{2} f_{,ij}(\mathbf{x}) \left[ \langle g(\mathbf{x}) x^i x^j \rangle - x^j \langle g(\mathbf{x}) x^i \rangle - x^i \langle g(\mathbf{x}) x^j \rangle + x^i x^j \langle g(\mathbf{x}) \rangle \right] + \dots
\end{aligned}$$

As can be seen by direct comparison of equation (2.2.1-5) and equation (2.2.1-2), the first term of equation (2.2.1-5) is equation (2.2.1-2). It must be recognized at this point that equation (2.2.1-5) is only accurate as an infinite series and, if we truncate it, the function  $f$  and all its remaining derivatives must be approximated by some averages as well. This point seemed to have been glossed over in Backus's (1962) paper. The use of Taylor-series truncations also entails an assumption of a smooth neighborhood of the function in question.

### 2.2.2: Application to linear elasticity

We will now venture to apply the averaging method that was discussed in the previous section in the realm of linear elasticity. First consider the constitutive relation of a linear elastic material below:

$$\sigma^{ij} = c_{..kl}^{ij} \epsilon^{kl}, \quad (2.2.2-1)$$

keeping in mind the difficulties above. The average of equation (2.2.2-1), by using the first two terms in relation (2.2.1-5), can be written as:

$$\begin{aligned}
\langle \sigma^{ij} \rangle &= \langle c_{..kl}^{ij} \epsilon^{kl} \rangle \\
&= C_{..kl}^{ij} \epsilon^{kl} + B_{..kl}^{ij..m} \epsilon_{..m}^{kl}
\end{aligned} \quad (2.2.2-2)$$

where

$$C_{..kl}^{ij} = \langle c_{..kl}^{ij} \rangle \quad \text{and} \quad B_{..kl}^{ij..m} = \langle c_{..kl}^{ij} x^m \rangle - x^m \langle c_{..kl}^{ij} \rangle.$$

The linear momentum equation in the absence of body forces is:

$$\sigma_{..j}^{ij} - \rho \dot{u}^i = 0. \quad (2.2.2-3)$$

Before considering the average of equation (2.2.2-3), we shall derive a couple of intermediate results. Consider:

$$\langle \sigma_{\dots j}^{ij} \rangle = \int_{V_\infty} w(\xi^i - x^i) \sigma_{\dots j}^{ij}(\xi^i) dV_\xi, \quad (2.2.2-4)$$

which can be cast in another form by the following reasoning:

$$\begin{aligned} \frac{\partial [w(\xi^i - x^i) \sigma_{\dots j}^{ij}(\xi^i)]}{\partial \xi^j} &= \frac{\partial w(\xi^i - x^i)}{\partial \xi^j} \sigma_{\dots j}^{ij}(\xi^i) + w(\xi^i - x^i) \frac{\partial \sigma_{\dots j}^{ij}(\xi^i)}{\partial \xi^j} \\ &= - \frac{\partial w(\xi^i - x^i)}{\partial x^j} \sigma_{\dots j}^{ij}(\xi^i) + w(\xi^i - x^i) \sigma_{\dots j}^{ij}(\xi^i). \end{aligned} \quad (2.2.2-5)$$

When relation (2.2.2-5) is used in equation (2.2.2-4) we have:

$$\begin{aligned} \langle \sigma_{\dots j}^{ij} \rangle &= \int_{V_\infty} \frac{\partial [w(\xi^i - x^i) \sigma_{\dots j}^{ij}(\xi^i)]}{\partial \xi^j} dV_\xi + \int_{V_\infty} \frac{\partial w(\xi^i - x^i)}{\partial x^j} \sigma_{\dots j}^{ij}(\xi^i) dV_\xi \\ &= \int_{S_\infty} [w(\xi^i - x^i) \sigma_{\dots j}^{ij}(\xi^i)] n_j dS_\xi + \frac{\partial}{\partial x^j} \int_{V_\infty} w(\xi^i - x^i) \sigma_{\dots j}^{ij}(\xi^i) dV_\xi \\ &= \langle \sigma_{\dots j}^{ij} \rangle_{,j}, \end{aligned} \quad (2.2.2-6)$$

where we have used the divergence theorem and the fact that  $w$  goes to zero on  $S_\infty$ . We shall now use equation (2.2.1-5) to recast the average of the product of density and particle acceleration as:

$$\langle \rho \ddot{u}^i \rangle = \ddot{u}^i \bar{\rho} + \ddot{u}_{,m}^i \mu^m + \ddot{u}_{,mn}^i v^{mn}, \quad (2.2.2-7)$$

where

$$\bar{\rho} = \langle \rho \rangle, \quad \mu^m = \langle \rho x^m \rangle - x^m \langle \rho \rangle,$$

and

$$v^{mn} = \frac{1}{2} \left( \langle \rho x^m x^n \rangle - x^m \langle \rho x^n \rangle - x^n \langle \rho x^m \rangle + x^m x^n \langle \rho \rangle \right).$$

Note that we have chosen the highest order of spatial differentiation in the displacement in order to be consistent with the terms kept for linear deformation in equation (2.2.2-2). The equation of motion (2.2.2-1) can be averaged in the following manner:

$$\langle \sigma_{..j}^{ij} \rangle - \langle \rho \ddot{u}^i \rangle = 0,$$

which, upon substitution of relations (2.2.2-6) and (2.2.2-7) becomes:

$$\langle \sigma^{ij} \rangle_{,j} - \ddot{u}^i \bar{\rho} - \ddot{u}_{..m}^i \mu^m - \ddot{u}_{..mn}^i v^{mn} = 0. \quad (2.2.2-8)$$

Using equation (2.2.2-2) in equation (2.2.2-8) results in:

$$\left[ C_{..kl}^{ij} \varepsilon^{kl} + B_{..kl}^{ij..m} \varepsilon_{..m}^{kl} \right]_{,j} - \ddot{u}^i \bar{\rho} - \ddot{u}_{..m}^i \mu^m - \ddot{u}_{..mn}^i v^{mn} = 0. \quad (2.2.2-9)$$

Equation (2.2.2-9) can be put into a more useful form by using the following relations:

$$\varepsilon^{kl} = \frac{1}{2} (u^{k,l} + u^{l,k}),$$

$$C_{..kl}^{ij} = C_{..lk}^{ij} \quad \text{and} \quad B_{..kl}^{ij..m} = B_{..lk}^{ij..m},$$

which upon introduction to equation (2.2.2-9) is transformed into:

$$\left[ C^{ijkl} u_{k,l} + B^{ijklm} u_{k,lm} \right]_{,j} - \ddot{u}^i \bar{\rho} - \ddot{u}_{..m}^i \mu^m - \ddot{u}_{..mn}^i v^{mn} = 0. \quad (2.2.2-10)$$

I have been able to gain some headway in deriving equation (2.2.2-10) as a direct consequence of Hamilton's principle as outlined in Bedford's (1985) book. This is an interesting mathematical exercise, but how can we use the new generalized continuum description to give us more information? As a step towards answering that question, we shall look at the simple situation of a plane wave propagating through this medium.

### 2.2.3: A plane-wave solution

Consider the possibility that there exist plane-wave solutions to equation (2.2.2-10) of the following form:

$$u^r = A p^r \exp(i [k_s x^s - \omega t]) = A p^r \exp(i k [n_s x^s - v t]) \quad (2.2.3-1)$$

where

$$\begin{aligned} u^r &\equiv \text{displacement vector,} \\ A &\equiv \text{amplitude,} \\ p^r &\equiv \text{unit polarization vector,} \\ k_s &\equiv \text{propagation vector,} \\ x^s &\equiv \text{spatial coordinate vector,} \\ \omega &\equiv \text{angular frequency,} \\ t &\equiv \text{time,} \\ k &\equiv \text{magnitude of propagation vector } |k| = \sqrt{k_s k^s} \end{aligned}$$

and

$$n_s \equiv \text{unit vector in direction of phase propagation.}$$

On substituting equation (2.2.3-1) in equation (2.2.2-10) and assuming **C** and **B** are constant tensors, we arrive at:

$$\left[ -C_{abcd} k^d k^b - i B_{abcde} k^d k^b k^e + \omega^2 \bar{\rho} \delta_{ac} + i \mu_e k^e \omega^2 \delta_{ac} - v_{ef} k^e k^f \omega^2 \delta_{ac} \right] p^c = 0, \quad (2.2.3-2)$$

where

$$\delta_{ac} \equiv \text{Kronecker delta.}$$

Using the identity  $k^d = k n^d$  we can recast equation (2.2.3-2) in the following form:

$$\left[ v^2 \delta_{ac} - C_{ac}^* \right] p^c = 0, \quad (2.2.3-3)$$

where

$$C_{ac}^* = \frac{\left( C_{abcd} n^d n^b \right) + i \left( k B_{abcde} n^d n^b n^e \right)}{\left( \bar{\rho} - k^2 v_{ef} n^e n^f \right) + i \left( k \mu_e n^e \right)}.$$

In order that equation (2.2.3-3) have nontrivial solutions, the following condition must be satisfied:

$$\det \left[ v^2 \delta_{ac} - C_{ac}^* \right] = 0. \quad (2.2.3-4)$$

Equation (2.2.3-4) is of the form of an eigenvalue problem. The eigenvalues resulting from its solution will be the phase velocities. It is interesting to note that when  $k = 0$ , equation (2.2.3-3) takes on the same form as the velocity equations in standard elastic media. This also means that if we have a finely layered composite we can use Backus's (1962) or Schoenberg and Muir's (1989) averaging scheme to get the elastic constants for  $\mathbf{C}$ . The velocities obtained from equation (2.2.3-4) will in general be complex, indicating attenuation and dispersion are possibilities. Once the eigenvalues are obtained, equation (2.2.3-3) can then be used to solve for the polarization vectors (eigenvectors).

This seems to be a reasonable means to find other dynamic relationships which could be used to describe a composite but it does seem to be a bit ad hoc. In the next section I will discuss a more general method which has the potential to set this direction of investigation on a more solid footing.

### 2.3: Other possible directions for investigation

It is probably a good idea to start from the basic definitions of deformation rather than the short-circuit method we have been using to describe the composite. I will use the Lagrangian, or material, description of motion. The notation I shall use is identical to that used in appendix B. I will describe it again here to avoid too much flipping back and forth.

As our composite continuum is deformed, the individual points of the continuum traverse different paths. If we now identify all the points within our continuum in some fixed reference configuration with a coordinate system, say  $X^I \ni I = 1,2,3$ , then we can track the motion of a particular point, for which we now have a unique label. We will set up another coordinate system to track the instantaneous motion of the labeled point. Let the coordinates of this system be symbolized by  $x^i \ni i = 1,2,3$ . When convenient I will also use vector notation such as  $\mathbf{X} \equiv (X_1, X_2, X_3)$  and  $\mathbf{x} = (x_1, x_2, x_3)$ . The actual motion of a point of concern can be written as

$$x_i = x_i(X_1, X_2, X_3, t), \quad (2.3-1a)$$

or

$$\mathbf{x} = (\mathbf{X}, t). \quad (2.3-1b)$$

Equation (2.3-1b) gives the location of point  $\mathbf{X} \equiv (X_1, X_2, X_3)$  at time  $t$ . If we were to track this same point for a period of time we would have a complete description of the motion of that point. Since we have this description for all points within our continuum, we also have a precise description of the deformation of the continuum. This is a very short summary of the Lagrangian (or material) description of deformation, for a very detailed analysis try volume 2 of the Continuum Physics series edited, and heavily contributed to by Eringen (1975). This is a very complete work and not an easy read.

We could attempt to describe, using equation (2.3-1b), all the motion of all constituent parts of our composite continuum. This, in many practical situations, is not an easy task since there may be many different constituent parts and the associated motion can be quite complex. One way we could proceed is to ask if there is any macroscopic phenomenon which can be observed that is of interest that is not completely tied to all the microscopic fluctuations within the continuum. If the answer is yes, then we can start to look for a mathematical means of isolating this macroscopic effect. A common method that is used assumes that the small fluctuations are random in some sense and tend to average out, so we can look at what happens if we average equation (2.3-1) using the same averaging scheme as in equation (2.2.1-1). When the average is applied we get

$$\langle x_i(\mathbf{X}, t) \rangle = \int_{V_\infty} w(\Xi) x_i(\mathbf{X} - \Xi, t) dV_\Xi, \quad (2.3-2)$$

where the integration is over material coordinates  $\Xi = (\Xi_1, \Xi_2, \Xi_3)$ . If we make the assumption that within the neighborhood specified by the weighting function,  $w$ , we are able to expand equation (2.3-1) as a Taylor's series around the material point  $\mathbf{X}$ , then we can write

$$x^i(\mathbf{X} - \Xi) = x^i(\mathbf{X}) + x^i_{,j}(\mathbf{X}) \Xi^j + \frac{1}{2} x^i_{,KL}(\mathbf{X}) \Xi^K \Xi^L + \dots, \quad (2.3-3)$$

where I have deliberately left out the explicit dependence on time,  $t$ . This is done to simplify the equation, and from this point, I will leave out the explicit dependence of the material point  $\mathbf{X}$ , since it is understood to be present as well. Substitution of equation (2.3-3) into equation (2.3-2) results in:

$$\begin{aligned} \langle x^i \rangle &= x^i + x^i_{,J} \int_{V_{\Xi}} w(\Xi) \Xi^J dV_{\Xi} + x^i_{,KL} \frac{1}{2} \int_{V_{\Xi}} w(\Xi) \Xi^K \Xi^L dV_{\Xi} + \dots \\ &= x^i + x^i_{,J} L1^J + x^i_{,KL} L2^{KL} + \dots, \end{aligned} \quad (2.3-4a)$$

where I have defined

$$L1^J = \int_{V_{\Xi}} w(\Xi) \Xi^J dV_{\Xi} \quad (2.3-4b)$$

and

$$L2^{KL} = \frac{1}{2} \int_{V_{\Xi}} w(\Xi) \Xi^K \Xi^L dV_{\Xi}. \quad (2.3-4c)$$

It is not too surprising that we can express the average of the motion as a function of the actual motion and its partial derivatives, but what we would like is the opposite; namely, the actual motion as a function of its average and the partial derivatives of its average. Towards this end we begin by taking the partial derivative of equation (2.3-4a) with respect to  $X_L$  and form a product with  $L1^L$ , which, with judicious change of dummy variables, allows us to write:

$$\langle x^i \rangle_{,J} L1^J = x^i_{,J} L1^J + x^i_{,JK} L1^J L1^K + x^i_{,JKL} L2^{JK} L1^L + \dots \quad (2.3-5a)$$

Upon subtracting equation(2.3-5a) from equation (2.3-4a)we arrive at:

$$\langle x^i \rangle - \langle x^i \rangle_{,J} L1^J = x^i + x^i_{,JK} (L2^{JK} - L1^J L1^K) + x^i_{,JKL} (L3^{JKL} - L2^{JK} L1^L) + \dots \quad (2.3-5b)$$

By repeating the process that gave us equations (2.3-5a) and (2.3-5b) we are able to bring all the averaged quantities to the left-hand side of the equation and leave only  $x^i$  on the right-hand side. We will go one step further to solidify the process. We will now take the second derivative of equation (2.3-4a) with respect to  $X_J$  and  $X_K$ , then form a product with  $(L2^{JK} - L1^J L1^K)$ . Again with judicious change of dummy variables, we get:

$$\langle x^i \rangle_{,JK} (L2^{JK} - L1^J L1^K) = x^i_{,JK} (L2^{JK} - L1^J L1^K) + x^i_{,JKL} L1^L (L2^{JK} - L1^J L1^K) + \dots \quad (2.3-6a)$$

Mirroring the step that gave us equation (2.3-5b), we subtract equation (2.3-6a) from equation (2.3-5b) to arrive at:

$$\langle x^i \rangle - \langle x^i \rangle_{,J} L1^J - \langle x^i \rangle_{,JK} (L2^{JK} - L1^J L1^K) = x^i + x^i_{,JKL} + x^i_{,JKL} [(L3^{JKL} - L2^{JK} L1^L) - L1^L (L2^{JK} - L1^J L1^K)] + \dots \quad (2.3-6b)$$

By repeated application of the process we arrive at:

$$x^i = \langle x^i \rangle + \langle x^i \rangle_{,J} \Lambda 1^J + \langle x^i \rangle_{,JK} \Lambda 2^{JK} + \langle x^i \rangle_{,JKL} \Lambda 3^{JKL} + \dots, \quad (2.3-7a)$$

where

$$\Lambda 1^J = -L1^J, \quad (2.3-7b)$$

$$\Lambda 2^{JK} = -(L2^{JK} - L1^J L1^K), \quad (2.3-7c)$$

$$\Lambda 3^{JKL} = -[L3^{JKL} - 2 L2^{JK} L1^L + L1^J L1^K L1^L], \quad (2.3-7d)$$

and so on. Equation (2.3-7a) tells us that the averages and their gradients have the potential to tell us about the actual motion. This means that meaningful dynamic relations can be derived from the averaged quantities and their gradients. One possible method is to truncate equations (2.3-7a) and substitute these into dynamic equations derived from  $x^i$ . Another more direct method is to assume that, in a composite the individual terms  $\langle x^i \rangle$ ,  $\langle x^i \rangle_{,J}$ ,  $\langle x^i \rangle_{,JK}$ , and so on, represent independent degrees of freedom, insert them into Lagrange's equation, and see what types of dynamic relations result from Hamilton's principle as outlined in Bedford's (1985) book.

There seem to be many avenues to investigate and many have been tried with mixed results. There is even an entire book by Christensen (1979) on this very subject but there is a lot of room for additional work. I believe that whole area of generalized continua has only seen cursory application in geophysics, such as in Biot mixtures (Biot, 1956). Perhaps the phenomena we will be investigating are second-order type effects; but from the lack of success of some of our standby methods to many real problems it is well

worth investigating. Real problems aside, the subject has enough depth to provide ample mental challenge for anyone with the interest.

### 3: Elastic tensors and their preferred frames of reference

#### 3.1: A brief review

Even though tensors have an existence independent of what frame we choose to represent them in, it is inevitable that we need to utilize the numbers representing the tensor in some particular frame of reference. The elastic tensor is no exception; if we choose the wrong frame of reference, the tensor components will in general all be nonzero, a situation that is cumbersome to work with, even though correct. If we choose the preferred frame, we gain two things: minimization of dependent nonzero elements and information as to the symmetry orientation represented by the elastic tensor. In real experiments where elastic constants are inverted from group- or phase-velocity measurements (Vestrum, Brown and Easley, 1996), we may not be fortunate enough to know exactly what the preferred frame is or even to what symmetry class the material, from which we took measurements, belongs. In this situation, when confronted by a bunch of elastic constants, a method to determine the preferred frame from these would be invaluable. I propose to approach the problem in a statistical manner (Easley and Brown, 1992, Easley, 1993b).

Many people have devised means to take an elastic tensor represented in an arbitrary frame and determine the symmetry properties of the underlying tensor. Most notable is the work of Backus (1970) who decomposed the representation of the elastic tensor to a series of vector bouquets and showed that, by direct observation of the symmetry of these bouquets, one can determine the symmetry of the underlying tensor. A second method is described by Baerheim (1993). He notes that the symmetric mapping of the asymmetric part of the representation of the elastic tensor is diagonal in the preferred frame of reference for all crystal classes except triclinic, monoclinic and trigonal cases. Thus the diagonalization of this matrix will yield eigenvectors that should represent the preferred coordinate system.

These are both good methods with some points which can be built upon. The method of Backus requires visual inspection, which can probably be automated, and there

is no work which shows how stable the technique is to small perturbations. The method of Baerheim is direct but is not universally applicable, and I have not seen the effects of small perturbations on this method. Thus I propose to study a statistical method that should be universal and, by its statistical nature, not sensitive to small perturbations. It is a good idea to have a good concept of how to deal with tensors and frames before proceeding to methods; so I will quickly review these aspects.

### 3.1.1: Preliminary mathematical considerations

We will use the definition that a tensor  $\mathbf{T}$  of order  $m$  is a multilinear functional on an  $n$ -dimensional vector space  $V_n$  equipped with an inner product  $(\cdot, \cdot)$ . These are all abstract quantities, which is the definition used by Backus (1970). The properties of  $\mathbf{T}$  are determined by choosing an arbitrary set of  $m$  vectors from  $V_n$  such as  $\{\mathbf{v}_1, \mathbf{v}_2, \dots, \mathbf{v}_m\}$ , and examining the scalar defined by  $\mathbf{T}(\mathbf{v}_1, \mathbf{v}_2, \dots, \mathbf{v}_m)$  and doing this for all sets of vectors  $\{\mathbf{v}_1, \mathbf{v}_2, \dots, \mathbf{v}_m\}$ . This method, though correct, is a rather daunting task. In practice, we choose an orthonormal basis in  $V_n$ , say  $\{\mathbf{x}_1, \mathbf{x}_2, \dots, \mathbf{x}_n\}$ , then represent the vectors above as  $\mathbf{v}_i = (\mathbf{v}_i, \mathbf{x}_j) \mathbf{x}_j$  for  $i = 1, \dots, m$ , summation on repeated indices being in effect. This convention differs from other sections by the fact that the indices do not have to be in a diagonal position for summation to be implied. This should be no problem since we will deal only with orthonormal basis throughout this section. With this in mind we can write:

$$\mathbf{T}(\mathbf{v}_1, \mathbf{v}_2, \dots, \mathbf{v}_m) = (\mathbf{v}_1, \mathbf{x}_{j_1})(\mathbf{v}_2, \mathbf{x}_{j_2}) \cdots (\mathbf{v}_m, \mathbf{x}_{j_m}) \mathbf{T}(\mathbf{x}_{j_1}, \mathbf{x}_{j_2}, \dots, \mathbf{x}_{j_m}), \quad (3.1.1-1)$$

where we have relied heavily on the multilinearity of  $\mathbf{T}$ , that is for any set of  $m$  scalars  $\{\alpha_1, \alpha_2, \dots, \alpha_m\}$  we have:  $\mathbf{T}(\alpha_1 \mathbf{v}_1, \alpha_2 \mathbf{v}_2, \dots, \alpha_m \mathbf{v}_m) = \alpha_1 \alpha_2 \cdots \alpha_m \mathbf{T}(\mathbf{v}_1, \mathbf{v}_2, \dots, \mathbf{v}_m)$ .

To cast equation (3.1.1-1) in a more familiar form, we can define the following scalars:

$$T_{j_1 j_2 \dots j_m} = \mathbf{T}(\mathbf{x}_{j_1}, \mathbf{x}_{j_2}, \dots, \mathbf{x}_{j_m}), \quad (3.1.1-2a)$$

$$v_1^{j_1} = (\mathbf{v}_1, \mathbf{x}_{j_1}), \quad (3.1.1-2b)$$

$$v_2^{j_2} = (\mathbf{v}_2, \mathbf{x}_{j_2}), \quad (3.1.1-2c)$$

⋮

$$v_m^{j_m} = (\mathbf{v}_m, \mathbf{x}_{j_m}) . \quad (3.1.1-2d)$$

The scalar on the left-hand side of equation (3.1.1-2a) is just the commonly used tensor component. The scalars on the left-hand sides of equations (3.1.1-2b)-(3.1.1-2d) are the components of the vectors. All of these scalars are defined only with respect to the basis we choose. Thus equation (3.1.1-1) can be rewritten with the aid of definition (3.1.1-2) as:

$$\mathbf{T}(\mathbf{v}_1, \mathbf{v}_2, \dots, \mathbf{v}_m) = v_1^{j_1} v_2^{j_2} \dots v_m^{j_m} T_{j_1 j_2 \dots j_m} . \quad (3.1.1-3)$$

Now consider the case when we have a different orthonormal basis  $\{\tilde{\mathbf{x}}_1, \tilde{\mathbf{x}}_2, \dots, \tilde{\mathbf{x}}_n\}$ . Then definition (3.1.1-2) and equation (3.1.1-3) give us:

$$\mathbf{T}(\tilde{\mathbf{x}}_{i_1}, \tilde{\mathbf{x}}_{i_2}, \dots, \tilde{\mathbf{x}}_{i_m}) = \tilde{T}_{i_1 i_2 \dots i_m} = \tilde{x}_{i_1}^{j_1} \tilde{x}_{i_2}^{j_2} \dots \tilde{x}_{i_m}^{j_m} T_{j_1 j_2 \dots j_m} , \quad (3.1.1-4a)$$

where

$$\tilde{x}_i^j = (\tilde{\mathbf{x}}_i, \mathbf{x}_j) , \quad (3.1.1-4b)$$

are just the direction cosines relating one frame to the other. Equation (3.1.1-4) shows that the components of a tensor can be quite different from one frame to the other, and this equation also provides a means of going from one to the other. The elastic tensor is no different. Its components are directly related in the same fashion to the frame of reference we choose to express it in. This is all the mathematics we need in order to develop the statistical technique that follows.

### 3.2: Statistical determination of elastic tensor's preferred frame

I will use the standard two-index notation for all the development. All bold-face capital letters will represent the tensor which underlies the matrix representation. It should be noted, that the matrix notation is only a short-hand used to list all the possible independent components of an elastic tensor and not the tensor itself. In other words, one must not confuse the matrix with the tensor itself. If one has this clearly in mind, then

equalities, such as the one in equation (3.2-5), should not confuse the reader. A reference for the two-index notation can be found in Baerheim's (1993) paper. I will be developing the idea for an elastic tensor of the cubic symmetry class. The ideas are easily transferred to other symmetry classes. The cubic elastic tensor represented in the preferred frame of reference has the following form in two-index notation:

$$\mathbf{C} = \begin{bmatrix} C_{11} & C_{12} & C_{12} & 0 & 0 & 0 \\ C_{12} & C_{11} & C_{12} & 0 & 0 & 0 \\ C_{12} & C_{12} & C_{11} & 0 & 0 & 0 \\ 0 & 0 & 0 & C_{44} & 0 & 0 \\ 0 & 0 & 0 & 0 & C_{44} & 0 \\ 0 & 0 & 0 & 0 & 0 & C_{44} \end{bmatrix}, \quad (3.2-5)$$

where  $C_{ij}$  are the elastic stiffness coefficients. This shows that the cubic elastic tensor has only three independent elements. Now consider the same tensor in some arbitrary frame of reference. In general its representation will no longer be as simple in appearance as equation (3.2-5) but will have many nonzero entries as:

$$\mathbf{C}' = \begin{bmatrix} A_{11} & A_{12} & A_{13} & A_{14} & A_{15} & A_{16} \\ A_{12} & A_{22} & A_{23} & A_{24} & A_{25} & A_{26} \\ A_{13} & A_{23} & A_{33} & A_{34} & A_{35} & A_{36} \\ A_{14} & A_{24} & A_{34} & A_{44} & A_{45} & A_{46} \\ A_{15} & A_{25} & A_{35} & A_{45} & A_{55} & A_{56} \\ A_{16} & A_{26} & A_{36} & A_{46} & A_{56} & A_{66} \end{bmatrix}, \quad (3.2-6)$$

where I have included a prime above  $\mathbf{C}$  to indicate another basis function has been used to represent this tensor. In our present discussion this means the tensor representation has been rotated into another configuration. In order to find the frame which causes equation (3.2-6) to become closest to equation (3.2-7), I propose to form the new matrix below:

$$\mathbf{B} = \begin{bmatrix} B_{11} & B_{12} & B_{12} & 0 & 0 & 0 \\ B_{12} & B_{11} & B_{12} & 0 & 0 & 0 \\ B_{12} & B_{12} & B_{11} & 0 & 0 & 0 \\ 0 & 0 & 0 & B_{44} & 0 & 0 \\ 0 & 0 & 0 & 0 & B_{44} & 0 \\ 0 & 0 & 0 & 0 & 0 & B_{44} \end{bmatrix}, \quad (3.2-7)$$

where

$$B_{11} = \frac{1}{3} (A_{11} + A_{22} + A_{33}) \quad ,$$

$$B_{44} = \frac{1}{3} (A_{44} + A_{55} + A_{66}) \quad ,$$

and 
$$B_{12} = \frac{1}{3} (A_{12} + A_{13} + A_{23}) \quad .$$

Of course, equation (3.2-7) is not the only representation we could choose, nor are we stuck with only one representation matrix. We could just as well choose several matrices like (3.2-7) and proceed equally with all of them through the following steps. We now form the difference  $\mathbf{E} = \mathbf{R}(\mathbf{B} - \mathbf{C}')$ , which I will call the error tensor. Note that if we did have several representation matrices,  $\mathbf{B}$ , we could index them and form a series of indexed error matrices,  $\mathbf{E}$ , before proceeding. The symbol  $\mathbf{R}(\cdot)$  represents the rotation from one frame of reference to another, as given by equation (3.1.1-4); this is where the distinction becomes important that the rotation is actually performed on the tensor and not its two-index matrix representation. The rotation can be represented by Euler angles or some other set of three appropriate variables. Let the matrix representation of  $\mathbf{E}$  have the elements  $E_{ij}$ . We now form the scalar:

$$\varepsilon = \sum_{i=1}^6 \sum_{j=1}^6 w_{ij} E_{ij}^2 \quad , \quad (3.2-8)$$

which shall be called the error term, in which weights  $w_{ij}$  have been introduced to add additional control. If we had more than one error matrix, we could at this point calculate an error term for each of them then form a weighted sum before going on. At this point we are free to use a number of optimization techniques (Press, Flannery, Teukolsky and Vetterling, 1988) to minimize equation (3.2-8). The template matrix,  $\mathbf{B}$ , can be customized for all symmetry systems in the same manner as above, and so is not restricted to cubic symmetry. When equation (3.2-8) is minimized, the resulting  $\mathbf{B}$  will be our closest representation of  $\mathbf{C}'$  within the confines of this fixed symmetry system. We can also examine the error matrix,  $\mathbf{E}$ , to see how the error is distributed and to see the magnitude of the individual terms. If we are to compare one symmetry class with another and have the error scalar have any meaning it is necessary to insure all the elements in the error matrix  $\mathbf{E}$  is as random as possible. Visual inspection is one way to determine randomness, but, a better way is to use a measure of randomness such as the Shannon

entropy measure or the varimax norm. With the error scalar and the entropy measure we can determine the best representation to be the one which minimizes the error scalar and maximizes the entropy. The Euler angles will define the new coordinate system, which provides information as to the underlying symmetry of the tensor, **A**. There is a host of error-minimization routines to perform just this task (Press, Flannery, Teukolsky and Vetterling, 1988). This procedure is represented in flowchart form in figure 3.2-1.

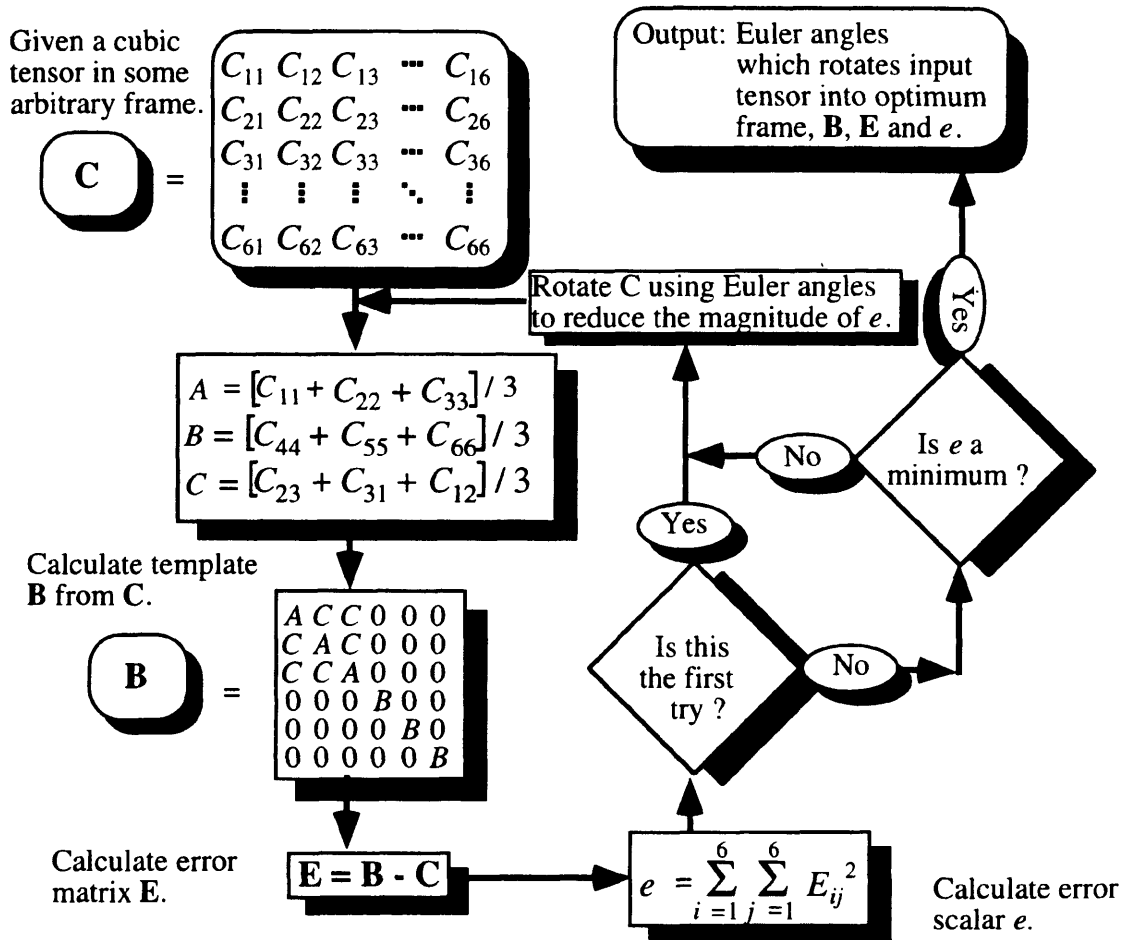


Fig. 3.2-1. Flowchart for a method to determine the preferred frame of reference of the elastic tensor (cubic example).

### 3.3: The proof of the pudding ( the numerical trial )

To see if this method works, I programmed the algorithm represented in figure 3.2-1. The numerical trial begins with a specific cubic elastic tensor in one of its preferred frames and represented in standard 6x6 matrix notation as:

$$\mathbf{C} = \begin{bmatrix} 3.1500 & 1.8500 & 1.8500 & 0.0000 & 0.0000 & 0.0000 \\ 1.8500 & 3.1500 & 1.8500 & 0.0000 & 0.0000 & 0.0000 \\ 1.8500 & 1.8500 & 3.1500 & 0.0000 & 0.0000 & 0.0000 \\ 0.0000 & 0.0000 & 0.0000 & 2.5000 & 0.0000 & 0.0000 \\ 0.0000 & 0.0000 & 0.0000 & 0.0000 & 2.5000 & 0.0000 \\ 0.0000 & 0.0000 & 0.0000 & 0.0000 & 0.0000 & 2.5000 \end{bmatrix}. \quad (3.3-1)$$

The frame of reference is then rotated by the Euler angles  $\theta = 35^\circ$ ,  $\varphi = 16^\circ$  and  $\psi = 52^\circ$ . This results in a matrix representation of  $\mathbf{C}$  very different from equation (3.3-1), as shown below:

$$\mathbf{C}' = \begin{bmatrix} 3.5169 & 1.8237 & 1.5094 & 0.0003 & 0.7344 & -0.1172 \\ 1.8237 & 3.3647 & 1.6616 & 0.5416 & -0.0610 & 0.2429 \\ 1.5094 & 1.6616 & 3.6789 & -0.5419 & -0.6734 & -0.1257 \\ 0.0003 & 0.5416 & -0.5419 & 2.3116 & -0.1257 & -0.0610 \\ 0.7344 & -0.0610 & -0.6734 & -0.1257 & 2.1594 & 0.0003 \\ -0.1172 & 0.2429 & -0.1257 & -0.0610 & 0.0003 & 2.4737 \end{bmatrix}. \quad (3.3-2)$$

The prime in equation (3.3-2) indicates that a rotation of the frame of reference has occurred, but we must keep in mind that we are still dealing with the same physical tensor. As can be seen by the representation of tensor  $\mathbf{C}$  in equation (3.3-2), it would be difficult to determine what symmetries, if any, may exist for this tensor. Following the recipe outlined by the flowchart in figure 3.2-1, we calculate the template associated with  $\mathbf{C}'$  as given by equation (3.3-2). This results in:

$$\mathbf{B}_1 = \begin{bmatrix} 3.5202 & 1.6649 & 1.6649 & 0.0000 & 0.0000 & 0.0000 \\ 1.6649 & 3.5202 & 1.6649 & 0.0000 & 0.0000 & 0.0000 \\ 1.6649 & 1.6649 & 3.5202 & 0.0000 & 0.0000 & 0.0000 \\ 0.0000 & 0.0000 & 0.0000 & 2.3149 & 0.0000 & 0.0000 \\ 0.0000 & 0.0000 & 0.0000 & 0.0000 & 2.3149 & 0.0000 \\ 0.0000 & 0.0000 & 0.0000 & 0.0000 & 0.0000 & 2.3149 \end{bmatrix}, \quad (3.3-3)$$

where the subscript 1 indicates that this is the template associated with the first iteration and that no rotations have been applied to equation (3.3-2). By direct comparison with

equation (3.3-1) we can see that there is a large difference between the two matrices. The error scalar associated with this template is  $\epsilon = 3.580657$ , which is rather large. We now attempt to find rotations which will minimize the error scalar. At each stage of minimization a new rotated realization of the elastic tensor  $\mathbf{C}'$  is calculated, as well as its associated template. This procedure is repeated until our optimization criterion is met. For this case, 14 iterations were necessary to satisfy the optimization criterion using Powell's method (Press, Flannery, Teukolsky and Vetterling, 1988). At this point the Euler angles were found to be  $\theta = -52.000027$ ,  $\phi = -16.000008$  and  $\psi = 55.000027$ . When these Euler angles are used to rotate equation (3.3-2), the following results:

$$\mathbf{C}' = \begin{bmatrix} 3.1500 & 1.8500 & 1.8500 & -0.0000 & -0.0000 & 0.0000 \\ 1.8500 & 3.1500 & 1.8500 & 0.0000 & -0.0000 & -0.0000 \\ 1.8500 & 1.8500 & 3.1500 & -0.0000 & 0.0000 & 0.0000 \\ -0.0000 & 0.0000 & -0.0000 & 2.5000 & 0.0000 & 0.0000 \\ -0.0000 & -0.0000 & 0.0000 & 0.0000 & 2.5000 & -0.0000 \\ 0.0000 & -0.0000 & 0.0000 & 0.0000 & -0.0000 & 2.5000 \end{bmatrix}. \quad (3.3-4)$$

By directly comparing  $\mathbf{C}'$  of equation (3.3-4) with  $\mathbf{C}$  of equation (3.3-1) we find that they are identical to four decimal places. The error scalar is zero also to four decimal places. We have come full circle and found a set of Euler angles which will give a reference frame in which our elastic tensor will have a representation in its standard form.

I have developed a rather simple statistical method to find the preferred frame of reference of an elastic tensor and was able to show that it works in the simple cubic symmetry case. Additional numerical trials would be useful to further test this method, as well as applying this method to real experimental data (Vestrum, Brown and Easley, 1996). The method used here is the most basic one as outlined in the flowchart of figure 3.2-1; the other symmetry classes may require some of the enhancements as outlined in section 3.2. This, however, is the stopping point I will choose for this chapter.

## 4: Synthetic seismograms for P and S waves using the Goupillaud model

### 4.1: A brief review

This chapter is based on research that I have had the privilege to work on with Darren Foltinek (Easley and Foltinek, 1993) as a part of the CREWES project. I must also thank Dr. Krebs for giving us a copy of his code for the calculations of Zoeppritz coefficients. The modeling method that is the workhorse of this method has a long history. Before I proceed we will quickly review some of material that comprises this method and some of the other work that has been done in this area.

The wave equation describes the propagation of plane waves within homogeneous layers as simple time delays; by this, I mean that the waveform is constant within any homogeneous layer, since there is no divergence or other geometrical effects and in a homogeneous layer there is no partitioning of the energy of a plane wave. The only perceptible change, at a point within the medium, is a time-delayed version of the waveform. When the wavefront impinges on an interface, the boundary conditions, along with the wave equation, specifies a partitioning of the wave field. This naturally gives rise to the definition of reflection and transmission coefficients. Imposing the constraint of having interfaces at discrete equal time intervals results in the Goupillaud model. This model has been studied by many researchers. For example Hubral, Treitel and Gutowski (1980) use this to study the spectral models of a layered earth system. Their studies are based on the z-transform, which is a frequency domain implementation of the Goupillaud model. Mendel, Nahi and Chan (1979) proposed a different formalism based on the state-space model. It is this method that is expanded upon here. The reason for using the state-space approach is the ease by which more sophisticated processes can be implemented, such as absorption (Aminzadeh and Mendel, 1983), isolation of multiples (Aminzadeh and Mendel, 1980), and the inclusion of P and S waves within the Goupillaud model, this last of which is our contribution to the subject. The time domain, the domain of the state-space model, also appeals more directly to the intuition.

## 4.2: A bit of the theory

It is always a good idea to go into a bit of the details of the method before looking at some of the results; so that is what we will now do.

### 4.2.1: Traditional nonnormally incident Goupillaud model

Consider horizontally layered elastic media bounded above and below by half-spaces, either or both of which may be a vacuum. Within the  $i$ th layer, we assume the existence of upward and downward propagating particle displacements with plane phase fronts. The notation I have adopted to represent these particle displacement disturbances are explained in figure 4.2.1-1, where:  $U$  stands for upward propagating,  $D$  stands for downward propagating,  $P$  represents compressional particle motion,  $S$  represents shear particle motion, subscripts represent the layer number to which the disturbances are confined and  $\tau$  is the delay time of a particular wave type within the layer. Therefore,  $DP_i(t)$  represents a downward propagating compressional wave in layer  $i$  at time  $t$ .

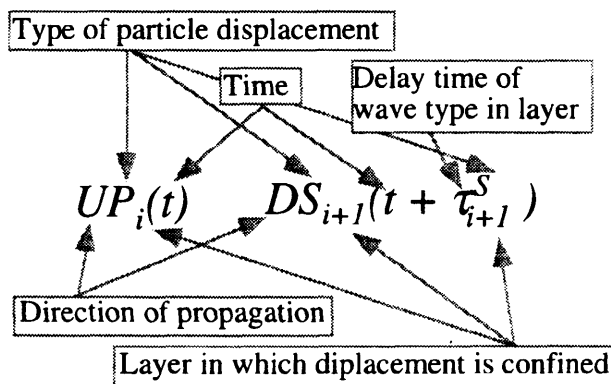


Fig. 4.2.1-1. Particle displacement notation.

When these disturbances impinge on an interface, the energy is partitioned into up- and downgoing compressional- (P) and shear- (S) waves (figure 4.2.1-2). From this partitioning, reflection and transmission coefficients are defined at an interface. Modifying Aminzadeh and Mendel's (1982) notation, it is assumed that at time  $t$  the downward propagating disturbance has reached the bottom of layer  $i$  ( $DP_i(t)$ ,  $DS_i(t)$ ), and the upward propagating disturbance has reached the top of layer  $i$  ( $US_i(t)$ ,  $UP_i(t)$ ). Additionally, the following disturbances are defined:

$$UP'_i(t) = UP_i(t + \tau_i^P) \equiv \text{upgoing P-wave at the bottom of layer } i,$$

$$DP'_i(t) = DP_i(t+\tau_i^P) \equiv \text{downgoing P-wave at the top of layer } i,$$

$$US'_i(t) = US_i(t+\tau_i^S) \equiv \text{upgoing S-wave at the bottom of layer } i,$$

and

$$DS'_i(t) = DS_i(t+\tau_i^S) \equiv \text{downgoing P-wave at the top of layer } i,$$

where  $\tau_i^P$  and  $\tau_i^S$  are the compressional- and shear-wave traveltimes of layer  $i$ . It is important to realize that at time  $t$  only the displacements defined at time  $t$  exist; for instance, all the primed disturbances will become the future unprimed variables when they reach the appropriate interfaces (figure 4.2.1-2). Using the transmission and reflection coefficients, we can relate these wavefields to each other by:

$$DP'_{i+1}(t) = R_i^{bPP}UP_{i+1}(t) + R_i^{bSP}US_{i+1}(t) + T_i^{tPP}DP_i(t) + T_i^{tSP}DS_i(t), \quad (4.2.1-1a)$$

$$DS'_{i+1}(t) = R_i^{bPS}UP_{i+1}(t) + R_i^{bSS}US_{i+1}(t) + T_i^{tPS}DP_i(t) + T_i^{tSS}DS_i(t), \quad (4.2.1-1b)$$

$$UP'_i(t) = R_i^{tPP}DP_i(t) + R_i^{tSP}DS_i(t) + T_i^{bPP}UP_{i+1}(t) + T_i^{bSP}US_{i+1}(t), \quad (4.2.1-1c)$$

and

$$US'_i(t) = R_i^{tPS}DP_i(t) + R_i^{tSS}DS_i(t) + T_i^{tPS}UP_{i+1}(t) + T_i^{bSS}US_{i+1}(t). \quad (4.2.1-1d)$$

The superscript  $b$  in reflection and transmission coefficients indicates partitioning of the wavefield as viewed from the bottom of an interface, and the superscript  $t$  indicates partitioning of the wavefield as viewed from the top of the interface. The first uppercase superscript indicates the incident wavetype and the second the scattered wavetype.

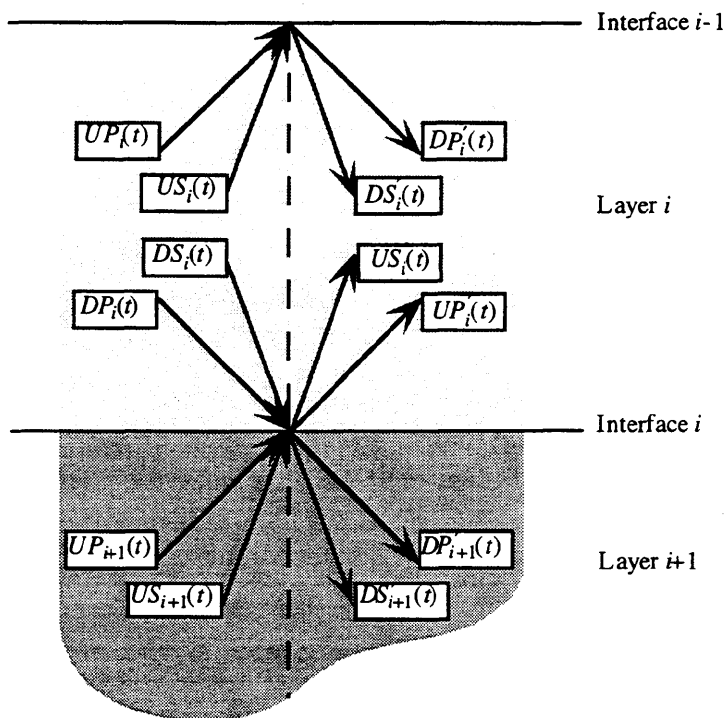


Fig.4.2.1-2. Partitioning of waves at interfaces.

These energy partitioning equations apply to plane waves within arbitrary horizontally layered models. The Goupillaud models are such that the traveltimes in all layers within a model are constant. By the device of interfaces with zero reflection coefficients and unit transmission coefficients, the approximation to a true depth model can be approached to any degree of accuracy by making the traveltime in each layer as small as necessary.

In plane horizontal layers with plane waves, the wave parameter,  $p = \sin \theta / V$  is constant (by Snell's law) and therefore the traveltime for each wavetype is constant within a single layer. But, the P- and S-wave traveltimes through a given layer differ from each other. This prohibits the use of a single Goupillaud model for modeling both wave types. It is important to note that the equations thus far deal with the entire wavefield within a single model, while the numerical scheme that is implemented separates the P and S wavefields into two separate Goupillaud models.

### 4.2.2: Coupled P- and S-wave Goupillaud models

The method used here to accommodate the differing P and S traveltimes is to run separate Goupillaud models for the P and S waves. These models are approximations of the true depth model. The approximation is accomplished by representing the traveltime in the  $i$ th depth layer as an integral multiple of a small constant time increment,  $\Delta t$ . This approximation constrains the  $V_P / V_S$  ratio within each layer of the coupled Goupillaud models to be a rational number. Since rational numbers are dense in the reals, we can achieve any degree of accuracy desired by reducing the time increment,  $\Delta t$ . The transformation from the true depth model to the coupled Goupillaud models is shown in figure 4.2.2-1. Note, however, that the coupled Goupillaud models represent an exact depth model which differs slightly from the original.

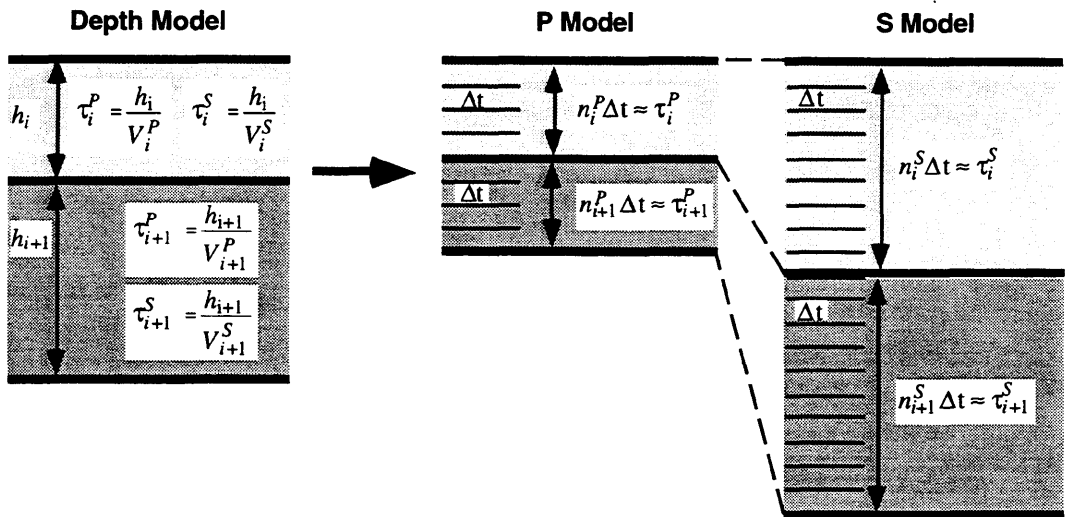


Fig 4.2.2-2. Transformation of depth model to P- and S-wave Goupillaud time models.

The rules for transforming the  $i$ th depth layer having P velocity  $V_i^P$ , S velocity  $V_i^S$ , and thickness  $h_i$  resulting in compression and shear traveltimes  $\tau_i^P$  and  $\tau_i^S$  respectively, into the two equal-time models are:

$$n_i^P \Delta t \approx \tau_i^P, \quad (4.2.2-1)$$

and

$$n_i^S \Delta t \approx \tau_i^S, \quad (4.2.2-2)$$

where  $n_i^P$  and  $n_i^S$  are integers determined by our chosen  $\Delta t$ . This procedure introduces a time error for both P- and S-wave traveltimes in the  $i$ th layer given by:

$$\delta_i^P = \tau_i^P - n_i^P \Delta t \quad (4.2.2-3)$$

and

$$\delta_i^S = \tau_i^S - n_i^S \Delta t \quad , \quad (4.2.2-4)$$

respectively. The total number of time layers within the two Goupillaud models will be:

$$M_p = \sum_{i=1}^N n_i^P \quad , \quad (4.2.2-5)$$

in the P-wave Goupillaud model, and

$$M_s = \sum_{i=1}^N n_i^S \quad , \quad (4.2.2-6)$$

for the S-wave Goupillaud model.

Since, we have discrete time intervals, it is appropriate to change the time variable,  $t$ , into a discrete variable,  $j$ , that is represented as a second subscript for each of the wave types. As stated previously, an upward propagating disturbance is assumed to have reached the top of layer  $i$  and the downward propagating disturbance to be at the bottom of this layer at discrete time indices. The wavefields designated with a prime are, by our convention, the same as the unprimed wavefields within the same layer advanced in time in the following manner:

$$DP'_{ij} = DP_{i,j+1} \quad , \quad (4.2.2-7a)$$

$$DS'_{ij} = DS_{i,j+1} \quad , \quad (4.2.2-7b)$$

$$UP'_{ij} = UP_{i,j+1} \quad , \quad (4.2.2-7c)$$

and

$$US'_{ij} = US_{i,j+1} , \quad (4.2.2-7d)$$

where the index  $j$  represents a discrete time variable with unit time step, and therefore  $t = j \Delta t$ . The relationships (4.2.2-7a-d) allows equations (4.2.2-8a-d) to be rewritten in their discrete form and separated into converted and non-converted modes as:

$$U^*_{i+1,j+1} = R_i^{t^{**}} D^*_{i+1,j} + T_i^{b^{**}} U^*_{i,j} , \quad (4.2.2-8a)$$

$$D^*_{i+1,j+1} = R_i^{b^{**}} U^*_{i+1,j} + T_i^{t^{**}} D^*_{i,j} , \quad (4.2.2-8b)$$

and for the converted waves:

$$U^\diamond_{i+1,j+1} = R_i^{t^{*\diamond}} D^*_{i,j} + T_i^{b^{*\diamond}} U^*_{i+1,j} , \quad (4.2.2-8c)$$

and

$$D^\diamond_{i+1,j+1} = R_i^{b^{*\diamond}} U^*_{i+1,j} + T_i^{t^{*\diamond}} D^*_{i,j} . \quad (4.2.2-8d)$$

Equations (4.2.2-8a), (4.2.2-8b), (4.2.2-8a) and (4.2.2-8b) explicitly give the state at time index  $j+1$  in terms of the states at time index  $j$  for all layers  $i$ ; therefore, these equations provide a means to generate all the states in all the layers from some given initial state at an initial time index. The symbol  $*$  represents the state within a single Goupillaud model and the  $\diamond$  symbol represents the converted state which must be introduced into the coupled Goupillaud model at the same time and appropriate layer. The reflection and transmission coefficients are calculated from the Zoeppritz equations (Aki and Richards, 1980). This provides all the necessary theory to generate full P and S body-wave synthetic seismograms within the Goupillaud framework.

### 4.3: Synthetic seismogram examples

Since all the descriptions above is for a computer algorithm so we shall now proceed to taste the fruits of our numerical implementation.

#### 4.3.1: The pictures that are worth a 1000 words

The following simple model was used to demonstrate the algorithm. The model consists of three layers with the following parameters:

Depth (m)	$V_P$ (m/s)	$V_S$ (m/s)	Density ( $\text{kg/m}^3$ )
0	4000	2100	2450
1200	4500	2700	2650
3000	5400	3100	2700

Figures 4.3-3 contains the synthetic seismic sections for the horizontal and vertical displacements associated with this model. The sample interval for this model is 2ms. The synthetic was generated with a P-wave source located on the surface and receivers at even depth intervals. Note the reflected up going P wave energy as well as the converted up going S-wave at the first interface. Further down in time the evidence of multiple energy of both wave types is clearly shown. The surface interface was defined as being a perfectly elastic reflector with no mode conversion taking place. This choice for surface conditions is arbitrary, we could have also defined it as a proper free surface. The purpose of this choice was to simplify the appearance of the synthetic seismogram.

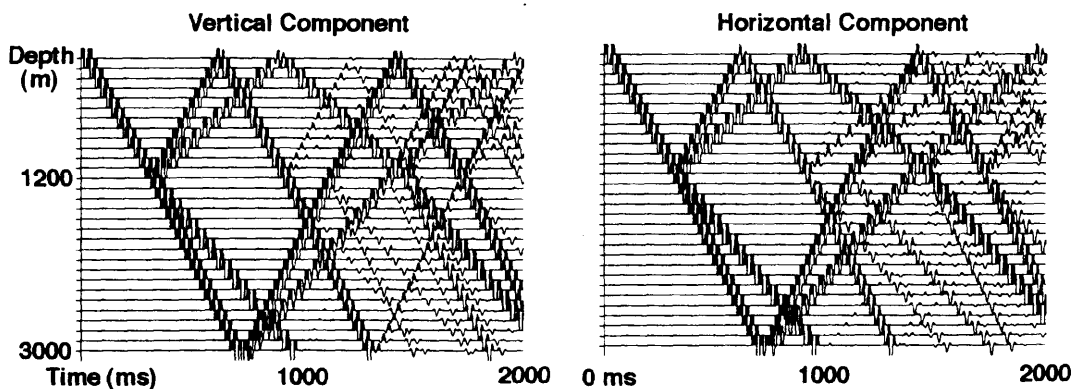


Fig 4.3-3. Vertical and horizontal VSP sections.

#### **4.3.2: At what cost ? (Run time Considerations)**

One of the major reasons for the development of this method of modeling is the speed at which the algorithm runs. For a 1200 layer Goupillaud model, a two second synthetic seismogram was generated on a Sun Sparcstation II in 23 seconds. Due to the nature of the algorithm, the code is highly parallelizable and therefore could easily take advantage of modern parallel computers.

#### **4.4: Always more to do. Possible enhancements**

The state space framework allows many easy to implement enhancements; some of these are the ability to generate primaries only seismograms as well as seismograms with any particular order of multiple, this is called Bremmer decomposition (Aminzadeh and Mendel, 1980). Absorption can also be incorporated (Aminzadeh and Mendel, 1983). To more closely match real data the plane wave synthetic seismograms can be combined to form line or point source seismograms (Aminzadeh and Mendel, 1982). The seismograms can also be generated at any offset.

## 5: Conclusions

### 5.1: Shear waves from vertical vibrators

The chapter dealing with this topic is split into two sections, each dealing with a different theoretical approach in the investigation of vertically incident shear waves from interacting vertical vibrators. As far as I am aware, up to this point, no theoretical analysis supports the existence of vertically incident shear waves from interacting vertical vibrators, though this phenomenon has been observed experimentally under many different situations.

The first approach generalizes the approach taken by Dankbaar (1983). He assumes vibrators in counterphase do not interact and act as vertical stresses in counterphase. In his analysis equations of motion are derived showing no evidence of vertically incident shear waves. I made the assumption that when the vibrators interact, the sources can be modeled as displacements in counterphase. With this assumption, I derived the equations of motion which show that, under this circumstance, the existence of vertically incident shear waves is a natural phenomenon. The actual interaction of vertical vibrators is probably not simple; therefore, both approaches tend to show the possibilities rather than the actual situation. In reality the system of forces best representing interacting vibrators is not a couple or double couple but a rather complicated system that is dominated by a few terms. This analysis proposes one such term which predicts the existence of vertically incident shear waves. More detailed experimental evidence may help to sort out which descriptions are more appropriate.

The second approach follows the development of Tan (1985). Tan's approach consists of fabrication of simple two-dimensional (2-D) mechanical models which are meant to mimic 2-D vibrators; these 2-D vibrators are placed on a frictionless surface of an elastic half-space and allowed to interact by coupling through the half-space. Since the equations governing the motion of the vibrators and the half-space is known, it is possible to calculate the displacement field of the combined system. Here again no vertically

incident shear waves were shown to exist. I believe the main cause of not observing vertically incident shear waves is due partly to the frictionless surface assumption. This method of modeling is, however, more general than the first method, and appears to assume less. I adapted the method by creating 3-D mechanical systems, I believe, better correspond to real vibrators and I assumed they were in welded contact with the free surface. I then derived all the equations necessary to model this new coupled system. A flowchart on how to compute the actual displacement field is given. Even though the development stops short of actual numerical implementation, it is not hard to imagine what would happen when a vibrator in welded contact with the free surface interacts with the Rayleigh waves, with retrograde elliptic motion, generated by another vibrator. I think it is difficult to conceive that this system would not generate some shear-waves in the near-vertical direction.

It is interesting to note that shear-wave generation from interacting vibrators did originally appear to be a strange phenomenon, yet after the analysis it is difficult to imagine an interacting system, unless highly artificial, that would not generate shear waves.

## **5.2: Composite media as generalized continua**

Backus's (1962) averaging method was generalized to develop a continuum theory that is not bound by the static assumption central to Backus's work. I derived a non-local description consistent with this method of averaging. Plane-wave solutions to this new description were examined. The waves are shown to be, in general, dispersive and attenuative. In real experiments it is known that seismic waves are both attenuated and dispersed and therefore the kinematic solutions provide only a partial description of the actual process. Generalized continuum theories can provide an additional tool to investigate the dynamic nature of seismic wave propagation.

## **5.3: Elastic tensors and their preferred frames of reference**

A statistical method to determine the preferred frame of reference of an elastic tensor of a particular symmetry class is developed. The method was tested using an

elastic tensor of cubic symmetry within an arbitrary frame. The method was able to extract the preferred frame. The method could also be used in a more general way to determine which symmetry class best describes the elastic tensor. To approach this problem one needs to include entropy measures, as discussed, along with the method tested. This method may provide a means of dealing with symmetries embodied with an arbitrary tensor.

#### **5.4: Synthetic seismograms for P and S waves using the Goupillaud model**

I have overcome the difficulty of modeling both P- and S-wave types using the Goupillaud model. This was accomplished using two coupled Goupillaud models, one was for P waves and the second for S waves. The wave propagation method I chose was Mendel's state-space method. I used this time-domain method due to its simplicity and availability of many enhancements. The Goupillaud model has been used in the seismic community for a long time and is known for its correctness in body-wave modeling as well and speed of computation. The new method I developed retains these characteristics and is borne out by my numerical trials.

## A: Radiation Field of a Vertical Vibrator Over a Half Space

### A.1: Introduction

The radiation pattern due to a mechanical vibrator has been studied by many authors with differing assumptions. This treatment is based on the work of Miller and Pursey (1953). I have not followed their development exactly but the differences do not affect the major results. The particular aspect of their work that we will be reviewing is the case of a vertically vibrating circular disk on an elastic half-space. This situation is represented in figure A.1-1.

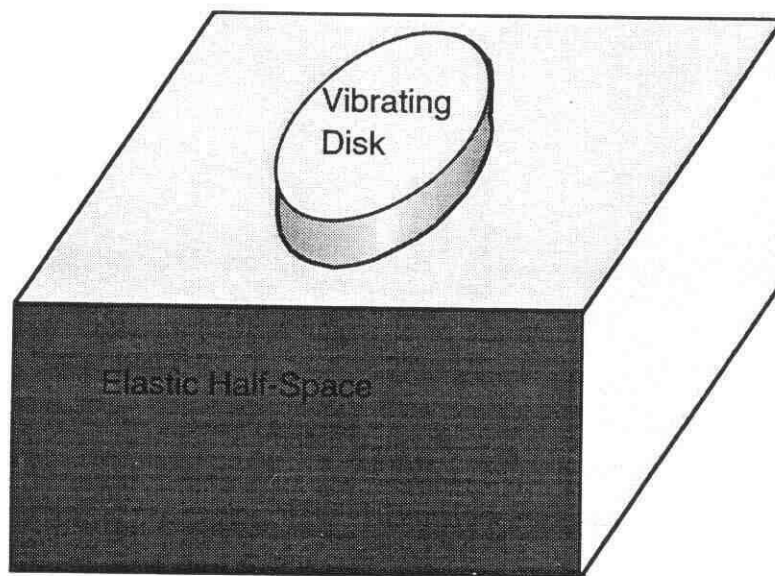


**Fig. A.1-1.** Vibrating circular disk over an elastic half-space.

Due to the cylindrical symmetry of the situation, some simplification can be obtained by using equations in cylindrical coordinates  $(r, \phi, z)$  as shown in figure A.1-2.

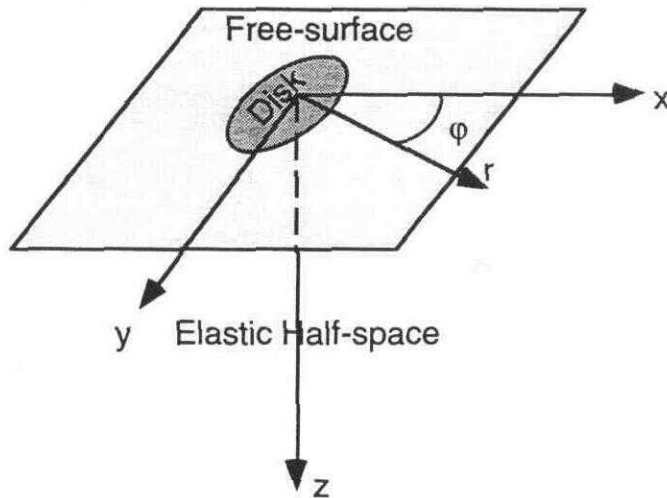


**Fig. A.1-2.** Cylindrical coordinates for vibrating disk problem.

The obvious consequence of the symmetry is that displacement in the  $\varphi$  direction,  $u_\varphi$ , is nonexistent and there are no changes in the  $\varphi$  direction, in other words all derivatives with respect to  $\varphi$  vanish as well. With this in mind let us collect some of the equations which describe the situation at hand.

## A.2: Equations of Motion

First we will collect the equations which describe the evolution of motion within the elastic half-space. These are the equations of motion as derived in appendix B and given by equations (B.4-39a), (B.4-39b) and (B.4-39c), which are in turn reproduced here as:

$$\ddot{u}_r \rho = (\lambda + 2\mu) \frac{\partial \Delta}{\partial r} - \frac{\mu}{r} \left[ \frac{\partial \omega_z}{\partial \varphi} - r \frac{\partial \omega_\varphi}{\partial z} \right] + f_r \rho, \quad (\text{A.2-1a})$$

$$\ddot{u}_\varphi \rho = (\lambda + 2\mu) \frac{\partial \Delta}{\partial \varphi} - \mu \left[ \frac{\partial \omega_r}{\partial z} - \frac{\partial \omega_z}{\partial r} \right] + f_\varphi \rho, \quad (\text{A.2-1b})$$

and

$$\ddot{u}_z \rho = (\lambda + 2\mu) \frac{\partial \Delta}{\partial z} - \frac{\mu}{r} \left[ \frac{\partial r \omega_\phi}{\partial r} - \frac{\partial \omega_r}{\partial \phi} \right] + f_z \rho, \quad (\text{A.2-1c})$$

where the dilatation is defined to be:

$$\Delta = \frac{\partial u_r}{\partial r} + \frac{u_r}{r} + \frac{1}{r} \frac{\partial u_\phi}{\partial \phi} + \frac{\partial u_z}{\partial z}, \quad (\text{A.2-2})$$

and the components of circulation are:

$$\omega_r = \frac{1}{r} \frac{\partial u_z}{\partial \phi} - \frac{\partial u_\phi}{\partial z}, \quad (\text{A.2-3a})$$

$$\omega_\phi = \frac{\partial u_r}{\partial z} - \frac{\partial u_z}{\partial r}, \quad (\text{A.2-3b})$$

and

$$\omega_z = \frac{1}{r} \left[ \frac{\partial r u_\phi}{\partial r} - \frac{\partial u_r}{\partial \phi} \right]. \quad (\text{A.2-3c})$$

Note, in all the equations above, that the curl is defined to be the negative of the ones found in appendix B. The sign reversal is partially justifiable, since the curl is a pseudovector, one which is defined up to an arbitrary sign. Normally the sign is defined by convention using the right-hand rule as a basis for specifying positive and negative senses of rotation.

Since we will be specifying the stress under the disk, we will have need of the constitutive relations, which relate the stresses,  $\sigma$ , supplied by the disk in the vertical direction,  $z$ , and the strains,  $e$ , resulting within the half-space. The appropriate components of stress and their corresponding constitutive relation, in cylindrical coordinates, are derived in appendix B as equations (B.4-29), (B.4-30) and (B.4-31) and reproduced here as:

$$\sigma_{rz} = 2\mu e_{rz} = \mu \left( \frac{\partial u_r}{\partial z} + \frac{\partial u_z}{\partial r} \right), \quad (\text{A.2-4a})$$

$$\sigma_{\varphi z} = 2\mu e_{\varphi z} = \mu \left( \frac{\partial u_{\varphi}}{\partial z} + \frac{1}{r} \frac{\partial u_z}{\partial \varphi} \right), \quad (\text{A.2-4b})$$

and

$$\sigma_{zz} = \lambda \Delta + 2\mu e_{zz} = \lambda \Delta + 2\mu \frac{\partial u_z}{\partial z}, \quad (\text{A.2-4c})$$

where I have moved all superscripts for the stress and strain to the subscript position, to simplify later developments. If we incorporate the symmetry conditions,  $u_{\varphi} = 0$ , implying the vanishing of all derivatives with respect to  $\varphi$  and the absence of all body forces, the equations above will take on simpler forms. The equations of motion become:

$$(\lambda+2\mu) \frac{\partial \Delta}{\partial r} + \mu \frac{\partial \omega_{\varphi}}{\partial z} - \ddot{u}_r \rho = 0 \quad (\text{A.2-5a})$$

and

$$(\lambda+2\mu) \frac{\partial \Delta}{\partial z} - \frac{\mu}{r} \frac{\partial r \omega_{\varphi}}{\partial r} - \ddot{u}_z \rho = 0, \quad (\text{A.2-5b})$$

where the dilatation is simplified to

$$\Delta = \frac{1}{r} \frac{\partial r u_r}{\partial r} + \frac{\partial u_z}{\partial z}, \quad (\text{A.2-6})$$

and the only surviving term of the circulation is

$$\omega_{\varphi} = \frac{\partial u_r}{\partial z} - \frac{\partial u_z}{\partial r}. \quad (\text{A.2-7})$$

The form of the constitutive relations given by equations (A.2-4a), and (A.2-4c) remain unchanged; equation (A.2-4b), however, is identically zero. We will try to find a system of equations which involve the dilatation  $\Delta$  and circulation  $\omega_{\varphi}$  of the displacement field only. The procedure, or recipe, to accomplish this can be represented symbolically by:

$$\frac{1}{r} \frac{\partial(\text{E.1-5a})}{\partial r} + \frac{\partial(\text{E.1-5b})}{\partial z},$$

followed by substitution of equation (A.2-6). This procedure results in:

$$\frac{1}{r} \frac{\partial}{\partial r} \left[ r \frac{\partial \Delta}{\partial r} \right] + \frac{\partial^2 \Delta}{\partial z^2} - \frac{\ddot{\Delta}}{V_p^2} = 0. \quad (\text{A.2-8a})$$

In the same fashion we can take

$$\frac{\partial(\text{E.1-5b})}{\partial r} - \frac{\partial(\text{E.1-5a})}{\partial z},$$

and substitute in equation (A.2-7) to arrive at:

$$\frac{\partial}{\partial r} \left[ \frac{1}{r} \frac{\partial r \omega_\phi}{\partial r} \right] + \frac{\partial^2 \omega_\phi}{\partial z^2} - \frac{\ddot{\omega}_\phi}{V_s^2} = 0. \quad (\text{A.2-8b})$$

In the two equations above we have defined two constants, namely

$$V_p = \sqrt{\frac{\lambda + 2\mu}{\rho}}, \quad (\text{A.2-9a})$$

and

$$V_s = \sqrt{\frac{\mu}{\rho}}; \quad (\text{A.2-9b})$$

these constants, not surprisingly, will turn out to be the compressional- and shear-wave velocities, respectively. By taking the second time derivative of equations (A.2-4a) and (A.4-4c) and substituting in equations (A.2-5a) and (A.2-5b) we transform the constitutive relations into a form which depends on  $\Delta$  and  $\omega_\phi$  explicitly. The new forms of the constitutive relations are:

$$\ddot{\sigma}_{rz} = \rho V_s^4 \left[ 2 m^2 \frac{\partial^2 \Delta}{\partial r \partial z} + \frac{\partial^2 \omega_\phi}{\partial z^2} - \frac{\partial}{\partial r} \left( \frac{1}{r} \frac{\partial r \omega_\phi}{\partial r} \right) \right], \quad (\text{A.2-10a})$$

and

$$\ddot{\sigma}_{zz} = \rho V_s^4 \left[ \frac{(m^2 - 2)}{V_s^2} \ddot{\Delta} + 2m^2 \frac{\partial^2 \Delta}{\partial z^2} - \frac{2}{r} \frac{\partial^2 r \omega_\varphi}{\partial r \partial z} \right]. \quad (\text{A.2-10b})$$

If we substitute equation (A.2-8a) into (A.2-10b), all the time derivatives on  $\Delta$  can be removed resulting in

$$\ddot{\sigma}_{zz} = \rho V_s^4 \left[ m^4 \frac{\partial^2 \Delta}{\partial z^2} + \frac{(m^2 - 2) m^2}{r} \frac{\partial}{\partial r} \left( r \frac{\partial \Delta}{\partial r} \right) - \frac{2}{r} \frac{\partial}{\partial r} \left( r \frac{\partial \omega_\varphi}{\partial z} \right) \right]. \quad (\text{A.2-10c})$$

where we have defined the  $V_p : V_s$  ratio to be

$$m = \frac{V_p}{V_s}. \quad (\text{A.2-10d})$$

We now have a system of equations, (A.2-8a), (A.2-8b), (A.2-10a) and (A.2-10b), which describe the evolution of deformation on and within our elastic half-space with the new quantities dilatation  $\Delta$  and circulation  $\omega_\varphi$  explicitly.

### A.3: Solving for Dilatation $\Delta$ and Circulation $\omega_\varphi$

The next step is to find solutions to the differential equations we have derived. I will not use the method of Miller and Pursey (1953), rather I will use the method of separation of variables (Pipes and Harvill, 1970). This method is more general and, for cases where the symmetry is not as convenient as the present one, such as a horizontal source (Cherry, 1962), this method will still lead to solutions.

The first equation we shall tackle is equation (A.2-8a) and the first step is to make the assumption that  $\Delta$  is separable, which means:

$$\Delta(r, z, t) = \Delta_r(r) \Delta_z(z) \Delta_t(t). \quad (\text{A.3-1})$$

Substitution of equation (A.3-1) into equation (A.2-8a) and rearranging terms yields

$$\frac{V_p^2}{r \Delta_r} \frac{\partial}{\partial r} \left( r \frac{\partial \Delta_r}{\partial r} \right) + \frac{V_p^2}{\Delta_z} \frac{\partial^2 \Delta_z}{\partial z^2} = \ddot{\Delta}_t. \quad (\text{A.3-2})$$

Note that the right-hand side of equation (A.3-2) is a function of the variable  $t$  only, while the left-hand side is a function of  $r$  and  $z$  only. For the two sides to be equal for all changes of the independent variables, they can at most be equal to a constant. Let this constant be  $-(2\pi f)^2$ . Therefore we can rewrite equation (A.3-2) as:

$$\ddot{\Delta}_t = -(2\pi f)^2 \Delta_t, \quad (\text{A.3-3a})$$

which has solutions of the form  $\Delta_t = e^{-i2\pi ft}$ . By the principle of linear superposition we can write a more general solution of the form

$$\Delta_t(t) = \frac{1}{2\pi} \int_{-\infty}^{\infty} \Delta_t^{(F)}(f) e^{-i2\pi ft} df, \quad (\text{A.3-3b})$$

which is nothing more than the Fourier transform, denoted by  $F$ . Then, using the inverse Fourier transform, we can write:

$$\Delta_t^{(F)}(f) = \int_{-\infty}^{\infty} \Delta_t(t) e^{i2\pi ft} dt. \quad (\text{A.3-3c})$$

The remainder of equation (A.3-2) can be written as:

$$\frac{1}{r \Delta_r} \frac{\partial}{\partial r} \left( r \frac{\partial \Delta_r}{\partial r} \right) = k_p^2 - \frac{1}{\Delta_z} \frac{\partial^2 \Delta_z}{\partial z^2}, \quad (\text{A.3-4a})$$

where we have defined the constant

$$k_p = \frac{2\pi f}{V_p}. \quad (\text{A.3-4b})$$

We again have, in equation (A.3-4a), the condition where the left-hand side of the equation is a function of  $r$  alone and the right-hand side is a function of only  $z$ . This can only be true if both sides are equal to a constant. Let this constant be  $\zeta^2$ . We can then write the right-hand side of equation (A.3-4a) as:

$$r \frac{\partial^2 \Delta_r}{\partial r^2} + \frac{\partial \Delta_r}{\partial r} + r \Delta_r \zeta^2 = 0. \quad (\text{A.3-5a})$$

Making the substitution:

$$y = \zeta r \quad (\text{A.3-5b})$$

into equation (A.3-5a) we arrive at the equation:

$$y \frac{\partial^2 \Delta_r}{\partial y^2} + \frac{\partial \Delta_r}{\partial y} + y \Delta_r = 0, \quad (\text{A.3-5c})$$

which is just Bessel's differential equation of order 0. This equation has solutions of the form (Pipes and Harvill, 1970):

$$\Delta_r = C_1 J_0(y) + C_2 Y_0(y), \quad (\text{A.3-5d})$$

where  $J_0$  is called Bessel's function of order 0 of the 1st kind, and  $Y_0$  is called Bessel's function of order 0 of the 2nd kind. Bessel's functions of the 2nd kind becomes singular at  $y = 0$ ; therefore we shall remove them from consideration. Now we shall follow the lead of the Fourier solution above and use linear superposition to write a more general solution of the form:

$$\Delta_r(r) = \int_0^\infty \Delta_r^{(B_0)}(\zeta) \zeta J_0(y) d\zeta, \quad (\text{A.3-5e})$$

where  $B_0$  denotes the *zeroth-order Fourier-Bessel transform*. We can use the inverse Fourier-Bessel transform to write:

$$\Delta_r^{(B_0)}(\zeta) = \int_0^\infty \Delta_r(r) r J_0(y) d\zeta. \quad (\text{A.3-5f})$$

The last remaining portion of equation (A.3-2) can be written as:

$$\frac{\partial^2 \Delta_z}{\partial z^2} = (\zeta^2 - k_p^2) \Delta_z, \quad (\text{A.3-6a})$$

which has solutions of the form

$$\Delta_z(z) = C_1 \exp(-z \sqrt{\zeta^2 - k_p^2}) + C_2 \exp(z \sqrt{\zeta^2 - k_p^2}), \quad (\text{A.3-6b})$$

where  $C_1$  and  $C_2$  are arbitrary constants. Since the second exponential blows up for large  $z$  we will exclude it from the final solution. Note that both  $\zeta$  and  $k_p$  have been set in the previous solutions so the most general solution for  $\Delta_z$  will be:

$$\Delta_z(z) = C_1 \exp(-z \sqrt{\zeta^2 - k_p^2}). \quad (\text{A.3-6c})$$

We can now recombine the separated solutions by using equation (A.3-1) to get:

$$\Delta(t,r,z) = \frac{C_1}{2\pi} \int_{f=-\infty}^{\infty} \Delta_t^{(F)}(f) e^{-i2\pi ft} \int_{\zeta=0}^{\infty} \Delta_r^{(B_0)}(\zeta) \zeta J_0(y) \exp(-z \sqrt{\zeta^2 - k_p^2}) d\zeta df,$$

which can be represented in the following more compact form:

$$\Delta(t,r,z) = \frac{C_1}{2\pi} \int_{-\infty}^{\infty} \int_0^{\infty} \Delta^{(F,B_0)}(f,\zeta) \exp(-z \sqrt{\zeta^2 - k_p^2}) \zeta J_0(y) e^{-i2\pi ft} d\zeta df. \quad (\text{A.3-7a})$$

This means that we can write the solution in the transformed domain as:

$$\Delta^{(F,B_0)}(f,\zeta,z) = A \exp(-z \sqrt{\zeta^2 - k_p^2}), \quad (\text{A.3-7b})$$

where for simplicity we have set  $A = C_1 \Delta^{(F, B_0)}(f, \zeta)$ .

The second equation we shall solve is equation (A.2-8b). The method we will employ is exactly the same as the one we used to solve equation (A.2-8a). We again begin by separating the variables to give:

$$\omega_{\varphi}(t, r, z) = \omega_t(t) \omega_r(r) \omega_z(z). \quad (\text{A.3-8})$$

By the same substitution method we are able to solve for the individual components of the separation. The solutions are:

$$\omega_t(t) = \frac{1}{2\pi} \int_{-\infty}^{\infty} \omega_t^{(F)}(f) e^{-i2\pi ft} df, \quad (\text{A.3-9a})$$

$$\omega_r(r) = \int_0^{\infty} \omega_r^{(B_1)}(\zeta) \zeta J_1(y) d\zeta, \quad (\text{A.3-9b})$$

where  $B_1$  denotes *first-order Fourier-Bessel transform*, and

$$\omega_z(z) = D_1 \exp(-z \sqrt{\zeta^2 - k_s^2}), \quad (\text{A.3-9c})$$

where  $k_s = \frac{2\pi f}{V_s}$ . Now we recombine equations (A.3-9a), (A.3-9b) and (A.3-9c) using equation (A.3-8) to give

$$\omega_{\varphi}(t, r, z) = \frac{D_1}{2\pi} \int_{f=-\infty}^{\infty} \omega_t^{(F)}(f) e^{-i2\pi ft} \int_{\zeta=0}^{\infty} \omega_r^{(B_1)}(\zeta) \zeta J_1(y) \exp(-z \sqrt{\zeta^2 - k_s^2}) d\zeta df,$$

which again can be made more compact by writing it as:

$$\omega_{\varphi}(t, r, z) = \frac{D_1}{2\pi} \int_{-\infty}^{\infty} \int_0^{\infty} \omega_{\varphi}^{(F, B_1)}(f, \zeta) \exp(-z \sqrt{\zeta^2 - k_s^2}) \zeta J_1(y) e^{-i2\pi ft} d\zeta df. \quad (\text{A.3-10a})$$

In the transform domain this can be expressed as

$$\omega_{\phi}^{(F,B_1)}(f, \zeta, z) = B \exp\left(-z \sqrt{\zeta^2 - k_s^2}\right), \quad (\text{A.3-10b})$$

where again to simplify things I have set  $B = D_1 \omega_{\phi}^{(F,B_1)}(f, \zeta)$ . In order to solve for  $A$  and  $B$  in equations (A.3-7b) and (A.3-10b) we will try to match boundary conditions. Since these equations are simplest in the Fourier and Fourier-Bessel transform domains, we will need to transform the constitutive equations as given by equations (A.2-10a) through (A.2-10c) before proceeding to matching boundary conditions. The  $n$ th order Fourier-Bessel transform of a function  $g(r)$  is given by:

$$B_n[g(r)] = g^{(B_n)}(\zeta) = \int_0^{\infty} g(r) r J_n(r\zeta) dr, \quad (\text{A.3-11a})$$

and the inverse transformation is

$$B_n^{-1}[g^{(B_n)}(\zeta)] = g(r) = \int_0^{\infty} g^{(B_n)}(\zeta) \zeta J_n(r\zeta) d\zeta. \quad (\text{A.3-11a'})$$

If we assume that  $g(r)$  and its derivative is either zero or dominated by  $J_n$  at infinity, then the following identities can be derived from equation (A.3-11a):

$$B_0\left[\frac{1}{r} \frac{\partial}{\partial r} \left(r \frac{\partial g}{\partial r}\right)\right] = \zeta B_1\left[\frac{\partial g}{\partial r}\right] = -\zeta^2 B_0[g] = -\zeta^2 g^{B_0}(\zeta), \quad (\text{A.3-11b})$$

and

$$B_1\left[\frac{\partial}{\partial r} \left(\frac{1}{r} \frac{\partial rg}{\partial r}\right)\right] = -\zeta B_0\left[\frac{1}{r} \frac{\partial rg}{\partial r}\right] = -\zeta^2 B_1[g] = -\zeta^2 g^{B_1}(\zeta), \quad (\text{A.3-11c})$$

where  $B_n[\cdot]$  represents the  $n$ th order Fourier-Bessel transform of the argument within the square brackets. The identities for the Fourier transform are well known and will not be repeated here. Applying transforms to equations (A.2-10a) through (A.2-10c) results in:

$$\sigma_{zz}^{(F,B_0)} = \frac{\rho V_s^4}{(2\pi f)^2} \left[ 2\zeta \frac{\partial \omega_\phi^{(F,B_1)}}{\partial z} - m^4 \frac{\partial^2 \Delta^{(F,B_0)}}{\partial z^2} + (m^2 - 2)m^2 \zeta^2 \Delta^{(F,B_0)} \right], \quad (\text{A.3-12a})$$

$$\sigma_{zz}^{(F,B_0)} = \frac{\rho V_s^4}{(2\pi f)^2} \left[ \frac{(m^2 - 2)}{k_s^2} \Delta^{(F,B_0)} - 2m^2 \frac{\partial^2 \Delta^{(F,B_0)}}{\partial z^2} + 2\zeta \frac{\partial \omega_\phi^{(F,B_1)}}{\partial z} \right], \quad (\text{A.3-12b})$$

and

$$\sigma_{rz}^{(F,B_0)} = \frac{\rho V_s^4}{(2\pi f)^2} \left[ 2m^2 \zeta \frac{\partial \Delta^{(F,B_0)}}{\partial z} - \frac{\partial^2 \omega_\phi^{(F,B_1)}}{\partial z^2} - \zeta^2 \omega_\phi^{(F,B_1)} \right]. \quad (\text{A.3-12c})$$

#### A.4: Matching Boundary Conditions

The boundary condition that we want to match is for a disk on the free surface that exerts a normal force on the free surface. The time history of the driving force, we will assume, is described by the function  $f_z(t)$ . This situation is represented by figure A.4-1.

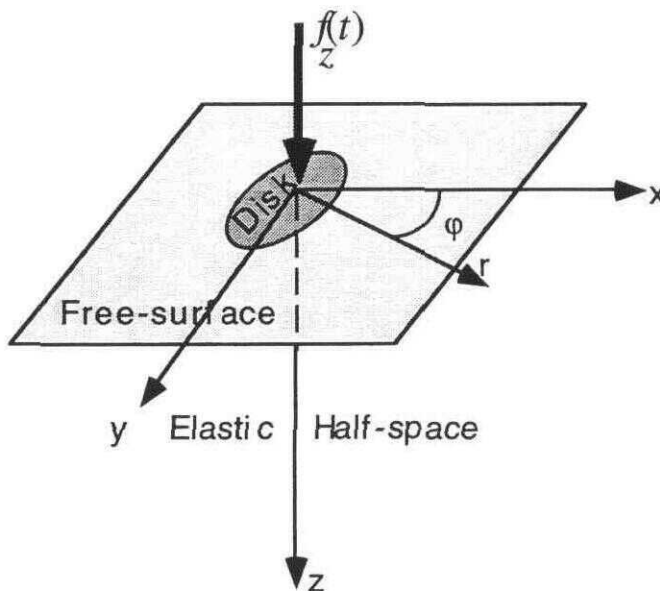


**Fig. A.4-1.** Disk on a free surface driven by a vertical force  $f_z(t)$ .

Mathematically these boundary conditions, for  $z = 0$ , can be written as:

$$\sigma_{zz} = \begin{cases} M f_z(t) : r < a \\ 0 : r > a \end{cases} \text{ and } \sigma_{rz} = 0 : \forall r, \quad (\text{A.4-1a})$$

where  $M$  is some reference magnitude of the driving force and  $a$  is the radius of the disk. We will now first take the Fourier-Bessel transform, followed by the Fourier transform of the boundary conditions given by equations (A.4-1a), to obtain:

$$B_0[\sigma_{zz}(t, r, z = 0)] = \sigma_{zz}^{(B_0)}(t, \zeta, z = 0) = \int_0^{\infty} \sigma_{zz}(t, r, z = 0) r J_0(r \zeta) dr,$$

$$\sigma_{zz}^{(B_0)}(t, \zeta, z = 0) = M f_z(t) \int_0^a r J_0(r \zeta) dr = M f_z(t) a J_1(a \zeta),$$

then:

$$\sigma_{zz}^{(F, B_0)}(f, \zeta, z = 0) = M f_z^{(F)}(f) a J_1(a \zeta). \quad (\text{A.4-2a})$$

Going through the same procedure with the second set of boundary conditions simply yields:

$$\sigma_{rz}^{(F, B_1)}(f, \zeta, z = 0) = 0. \quad (\text{A.4-2b})$$

Substitution of equations (A.3-7b) and (B.3-10b) into the transformed stress equations (A.3-12a) and (A.3-12c) and placing them in matrix form results in:

$$\begin{bmatrix} \sigma_{zz}^{(F, B_0)} \\ \sigma_{rz}^{(F, B_1)} \end{bmatrix} = \frac{1}{c} \begin{bmatrix} (m^2 - 2)m^2 \zeta^2 - m^2 \tilde{\alpha}^2, & -2 \beta \zeta \\ -2m^2 \tilde{\alpha} \zeta, & -\beta^2 - \zeta^2 \end{bmatrix} \begin{bmatrix} \Delta^{(F, B_0)} \\ \omega_{\phi}^{(F, B_1)} \end{bmatrix}, \quad (\text{A.4-3a})$$

where I have defined

$$\tilde{\alpha} = \sqrt{\zeta^2 - k_p^2}, \quad (\text{A.4-3b})$$

$$\beta = \sqrt{\zeta^2 - k_s^2}, \quad (\text{A.4-3c})$$

and

$$c = \frac{(2\pi f)^2}{\rho V_s^4} = \frac{k_s^4}{\rho (2\pi f)^2}, \quad (\text{A.4-3d})$$

to shorten the formula a bit. To match the boundary conditions and finally solve for the unknowns  $A$  and  $B$  we need to invert equation (A.4-3a) to find:

$$\begin{bmatrix} \Delta_{(F,B_0)} \\ \omega_{\phi}^{(F,B_1)} \end{bmatrix} = \frac{c}{D} \begin{bmatrix} -\beta^2 - \zeta^2, & 2m^2 \alpha \zeta \\ 2\beta \zeta, & (m^2 - 2)m^2 \zeta^2 - m^2 \alpha^2 \end{bmatrix} \begin{bmatrix} \sigma_{zz}^{(F,B_0)} \\ \sigma_{rz}^{(F,B_1)} \end{bmatrix}, \quad (\text{A.4-4a})$$

where the determinant,  $D$ , is given by:

$$D = \begin{vmatrix} (m^2 - 2)m^2 \zeta^2 - m^2 \alpha^2, & -2\beta \zeta \\ -2m^2 \alpha \zeta, & -\beta^2 - \zeta^2 \end{vmatrix} = m^2 F(\zeta), \quad (\text{A.4-4b})$$

and

$$F(\zeta) = (\beta^2 + \zeta^2)^2 - 4\alpha\beta\zeta^2 = (2\zeta^2 - k_s^2)^2 - 4\zeta^2 \sqrt{\zeta^2 - k_p^2} \sqrt{\zeta^2 - k_s^2}. \quad (\text{A.4-4c})$$

Therefore, matching boundary conditions in the transform domain, as given by equations (A.4-2a) and (A.4-2b) at  $z = 0$ , equation (A.4-4a) becomes:

$$\begin{bmatrix} A \\ B \end{bmatrix} = \frac{k_s^4}{\rho (2\pi f)^2 m^2 F(\zeta)} \begin{bmatrix} -\beta^2 - \zeta^2, & 2m^2 \alpha \zeta \\ 2\beta \zeta, & (m^2 - 2)m^2 \zeta^2 - m^2 \alpha^2 \end{bmatrix} \begin{bmatrix} M f_z^{(F)} a J_1(a \zeta) \\ 0 \end{bmatrix}. \quad (\text{A.4-5})$$

From equation (A.4-5) we can solve for  $A$  and  $B$  which can in turn be substituted into equations (A.3-7b) and (A.3.10b) to give the complete form of the dilatation and circulation. These will be respectively:

$$\Delta^{(F,B_0)}(f, \zeta, z) = \frac{k_s^4 M a}{(2\pi f)^2 \rho m^2} f_z^{(F)}(f) \frac{(k_s^2 - 2\zeta^2) J_1(\zeta a)}{\zeta F(\zeta)} \exp(-z \sqrt{\zeta^2 - k_p^2}), \quad (\text{A.4-6a})$$

and

$$\omega_\phi^{(F,B_1)}(f, \zeta, z) = \frac{2 k_s^4 M a}{(2\pi f)^2 \rho} f_z^{(F)}(f) \frac{\sqrt{\zeta^2 - k_p^2} J_1(\zeta a)}{F(\zeta)} \exp(-z \sqrt{\zeta^2 - k_s^2}). \quad (\text{A.4-6b})$$

By using the Fourier-Bessel transform identities given by equations (A.3-11b) and (A.3-11c) and the Fourier transform, the equations of motion embodied by equations (A.2-5a) and (A.2-5b) can be written as:

$$u_r^{(F,B_1)}(f, \zeta, z) = \frac{\zeta}{k_p^2} \Delta^{(F,B_0)} - \frac{1}{k_s^2} \frac{\partial \omega_\phi^{(F,B_1)}}{\partial z}, \quad (\text{A.4-7a})$$

and

$$u_z^{(F,B_0)}(f, \zeta, z) = \frac{\zeta}{k_s^2} \omega^{(F,B_1)} - \frac{1}{k_p^2} \frac{\partial \Delta^{(F,B_0)}}{\partial z}. \quad (\text{A.4-7b})$$

Direct substitution of equations (A.4-6a) and (A.4-6b) into equations (A.4-7a) and (A.4-7b) results in the transformed particle-displacement equations:

$$u_r^{(F,B_1)}(f, \zeta, z) = \frac{M a k_s^2}{(2\pi f)^2 \rho} f_z^{(F)}(f) \frac{J_1(\zeta a)}{F(\zeta)} \times \left[ (k_s^2 - 2\zeta^2) e^{(-z \sqrt{\zeta^2 - k_p^2})} + 2 \sqrt{\zeta^2 - k_p^2} \sqrt{\zeta^2 - k_s^2} e^{(-z \sqrt{\zeta^2 - k_s^2})} \right], \quad (\text{A.4-8a})$$

and

$$u_z^{(F,B_0)}(f, \zeta, z) = \frac{M a k_s^2}{(2\pi f)^2 \rho} f_z^{(F)}(f) \frac{J_1(\zeta a) \sqrt{\zeta^2 - k_p^2}}{\zeta F(\zeta)} \times \left[ 2\zeta^2 e^{(-z \sqrt{\zeta^2 - k_s^2})} + (k_s^2 - 2\zeta^2) e^{(-z \sqrt{\zeta^2 - k_p^2})} \right]. \quad (\text{A.4-8b})$$

To simplify the equations above and to bring them into a form more similar to the development of Miller and Pursey, we will make the following substitutions:

$$\zeta = \alpha \xi, \quad (\text{A.4-9a})$$

$$b = \frac{a}{\alpha}, \quad (\text{A.4-9b})$$

and

$$\alpha = |k_p|, \quad (\text{A.4-9c})$$

into equations (A.4-8a) and (A.4-8b). Then, keeping in mind we have incorporated the change of variable given by equation (A.4-9a), we will take the inverse Fourier-Bessel transform resulting in:

$$u_r^{(F)}(f, r, z) = K(f) \sqrt{\alpha} \times \int_0^{\infty} \frac{\xi J_1(\xi b)}{F_0(\xi)} \left[ (m^2 - 2\xi^2) e^{-\alpha z \sqrt{\xi^2 - 1}} + 2 \sqrt{\xi^2 - 1} \sqrt{\xi^2 - m^2} e^{-\alpha z \sqrt{\xi^2 - m^2}} \right] J_0(\alpha \xi r) d\xi \quad (\text{A.4-10a})$$

and

$$u_z^{(F)}(f, r, z) = \text{sgn}(k_p) K(f) \sqrt{\alpha} \times \int_0^{\infty} \frac{J_1(\xi b) \sqrt{\xi^2 - 1}}{F_0(\xi)} \left[ 2\xi^2 e^{-\alpha z \sqrt{\xi^2 - m^2}} + (m^2 - 2\xi^2) e^{-\alpha z \sqrt{\xi^2 - 1}} \right] J_0(\alpha \xi r) d\xi \quad (\text{A.4-10b})$$

where we have defined

$$K(f) = \frac{M a m^2 \sqrt{\alpha}}{(2\pi f)^2 \rho} f_z^{(F)}(f), \quad (\text{A.4-10c})$$

$$F_0(\xi) = (2\xi^2 - m^2)^2 - 4\xi^2 \sqrt{\xi^2 - 1} \sqrt{\xi^2 - m^2}, \quad (\text{A.4-10d})$$

and the sign function is defined as

$$\text{sgn}(x) = \begin{cases} -1 & : x < 1 \\ +1 & : x > 1 \end{cases}. \quad (\text{A.4-10e})$$

Note, also that a factor of  $\sqrt{\alpha}$  was kept out as well as in our definition of  $K(f)$  in equation (A.4-10c); this was done deliberately, since later in our approximation of the zeroth-order Bessel function this factor will cancel. Equation (A.4-10d) defines Rayleigh's function. It is central to the behavior of our integral equations of motion, since its zeros are the poles of the integrand and its radicals are the same as the ones present throughout the integrand. Understanding this function will lead us quite far in solving equations (A.3-10a) and (A.3-10b), so we will be spending quite a bit of effort in the next section towards this end. In Miller and Pursey's (1953) paper they make one further assumption namely  $k_p = 1$ , which would imply:

$$\text{sgn}(k_p) = 1, \quad (\text{A.4-11a})$$

$$b = a, \quad (\text{A.4-11b})$$

and

$$\alpha = 1. \quad (\text{A.4-11c})$$

If we were to make these substitutions into equation (A.4-10a) and (A.4-10b) we would find them equivalent to equations (72) and (73) in Miller and Pursey's paper up to within a single Fourier transform. This is because their analysis is based on a monochromatic source while I have not made that assumption. I could, however, make the assumption that the input signal is analytic by replacing the source signature  $f_z(t)$  with its analytic

extension  $f_z(t) + i H[f_z(t)]$ , where  $H[\cdot]$  is the Hilbert transform of the argument. This would cause its Fourier transform to become one-sided; in this situation only positive frequencies  $f$  would be present allowing us to drop the term  $\text{sgn}(k_p)$  since it would always be equal to one. This procedure poses no difficulty if we make sure only to consider the real part of the relevant function when we deal with measurable quantities.

## E5: Branch cuts and poles of Rayleigh's function

As mentioned in the previous section, Rayleigh's function, given by equation (A.4-10d) and reproduced here as:

$$F_0(\xi) = (2\xi^2 - m^2)^2 - 4\xi^2 \sqrt{\xi^2 - 1} \sqrt{\xi^2 - m^2}, \quad (\text{A.5-1})$$

is central to the understanding and solution of equations (A.4-10a) and (A.4-10b), the integral equations of motion. The first point we shall address is the multiple-valued nature of  $F_0(\xi)$ , which arises from the multivalued nature of the radicals. To make future developments easier, I will factor and regroup the radicals in equation (A.5-1) in the form:

$$F_0(\xi) = (2\xi^2 - m^2)^2 - 4\xi^2 ( \sqrt{(\xi - 1)} \sqrt{(\xi - m)} ) ( \sqrt{(\xi + 1)} \sqrt{(\xi + m)} ), \quad (\text{A.5-2})$$

I will now analyze in some painful detail the behavior of the radicals in equation (A.5-2). If the reader is already familiar with this, skip to the next section A.5.2.

### A.5.1: Branch Cuts

Rayleigh's function consists of, among other things, products of terms of the form

$$w = \sqrt{(\xi - \kappa)} : \kappa = 1, m. \quad (\text{A.5.1-3a})$$

We will transform equation (A.5.1-3a) using polar coordinates centered about the point  $\kappa$ . To accomplish this we set  $\theta = \arg(\xi - \kappa)$  and  $r = |\xi - \kappa|$  as shown in figure A.5.1-1.

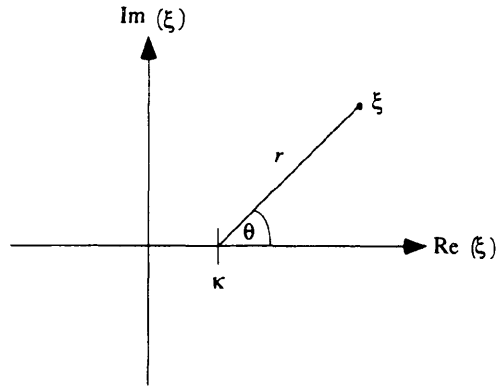


**Fig. A.5.1-1.** Polar coordinate transformation.

With this definition we can rewrite equation (A.5.1-3a) as:

$$w = \sqrt{r} e^{i\theta/2} = \rho e^{i\varphi}. \quad (\text{A.5.1-3b})$$

From this we can see that for fixed  $\theta = \theta_0 = \theta_0 + 2\pi$  and  $r$ , which specifies a unique point  $\xi_0$  in the  $\xi$  plane, we will have two distinct values in the  $w$  (figure A.5.1-2) plane given by:

$$w_0 = \sqrt{r} e^{i\theta_0/2} = \rho e^{i\varphi_0} \quad (\text{A.5.1-3c})$$

and

$$w_1 = \sqrt{r} e^{i(\theta_0 + 2\pi)/2} = \rho e^{i\varphi_1}. \quad (\text{A.5.1-3d})$$

The mapping from the  $\xi$  plane to the  $w$  plane is represented in figure A.5.1-2.

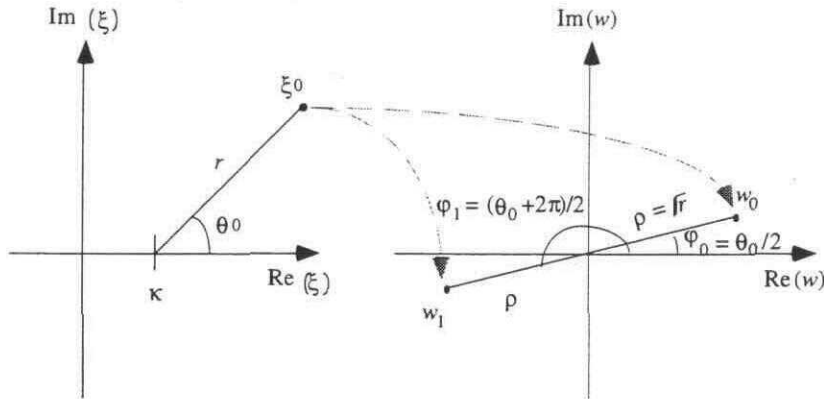


**Fig. A.5.1-2.** Mapping of a point in the  $\xi$  plane into points in the  $w$  plane, as determined by the function  $w = \sqrt{(\xi - \kappa)}$ .

In order to have a unique value for equation (A.5.1-3a) we introduce the device of a branch cut. The branch cut is an imaginary line on the  $\xi$  plane which we will not allow a continuous path to cross. In our case, a convenient choice, of infinitely many possibilities, is to start at the branch point  $\kappa$  and follow the real  $\xi$  axis. More formally this branch cut can be defined as the locus of all points in the complex  $\xi$  plane such that  $\text{Re}(\xi) \geq \kappa$  and  $\text{Im}(\xi) = 0$  as shown in figure A.5.1-3a by the bold line in the complex  $\xi$  plane.

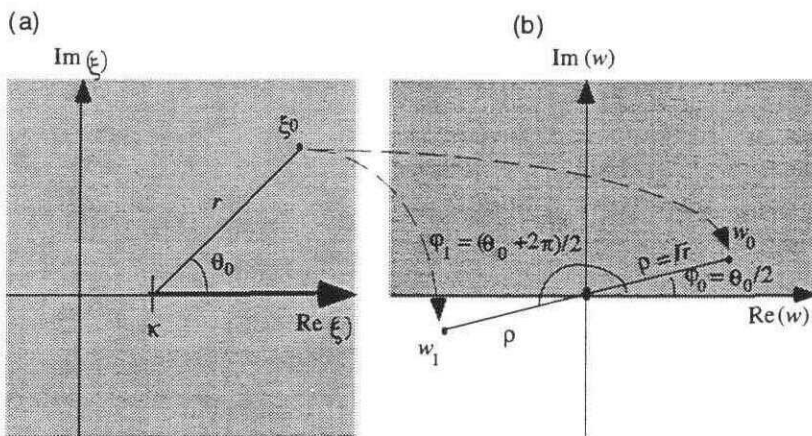


**Fig. A.5.1-3.** A particular branch cut of the function  $w = \sqrt{(\xi - \kappa)}$  and the mapping of the resultant  $\xi$  plane into the reduced  $w$  plane as shown in grey.

This branch cut effectively constrains  $\xi = r e^{i\theta}$  to be such that  $r > 0$  and  $0 < \theta < 2\pi$ , which in turn constrains  $w = \sqrt{r} e^{i\theta/2} = \rho e^{i\varphi}$ , to be defined only when  $\rho > 0$  and  $0 < \varphi < \pi$ . These regions are represented by grey excluding the branch cut in figure A.5.1-

3a and the origin in figure A.5.1-3b. Another useful method to visualize the multivalued nature of a function is using the device of Riemann sheets. For the present problem we separate the  $\xi$  plane into two distinct planes, then we cut both planes along the branch cut and fuse the two sheets along the branch cuts. Each sheet represents a certain unique range of the argument  $\theta$  that maps uniquely into the  $w$  plane. This is represented in figure A.5.1-4

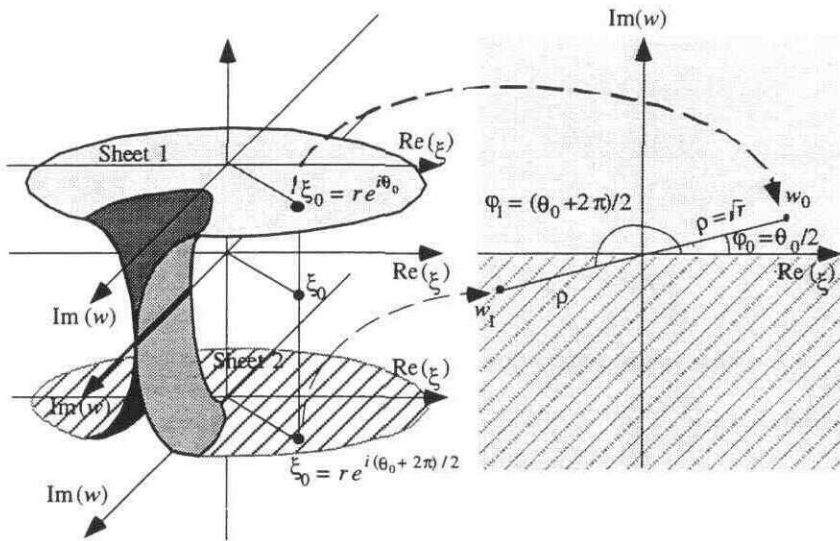


**Fig. A.5.1-4.** Riemann sheets in the  $\xi$  plane and its corresponding image in the  $w$  plane as determined by the function  $w = \sqrt{(\xi - \kappa)}$ .

The two Riemann sheets help to clarify the multiple-valued nature of the function  $w = \sqrt{(\xi - \kappa)}$ , as well as showing how we must go from one sheet to another when we cross the branch cut.

Now we will consider the case where we have a product of functions of the form given by equation (A.5.1-3a), where

$$W = \sqrt{\xi - \kappa_1} \sqrt{\xi - \kappa_2}, \quad (\text{A.5.1-4a})$$

such that  $\kappa_1$  and  $\kappa_2$  are positive real numbers. Two special cases, of course, are 1 and  $m$ . As in the previous discussion, we will introduce shifted polar coordinates for each of the radicals, as shown in figure A.5.1-5. In these polar coordinates equation (A.5.1-4a) becomes:

$$W = \sqrt{r_1 r_2} e^{i(\theta_1 + \theta_2)/2} \quad (\text{A.5.1-4b})$$

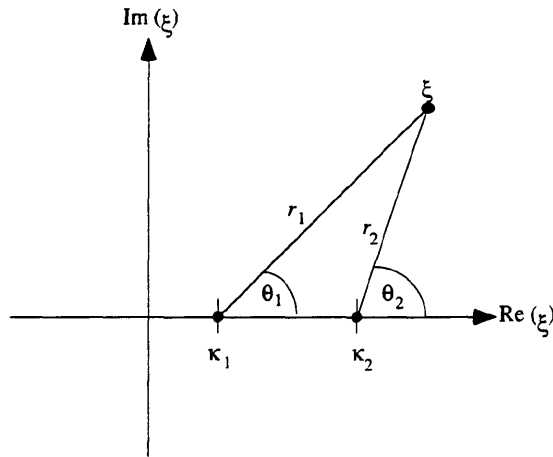


**Fig. A.5.1-5.** Shifted polar coordinates for the function  $W = \sqrt{\xi - \kappa_1} \sqrt{\xi - \kappa_2}$ .

again we can see the multivalued nature of this function. The simplest way to obtain uniqueness for this function is to consider each radical in turn, and each corresponding branch cut. Then the combined domain common to both and not crossing either branch cut will yield a specific branch for  $D$ . Using the branch cuts as previously defined for equation (A.5.1-3a) for each of the radicals yields a specific branch of  $D$ . The branch cut can be defined to be the locus of points in the complex  $\xi$  plane such that  $\text{Re}(\xi) > \kappa_1$  and  $\text{Im}(\xi) = 0$ , which is the half-line on the real axis starting at  $\kappa_1$  and extending to positive infinity. This branch cut in the  $\xi$  plane defines a domain given by  $r_1 > 0$ ,  $r_2 > 0$  and  $0 < \theta_k < 2\pi$  in which  $W$  is single-valued and analytic (figure A.5.1-6).

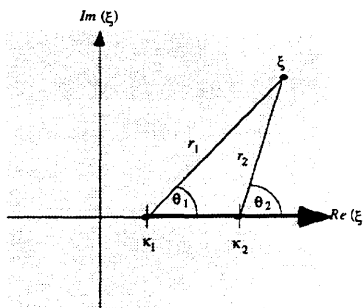


**Fig. A.5.1-6.** A possible branch cut and domain of the function  $W = \sqrt{\xi - \kappa_1} \sqrt{\xi - \kappa_2}$ .

This, however, is not the largest domain in which  $W$  is analytic. To see this, we will recast equation (A.5.1-4b), along with its reduced domain of definition, as:

$$W_0 = \sqrt{r_1 r_2} e^{i(\theta_1 + \theta_2)/2}; r_1 > 0, r_2 > 0, 0 < \theta_k < 2\pi, k = 1, 2, \quad (\text{A.5.1-5a})$$

where I have introduced a subscript to emphasize this particular branch. Now we shall introduce another branch that has a domain and branch cut as shown in figure A.5.1-7.

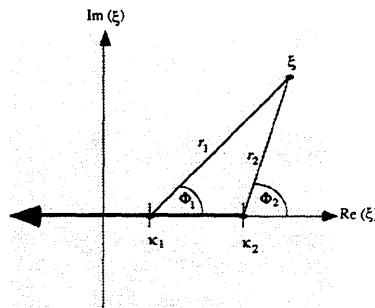


**Fig. A.5.1-7.** Another equally good branch cut and domain of the function  $W = \sqrt{\xi - \kappa_1} \sqrt{\xi - \kappa_2}$ .

This would give us a new branch and domain of definition represented symbolically as

$$W_1 = \sqrt{r_1 r_2} e^{i(\Phi_1 + \Phi_2)/2}; r_1 > 0, r_2 > 0, 0 < \Phi_k < 2\pi, k = 1, 2. \quad (\text{A.5.1-5b})$$

What I am attempting to show is that  $W_0$  is analytic even on the half-line  $\text{Re}(\xi) > \kappa_2$  and  $\text{Im}(\xi) = 0$ . Towards this end we notice that when  $\xi$  is above this half-line  $W_0 = W_1$ . To see this one only has to notice that  $\theta_k = \Phi_k, k = 1, 2$  within this domain. When  $\xi$  is below the half-line  $\theta_k = \Phi_k + 2\pi, k = 1, 2$  then  $e^{i\theta_k/2} = e^{i(\Phi_k + 2\pi)/2} = -e^{i\Phi_k/2}$ , which means again we have  $W_0 = W_1$ . Since we have  $W_0 = W_1$  in a domain containing the half-line  $\text{Re}(\xi) > \kappa_2$  and  $\text{Im}(\xi) = 0$ , and by the domain defined in equation (A.5.1-6b)  $W_1$  is analytic there, then  $W_0$  must also be analytic there. This means we can expand the domain of definition for our branch as shown in figure A.5.1-8.

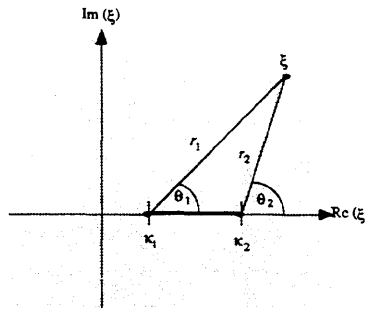


**Fig. A.5.1-8.** Final branch cut and domain of definition for the function  $W = \sqrt{\xi - \kappa_1} \sqrt{\xi - \kappa_2}$ .

To see that this is the largest domain on which  $W$  is analytic we need only to observe what happens as we approach the branch cut from either direction. Consider a point  $\xi$  at a distance  $\epsilon$  perpendicularly above the branch cut, as shown in figure A.5.1-9a.

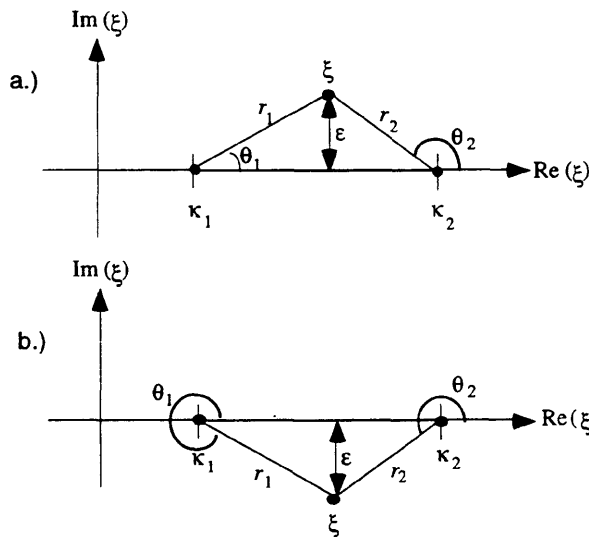


**Fig. A.5.1-9.** Behavior of  $W = \sqrt{\xi - \kappa_1} \sqrt{\xi - \kappa_2}$  around branch cut.

As  $\epsilon$  approaches zero (figure A.5.1-9a), then  $\theta_1 \rightarrow 0$  and  $\theta_2 \rightarrow \pi$ , which means

$$W_0 = \sqrt{r_1 r_2} e^{i(\theta_1 + \theta_2)/2} \rightarrow i \sqrt{r_1 r_2}, \tag{A.5.1-6a}$$

and as  $\epsilon$  approaches zero in figure A.5.1-9a, then  $\theta_1 \rightarrow 2\pi$  and  $\theta_2 \rightarrow \pi$  which means

$$W_0 = \sqrt{r_1 r_2} e^{i(\theta_1 + \theta_2)/2} \rightarrow -i \sqrt{r_1 r_2}. \tag{A.5.1-6b}$$

From relations (A.5.1-6a) and (A.5.1-6b) we can see that  $W_0$  is not even continuous at the branch cut, so no extension is possible; therefore we have the largest domain defined. We can write this branch of the function  $W = \sqrt{\xi - \kappa_1} \sqrt{\xi - \kappa_2}$  symbolically as

$$w = \sqrt{r_1 r_2} e^{i(\theta_1 + \theta_2)/2}; r_k > 0, r_1 + r_2 > \kappa_2 - \kappa_1, 0 \leq \theta_k \leq 2\pi, k = 1, 2. \quad (\text{A.5.1-7})$$

Now we shall examine the mapping from the  $\xi$  plane onto the  $w$  plane. First consider the open half-line perpendicular and centred on the branch cut in the  $\xi$  plane, where  $\theta_1 + \theta_2 = \pi$  and  $r_1 = r_2 > (\kappa_2 + \kappa_1) / 2$ . This open half-line maps onto the open half-line  $\text{Im}(w) > \frac{|\kappa_2 - \kappa_1|}{2}$  and  $\text{Re}(w) = 0$  in the  $w$  plane. By the same argument, the negative half of this line in the  $\xi$  plane maps onto the half-line  $\text{Im}(w) < -\frac{|\kappa_2 - \kappa_1|}{2}$  and  $\text{Re}(w) = 0$ . Furthermore each point in the upper half of the  $\xi$  plane maps onto the upper half of the  $w$  plane. The same goes for the lower half-planes (figure A.5.1-10).

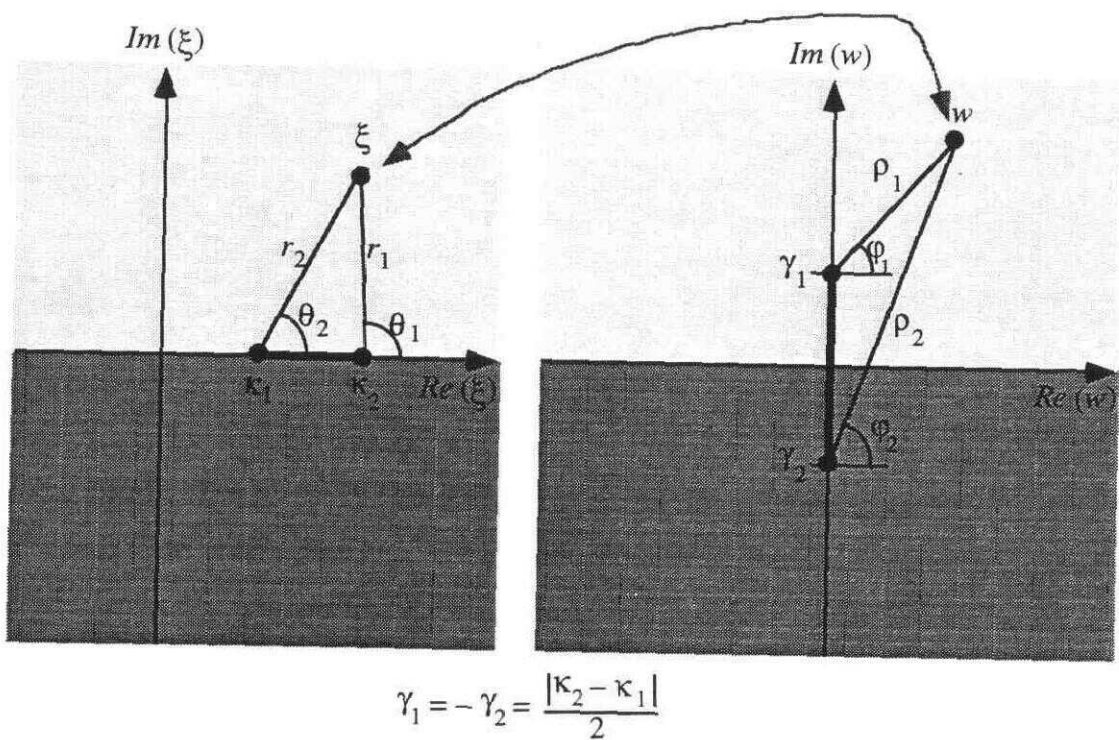


**Fig. A.5.1-10.** Mapping between  $\xi$  and  $w$  planes due to the function  $w = \sqrt{\xi - \kappa_1} \sqrt{\xi - \kappa_2}$ .

The mapping, as illustrated in figure A.5.1-10, with branch cuts as drawn, can be shown to be a one-one, onto mapping between the two cut planes. For a more detailed discussion

refer to (Churchill, Brown and Verhey, 1976). For completeness I will construct the Riemann surfaces for the function  $W = \sqrt{\xi - \kappa_1} \sqrt{\xi - \kappa_2}$ . To see what happens as we move around the complex  $\xi$  plane, we shall consider three cases. This will help make sense of our eventual Riemann-surface diagram. First, referring to figure A.5.1-10, consider what happens when a point  $\xi$  is moved around the branch cut  $n$  times in a counter-clockwise direction, where  $n$  is a positive integer. Symbolically,

$$\theta_1 \rightarrow \theta_1 + 2n\pi, \quad (\text{A.5.1-8a})$$

$$\theta_2 \rightarrow \theta_2 + 2n\pi \quad (\text{A.5.1-8b})$$

$$\begin{aligned} W &= \sqrt{r_1 r_2} e^{i(\theta_1 + \theta_2)/2} \rightarrow \sqrt{r_1 r_2} e^{i(\theta_1 + \theta_2)/2} e^{i4n\pi/2} \\ &= \sqrt{r_1 r_2} e^{i(\theta_1 + \theta_2)/2}. \end{aligned} \quad (\text{A.5.1-8c})$$

This shows that circling the branch cut keeps us on the same branch of  $D$ . The results would be the same if we went in a clockwise direction. Secondly we will consider what happens when we circle the branch point  $\kappa_1$  an even number of times, say  $2n$ , in a counter-clockwise direction. In this case we have:

$$\theta_1 \rightarrow \theta_1 + 4n\pi, \quad (\text{A.5.1-9a})$$

$$\theta_2 \rightarrow \theta_2, \quad (\text{A.5.1-9b})$$

$$\begin{aligned} W &= \sqrt{r_1 r_2} e^{i(\theta_1 + \theta_2)/2} \rightarrow \sqrt{r_1 r_2} e^{i(\theta_1 + \theta_2)/2} e^{i4n\pi/2} \\ &= \sqrt{r_1 r_2} e^{i(\theta_1 + \theta_2)/2}. \end{aligned} \quad (\text{A.5.1-9c})$$

Here again we remain on the same branch. This argument is independent of which branch point we choose or the direction of rotation. Thirdly we will consider what happens when we circle the branch point  $\kappa_1$  an odd number of times, say  $(2n - 1)$ , in a counter-clockwise direction. This time we have:

$$\theta_1 \rightarrow \theta_1 + (2n - 1) 2\pi, \quad (\text{A.5.1-10a})$$

$$\theta_2 \rightarrow \theta_2, \quad (\text{A.5.1-10b})$$

$$\begin{aligned} W_0 &= \sqrt{r_1 r_2} e^{i(\theta_1 + \theta_2)/2} \rightarrow \sqrt{r_1 r_2} e^{i(\theta_1 + \theta_2)/2} e^{i(2n-1)\pi/2} \\ &= -\sqrt{r_1 r_2} e^{i(\theta_1 + \theta_2)/2}. \end{aligned} \quad (\text{A.5.1-10c})$$

Now we have arrived at the second branch of our function  $D$ . Again this is independent of the branch point we choose or the direction of rotation. With this in mind, we will construct the Riemann sheets as shown in figure A.5.1-11.

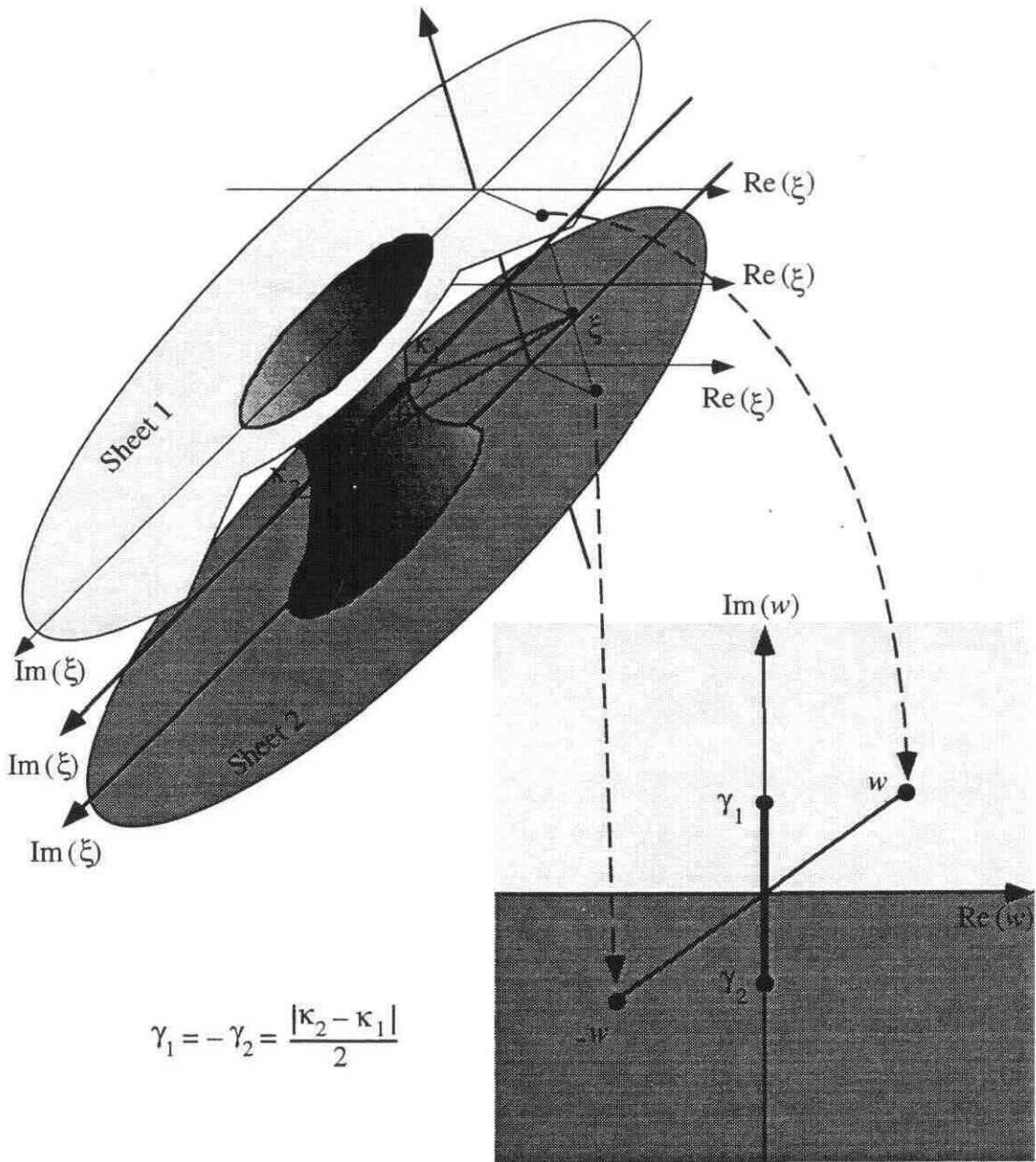


**Fig. A.5.1-11.** Riemann sheets for the function  $W = \sqrt{\xi - \kappa_1} \sqrt{\xi - \kappa_2}$ .

It is interesting to note that if we introduce a branch cut, as indicated in figures A.5.1-10 and A.5.1-11, in the  $w$  plane it is possible to define an inverse mapping that takes values in the  $w$  plane onto the  $\xi$  plane. It should be possible to introduce similar Riemann sheets for the  $w$  plane and define a one-one, onto mapping based on the function

$$W = \sqrt{\xi - \kappa_1} \sqrt{\xi - \kappa_2}.$$

Finally we are led to consider the mapping:

$$w = \left( \sqrt{(\xi - \kappa_1)} \sqrt{(\xi - \kappa_2)} \right) \left( \sqrt{(\xi + \kappa_1)} \sqrt{(\xi + \kappa_2)} \right). \quad (\text{A.5.1-11})$$

This is nothing more than what we have considered in formula (A.5.1-4a) in the previous paragraph with an additional product of radicals. The behavior of this function can be studied in exactly the same fashion as its predecessor. Its branch cuts will be given by  $\kappa_1 < \text{Re}(\xi) < \kappa_2$  and  $\text{Im}(\xi) = 0$  and shown in figure A.5.1-12.

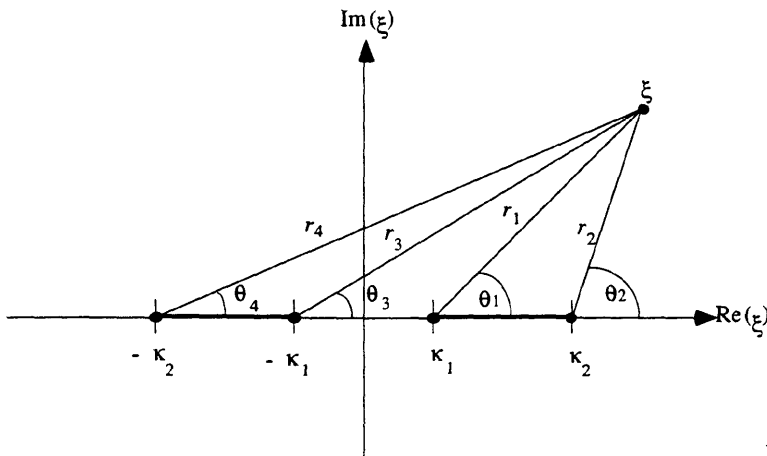


**Fig. A.5.1-12.** Branch cuts and domain of definition for the function  $w = \left( \sqrt{(\xi - \kappa_1)} \sqrt{(\xi - \kappa_2)} \right) \left( \sqrt{(\xi + \kappa_1)} \sqrt{(\xi + \kappa_2)} \right)$ .

Again, comparison to the previous case and examination of figure A.5.1-12 lead us to define a particular branch of this function to be

$$w = \sqrt{r_1 r_2 r_3 r_4} e^{i(\theta_1 + \theta_2 + \theta_3 + \theta_4)/2},$$

$$r_k > 0, r_1 + r_2 \text{ and } r_3 + r_4 > \kappa_2 - \kappa_1, 0 \leq \theta_k \leq 2\pi, k = 1, 2. \quad (\text{A.5.1-12})$$

To see that equation (A.5.1-12) is indeed a branch of the function  $w$ , one only has to go through the same argument as in the previous case and consider what happens as we allow a point to cross one branch cut and return to the same location, noting that the other branch cut would give no contribution. Secondly, we can show that crossing one branch cut then the other and returning to the same point leaves the function unaltered, just as

going through the same branch cut twice would do. With this in mind, we know that there must be two Riemann sheets for this function, as show in figure A.5.1-13.

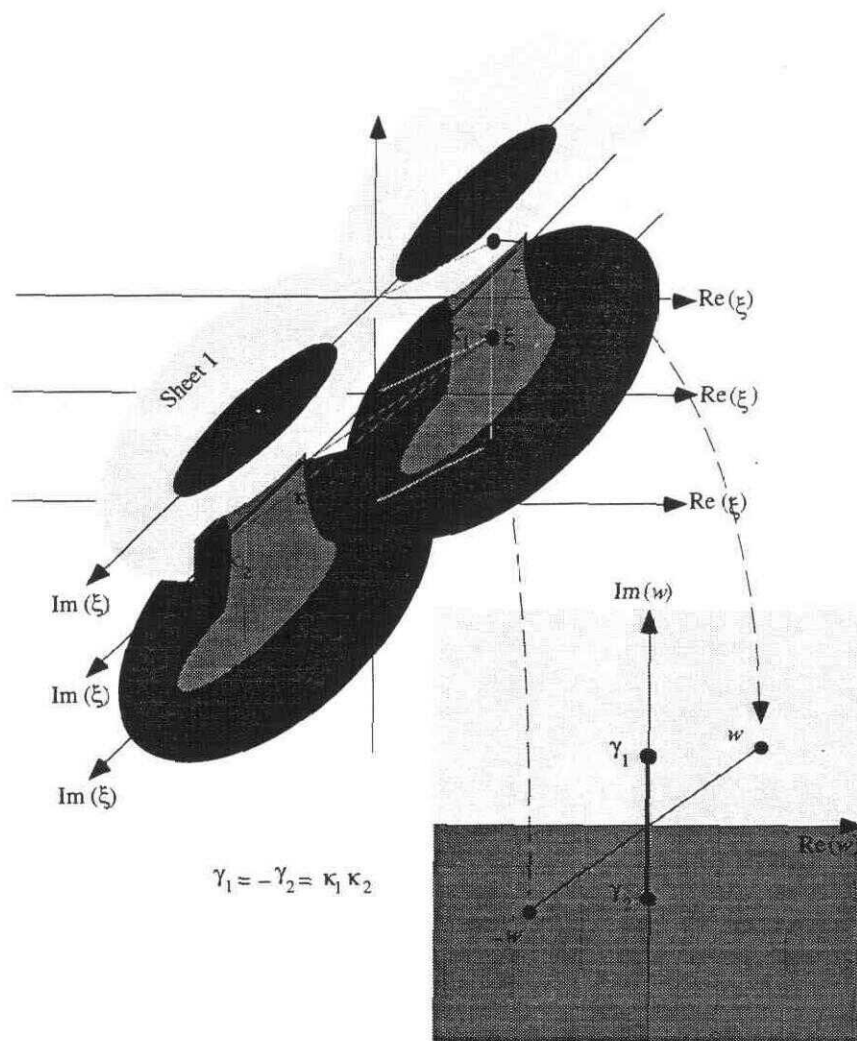


**Fig. A.5.1-13.** Riemann sheets for the function  
 $w = \left( \sqrt{(\xi - \kappa_1)} \sqrt{(\xi - \kappa_2)} \right) \left( \sqrt{(\xi + \kappa_1)} \sqrt{(\xi + \kappa_2)} \right)$ .

With the preliminary work done, we can finally deal with Rayleigh's function as given by equation (A.5-2). The radicals in Rayleigh's function have exactly the form as given by equation (A.5.1-11). Since the rest of the terms in Rayleigh's function are single-valued and analytic, the branch cuts will be identical to those represented by equation (A.5.1-11) and shown in figure A.5.1-12. The only alterations are to define the constants  $\kappa_1 = 1$  and  $\kappa_2 = m$ . Now we can proceed to finding the zeros of the Rayleigh' function as given by equations (A.5-1) and (A.5-2), which, as mentioned is central to any analysis of the integral equations of motion, equations (A.4-10a) and (A.4-10b).

### A.5.2: Zeros of Rayleigh's Function

For convenience, I will again reproduce Rayleigh's equation (A.5-1) here as:

$$F_0(\xi) = (2\xi^2 - m^2)^2 - 4\xi^2 \sqrt{\xi^2 - 1} \sqrt{\xi^2 - m^2}. \quad (\text{A.5.2-1})$$

To study the zeros of this equation, we need a result from complex analysis (Churchill, Brown and Verhey, 1976, p. 296-297), which states that an analytic function,  $f$ , with a finite number of simple poles and zeros within, and not on, a closed contour  $C$  described in the positive sense (counter-clockwise) will satisfy the relationship:

$$\frac{1}{2\pi i} \int_C \frac{f'(\xi)}{f(\xi)} d\xi = Z - P, \quad (\text{A.5.2-2})$$

where  $Z$  is the number of zeros and  $P$  is the number of poles of  $f$  within  $C$ . The proof of the relationship given by equation (A.5.2-2) rests on two simple facts: firstly, the zeros of order  $m_0$  of  $f$  map into poles of  $f'/f$  with residue  $m_0$ ; and secondly, the poles of order  $m_p$  of  $f$  map into poles of  $f'/f$  with residue  $m_p$ . This can be seen by considering a single isolated zero of order  $m_0$  of  $f$ , say  $\xi_0$ , which means in some neighborhood of  $\xi_0$  we can write:

$$f(\xi) = (\xi - \xi_0)^{m_0} g(\xi), \quad (\text{A.5.2-3a})$$

such that  $g(\xi)$  is by definition analytic within that neighborhood and  $g(\xi_0) \neq 0$ . From equation (A.5.2-3a) we get:

$$f'(\xi) = m_0 (\xi - \xi_0)^{m_0-1} g(\xi) + (\xi - \xi_0)^{m_0} g'(\xi). \quad (\text{A.5.2-3b})$$

Combining equations (A.5.2-3a) and (A.5.2-3b) results in:

$$\frac{f'(\xi)}{f(\xi)} = \frac{m_0}{(\xi - \xi_0)} + \frac{g'(\xi)}{g(\xi)}, \quad (\text{A.5.2-3c})$$

which, as mentioned earlier, has a simple pole with residue  $m_0$ . In the same fashion, if we consider a single isolated pole of order  $m_p$  of  $f$ , say  $\xi_p$ , then within some neighborhood of  $\xi_p$  we have:

$$f(\xi) = (\xi - \xi_p)^{-m_p} h(\xi), \quad (\text{A.5.2-4a})$$

where again  $h(\xi)$  is analytic within the neighborhood and  $h(\xi_0) \neq 0$ . Again we take the derivative of equation (A.5.2-4a) to get:

$$f'(\xi) = -m_p (\xi - \xi_p)^{-m_p - 1} h(\xi) + (\xi - \xi_p)^{-m_p} h'(\xi). \quad (\text{A.5.2-4b})$$

Dividing equation (A.5.2-4b) by equation (A.5.2-4a) results in:

$$\frac{f'(\xi)}{f(\xi)} = -\frac{m_p}{(\xi - \xi_p)} + \frac{h'(\xi)}{h(\xi)}, \quad (\text{A.5.2-4c})$$

which again has a simple pole with residue  $-m_p$ . Now if we introduce closed contours around all the poles and zeros of  $f$  within  $C$ , evaluate the integral given in equation (A.5.2-2) with the new path described, and add up all the residues, equation (A.5.2-2) would be the result. Now we will apply these results to Rayleigh's function. A good discussion of this material can be found in Achenbach (1980).

By examination of Rayleigh's equation (A.5.2-1) we can immediately tell that there are no poles within any given contour  $C$ ; therefore, if we apply the result from equation (A.5.2-2) to Rayleigh's equation, we would get:

$$\frac{1}{2\pi i} \int_C \frac{F_0'(\xi)}{F_0(\xi)} d\xi = Z, \quad (\text{A.5.2-5})$$

where  $Z$  is the number of zeros of Rayleigh's function. Knowing the branch cuts of Rayleigh's function to be the same as the one given in figure A.5.1-12, we will choose a path of integration  $C$  for equation (A.5.2-5) as shown in figure A.5.2-1 below.

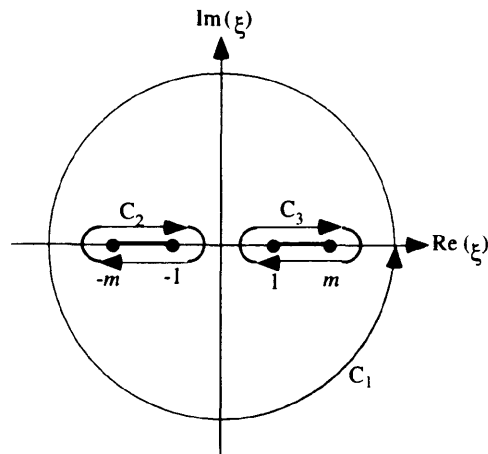


**Fig. A.5.2-1.** Contour of integration to find numbers of zeroes of Rayleigh's function.

As shown in figure A.5.2-1 we have broken the contour of integration  $C$  into three parts such that  $C = C_1 + C_2 + C_3$  and the sense of integration over each contour is indicated by the arrowheads. Now we shall map the integral given by equation (A.5.2-5) into the  $\zeta$  plane using the mapping

$$\zeta = F_0(\xi), \quad (\text{A.5.2-6})$$

where  $F_0$  is again the Rayleigh's function given by equation (A.5.2-1). The mapping above transforms both the integrand and the path of integration, which we will write as

$$\frac{1}{2\pi i} \int_{C_\zeta} \frac{d\zeta}{\zeta} = Z. \quad (\text{A.5.2-7})$$

The path,  $C_\zeta$ , is determined by the mapping of path  $C$  by equation (A.5.2-6). The first thing that we notice is that the integrand in equation (A.5.2-7) has only one simple pole at  $\zeta = 0$ , with residue 1; this means that the integral is solely determined by how many times the new path  $C_\zeta$  circles the origin. The number of times  $C_\zeta$  circles the origin, in the counter-clockwise direction, will exactly equal the number of zeroes Rayleigh's function actually has. This is known as the argument principle and is discussed in some detail by Churchill, Brown and Verhey (1976). So we will examine how our path  $C$  maps into the  $\zeta$  plane.

Due to the bilateral symmetry about the  $\text{Im}(\xi)$  axis, we will consider in detail the mapping of only one of the paths around the branch cuts, namely the mapping of the path  $C_3$ , as shown in figure A.5.2-1 and expanded in figure A.5.2-2 below.

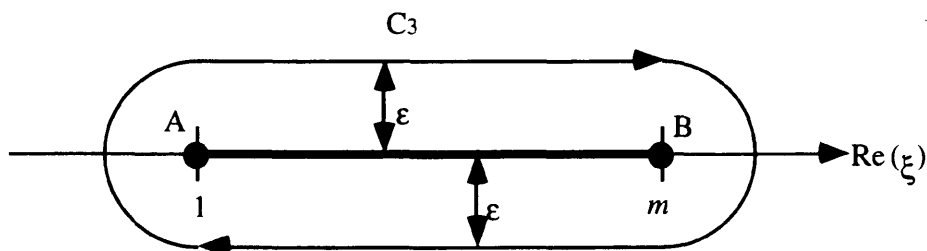


**Fig. A.5.2-2.** One branch cut of Rayleigh's function and path of integration  $C_3$ .

In figure A.5.2-2 I have introduced a small positive quantity  $\epsilon$  to indicate that the path  $C_3$  is to be considered as arbitrarily close to the branch cut from point A to point C. Now consider the different parts of the path  $C_3$  that is almost on the branch cut first, at point A,

$$F_0(1) = (2 - m^2)^2. \quad (\text{A.5.2-8a})$$

Second, between points A and B but above the branch cut,

$$F_0(\xi) = (2\xi^2 - m^2)^2 - i 4\xi^2 \sqrt{\xi^2 - 1} \sqrt{m^2 - \xi^2}. \quad (\text{A.5.2-8b})$$

Third, between points A and B but below the branch cut,

$$F_0(\xi) = (2\xi^2 - m^2)^2 + i 4\xi^2 \sqrt{\xi^2 - 1} \sqrt{m^2 - \xi^2}. \quad (\text{A.5.2-8c})$$

Finally, at point B,

$$F_0(\xi) = m^4. \quad (\text{A.5.2-8d})$$

To see how to obtain relations (A.5.2-8b) and (A.5.2-8c), refer to the arguments surrounding figure A.5.1-9 and equations (A.5.1-6a) and (A.5.1-6b). The mapping is shown in figure A.5.2-3 for the special case of  $m = 2$ . One thing is certain the path never circles the origin in the  $\zeta$  plane.

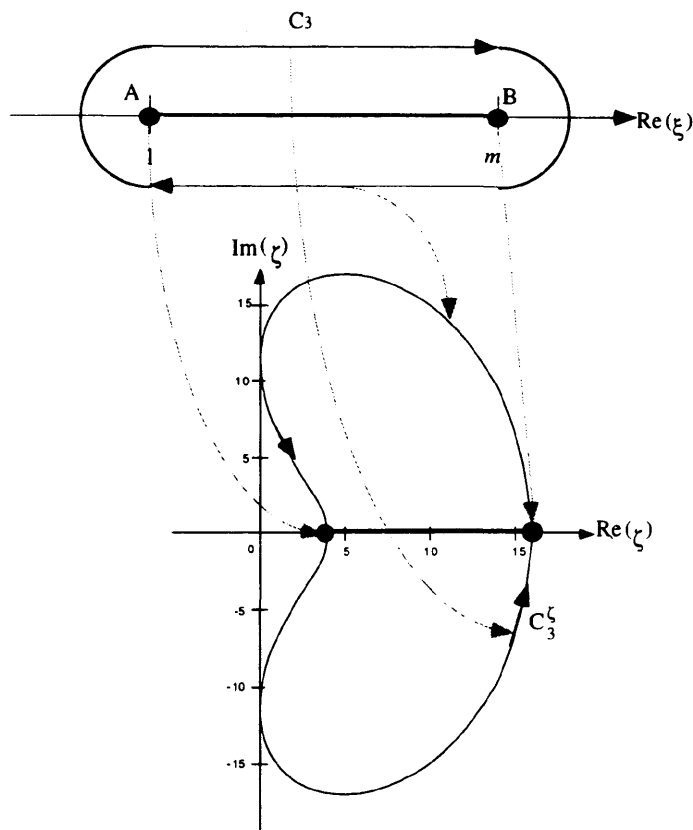


**Fig. A.5.2-3.** Mapping of path  $C_3$  in the  $\xi$  plane onto path  $C_3^\zeta$  in the  $\zeta$  plane, for the case where  $m = 2$ .

As mentioned before, the other branch cut will just be the mirror image of this one, and so will be ignored. Since we only have a simple pole at the origin, the two mapped contours,  $C_3^\zeta$  and  $C_2^\zeta$ , associated with the branch cuts will have no contribution to the total integral given by equation (A.5.2-7). Now we need to consider the large circular path  $C_1$  in the  $\xi$  plane; on this path  $|\xi|$  is large. When  $|\xi| \gg m > 1$  we can factor out  $|\xi|$  from each of the radicals in Rayleigh's function and then expand them in a binomial series, which after cross-multiplication and cancellation of terms becomes:

$$F_0(\xi) = 2 \xi^2 (1 - m^2) + O(1). \quad (\text{A.5.2-9})$$

From equation (A.5.2-9) we can see that for very large  $|\xi|$ , Rayleigh's function behaves like  $\xi^2$ , which means that for  $\xi = r e^{i\theta}$ ,  $0 \leq \theta \leq 2\pi$ , we have  $\zeta = \xi^2 = r^2 e^{i2\theta} = \rho e^{i\varphi}$ ,  $0 \leq \varphi \leq 4\pi$ , where I have ignored scalar terms. This shows that as we circumnavigate the path  $C_1$  once in the  $\xi$  plane, the equivalent path  $C_1^\zeta$  in the  $\zeta$  plane will have been circled

twice. From this argument we can see that the integral in equation (A.5.2-7) is identically two. This in turn means we have only two zeros to Rayleigh's function.

There is more that can be said about these two zeros. Firstly, since Rayleigh's function is an equation in  $\xi^2$ , the zeros must be the negative of each other; in other words, if  $\xi_0$  is a zero of Rayleigh's function so is  $-\xi_0$ . Secondly, we have:

$$F_0(m) = m^4 > 0, \quad (\text{A.5.2-10a})$$

and by equation (A.5.2-9) for very large  $\xi$  say  $\xi = \xi_L$ , we can write:

$$F_0(\xi_L) \rightarrow 2 \xi_L^2 (1 - m^2) < 0, \quad (\text{A.5.2-10b})$$

which is true since  $m = V_p / V_s > 1$ . This means that, for some real number between the real numbers  $m$  and  $\xi_L$ , the function  $F_0$  must be zero or else it would be discontinuous, which in turn means that the two zeros of  $F_0$  are real numbers. Finally, we get the result that the zero is greater than  $|m|$ , which follows directly from our second point.

Summarizing the results for the zeros of Rayleigh's equation:

$$\text{there are only two zeros of } F_0; \quad (\text{A.5.2-11a})$$

$$\text{if } \xi_0 \text{ is a zero of } F_0 \text{ so is } -\xi_0; \quad (\text{A.5.2-11b})$$

$$\xi_0 \text{ is a real number, and} \quad (\text{A.5.2-11c})$$

$$|\xi_0| > m. \quad (\text{A.5.2-11d})$$

The reasons I have spent the effort to analyze in detail the zeros of Rayleigh's equation are threefold: the first is to give a method of choosing zeros for Rayleigh's equations after rationalization (this, I believe, was done incorrectly by Miller and Pursey (1953) which caused me quite a bit of confusion); second, a good understanding of the behavior of the branchcuts of Rayleigh's equation will help when we find approximate solutions to the integral equations of motion using the method of steepest descent; and finally, the material covered comes from a few sources and it never hurts to put it all in one place.

Now we proceed to the standard method of finding the zeros of Rayleigh's function, guided by points (A.5.2-11a) through (A.5.2-11d). If we take Rayleigh's equation (A.5.2-1), set it to zero, move the radicals to one side of the equation, and then square the expression, the result would be

$$(2\xi^2 - m^2)^4 = 16\xi^4(\xi^2 - 1)(\xi^2 - m^2), \quad (\text{A.5.2-12})$$

which after substitution of  $\omega = \zeta^2$  and multiplying out all terms becomes:

$$A\omega^3 + B\omega^2 + C\omega + D = 0, \quad (\text{A.5.2-13a})$$

where

$$A = 16(1 + m^2), \quad (\text{A.5.2-13b})$$

$$B = 8(3m^3 - 2)m^2, \quad (\text{A.5.2-13c})$$

$$C = -8m^6 \quad (\text{A.5.2-13d})$$

and

$$D = m^8. \quad (\text{A.5.2-13e})$$

Equation (A.5.2-13a) has, by the fundamental theorem of algebra, three solutions (Churchill, Brown and Verhey, 1976), only one of which is also a solution to Rayleigh's equation. Let the roots of equation (A.5.2-13a) be  $\omega_1$ ,  $\omega_2$  and  $\omega_3$ . Then (Spiegel, 1968)

$$\omega_1 = S + T - \frac{1}{3}a = p, \quad (\text{A.5.2-14a})$$

$$\omega_2 = \left[ -\frac{1}{2}(S + T) - \frac{1}{3}a \right] + i \left[ \frac{\sqrt{3}}{2}(S - T) \right], \quad (\text{A.5.2-14b})$$

and

$$\omega_3 = \left[ -\frac{1}{2}(S + T) - \frac{1}{3}a \right] - i \left[ \frac{\sqrt{3}}{2}(S - T) \right], \quad (\text{A.5.2-14c})$$

where

$$S = \left( R + \sqrt{Q^3 + R^2} \right)^{\frac{1}{3}},$$

$$T = \left( R - \sqrt{Q^3 + R^2} \right)^{\frac{1}{3}},$$

$$Q = \frac{3b - a^2}{9},$$

$$R = \frac{9ab - 27c - 2a^3}{54},$$

$$a = \frac{B}{A}, \quad b = \frac{C}{A} \quad \text{and} \quad c = \frac{D}{A}.$$

I have given the first root two symbols,  $\omega_1$  and  $p$ , anticipating the following development as well as simplifying notation used later. To see which root is legitimate, we need to consider the next three graphs in figures A.5.2-4a through A.5.2-4c. From these graphs it is obvious that only the first root, which is always real, fits all the criteria (A.5.2-11a) through (A.5.2-11d).

**Square of the first root of  
Rayleigh's Equation**

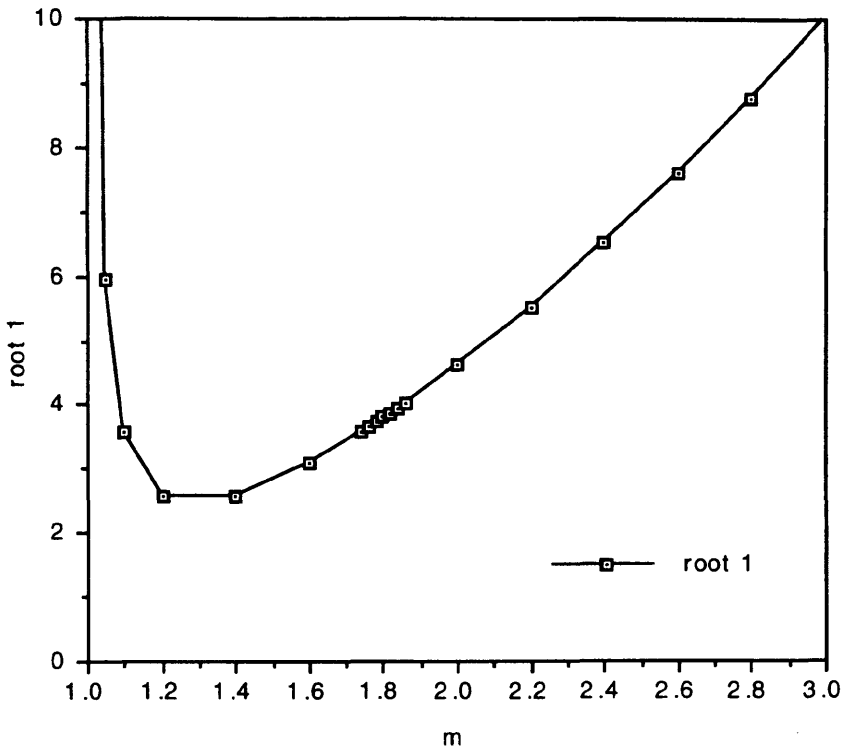


**Fig. A.5.2-4a.** First root of the rationalized Rayleigh's equation.

**Real and imaginary parts of  
the second root of the rationalized  
Rayleigh's equation**

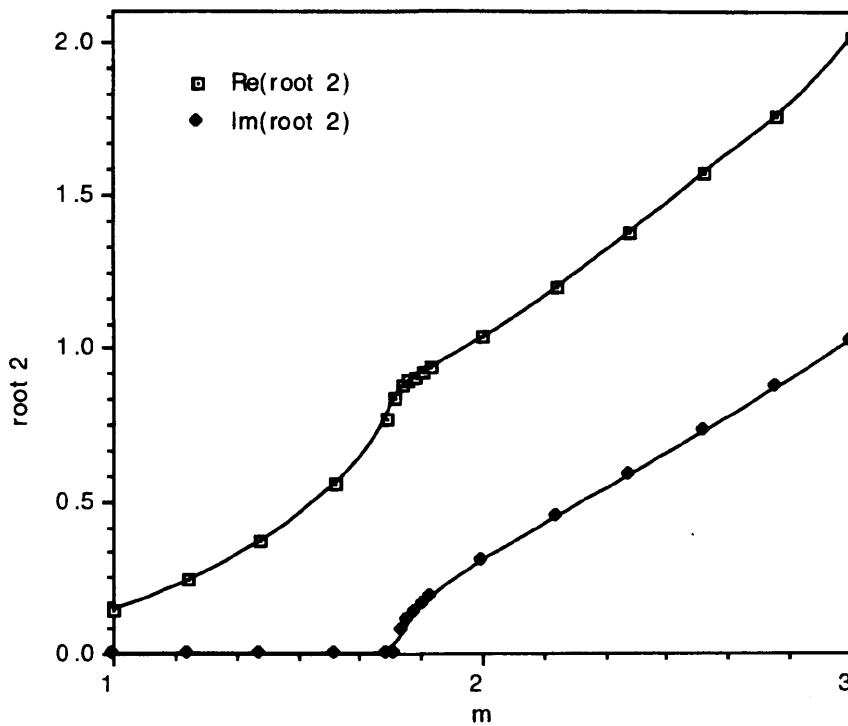


**Fig. A.5.2-4b.** Second root of the rationalized Rayleigh's equation.

**Real and imaginary parts of the  
third root of the rationalized  
Rayleigh's equation**

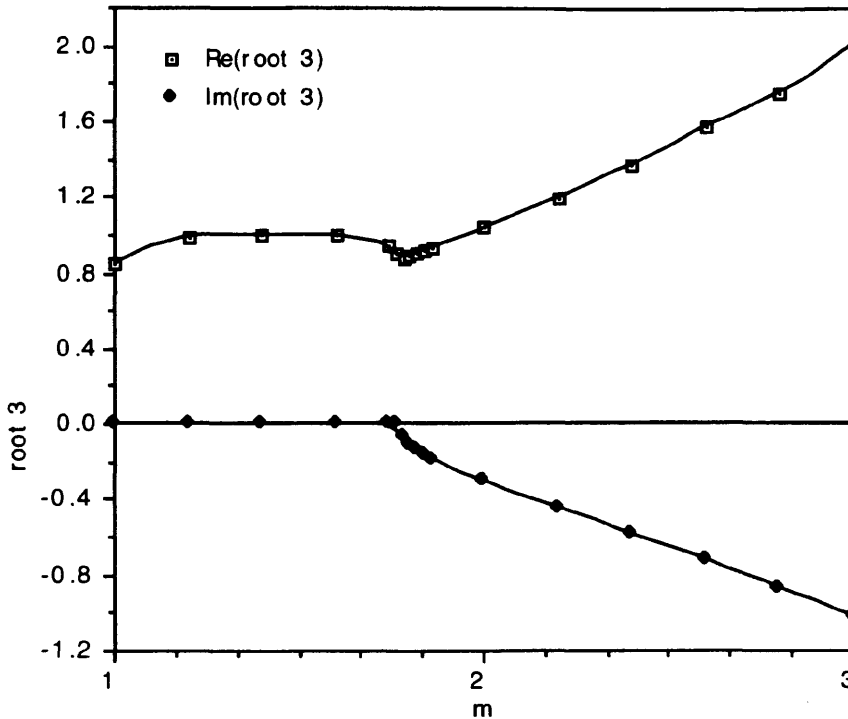


**Fig. A.5.2-4c.** Third root of the rationalized Rayleigh's equation.

Now that we have investigated the multivalued nature of Rayleigh's equation and its zeros, we are set up to try and obtain solutions to the integral equations of motion (A.4-10a) and (A.4-10b). This is the subject of the next section.

## **A.6: The Integral Equations of Motion and the Field at Infinity**

Before proceeding to finding approximate or far-field solutions to the integral equations of motion, we should address the problem of branch cuts and poles existing along the real axis. First, we will need to transform the equations of motion, given by integral equations (A.4-10a) and (A.4-10b), into a more useful form by using Hankel functions. That is:

$$u_r^{(F)}(f, r, z) = \frac{K(f)}{2} \sqrt{\alpha} \times \int_{-\infty}^{\infty} \frac{\xi J_1(\xi b)}{F_0(\xi)} \left[ (m^2 - 2\xi^2) e^{(-\alpha z \sqrt{\xi^2 - 1})} + 2 \sqrt{\xi^2 - 1} \sqrt{\xi^2 - m^2} e^{(-\alpha z \sqrt{\xi^2 - m^2})} \right] H_1^{(1)}(\alpha \xi r) d\xi$$

(A.6-1a)

and

$$u_z^{(F)}(f, r, z) = \text{sgn}(k_p) \frac{K(f)}{2} \sqrt{\alpha} \times \int_{-\infty}^{\infty} \frac{J_1(\xi b) \sqrt{\xi^2 - 1}}{F_0(\xi)} \left[ 2\xi^2 e^{(-\alpha z \sqrt{\xi^2 - m^2})} + (m^2 - 2\xi^2) e^{(-\alpha z \sqrt{\xi^2 - 1})} \right] H_0^{(1)}(\alpha \xi r) d\xi.$$

(A.6-1b)

The derivation of equations (A.6-1a) and (A.6-1b) from equations (A.4-10a) and (A.4-10b) is outlined in box A.6.a. The two integral equations of motion above are in the form that we will be dealing with from this point forward.

**Box A.6.a:** Use of Hankel functions to transform the integral equations of motion.

Note that all the integrals of equations implicit within (A.4-10a) and (A.4-10b) can be represented by the forms

$$I_1 = \int_0^{\infty} E(\xi) e^{-\alpha z \sqrt{\xi^2 - v^2}} J_1(\alpha r \xi) d\xi \quad (\text{A.6.a-1})$$

and

$$I_2 = \int_0^{\infty} O(\xi) e^{-\alpha z \sqrt{\xi^2 - v^2}} J_0(\alpha \xi r) d\xi, \quad (\text{A.6.a-2})$$

where  $E$  and  $O$  are even and odd functions of  $\xi$  respectively and  $v$  can be either 1 or  $m$ . Bessel functions are related to Hankel functions (Morse and Feshbach, 1953, p. 624) by:

$$J_n(\xi) = \frac{H_n^{(1)}(\xi) + H_n^{(2)}(\xi)}{2}, \quad (\text{A.6a-3})$$

where  $H_n^{(1)}(\xi)$  and  $H_n^{(2)}(\xi)$  are Hankel functions of the 1st and 2nd kinds and of order  $n$ . According to Cherry (1962, p. 30) Hankel functions have the property:

$$H_n^{(1)}(\xi e^{i\pi}) = -e^{in\pi} H_n^{(2)}(\xi). \quad (\text{A.6.a-4})$$

Substitution of equation (A.6.a-4) into (A.6.a-3) for  $n = 0$  and 1 results in

$$J_0(\alpha \xi r) = \frac{H_0^{(1)}(\alpha \xi r) - H_0^{(1)}(-\alpha \xi r)}{2} \quad (\text{A.6.a-5a})$$

and

$$J_1(\alpha \xi r) = \frac{H_1^{(1)}(\alpha \xi r) + H_1^{(1)}(-\alpha \xi r)}{2}. \quad (\text{A.6.a-5b})$$

If equations (A.6.a-5a) and (A.6.a-5b) are in turn substituted into equations (A.6.a-1) and (A.6.a-2), accompanied by a simple change of the sign of one of the resulting integrals, we can write

$$I_1 = \frac{1}{2} \int_{-\infty}^{\infty} E(\xi) e^{-\alpha z \sqrt{\xi^2 - v^2}} H_1^{(1)}(\alpha \xi r) d\xi \quad (\text{A.6.a-6a})$$

and

$$I_2 = \frac{1}{2} \int_{-\infty}^{\infty} O(\xi) e^{-\alpha z \sqrt{\xi^2 - v^2}} H_0^{(1)}(\alpha \xi r) d\xi, \quad (\text{A.6.a-6b})$$

which is the form we used in equations (A.6-1a) and (A.6-1b).

In order to have well behaved integral equations we need to deform the contour of integration around the branch cuts and poles encountered. To properly deform the contour of integration we will first examine what happens to the branch points in the case of a particular type of dissipative material. The material we will consider is a particular viscoelastic material where the stress is not only linearly related to the strain but also to the rate of change of strain. One possible way of representing this is to consider the stress-strain relations given by equations (A.2-4a) through (A.2-4c) and add the time rate of change of strain, for instance equation (A.2-4a),

$$\sigma_{rz} = 2\mu e_{rz}, \quad (\text{A.6-2a})$$

becomes

$$\sigma_{rz} = 2\mu \left( e_{rz} + \epsilon_1^2 \frac{\partial e_{rz}}{\partial t} \right), \quad (\text{A.6-2b})$$

where the small positive quantity  $\epsilon_1^2$  ensures a lossy medium and not one that gains energy by deformation caused by stresses. By Fourier transforming equation (A.6-2b) we get:

$$\sigma_{rz}^{(F)} = 2\mu^* e_{rz}^{(F)}, \quad (\text{A.6-2c})$$

such that

$$\mu^* = \mu (1 + i\omega\epsilon_1^2). \quad (\text{A.6-2d})$$

By direct comparison of equation (A.6-2a) and equation (A.6-2c), we see that in the Fourier domain they have the exact same form, except that the elastic constant has

changed from a real quantity to a complex one. The new elastic constant is complex but otherwise would play the same role in subsequent derivation of equations of motion, and so on. The same arguments used to get the new elastic constant  $\mu^*$  can be used on equation (A.2-4c) to arrive at:

$$\sigma_{zz}^{(F)} = (\lambda + 2\mu)^* e_{zz}^{(F)} + \lambda^* (e_{rz}^{(F)} + e_{\phi z}^{(F)}), \quad (\text{A.6-3a})$$

where

$$(\lambda + 2\mu)^* = (\lambda + 2\mu) [1 + i\omega\epsilon_2^2], \quad (\text{A.6-3b})$$

and

$$\lambda^* = \lambda [1 + i\omega\epsilon_3^2]. \quad (\text{A.6-3c})$$

In this situation we can see that the quantities  $k_p^2$  and  $k_s^2$ , for finite  $\omega$  and very small  $\epsilon$ , will be, to first order:

$$(k_p^*)^2 = \frac{\omega^2 \rho}{(\lambda + 2\mu)^*} \approx \frac{\omega^2 \rho}{(\lambda + 2\mu)} (1 - i\omega\epsilon_2^2) = k_p^2 (1 - i\omega\epsilon_2^2) \quad (\text{A.6-4a})$$

and

$$(k_s^*)^2 = \frac{\omega^2 \rho}{\mu^*} \approx \frac{\omega^2 \rho}{\mu} (1 - i\omega\epsilon_1^2) = k_s^2 (1 - i\omega\epsilon_1^2) \quad (\text{A.6-4b})$$

respectively. Note that I have kept the star notation to distinguish between the quantities belonging to the lossy and elastic media. This means the branch points in a viscoelastic media would move from the elastic case on the real axis to the second and fourth quadrants in the complex plane. The two zeros of Rayleigh's equation are moved in the same fashion. To see this we will perturb Rayleigh's equation,  $F(\zeta) = 0$ , as given by equation (A.4-4c). If we allow  $k_p$  and  $k_s$  to vary in Rayleigh's equation, we could write

$$F(\zeta; k_p, k_s) = 0, \quad (\text{A.6-5a})$$

so that

$$\frac{\partial F}{\partial \zeta} \delta \zeta + \frac{\partial F}{\partial k_p} \delta k_p + \frac{\partial F}{\partial k_s} \delta k_s = 0. \quad (\text{A.6-5b})$$

Taking the partial derivatives of equation (A.4-4c) and substituting them back into equation (A.6-5b), we arrive at:

$$\zeta \delta \zeta = \frac{\left[ (k_s^2 - 2\zeta^2) \sqrt{\zeta^2 - k_p^2} \sqrt{\zeta^2 - k_s^2} + \zeta^4 - k_p^2 \zeta^2 \right] k_s \delta k_s + \left[ \zeta^2 (\zeta^2 - k_s^2) \right] k_p \delta k_p}{2(k_s^2 - 2\zeta^2) \sqrt{\zeta^2 - k_p^2} \sqrt{\zeta^2 - k_s^2} + 2k_p^2 k_s^2 + 4\zeta^4 - 3k_p^2 \zeta^2 - 3k_s^2 \zeta^2} \quad (\text{A.6-6})$$

which, after substitution of  $\zeta = k_p \xi$  and  $m = \frac{V_p}{V_s} = \frac{k_s}{k_p}$ , as given by equations (A.4-9a) and (A.2-10d) respectively, becomes:

$$\delta \zeta = f_1(\xi; m) \delta k_p + f_2(\xi; m) \delta k_s, \quad (\text{A.6-7a})$$

where

$$f_1(\xi; m) = \frac{(\xi^2 - m^2) \xi^2}{g(\xi; m)}, \quad (\text{A.6-7b})$$

$$f_2(\xi; m) = \frac{m(m^2 - 2\xi^2) \sqrt{\xi^2 - m^2} \sqrt{\xi^2 - 1} + (\xi^2 - 1) \xi^2}{g(m; \xi)}, \quad (\text{A.6-7c})$$

and

$$g(\xi; m) = \left[ 2(m^2 - 2\xi^2) \sqrt{\xi^2 - m^2} \sqrt{\xi^2 - 1} + 2m^2 + 4\xi^4 - 3m^2 \xi^2 - 3\xi^2 \right] \xi. \quad (\text{A.6-7d})$$

The relationship I have obtained, given by equation (A.6-7a), is quite different from Miller and Pursey's (1953) equation (76), and the perturbation of the affixes (or the initial positions) of the zeroes is not simple. It is true, however, that the zeroes for the two cases considered in Miller and Pursey's paper, namely for  $m = 2$  and  $\sqrt{3}$ , the zeroes do move obviously to the second and fourth quadrants. This does not appear to be the case in

general, as shown in the following development. From our discussion of the zeros of Rayleigh's equation we found that if  $\xi$  is a zero then  $1 < m < |\xi|$ , as given by condition (A.5.2-11d). Therefore, we need only consider values of  $m > 1$ . Since the zero,  $\xi$ , of Rayleigh's equation is directly related to  $m$  we can plot the behavior of  $f_1$  and  $f_2$  as functions of  $m$  alone. As can be seen, for the positive root of Rayleigh's equation (figures A.6-1a and A.6-1b), the two factors are not of the same sign for the most part. This makes the choice of an integration path slightly more difficult. For negative roots, the two graphs A.6-1a and A.6-1b are just the negative of the ones shown.

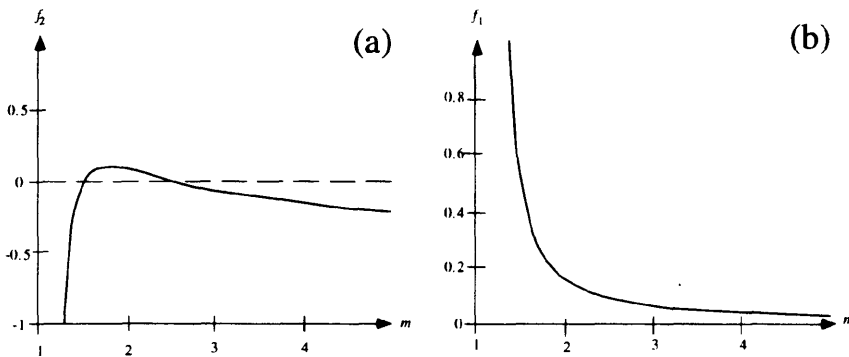


**Fig. A.6-1.** Multiplicative factors in the perturbation equation.

When the sign of both multiplicative factors  $f_1$  and  $f_2$  are positive, then the zeros of Rayleigh's equation move to the second and fourth quadrants. To see this consider equations (A.6-4a) and (A.6-4b), which give:

$$k_p^* = k_p \sqrt{1 - i \omega \epsilon_2^2} \approx k_p \left( 1 - i \frac{\omega \epsilon_2^2}{2} \right) = k_p + \delta k_p, \tag{A.6-8a}$$

and

$$k_s^* = k_s \sqrt{1 - i \omega \epsilon_1^2} \approx k_s \left( 1 - i \frac{\omega \epsilon_1^2}{2} \right) = k_s + \delta k_s, \tag{A.6-8b}$$

which upon substitution into equation (A.6-7a) results in

$$\delta \zeta = f_1 \delta k_p + f_2 \delta k_s = -i \omega \left( \frac{f_1 \epsilon_2^2 + f_2 \epsilon_1^2}{2} \right) = -i \alpha, \tag{A.6-8c}$$

where  $\alpha$  is a real number with the same sign as the root  $\zeta$ . Following the same notation, we can write the perturbed root as

$$\zeta^* = \zeta + \delta\zeta = \zeta - i\alpha. \quad (\text{A.6-9})$$

In this situation alone, we can choose the integration path to be the one shown in figure A.6-2, with  $R$  arbitrarily large and the smaller indentations on the real axis arbitrarily small.

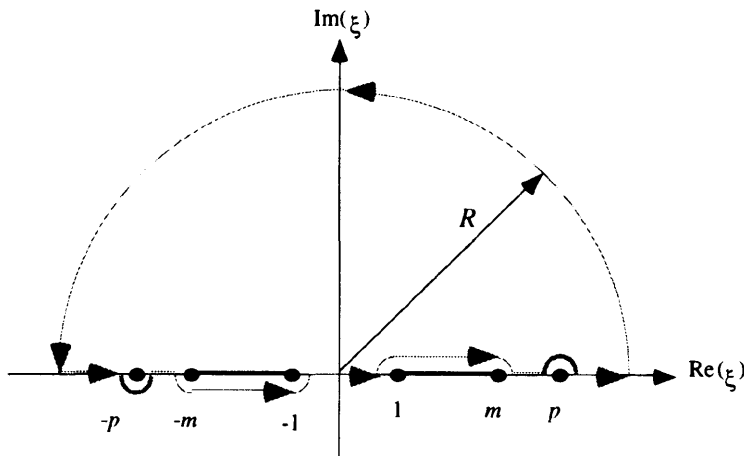


**Fig. A.6-2.** A possible contour of integration for the integral equations of motion.

Before proceeding to the far-field approximations, which constitute the next topic, we will associate all the terms in the template equations (A.6.a-6a) and (A.6.a-6b) with our integral equations of motion (A.6-1a) and (A.6-1b). The first correspondence is with equation (A.6-1a) where the even function in (A.6.a-6a) is related to the two even terms by:

$$E(\xi) = \left\{ \begin{array}{l} \frac{\xi J_1(b\xi)}{F_0(\xi)} (m^2 - 2\xi^2) \\ \frac{\xi J_1(b\xi)}{F_0(\xi)} 2\sqrt{\xi^2 - 1}\sqrt{\xi^2 - m^2} \end{array} \right\}, \quad (\text{A.6-10a})$$

where the two terms have  $\nu = 1$  and  $m$ , respectively. The second correspondence is with equation (A.6-1b) where the odd function in (A.6.a-6b) is related to the two odd terms by:

$$O(\xi) = \left\{ \begin{array}{l} \frac{J_1(b\xi) \sqrt{\xi^2 - 1}}{F_0(\xi)} 2\xi^2 \\ \frac{J_1(b\xi) \sqrt{\xi^2 - 1}}{F_0(\xi)} (m^2 - 2\xi^2) \end{array} \right\}, \quad (\text{A.6-10b})$$

and in this case we have  $v = m$  and  $1$ , respectively.

Now we proceed to the far-field case, where  $r$  is assumed to be large. In this case it is appropriate to use the asymptotic expansion of the Hankel function

$$H_n^{(1)}(\alpha \xi r) \sim \sqrt{\frac{2}{\pi \alpha \xi r}} \exp\left[i\left(\alpha \xi r - \frac{n\pi}{2} - \frac{\pi}{4}\right)\right]. \quad (\text{A.6-11})$$

There is the problem of the case when  $\xi = 0$  but, as we shall see, the origin will not influence the integral since the path of integration we will finally take does not pass through this point. Upon substitution of (A.6-11) into the prototype equations (A.6.a-6a) and (A.6.a-6b) we get:

$$I_1 \sim \frac{e^{-i(3\pi)/4}}{\sqrt{\alpha}} \sqrt{\frac{1}{2\pi r}} \int_{-\infty}^{\infty} \frac{E(\xi)}{\sqrt{\xi}} e^{i\alpha r \xi - \alpha z \sqrt{\xi^2 - v^2}} d\xi \quad (\text{A.6-12a})$$

and

$$I_2 \sim \frac{e^{-i\pi/4}}{\sqrt{\alpha}} \sqrt{\frac{1}{2\pi r}} \int_{-\infty}^{\infty} \frac{O(\xi)}{\sqrt{\xi}} e^{i\alpha r \xi - \alpha z \sqrt{\xi^2 - v^2}} d\xi. \quad (\text{A.6-12b})$$

Note, the factor,  $\sqrt{\alpha}$ , in equations (A.6-12a) and (A.6-12b) will cancel the same factor in equations (A.4-10a) and (A.4-10b) when the final substitutions are made below. If we make the following substitutions

$$z = R \cos \theta, \quad (\text{A.6-13a})$$

$$r = R \sin \theta, \quad (\text{A.6-13b})$$

$$f(\xi) = i \alpha \xi \sin \theta - \alpha \cos \theta \sqrt{\xi^2 - v^2}, \quad (\text{A.6-13c})$$

and

$$\chi(\xi) = \left\{ \begin{array}{l} \frac{e^{-i(3\pi)/4}}{\sqrt{\alpha}} \sqrt{\frac{1}{2\pi r}} \frac{E(\xi)}{\sqrt{\xi}} \\ \frac{e^{-i\pi/4}}{\sqrt{\alpha}} \sqrt{\frac{1}{2\pi r}} \frac{O(\xi)}{\sqrt{\xi}} \end{array} \right\} \quad (\text{A.6-13d})$$

into equations (A.6-12a) and (A.6-12b), we get equations of the form:

$$I = \int_{-\infty}^{\infty} \chi(\xi) e^{R f(\xi)} d\xi. \quad (\text{A.6-14})$$

The substitutions above have the geometric interpretation as indicated in figure A.6-3a.

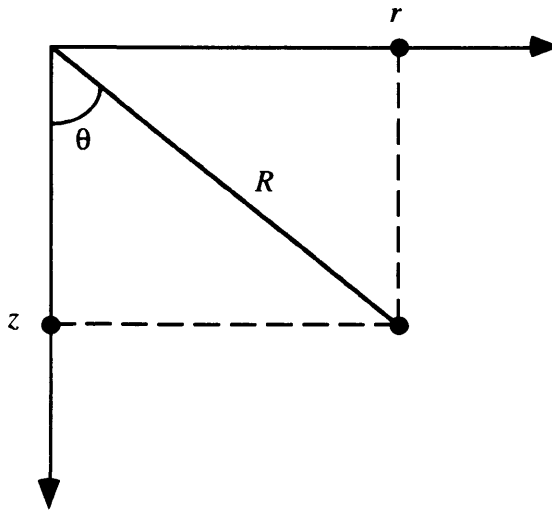


**Fig. A.6-3a.** Polar coordinate transformation.

Equation (A.6-14) is of exactly the same form as equation (D.1-1) in appendix D, so we can use the method of steepest descent, or saddle-point method, to obtain an approximate solution.

The first step in the method of steepest descent is to determine the saddle point, which is found by solving the equation

$$\frac{df(\xi)}{d\xi} = 0. \quad (\text{A.6-15a})$$

Substitution of equation (A.6-13c) into equation (A.6-15a) results in the equation

$$i \sin \theta = \frac{\xi \cos \theta}{\sqrt{v^2 - \xi^2}}. \quad (\text{A.6-15b})$$

By inspection of the right-hand side of equation (A.6-15b) one would suspect that the solution would be some simple trig-relation. The relation which solves equation (A.6-15a) is represented in figure A.6-3b and given by:

$$\xi_0 = -v \sin \theta. \quad (\text{A.6-15c})$$

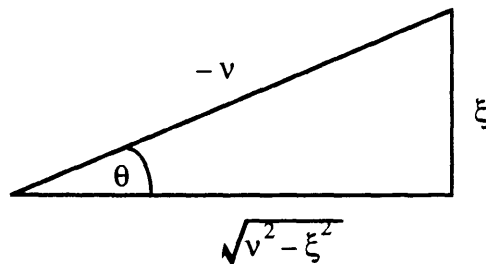


**Fig. A.6-3b.** Pictorial representation of the solution to equation (A.6-15b)

This is the saddle point. The asymptotic solution for equation (A.6-14) when  $R$  is very large, is given by equation (D.3-31) in appendix D and duplicated here as:

$$I = \frac{\sqrt{2\pi} \chi(\xi_0) e^{Rf(\xi_0)} e^{i\beta}}{\sqrt{R \left| \frac{d^2 f}{d\xi^2} \right|_{\xi_0}}}, \quad (\text{A.6-16})$$

where I have used the symbols  $R$  and  $\beta$  instead of the  $t$  and  $\alpha$  used in appendix D. By equation (D.3-24) and (D.3-26) in appendix D we can write:

$$\xi - \xi_0 = \sqrt{2 \left( \frac{f(\xi) - f(\xi_0)}{\left. \frac{d^2 f}{d\xi^2} \right|_{\xi_0}} \right)}. \quad (\text{A.6-17a})$$

Now we use equation (D.3-29a) to transform equation (A.6-17a) into

$$|\xi - \xi_0| e^{i\beta} = \sqrt{2 \left( \frac{f(\xi) - f(\xi_0)}{\left. \frac{d^2 f}{d\xi^2} \right|_{\xi_0}} \right)}, \quad (\text{A.6-17b})$$

or in another form

$$\beta = \arg \left( \sqrt{2 \left( \frac{f(\xi) - f(\xi_0)}{\left. \frac{d^2 f}{d\xi^2} \right|_{\xi_0}} \right)} \right), \quad (\text{A.6-17c})$$

where I have used  $\beta$  instead of the  $\alpha$  used in appendix D, since the symbol  $\alpha$  has another meaning within this equation. Now we will explicitly derive all the terms that the approximation (A.6-16) requires. From equation (A.6-13c) we can get:

$$f(\xi_0) = f(-v \sin \theta) = -i \alpha v, \quad (\text{A.6-18a})$$

$$\left. \frac{d^2 f}{d\xi^2} \right|_{\xi_0} = \left. \frac{d^2 f}{d\xi^2} \right|_{(-v \sin \theta)} = \frac{i \sec^2 \theta}{v}, \quad (\text{A.6-18b})$$

and from equation (A.6-17c)

$$\beta = \frac{\pi}{4}. \quad (\text{A.6-18c})$$

If we substitute equations (A.6-18a) through (A.6-18c) into our asymptotic approximation given by equation (A.6-16), it results in:

$$I \sim \sqrt{\frac{2 \pi v}{R}} e^{i((\pi/4) - \alpha R v)} \cos \theta \chi(-v \sin \theta), \quad (\text{A.6-19a})$$

which upon substitution from equations (A.6-13d) becomes the equations:

$$I \sim -\frac{e^{-i\alpha R v}}{\sqrt{\alpha} R} \cot \theta \left\{ \begin{array}{l} E(-v \sin \theta) \\ i O(-v \sin \theta) \end{array} \right\}. \quad (\text{A.6-19b})$$

By using the correspondences given by equations (A.6-10a) and (A.6-10b), equations (A.6-19b) can be used directly on the integral equations of motion (A.6-1a) and (A.6-1b) to obtain an asymptotic far-field solution. Prior to doing that, one more approximation is customarily made. The radius of the vibrating disk is assumed to be very small. This means that the term  $b\xi$  is small, so that we can include only the first terms of the power series of the Bessel functions (Spiegel, 1968, p. 136) and write

$$J_n(b\xi) \sim \frac{b^n \xi^n}{2^n n!}. \quad (\text{A.6-20})$$

With approximation (A.6-20), keeping in mind  $v$  can be either 1 or  $m$ , we can find the new form of the odd and even terms in equation (A.6-19b) at the saddle points to be

$$E(\xi_0) = E\left(\begin{array}{l} -\sin \theta \\ -m \sin \theta \end{array}\right) \sim \left\{ \begin{array}{l} \frac{b \sin^2 \theta}{2 F_0(-\sin \theta)} (m^2 - 2 \sin^2 \theta) \\ i \frac{b m^3 \sin^2 \theta |\cos \theta|}{F_0(-m \sin \theta)} \sqrt{m^2 \sin^2 \theta - 1} \end{array} \right\}, \quad (\text{A.6-21a})$$

and

$$O(\xi_0) = O\left(\begin{array}{l} -m \sin \theta \\ -\sin \theta \end{array}\right) \sim \left\{ \begin{array}{l} -\frac{b m^3 \sin^3 \theta \sqrt{m^2 \sin^3 - 1}}{F_0(-m \sin \theta)} \\ -i \frac{b \sin \theta |\cos \theta|}{2 F_0(-\sin \theta)} (m^2 - 2 \sin^2 \theta) \end{array} \right\}. \quad (\text{A.6-21b})$$

Now we have collected all the pieces needed to write out the far-field solution, for the particle motion, where  $(r\xi)$  is large and  $(b\xi)$  is small. Using equations (A.6-21a), (A.6-21b) and (A.6-19b) we can approximate the integral equations of motion (A.6-1a) and (A.6-1b) as:

$$u_r^{(F)}(R, \theta, f) = \frac{-K(f) b \sin \theta \cos \theta}{R} \times \left[ e^{-i \alpha R} \frac{m^2 - 2 \sin^2 \theta}{2 F_0(-\sin \theta)} + i e^{-i \alpha m R} \frac{m^3 |\cos \theta|}{F_0(-m \sin \theta)} \sqrt{m^2 \sin^2 \theta - 1} \right], \quad (\text{A.6-22a})$$

and

$$u_z^{(F)}(R, \theta, f) = \frac{-\text{sgn}(k_p) K(f) b \cos \theta}{R} \times \left[ e^{-i \alpha R} \frac{|\cos \theta|}{F_0(-\sin \theta)} (m^2 - 2 \sin^2 \theta) - i e^{-i \alpha m R} \frac{m^3 \sin^2 \theta \sqrt{m^2 \sin^2 \theta - 1}}{F_0(-m \sin \theta)} \right]. \quad (\text{A.6-22b})$$

From this point forward, we shall consider positive frequencies only; then  $\text{sgn}(k_p)$  will always equal plus one. Next, for consistency and simplicity we shall transform equations (A.6-22a) and (A.6-22b) using polar coordinates. The transformation equations are:

$$u_R^{(F)} = u_z^{(F)} \cos \theta + u_r^{(F)} \sin \theta \quad (\text{A.6-23a})$$

and

$$u_\theta^{(F)} = u_r^{(F)} \cos \theta - u_z^{(F)} \sin \theta. \quad (\text{A.6-23b})$$

If equations (A.6-22a) and (A.6-22b) are substituted into equations (A.6-23a) and (A.6-23b) we arrive at the polar form of the far-field particle displacements

$$u_R^{(F)}(R, \theta, f) \sim -b K(f) \frac{e^{-i \alpha R}}{R} \frac{\cos \theta (m^2 - 2 \sin^2 \theta)}{2 F_0(-\sin \theta)} \quad (\text{A.6-24a})$$

and

$$u_\theta^{(F)}(R, \theta, f) \sim -i b K(f) m^3 \frac{e^{-i \alpha m R}}{R} \frac{\sin 2\theta \sqrt{m^2 \sin^2 \theta - 1}}{2 F_0(-m \sin \theta)}. \quad (\text{A.6-24b})$$

I find it interesting that, after all the gyrations we go through, the final solutions take this rather simple form. This is, however, not the end of the story. We need to see just what our steepest descent path looks like, since we may need to consider the contributions

from the Rayleigh poles, which can be found from equation (A.5.2-14a). The steepest descent path is discussed in appendix D; the facts relevant to the present case are:

- (1) The path crosses the real axis at the saddle point given by

$$\xi_0 = -v \sin \theta \quad (\text{A.6-15c})$$

as found previously.

- (2) From equation (D.3-10) in appendix D we know that the steepest descent path is characterized by the conditions that  $\text{Im}[f(\xi)]$  is constant and  $f(\xi)$  decreases away from the saddle point, given in the first fact. This means that  $f(\xi) - f(\xi_0)$  must be a nonpositive real quantity along the path.

- (3) The path crosses the  $\text{Re}[\xi]$  axis if  $\text{Im}[f(\xi) - f(\xi_0)] = 0$  and  $\xi$  is real. From equations (A.6-13c) and (A.6-18a) we have

$$f(\xi) - f(\xi_0) = -\alpha \cos \theta \sqrt{\xi^2 - v^2} + i(\xi \sin \theta + v), \quad (\text{A.6-25a})$$

so that the only other point at which the steepest decent path crosses the real axis is given by

$$\xi_1 = -v \csc \theta. \quad (\text{A.6-25b})$$

Facts (1) and (3) provide points at which the path crosses the real axis; and fact (2) gives the global description of the path. It is fact (2) that we will now develop fully. From fact (2) and equation (A.6-25a) we can write:

$$i(\xi \sin \theta + v) - \alpha \cos \theta \sqrt{\xi^2 - v^2} = -X^2, \quad (\text{A.6-26a})$$

where  $X \in \{\text{Reals}\}$ . If we rationalize equation (A.6-26a) we can put it in the form:

$$\xi^2 + B\xi + C = 0, \quad (\text{A.6-26b})$$

where

$$B = -2i\alpha \sin \theta \quad (\text{A.6-26c})$$

and

$$C = X^4 + 2 i m X^2 - m^2(1 + \cos^2\theta). \quad (\text{A.6-26d})$$

Equation (A.6-26b) is just a quadratic in  $\xi$  and can be easily solved. The solution, after substituting back from equations (A.6-26c) and (A.6-26d) is:

$$\xi = (m - i X^2) \sin \theta \pm \sqrt{(X^4 \cos^2\theta + m^2 \sin^2\theta) + i(2 m X^2 \cos^2\theta)}. \quad (\text{A.6-26e})$$

In order to separate equation (A.6-26e) into real and imaginary parts, we will put the quantity within the radical sign in polar form by defining

$$(X^4 \cos^2\theta + m^2 \sin^2\theta) + i(2 m X^2 \cos^2\theta) = \beta e^{i\phi}, \quad (\text{A.6-26f})$$

where

$$\beta^2 = (X^4 \cos^2\theta + m^2 \sin^2\theta)^2 + (2 m X^2 \cos^2\theta)^2 \quad (\text{A.6-26g})$$

and

$$\tan \phi = \frac{2 m X^2 \cos^2\theta}{X^4 \cos^2\theta + m^2 \sin^2\theta}. \quad (\text{A.6-26h})$$

Substitution of equation (A.6-26f) into equation (A.6-26e) allows us to write:

$$\xi = \left[ m \sin \theta \pm \sqrt{\beta} \cos \frac{\phi}{2} \right] + i \left[ -X^2 \sin \theta \pm \sqrt{\beta} \sin \frac{\phi}{2} \right]. \quad (\text{A.6-26i})$$

As the variable  $X$  in equation (A.6-26i) evolves, the real and imaginary parts of  $\xi$  mark out the path of steepest descent. To further define the path of steepest descent we will see what happens to it as  $X$  approaches infinity. From equation (A.6-26h) we can see that

$$\lim_{X \rightarrow \pm\infty} \phi = 0, \quad (\text{A.6-26j})$$

and from equation (A.6-26g) we can deduce that

$$\lim_{X \rightarrow \pm\infty} \sqrt{\beta} = X^2 \cos \theta. \quad (\text{A.6-26k})$$

From equations (A.6-26j) (A.6-26k) and (A.6-26i) we arrive at the expression:

$$\lim_{X \rightarrow \pm\infty} \xi = [\pm X^2 \cos \theta] + i[-X^2 \sin \theta], \quad (\text{A.6-26l})$$

which also means that

$$\lim_{X \rightarrow \pm\infty} \arg[\xi] = \pm \theta. \quad (\text{A.6-26m})$$

Equation (A.6-26m) means the path of steepest descent is asymptotic to the lines at angles  $\theta$  and  $-\theta$  to the  $\text{Re}[\xi]$  axis. All of the facts with respect to the path of steepest descent are summarized in figure A.6-4.

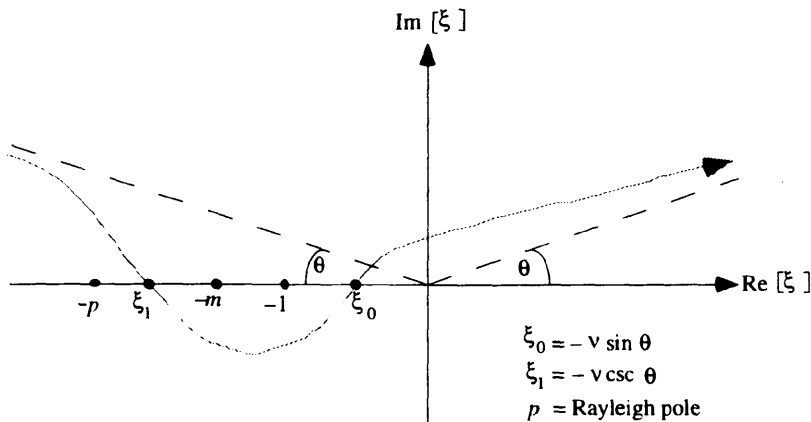


**Fig. A.6-4.** Path of steepest descent.

As can be seen from figure A.6-4 the point  $\xi_1 = -v \csc \theta$  will move to the left of the Rayleigh pole,  $-p$ , when  $-p > \xi_1$ , which in turn means that the condition for the path enclosing the Rayleigh pole is met for angles  $\theta$ , where

$$\theta < \text{arccsc}\left(\frac{p}{v}\right), \quad \exists \frac{\pi}{2} > \theta > 0. \quad (\text{A.6-27})$$

Under these conditions we need to consider the contribution to the integral from the Rayleigh pole which certainly contributed to the integral before we deformed the path shown in figure A.6-2. From the theory of complex variables (Churchill, Brown and

Verhey, 1976, p. 172-173) we know that the contribution of the Rayleigh pole is given by the residue theorem to be

$$2 \pi i \left[ \text{residue of } \left( e^{R f(\xi)} \chi(\xi) \right) \text{ at } \xi = -p \right]. \quad (\text{A.6-28a})$$

If we let the residue be  $b_0$  and write

$$\chi(\xi) = \frac{\Psi(\xi)}{F_0(\xi)}, \quad (\text{A.6-28b})$$

which we can always do, then the residue (Churchill, Brown and Verhey, 1976, p. 178) can be expressed as:

$$b_0 = \frac{\Psi(-p) e^{R f(-p)}}{F_0(-p)}. \quad (\text{A.6-28c})$$

So the solution with contributions from both the saddle point and the Rayleigh pole will be the combination of equation (A.6-19a) and (A.6-28a) taking the form:

$$I \sim \sqrt{\frac{2 \pi v}{R}} e^{i((\pi/4) - Rv)} \cos \theta \chi(-v \sin \theta) + 2\pi i b_0. \quad (\text{A.6-29})$$

In the cases where the Rayleigh pole is not included within the contour of integration, it does not mean that the Rayleigh pole has no contribution; we must include it within a separate contour as shown in figure A.6-5. In this situation, the path  $C_1$  gives the Rayleigh pole contribution and the path  $C_2$  has the same asymptotic solution as before.

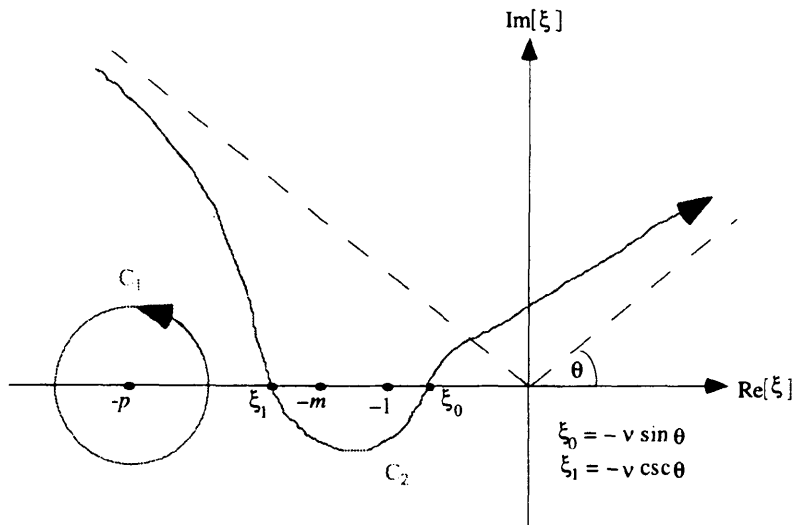


**Fig. A.6-5.** Path of steepest descent including Rayleigh pole outside of main path.

One other situation can occur when  $\theta$  approaches  $\pi/2$ : in this situation the two points  $\xi_1$  and  $\xi_2$  approach one of the branch points, which requires additional modification of the path of integration. The new path (figure A.6-6) has basically three paths  $C_1$ ,  $C_2$  and  $C_3$ . The first two paths,  $C_1$  and  $C_2$ , give rise to the Rayleigh pole contribution and the asymptotic solution already derived; the last path  $C_3$ , according to Miller and Pursey (1953), can be dealt with by the method of steepest descent which gives a solution that decays faster than the other solutions. I have expanded on this in box A.6.b. Since, the path  $C_3$  gives rise to a quickly decaying wave type, we shall ignore this wave. Aki and Richards (1980, p. 220-221) discuss this path for a slightly different problem, namely that of a buried point source, and say that this path corresponds to a surface S-wave. So, we should be aware that, by ignoring this path we may not get a very complete description of what we may find on the free surface.

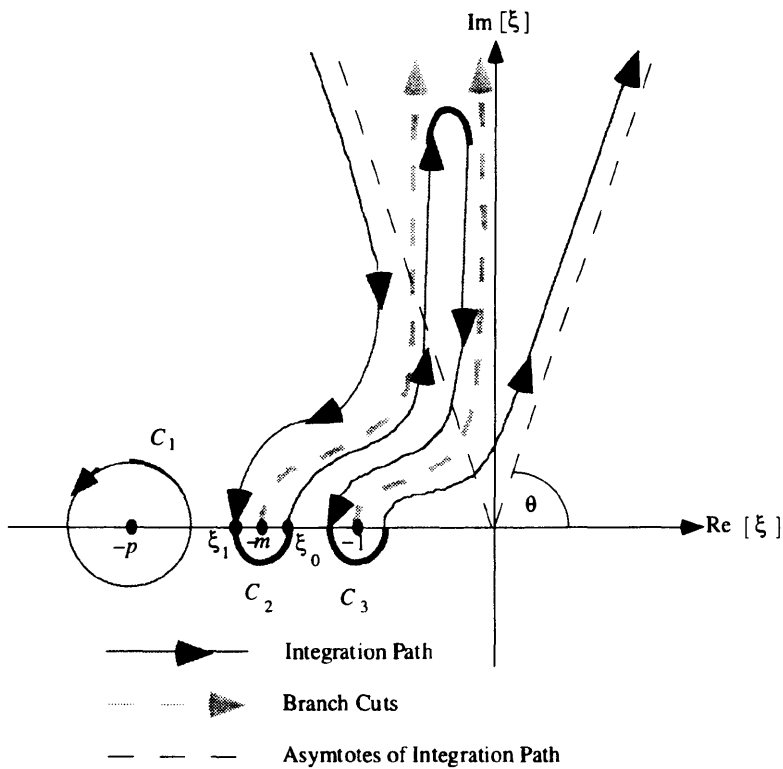


Fig. A.6-6. Path of integration when  $\theta$  approaches  $\frac{\pi}{2}$ .

**Box A.6.b:** Asymptotic solutions as  $\theta$  approaches  $\frac{\pi}{2}$ .

As can be seen in figure A.6-6 the integral (A.6-14) can be approximated by the sum of three integrals

$$I = I_1 + I_2 + I_3 \tag{A.6.b-1}$$

$$= \int_{C_1} e^{R f(\xi)} \chi(\xi) d\xi + \int_{C_2} e^{R f(\xi)} \chi(\xi) d\xi + \int_{C_3} e^{R f(\xi)} \chi(\xi) d\xi.$$

The first two integrals,  $I_1$  and  $I_2$ , in equation (A.6.b-1) gives rise to solutions from the Rayleigh pole and the asymptotic solution from the saddle point, respectively. These two solutions have been discussed in the previous section culminating in equations (A.6-19a) and (A.6-28a) and combined in equation (A.6-29) and will not be elaborated upon here. The third integral,  $I_3$ , is somewhat of a different beast, but the techniques used to obtain an asymptotic solution will yield a tool that allows us to find a solution in this case as well. First we will show that most of the contribution to the integral along path  $C_3$  comes from the region around the branch point  $\xi = -1$ . To see this, simply consider the case when  $\theta$  approaches  $\frac{\pi}{2}$ , then

$$\lim_{\theta \rightarrow \frac{\pi}{2}} f(\xi) = i \xi. \quad (\text{A.6.b-1})$$

Now if  $\xi = \bar{a} + i \bar{b}$  then

$$e^{R f(\xi)} \rightarrow e^{-R \bar{b}} e^{i R \bar{a}}. \quad (\text{A.6.b-2})$$

Since we have assumed that  $R$  is very large, the only places where the integral will have significant contribution, with (A.6.b-2) as a factor, will be when  $\bar{b} \rightarrow 0$ , which in the case of path  $C_3$  is in the neighborhood of the point  $\xi = -1$ . We can try to find a path of steepest descent away from  $\xi = -1$ , which takes on the role of the saddle point. Since we now seek a path on which  $f(\xi)$  is real and non-positive away from  $\xi = -1$ , we can parameterize such a path by letting

$$f(\xi) - f(-1) = -Y, \quad (\text{A.6.b-3})$$

where

$$Y \in \{\text{Positive Real Numbers}\}.$$

Equation (A.6.b-3) reduces to a quadratic equation:

$$A \xi^2 + B \xi + C = 0, \quad (\text{A.6.b-4a})$$

where

$$A = \left(\frac{\tan \theta}{\alpha}\right)^2 + 1 \quad (\text{A.6.b-4b})$$

$$B = \frac{2 \tan \theta}{\alpha} \left[ \sqrt{v^2 - 1} + \frac{\tan \theta}{\alpha} - i \frac{Y}{\cos \theta} \right] \quad (\text{A.6.b-4c})$$

and

$$C = \left(\frac{\tan \theta}{\alpha}\right)^2 \left[ 1 + \frac{\sqrt{v^2 - 1}}{\tan \theta} - \left(\frac{Y}{\sin \theta}\right)^2 \right] + i \frac{2 Y}{\alpha \cos \theta} \left[ \frac{\tan \theta}{\alpha} + \sqrt{v^2 - 1} \right]. \quad (\text{A.6.b-4d})$$

We can solve equation (A.6.b-4a) by using the quadratic formula:

$$\xi = -\frac{B \pm \sqrt{B^2 - 4 A C}}{2 A}. \quad (\text{A.6.b-5})$$

This will give us the steepest descent path we have been looking for. We will deform the path  $C_3$  so that the two main branches, which I will call  $\Gamma_1$  and  $\Gamma_2$ , will be close and parallel to the steepest descent path and cross the point  $\xi = -1$ .

This situation is shown in figure A.6.b-1.

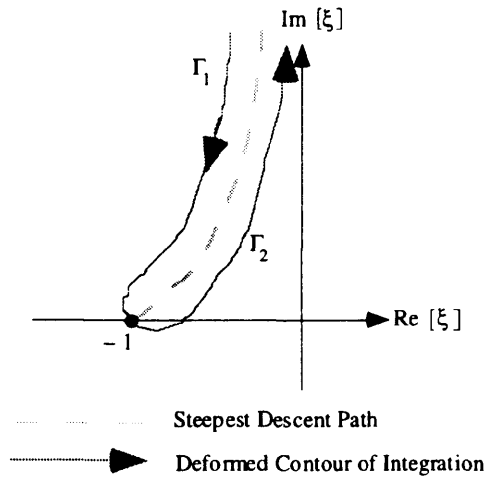


**Fig. A.6.b-1.** Steepest descent path for  $C_3$ .

Now we shall use a device used by Miller and Pursey (1953); that is, we assume the paths  $\Gamma_1$  and  $\Gamma_2$  are arbitrarily close to the path of steepest descent and that the value of  $\chi(\xi)$  is  $\chi_1(\xi)$  on  $\Gamma_1$  and  $\chi_2(\xi)$  on  $\Gamma_2$ . Then using the parameterization of the path of steepest descent, we can rewrite the integral  $I_3$  as:

$$I_3 \approx e^{R f(-1)} \int_0^\infty e^{-R Y} F(\xi(Y)) dY, \tag{A.6.b-6a}$$

where

$$F(\xi) = (\chi_2(\xi) - \chi_1(\xi)) \frac{d\xi}{dY}. \tag{A.6.b-6b}$$

Equation (A.6.b-6a) is of a form for which we can apply equation (D.2.a-21) in order to find an asymptotic solution. The asymptotic solution would be of the form:

$$I_3 \sim e^{R f(-1)} \sum_{j=0}^{n-1} a_j \frac{j!}{R^{j+1}}, \tag{A.6.b-7a}$$

where

$$a_j = \left[ \frac{d^j F}{d\xi^j} \right]_{\xi=-1} \frac{1}{j!}. \quad (\text{A.6.b-7b})$$

Since  $\chi_1(-1) = \chi_2(-1)$  this implies that  $F(-1) = 0$ , which in turn means that  $a_0 = 0$ . Therefore, the first nonzero term will be  $O(R^{-2})$ , which certainly decays faster than the other terms but is still not zero. There is one difficulty with this argument. If we consider only the next term in the asymptotic expansion we find that

$$a_1 = \left[ \frac{dF}{d\xi} \right]_{\xi=-1} \quad (\text{A.6.b-8a})$$

$$= \left[ \left( \frac{d\chi_1}{d\xi} - \frac{d\chi_2}{d\xi} \right) \left( \frac{\partial f}{\partial \xi} \right)^{-1} + (\chi_1 - \chi_2) \frac{\partial^2 f}{\partial \xi^2} \left( \frac{\partial f}{\partial \xi} \right)^{-1} \right]_{\xi=-1},$$

where we have used

$$\frac{d\xi}{dY} = - \left( \frac{\partial f}{\partial \xi} \right)^{-1} \quad (\text{A.6.b-8b})$$

derived by implicit differentiation of equation (A.6.b-3). Now we substitute in equation (A.6-13c) to get

$$- \left( \frac{\partial f}{\partial \xi} \right)^{-1} = \frac{\sqrt{\xi^2 - v^2}}{\alpha \xi \cos \theta - i \sin \theta \sqrt{\xi^2 - v^2}}, \quad (\text{A.6.b-9a})$$

and

$$\frac{\partial^2 f}{\partial \xi^2} \left( \frac{\partial f}{\partial \xi} \right)^{-2} = \frac{\alpha v^2 \cos \theta}{(\alpha \xi \cos \theta)^2 - (\xi^2 - v^2) \sin^2 \theta - i 2 \alpha \xi \sqrt{\xi^2 - v^2} \sin 2\theta}.$$

(A.6.b-9b)

As can be seen from equation (A.6.b-8a), the same argument of  $\chi_1(-1) = \chi_2(-1)$  causing  $a_0$  to be identically zero will also cause all terms to be zero. The only mitigating circumstance is the presence of factors like (A.6.b-9b) that are infinite when  $\theta \rightarrow \pi / 2$ , which points to the need for further analysis.

This concludes our analysis and update of Miller and Pursey's (1953) paper. The differences between their paper and this treatment are developmental and lie in certain points of analysis. The development here is more general than the one given by Miller and Pursey and allows one a more convenient starting point for other developments such as Cherry's (1962) work on horizontal stresses. No attempt at terseness was made since this is meant to be tutorial in nature and an easy jumping-off point for further developments. The radiation patterns could be displayed at this point but to speed things up a little the reader is referred to Miller and Pursey's (1953) paper. There should be no difference in these patterns since the final equations are the same.

## B: Review of the Theory of an Elastic Continuum

### B.1: Conservation laws

Consider the forces acting on a material volume  $V$ , enclosed by an orientable surface  $S$ . The material within  $V$  is acted upon by forces through the surface  $S$  and action at a distance type forces, for example the gravitational forces, throughout the volume. First consider the surface element  $dS$  with outward normal  $\mathbf{n}$ . The net force per unit area or traction acting on this element will be  $\mathbf{t}_n$ . Secondly, a net force per unit volume, or body force,  $\mathbf{f}$ , will act upon elemental volume  $dV$  around point  $P$ . This situation is represented in figure B.1-1.

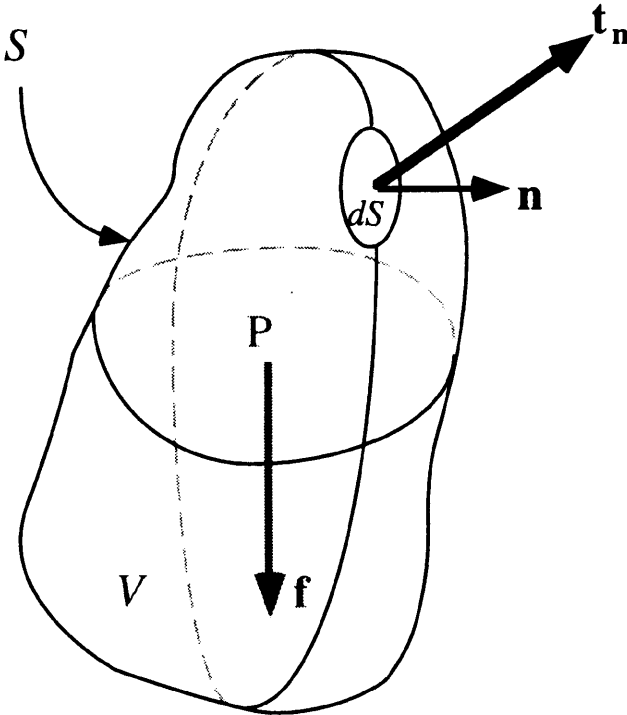


Fig. B.1-1. Forces acting on a material volume.

To study the motion of the material points in volume  $V$ , due to the forces mentioned in the previous paragraph, the conservation laws for a continuum will be invoked. The laws that will be considered are the conservation of mass, the conservation of momentum, the conservation of moment of momentum, and the conservation of mechanical energy. The equations representing these conservation laws are respectively:

$$\frac{d}{dt} \int_V \rho dV = 0, \quad (\text{B.1-1})$$

$$\frac{d}{dt} \int_V v^i \rho dV = \oint_S t_{\mathbf{n}}^i dS + \int_V f^i \rho dV, \quad (\text{B.1-2})$$

$$\frac{d}{dt} \int_V g^{il} \epsilon_{ljk} x^j v^k \rho dV = \oint_S g^{il} \epsilon_{ljk} x^j t_{\mathbf{n}}^k dS + \int_V g^{il} \epsilon_{ljk} x^j f^k \rho dV, \quad (\text{B.1-3})$$

$$\frac{d}{dt} \int_V [g_{ij} v^i v^j + U] \rho dV = \oint_S g_{ij} t_{\mathbf{n}}^i v^j dS + \int_V g_{ij} f^i v^j \rho dV, \quad (\text{B.1-4})$$

where

$\frac{d}{dt} \equiv$  material time derivative,

$\rho \equiv$  mass density,

$\mathbf{n} \equiv$  outward normal of surface  $S$ ,

$x^i \equiv$  covariant position vector,

$g_{ij} \equiv$  contravariant metric tensor,

$\epsilon_{ijk} = \sqrt{g} e_{ijk} \equiv$  permutation tensor,

such that,  $g = \det[g_{ij}] = |g_{ij}|$  and  $e_{ijk} \equiv$  permutation symbols,

$$v^i = \frac{d}{dt}x^i = \dot{x}^i \equiv \text{material velocity,}$$

and  $U \equiv$  internal energy per unit mass.

These balance or conservation equations are based on many assumptions, one of which is the adequacy of just the traction (force per unit area) and body force (force per unit volume) in describing the interaction with the volume. The form of the equations would be quite different if other interactions were allowed, for example if couples were present, as is appropriate for the case of rigid bodies. This possibility is explored in appendix C. The material in appendix C directly parallels the development here but includes much more detail in some areas and less in others.

The normal tensor notation, as can be found in Colburn (1970), Spain (1965) and Eringen (1971), has been followed. I will tend to call symbols of the form,  $a^i$  and  $b^{ij}$ , contravariant vectors and tensors, respectively, when I mean the contravariant components of vectors and tensors. The same convention will be followed for covariant and mixed vectors and tensors. This is also the convention used in Spain's (1965) book. Since there are some discrepancies in notation between the books, a short descriptions will be included along with the development. Summation on diagonally repeated indices will always be in effect, such as  $x_i u^i = x_1 u^1 + x_2 u^2 + x_3 u^3$ . To suppress summation the indices will be in Greek letters, such as  $x_\alpha u^\alpha$ , which represents any one of  $x_1 u^1$ ,  $x_2 u^2$ , or  $x_3 u^3$ .

## Differential form of the conservation laws

### Conservation of mass

It is useful to cast equations (B.1-1) – (B.1-4) in their differential form. Since the material (Lagrangian) frame of reference is assumed, the material time derivative can be taken within the integral sign. A direct outcome of this is equation (B.1-1) can be rewritten in its differential form as:

$$\int_V \frac{d}{dt} \rho \, dV = 0 = \dot{\rho} . \quad (\text{B.1-5})$$

### Conservation of momentum

Calling upon the tetrahedron argument, as summarized in Appendix E, the traction can be recast in the following form:

$$t_{\mathbf{n}}^i = \sigma^{ij} n_j, \quad (\text{B.1-6})$$

where  $\sigma^{ij}$  is the stress tensor (or more accurately called the first Piola-Kirchhoff stress) and  $n_j$  is the covariant vector normal to the surface element. Substitution of equation (B.1-6) into equation (B.1-2) and applying the divergence theorem results in:

$$\int_V (\dot{v}^i \rho - \sigma_{\dots j}^{ij} - f^i \rho) dV = 0, \quad (\text{B.1-7})$$

where

$$\sigma_{\dots j}^{ij} = \frac{\partial \sigma}{\partial x^j} + \left\{ \begin{matrix} i \\ rj \end{matrix} \right\} \sigma^{rj} + \left\{ \begin{matrix} j \\ rj \end{matrix} \right\} \sigma^{ir} \equiv \text{covariant partial derivative,}$$

and

$$\left\{ \begin{matrix} i \\ rj \end{matrix} \right\} \equiv \text{Christoffel symbol of the second kind,}$$

which is defined as:

$$\left\{ \begin{matrix} i \\ rj \end{matrix} \right\} = g^{ik} [rj, k] = g^{ik} \frac{1}{2} \left( \frac{\partial g^{rk}}{\partial x^j} + \frac{\partial g^{jk}}{\partial x^r} - \frac{\partial g^{rj}}{\partial x^k} \right).$$

Covariant differentiation of tensors creates other tensors that transform as tensors should: the operation plays the role of partial differentiation in rectangular Cartesian coordinates and reduces to ordinary partial differentiation in that case. Since the volume of integration is arbitrary we have the differential or local form of equation (B.1-7):

$$\dot{v}^i \rho - \sigma_{\dots j}^{ij} - f^i \rho = 0. \quad (\text{B.1-8})$$

Equation (B.1-8) is often called the equation of motion.

### Conservation of moment of momentum

Manipulation of equation (B.1-3), following a similar recipe as the one used to manipulate equation (B.1-2), results in:

$$g^{il} \varepsilon_{ijk} x_{,m}^j \sigma^{km} = 0. \quad (\text{B.1-9})$$

Equation (B.1-9) shows the stress tensor  $\sigma^{km}$  to be symmetric. This can readily be seen in the special case of rectangular Cartesian coordinates.

### Conservation of energy

Finally, manipulation of equation (B.1-4) yields its local form:

$$\dot{U} \rho = g_{ij} \sigma^{ip} v_{,p}^j. \quad (\text{B.1-10})$$

Equations (B.1-5), (B.1-8), (B.1-9), and (B.1-10) are assumed to fully describe the dynamics of the material considered. These equations do not assume anything about the material itself and can be used to describe a host of materials. To make these relations useful, however, a description of how the material itself will respond to deformation is necessary. This type of description is called a constitutive relationship.

## **B.2: Constitutive relationships**

As the material under consideration deforms, there is usually a tendency for the material to resist the deformation. The quantification of this resistance results in the constitutive relationships. Some effects will be ignored such as the effects of temperature and temperature gradient. The deformation will be described with respect to some initial reference configuration in a frame of reference call the material (Lagrangian) frame. The position vector within the material frame will have components designated by the capital letter  $X$  and all reference to this frame in terms of subscripts and superscripts will also be in capital letters. The actual configuration of the material at some time will be described

with a frame of reference called the spatial (Eulerian) frame. The position vector in this frame will be designated by the small letter  $x$  and all reference to this frame in terms of subscripts and superscripts will also be in small letters. The squares of the arc distances traced out by the position vector in the spatial and material (Eulerian and Lagrangian) frames are respectively:

$$(ds)^2 = g_{kl} dx^k dx^l \quad (\text{B.2-1a})$$

and

$$(dS)^2 = G_{KL} dX^K dX^L \quad (\text{B.2-1b})$$

where the metric tensors are self-defined by these equations for each frame of reference. Now consider an infinitesimal directed line segment in the material frame and its image in the spatial frame. They will be related by the following formula:

$$dx^k = \frac{\partial x^k}{\partial X^K} dX^K = x^k{}_{;K} dX^K \quad (\text{B.2-2a})$$

or

$$dX^K = \frac{\partial X^K}{\partial x^k} dx^k = X^K{}_{;k} dx^k, \quad (\text{B.2-2b})$$

where the semicolon designates ordinary partial differentiation. By direct comparison of equations (B.2-2a) and (B.2-2b) to equations (B.2-1a) and (B.2-1b) it can be seen that the arc distance is just the inner product of equations (B.2-2a) and (B.2-2b), which takes the form:

$$(ds)^2 = g_{kl} x^k{}_{;K} x^l{}_{;L} dX^K dX^L \quad (\text{B.2-3a})$$

and

$$(dS)^2 = G_{KL} X^K{}_{;k} X^L{}_{;l} dx^k dx^l. \quad (\text{B.2-3b})$$

A good measure of deformation would be the difference of squared lengths in the undeformed and deformed bodies along the same material points. The deformation measure generated in this way could be used as a variable to determine how the deformation energy is stored in the material (materials which generate energy when deformed are not considered). With this in mind we write the following formula:

$$\begin{aligned} (ds)^2 - (dS)^2 &= (g_{kl} x^k_{;K} x^l_{;L} - G_{KL}) dX^K dX^L \\ &= (g_{kl} - G_{KL} X^K_{;k} X^L_{;l}) dx^k dx^l \end{aligned} \quad (\text{B.2-4})$$

Equation (B.2-4) gives a measure of deformation in a body. The terms within the parenthesis, therefore, provide a measure of this length change in the material and spatial frame respectively. The names Lagrangian and Eulerian strain tensors will be attached to these quantities and the following symbols will be used to represent them:

$$2E_{KL} = 2E_{LK} = g_{kl} x^k_{;K} x^l_{;L} - G_{KL} \quad (\text{B.2-5a})$$

and

$$2e_{kl} = 2e_{lk} = g_{kl} - G_{KL} X^K_{;k} X^L_{;l}. \quad (\text{B.2-5b})$$

The symmetry of the strain tensors is obvious since the metric tensor is assumed to be symmetric. In order to relate the stress to strain, it is appropriate to consider the internal energy. Assume the internal energy of the body,  $U$ , be altered only by the deformation. In other words the energy is in some way stored by the body when deformed. This means  $U$  can be written as:

$$U = U(E_{LK}), \quad (\text{B.2-6})$$

which in turn implies:

$$\rho \dot{U} = \rho \frac{\partial U}{\partial E_{IJ}} \dot{E}_{IJ}. \quad (\text{B.2-7})$$

Equation (B.1-10) can be manipulated into the form of (B.2-7) by the following steps:

$$\begin{aligned}
 \dot{U} \rho &= g_{ij} \sigma^{ip} v_{,p}^j , \\
 &= g_{ij} \sigma^{ip} \dot{x}_{;J}^j X_{;p}^J , && \text{(chain rule)} \\
 &= g_{ij} \dot{x}_{;J}^j x_{;M}^i X_{;p}^J X_{;l}^M \sigma^{lp} , && (\delta_l^i = x_{;M}^i X_{;l}^M ) \\
 &= \frac{1}{2} \dot{E}_{JM} X_{;p}^J X_{;l}^M \sigma^{lp} , && \text{(define: } \dot{E}_{JM} = 2 g_{ij} \dot{x}_{;J}^j x_{;M}^i \text{)} \\
 &= \dot{E}_{JM} \Phi^{JM} . && \text{(define: } \Phi^{JM} = \frac{1}{2} X_{;p}^J X_{;l}^M \sigma^{lp} \text{)} \quad \text{(B.2-8)}
 \end{aligned}$$

Subtracting equation (B.2-7) from (B.2-8) results in:

$$\left( \Phi^{IJ} - \rho \frac{\partial U}{\partial E_{IJ}} \right) \dot{E}_{IJ} = 0 . \quad \text{(B.2-9)}$$

If it is assumed that the factor within parenthesis is independent of the factor outside, then:

$$\Phi^{IJ} = \rho \frac{\partial U}{\partial E_{IJ}} . \quad \text{(B.2-10)}$$

Substitution of the last definition in equation (B.2-8) into equation (B.2-10) and solving for the stress gives:

$$\sigma^{lp} = 2 \rho x_{;J}^p x_{;M}^l \frac{\partial U}{\partial E_{IJ}} . \quad \text{(B.2-11)}$$

Equation (B.2-11) is one form of the constitutive relationship but is in a far more general form than is required. Since the problems under consideration will be in the small-displacement regime, linearization is an appropriate simplification for equation (B.2-11).

### B.3: Linearization

#### Internal Energy

As a first step towards linearization of equation (B.2-11) consider the behavior of the internal energy close to the undeformed state of the body. To do this the internal energy is expanded as a Taylor's series around the undeformed state where the density is assumed to take on the value  $\rho_0$ . Recalling  $U = U(E_{IJ})$  the internal energy can be written as:

$$\rho_0 U = a + b^{IJ} E_{IJ} + \frac{1}{2} c^{IJKL} E_{IJ} E_{KL} + \dots, \quad (\text{B.3-1})$$

where  $a$ ,  $b^{IJ}$ , and  $c^{IJKL}$  are assumed to be constant material scalar, dyadic and tetrads respectively, which determine the behavior of the material considered. The higher-order terms, of course, have higher-order polyadics, which have not been explicitly represented. If the assumption is made that the internal energy is zero when the body is undeformed, then the scalar  $a$  must be zero; if a further assumption is made that the undeformed state is a state of zero stress, (i.e.  $\sigma^{ij} = 0$ ), the definition in equation (B.2-8) can be used to show that

$$\rho_0 \dot{U} = \Phi^{IJ} \dot{E}_{IJ} = \left( \frac{1}{2} X^I_{;i} X^J_{;j} \sigma^{ij} \right) \dot{E}_{IJ} = 0. \quad (\text{B.3-2})$$

Differentiating equation (B.3-1) with respect to time will result in:

$$\begin{aligned} \rho_0 \dot{U} &= b^{IJ} \dot{E}_{IJ} + c^{IJKL} \dot{E}_{IJ} E_{KL} + \dots \\ &= (b^{IJ} + c^{IJKL} E_{KL}) \dot{E}_{IJ} + \dots. \end{aligned} \quad (\text{B.3-3})$$

Then, by directly comparing equation (B.3-3) with equation (B.3-2), the conclusion  $b^{IJ} = 0$  can be drawn. With this in mind, the internal energy can then be written as:

$$\rho_0 U = \frac{1}{2} c^{IJKL} E_{IJ} E_{KL} + \dots. \quad (\text{B.3-4})$$

It is natural to consider the role that displacement plays, since it is a natural variable to use in describing the evolution of the material body.

## Displacement

Prior to deformation the body under consideration is referred to as the reference body; after deformation has taken place the same body having undergone deformation is referred to as the deformed body. The displacement vector  $\mathbf{u}$  is the vector which starts from a point located at position vector  $\mathbf{P}$  for a particular material point in the reference body and ends at a point located at position vector  $\mathbf{p}$  for the same material point in the deformed body. This situation is represented by figure B.3-1. The symbols used in the figure are:

$V \equiv$  volume of reference material body,

$S \equiv$  surface of reference material body,

$X^i \equiv$  curvilinear coordinates in the material frame of reference,

$\mathbf{G}_i \equiv$  covariant basis vectors in the material frame of reference,

$(X, Y, Z) \equiv$  rectangular Cartesian coordinates in the material frame,

$\mathbf{I}_i \equiv$  orthonormal basis vectors for  $(X, Y, Z)$ ,

$\mathbf{P} \equiv$  position vector of a material point in the reference body,

$V_t \equiv$  volume of deformed body,

$S_t \equiv$  surface of deformed body,

$x^i \equiv$  curvilinear coordinates in the spatial frame of reference,

$\mathbf{g}_i \equiv$  covariant basis vectors in the spatial frame of reference,

$(x, y, z) \equiv$  rectangular Cartesian coordinates in the material frame,

$\mathbf{i}_i \equiv$  orthonormal basis vectors for  $(x, y, z)$ ,

$\mathbf{p}$   $\equiv$  position vector of a material point in the deformed body,

$\mathbf{b}$   $\equiv$  vector starting from the origin of the material frame and ending at the origin of the spatial frame,

$\mathbf{u}$   $\equiv$  displacement vector as defined in the opening paragraph,

$i$   $\equiv$  a counter that identifies objects in the different frames as defined in figure B.3-1.

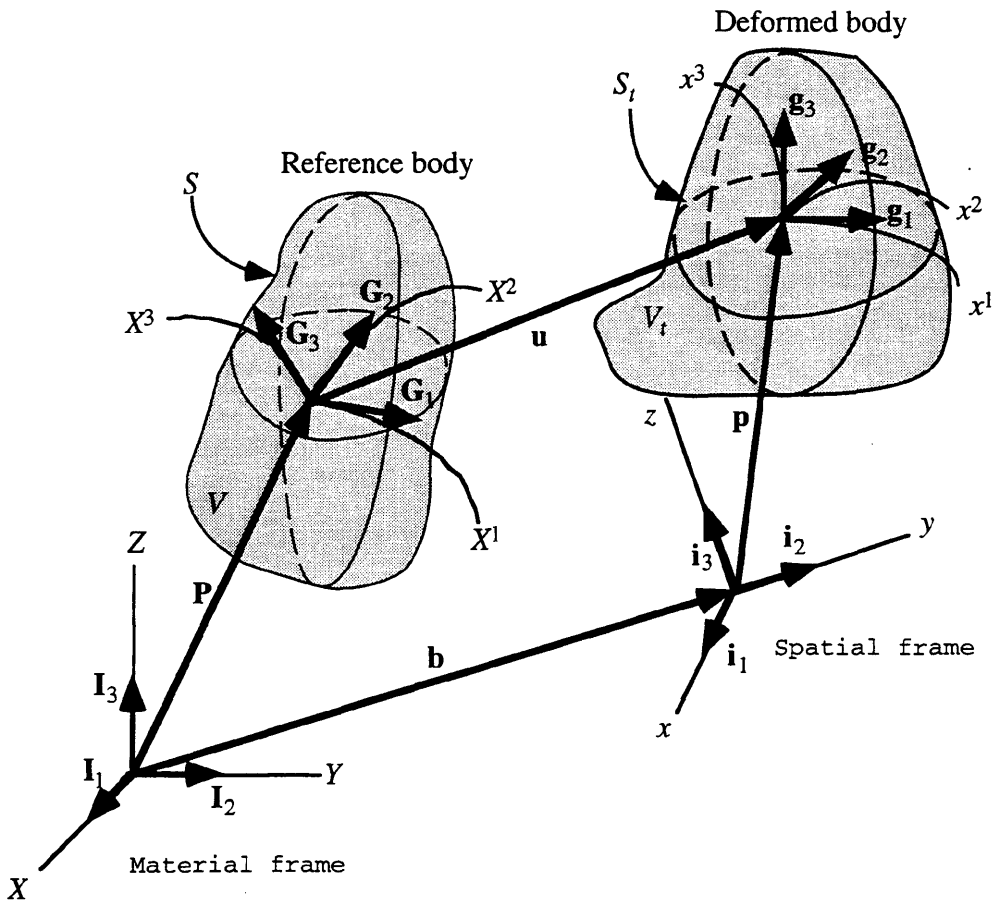


**Fig. B.3-1.** Frames of reference and motion.

As an intermediate step towards relating displacement to the Eulerian and Lagrangian strains, a different deformation measure will be considered. To begin, consider infinitesimal vectors due to a change in the position vectors  $\mathbf{p}$  and  $\mathbf{P}$ . These can be written as:

$$\begin{aligned}
 d\mathbf{p} &= \mathbf{p}_{;J} dX^J \\
 &= \mathbf{p}_{;i} x^i_{;J} dX^J && \text{(by the chain rule)} \\
 &= \mathbf{C}_I dX^I, && \text{(define: } \mathbf{C}_I = \mathbf{p}_{;i} x^i_{;I} \text{)} \quad (\text{B.3-5a})
 \end{aligned}$$

and, in the same fashion,

$$\begin{aligned}
 d\mathbf{P} &= \mathbf{P}_{;i} dx^i \\
 &= \mathbf{c}_i dx^i && \text{(define: } \mathbf{c}_i = \mathbf{P}_{;i} x^i_{;i} \text{)} \quad (\text{B.3-5b})
 \end{aligned}$$

From equations (B.3-5a) and (B.3-5b) we have a second method to obtain the square of the arc length in the material and spatial frames. The square of the arc length will have the form:

$$\begin{aligned}
 (dS)^2 &= d\mathbf{P} \cdot d\mathbf{P} \\
 &= (\mathbf{c}_i \cdot \mathbf{c}_j) dx^i dx^j && \text{(substitution of equation B.3-5b)} \\
 &= c_{ij} dx^i dx^j && \text{(define: } c_{ij} = \mathbf{c}_i \cdot \mathbf{c}_j \text{)}, \quad (\text{B.3-6a})
 \end{aligned}$$

and, in a like fashion,

$$(ds)^2 = C_{IJ} dX^I dX^J \quad \text{(define: } C_{IJ} = \mathbf{C}_I \cdot \mathbf{C}_J \text{)}. \quad (\text{B.3-6b})$$

The tensors  $C_{IJ}$  and  $c_{ij}$  can be used as deformation measures and are called Green and Cauchy deformation tensors, respectively. The relationship between these tensors and the Lagrangian and Eulerian strain tensors are:

$$(ds)^2 - (dS)^2 = (C_{IJ} - G_{IJ}) dX^I dX^J = 2E_{IJ} dX^I dX^J, \quad (\text{B.3-7a})$$

and

$$(ds)^2 - (dS)^2 = (c_{ij} - g_{ij})dx^i dx^j = 2e_{ij}dx^i dx^j \quad (\text{B.3-7b})$$

Now the relationship between the deformation measures and displacement can be made. From the definition of displacement and figure B.3-1 one can write:

$$\mathbf{u} = \mathbf{p} - \mathbf{P} + \mathbf{b}. \quad (\text{B.3-8})$$

If we take the partial derivative of (B.3-8) with respect to the material and spatial coordinates and compare this to the definitions in equations (B.3-5a) and (B.3-5b) we find:

$$\begin{aligned} \mathbf{C}_K &= \mathbf{P}_{;K} + \mathbf{u}_{;K} \\ &= \mathbf{G}_K + (U^I \mathbf{G}_I)_{;K} \quad (\text{expansion of } \mathbf{u} \text{ in terms of } \mathbf{G}_I) \\ &= \mathbf{G}_K + U^I_{;K} \mathbf{G}_I \quad (\text{definition of covariant derivative}) \end{aligned} \quad (\text{B.3-9a})$$

and in the same fashion:

$$\mathbf{c}_k = \mathbf{g}_k + u^I_{;k} \mathbf{g}_I. \quad (\text{B.3-9b})$$

Equations (B.3-9a) and (B.3-9b) immediately furnishes the definition of the Green and Cauchy deformation tensors in terms of displacements as:

$$\begin{aligned} C_{KL} &= \mathbf{C}_K \cdot \mathbf{C}_L \quad (\text{by definition}) \\ &= (\mathbf{G}_K + U^I_{;K} \mathbf{G}_I) \cdot (\mathbf{G}_L + U^J_{;L} \mathbf{G}_J) \quad (\text{by equation B.3-9a}) \\ &= G_{KL} + U_{L,K} + U_{K,L} + U_{I,K} U^I_{;L} \quad (\text{inner product expansion}) \end{aligned} \quad (\text{B.3-10a})$$

and

$$c_{kl} = g_{kl} + u_{l,k} + u_{k,l} + u_{i,k}u_{,l}^i. \quad (\text{B.3-10b})$$

By substitution of equations (B.3-10a) and (B.3-10b) into equations (B.3-7a) and (B.3-7b), the relationships between Lagrangian and Eulerian strain tensors and displacements are found to be:

$$E_{KL} = \frac{1}{2} (U_{L,K} + U_{K,L} + U_{i,K}U_{,L}^i), \quad (\text{B.3-11a})$$

and

$$e_{kl} = \frac{1}{2} (u_{l,k} + u_{k,l} - u_{i,k}u_{,l}^i). \quad (\text{B.3-11b})$$

If the material and spatial gradients are assumed to be small in the following sense:

$$|U_{L,K}| \ll 1 \text{ and } |u_{l,k}| \ll 1, \quad (\text{B.3-12})$$

then the Lagrangian and Eulerian strain tensors will be approximately equal and have the linear form:

$$E_{kl} = e_{kl} = \frac{1}{2} (u_{l,k} + u_{k,l}). \quad (\text{B.3-13})$$

The ideas above can now be incorporated with the equation of motion (B.1-8) to give the linearized equation of motion.

### Linearized equation of motion and isotropy

If the linearized strain tensor of equation (B.3-13) is substituted into the internal energy equation (B.3-4) the following relationship is derived:

$$\rho_0 U = \frac{1}{2} W \approx \frac{1}{2} c^{ijkl} e_{ij} e_{kl} + \dots \quad (\text{B.3-14})$$

By the same procedure the constitutive relationship can be written as:

$$\begin{aligned}\sigma^{ij} &= 2 \rho_0 \frac{\partial U}{\partial e_{ij}} \\ &= \frac{\partial W}{\partial e_{ij}}.\end{aligned}\tag{B.3-15}$$

By ignoring higher-order terms, the following set of linearized equations can be written:

$$W = c^{ijkl} e_{ij} e_{kl},\tag{B.3-16a}$$

$$\sigma^{ij} = \frac{\partial W}{\partial e_{ij}} = c^{ijkl} e_{kl},\tag{B.3-16b}$$

and

$$e_{kl} = \frac{1}{2} (u_{l,k} + u_{k,l}).\tag{B.3-16c}$$

Substitution of equations (B.3-16b) and (B.3-16c) into the equations of motion (B.1-8) results in:

$$\begin{aligned}\ddot{u}^i \rho &= (c^{ijkl} u_{k,l})_{,j} + f^i \rho \\ &= c^{ijkl} u_{k,lj} + c^{ijkl} u_{k,l} + f^i \rho.\end{aligned}\tag{B.3-17}$$

Equation (B.3-17) is one form of the linearized equation of motion. If we make the additional assumption of isotropy then:

$$c^{ijkl} = \lambda \delta^{ij} \delta^{kl} + \mu (\delta^{ik} \delta^{jl} + \delta^{il} \delta^{jk}),\tag{B.3-18}$$

where  $\lambda$  and  $\mu$  are the Lamé constants. If, further, the assumption of homogeneity is made then equation (B.3-17) becomes:

$$\ddot{u}^i \rho = (\lambda + \mu) g^{ij} u^l_{,lj} + \mu g^{jl} u^i_{,jl} + f^i \rho,\tag{B.3-19a}$$

which can be put in a more widely used form:

$$\ddot{u}^i \rho = (\lambda + 2\mu) g^{ij} \Delta_{,j} - \mu \varepsilon^{ijk} \omega_{k,j} + f^i \rho, \quad (\text{B.3-19b})$$

where the definitions:

$$\Delta = e^k_{,k} = u^k_{,k}, \quad (\text{B.3-19c})$$

and:

$$\omega_k = \varepsilon_{klm} g^{ln} u^m_{,n}, \quad (\text{B.3-19d})$$

have been made. To get from equation (B.3-19a) to equation (B.3-19b) the reasoning in the following box was used.

### Box I

Given:

$$\varepsilon^{ijk} \varepsilon_{klm} = e^{ijk} e_{klm} = \delta_{lm}^{ij} = (\delta_l^i \delta_m^j - \delta_m^i \delta_l^j), \quad (\text{B.3-I-i})$$

where:

$\delta_{lm}^{ij} \equiv$  the generalized Kronecker delta,

and:

$\delta_l^i = \begin{cases} 1 & : i = l \\ 0 & : i \neq l \end{cases} \equiv$  the Kronecker delta,

then,

$$\begin{aligned} \varepsilon^{ijk} \varepsilon_{klm} V_{..j}^{lm} &= (\delta_l^i \delta_m^j - \delta_m^i \delta_l^j) V_{..j}^{lm} \\ &= V_{..j}^{ij} - V_{..j}^{ji} \end{aligned} \quad (\text{B.3-I-ii})$$

The following term from equation (B.3-19a) can be rewritten using equation (B.3-I-ii) as:

$$\begin{aligned} g^{jl} u^i_{,jl} &= V^{ji}_{,j} = V^{ij}_{,j} - \varepsilon^{ijk} \varepsilon_{klm} V^{lm}_{,j} \\ &= g^{il} u^j_{,jl} - \varepsilon^{ijk} \varepsilon_{klm} g^{ln} u^m_{,jn} \end{aligned} \quad (\text{B.3-I-iii})$$

Upon substitution of equation (B.3-I-iii) into equation (B.3-19a) the following results:

$$\ddot{u}^i \rho = (\lambda + 2\mu) g^{ij} u^l_{,lj} - \mu \varepsilon^{ijk} \varepsilon_{klm} g^{ln} u^m_{,nj} + f^i \rho \quad (\text{B.3-I-iv})$$

Since  $e_{klm,j} = 0$  and by Ricci's lemma (Colburn, 1970)  $g^{ln}_{,j} = 0$ , equation (B.3-I-iv) can be recast in the form:

$$\ddot{u}^i \rho = (\lambda + 2\mu) g^{ij} u^l_{,lj} - \mu \varepsilon^{ijk} [\varepsilon_{klm} g^{ln} u^m_{,n}]_{,j} + f^i \rho \quad (\text{B.3-I-v})$$

If definitions (B.3-19c) and (B.3-19b) are introduced into equation (B.3-I-v) then equation (B.3-19b) results.

Equation (B.3-19a) and (B.3-19b) are the covariant form of the equations of motion for a homogeneous isotropic medium. This equation is true for any curvilinear coordinate system but, in general, it is the physical components and not the covariant components which we work with. So it is appropriate to look at the general tensor relationships within a few standard coordinate systems.

## B.4: Equations of linear elasticity in orthogonal Cartesian and cylindrical coordinates

### Cartesian orthogonal coordinates

The most commonly used coordinate system is the rectangular Cartesian system. In this system the relationships between contravariant components and physical components are simply:

$$x^1 = x, x^2 = y, \text{ and } x^3 = z . \quad (\text{B.4-1})$$

Since the squared arc length has the form:

$$\begin{aligned} (ds)^2 &= g_{ij} dx^i dx^j \\ &= x^2 + y^2 + z^2 , \end{aligned} \quad (\text{B.4-2})$$

from which the metric tensor can be seen to have the simple form:

$$g_{ij} = \delta_{ij} . \quad (\text{B.4-3})$$

From equation (B.4-3) it can be seen that:

$$\left\{ \begin{matrix} i \\ jk \end{matrix} \right\} = g^{il} \left( \frac{\partial g_{jl}}{\partial x^k} + \frac{\partial g_{kl}}{\partial x^j} - \frac{\partial g_{jk}}{\partial x^l} \right) = 0 . \quad (\text{B.4-4})$$

This in turn means that all covariant derivatives reduce to the familiar partial derivatives. Since  $g^{ij} = (g_{ij})^{-1} = g_{ij}$ , the covariant and contravariant components are equal. This allows one to drop the super- and subscript notation distinguishing between the two. With this in mind all the formulas of linear elasticity take on the familiar forms. Some of these are: the relation between displacement and linear strain,

$$e_{ij} = \frac{1}{2}(u_{i;j} + u_{j;i}) = \frac{1}{2} \left( \frac{\partial u_i}{\partial x_j} + \frac{\partial u_j}{\partial x_i} \right) , \quad (\text{B.4-5a})$$

the constitutive relation, in the case of isotropy,

$$\begin{aligned}\sigma_{ij} &= c_{ijkl} e_{kl} \\ &= [\lambda \delta_{ij} \delta_{kl} + \mu (\delta_{ik} \delta_{jl} + \delta_{il} \delta_{jk})] e_{kl} ,\end{aligned}\tag{B.4-5b}$$

and the equation of motion,

$$\ddot{u}_i \rho = (\lambda + \mu) u_{l;li} + \mu u_{i;ll} + f_i \rho .\tag{B.4-5c}$$

By using the permutation tensor or permutation symbol, which are the same in this case, the equations of motion can be cast in a more widely used form:

$$\ddot{u}_i \rho = (\lambda + 2\mu) u_{l;li} - \mu \epsilon_{ijk} \epsilon_{klm} u_{m;jl} + f_i \rho .\tag{B.4-5d}$$

Equations (B.4-5a) through (B.4-5d) can be written in vector notation respectively as:

$$\mathbf{e} = \frac{1}{2} (\nabla \mathbf{u} + \mathbf{u} \nabla),\tag{B.4-6a}$$

$$\boldsymbol{\sigma} = \mathbf{c} \mathbf{e},\tag{B.4-6b}$$

$$\ddot{\mathbf{u}} \rho = (\lambda + \mu) \nabla \nabla \cdot \mathbf{u} + \mu \nabla \cdot \nabla \mathbf{u} + \mathbf{f} ,\tag{B.4-6c}$$

and

$$\ddot{\mathbf{u}} \rho = (\lambda + 2\mu) \nabla \nabla \cdot \mathbf{u} - \mu \nabla \times \nabla \times \mathbf{u} + \mathbf{f} .\tag{B.4-6d}$$

As seen from the development above, all the equations take on the familiar forms that is determined by the choice of rectangular orthogonal coordinates. Of course the vector notation is also coordinate independent by less informative. Now consider another coordinate system.

## Cylindrical coordinates

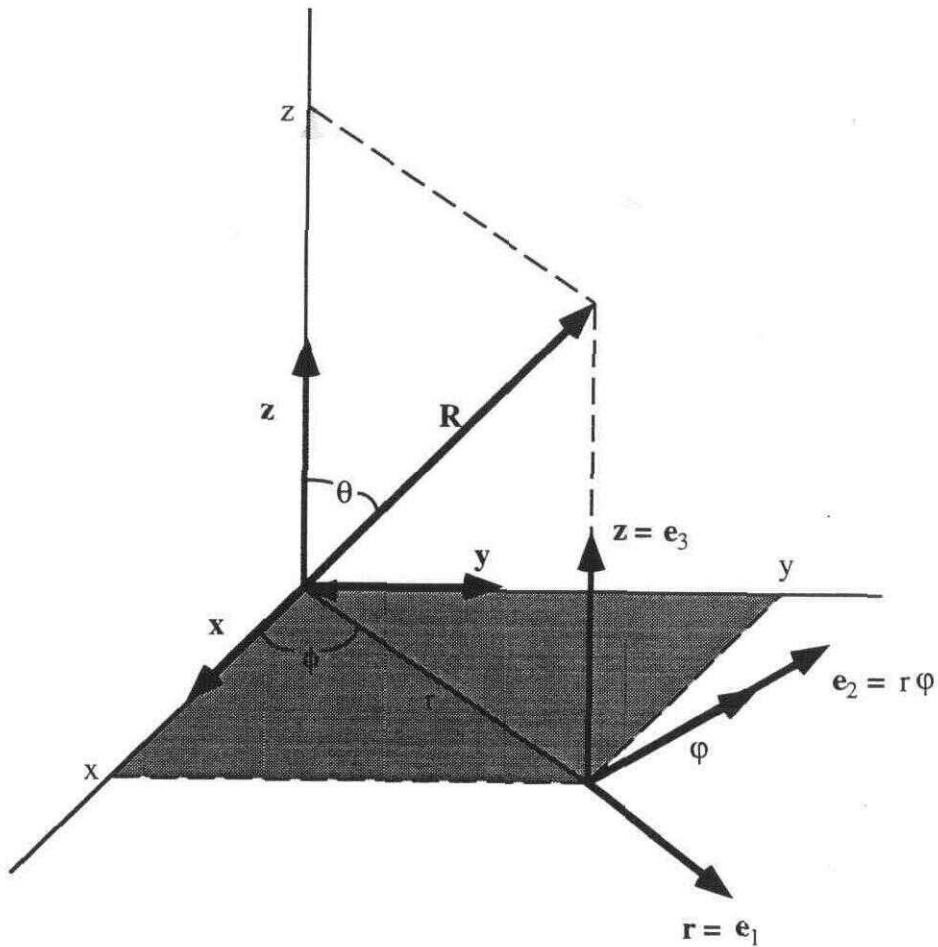


Fig. B.4-1. Cylindrical coordinates.

The results from Cartesian coordinates will be used to develop the relationships in cylindrical coordinates. From figure B.4-1 relationships between the two physical coordinates and their normalized basis vectors can be seen to be:

$$x = r \cos \varphi, \quad (\text{B.4-7a})$$

$$y = r \sin \varphi, \quad (\text{B.4-7b})$$

$$z = z, \quad (\text{B.4-7c})$$

$$\mathbf{r} = \sin(\varphi) \mathbf{y} + \cos(\varphi) \mathbf{x}, \quad (\text{B.4-7d})$$

$$\boldsymbol{\varphi} = \cos(\varphi) \mathbf{y} - \sin(\varphi) \mathbf{x} , \quad (\text{B.4-7e})$$

and

$$\mathbf{z} = \mathbf{z} . \quad (\text{B.4-7f})$$

The covariant basis vectors will be, by definition:

$$\mathbf{e}_1 = \frac{\partial \mathbf{R}}{\partial r} , \quad (\text{B.4-8a})$$

$$\mathbf{e}_2 = \frac{\partial \mathbf{R}}{\partial \varphi} , \quad (\text{B.4-8b})$$

and

$$\mathbf{e}_3 = \frac{\partial \mathbf{R}}{\partial z} . \quad (\text{B.4-8c})$$

These basis vectors need not be unit vectors. By direct application of the chain rule and substitution of equations (B.4-7a) through (B.4-7f) into equations (B.4-8a) through (B.4-8c), as in the following example:

$\mathbf{e}_2 = \frac{\partial \mathbf{R}}{\partial \varphi} = \frac{\partial \mathbf{R}}{\partial x} \frac{\partial x}{\partial \varphi} + \frac{\partial \mathbf{R}}{\partial y} \frac{\partial y}{\partial \varphi} + \frac{\partial \mathbf{R}}{\partial z} \frac{\partial z}{\partial \varphi} \quad (\text{by the chain rule})$
$= \mathbf{x} \frac{\partial x}{\partial \varphi} + \mathbf{y} \frac{\partial y}{\partial \varphi} + \mathbf{z} \frac{\partial z}{\partial \varphi} \quad \left( \begin{array}{l} \text{by definition of } \mathbf{R} \text{ in rectangular} \\ \text{Cartesian coordinates} \end{array} \right)$
$= -\mathbf{x} r \sin(\varphi) + \mathbf{y} r \cos(\varphi) \quad (\text{by equations B.4-7a to 7c})$
$= r \boldsymbol{\varphi} \quad (\text{by equation B.4-7e})$

we obtain:

$$\mathbf{e}_1 = \mathbf{r}, \quad (\text{B.4-9a})$$

$$\mathbf{e}_2 = r \boldsymbol{\phi}, \quad (\text{B.4-9b})$$

and

$$\mathbf{e}_3 = \mathbf{z}. \quad (\text{B.4-9c})$$

To get a handle on the metric tensor, one can first consider the differential of the position vector  $d\mathbf{R}$ , which has the representation:

$$d\mathbf{R} = dx^i \mathbf{e}_i = dr \mathbf{r} + d\phi r \boldsymbol{\phi} + dz \mathbf{z}. \quad (\text{B.4-10})$$

By comparing terms in equation (B.4-10) and using equations (B.4-9a) through (B.4-9c) the following can be deduced:

$$dx^1 = dr, \quad dx^2 = d\phi \quad \text{and} \quad dx^3 = dz.$$

Keeping this in mind and using equation (B.4-10), the differential arc-length can be computed:

$$(ds)^2 = d\mathbf{R} \cdot d\mathbf{R} = g_{ij} dx^i dx^j = (dr)^2 + (r d\phi)^2 + (dz)^2. \quad (\text{B.4-11})$$

This, in turn, gives the definition of the metric tensor, which can be written in matrix form as:

$$[g_{ij}] = \begin{bmatrix} 1 & 0 & 0 \\ 0 & (r)^2 & 0 \\ 0 & 0 & 1 \end{bmatrix} = \begin{bmatrix} 1 & 0 & 0 \\ 0 & (x^1)^2 & 0 \\ 0 & 0 & 1 \end{bmatrix}, \quad (\text{B.4-12a})$$

and

$$[g^{ij}] = [g_{ij}]^{-1} = \begin{bmatrix} 1 & 0 & 0 \\ 0 & (r)^{-2} & 0 \\ 0 & 0 & 1 \end{bmatrix} = \begin{bmatrix} 1 & 0 & 0 \\ 0 & (x^1)^{-2} & 0 \\ 0 & 0 & 1 \end{bmatrix}. \quad (\text{B.4-12b})$$

The metric tensor can also be defined by the inner or dot product of the covariant basis vectors in the following manner:

$$\mathbf{e}_i \cdot \mathbf{e}_j = g_{ij}. \quad (\text{B.4-13a})$$

Equation (B.4-13a) provides an alternate means of obtaining the length of the covariant basis vectors. Since the covariant basis vectors are not unit vectors in general, but lie in the same directions as the physical unit vectors, the length of the covariant basis provides a link between the physical and contravariant components of the vectors. The lengths of the covariant basis vectors are:

$$|\mathbf{e}_i|^2 = \mathbf{e}_i \cdot \mathbf{e}_i = g_{ii}. \quad (\text{B.4-13b})$$

This supplies a link between the contravariant components of a vector and its physical components through the metric tensor. Let  $\mathbf{u}_i$  be unit vectors along the covariant vectors  $\mathbf{e}_i$ . Then for any vector  $\mathbf{v}$  the relationship:

$$\mathbf{v} = \tilde{v}^i \mathbf{u}_i = v^i \mathbf{e}_i, \quad (\text{B.4-14})$$

holds. The tilde specifies the physical components. Examining equation (B.4-13b) and equation (B.4-14) shows the components are related by:

$$\tilde{v}^\alpha = \sqrt{g_{\alpha\alpha}} v^\alpha \quad (\text{recall, no summation on Greek letters}). \quad (\text{B.4-15})$$

The previous development allows the calculation of the Christoffel symbols. For cylindrical coordinates in a Euclidean space, the Christoffel symbols will have the form:

$$\left\{ \begin{matrix} i \\ jk \end{matrix} \right\} = g^{il} [jk;l] = \frac{g^{il}}{2} \left[ \frac{\partial g_{jl}}{\partial x^k} + \frac{\partial g_{kl}}{\partial x^j} - \frac{\partial g_{jk}}{\partial x^l} \right]$$

$$= \frac{g^{i\alpha}}{2} \left[ \frac{\partial g^{j\alpha}}{\partial x^k} + \frac{\partial g^{k\alpha}}{\partial x^j} - \frac{\partial g^{jk}}{\partial x^\alpha} \right] \quad (\text{again, no summation on } \alpha). \quad (\text{B.4-16a})$$

Since:

$$\frac{\partial g_{ij}}{\partial x^k} = \begin{cases} 2x^1 = 2r & : i = j = 2, k = 1 \\ 0 & : \text{otherwise} \end{cases}$$

$$= 2r \delta_{i2} \delta_{j2} \delta_{k1},$$

then:

$$[ij;k] = r (\delta_{i2} \delta_{k2} \delta_{j1} + \delta_{j2} \delta_{k2} \delta_{i1} - \delta_{i2} \delta_{j2} \delta_{k1}). \quad (\text{B.4-16b})$$

Substitution of equation (B.4-16b) into equation (B.4-16a) shows that there are only three nonzero elements of the Christoffel symbol, these are:

$$\left\{ \begin{matrix} 2 \\ 21 \end{matrix} \right\} = \left\{ \begin{matrix} 2 \\ 12 \end{matrix} \right\} = \frac{1}{r} \quad (\text{B.4-17a})$$

and

$$\left\{ \begin{matrix} 1 \\ 22 \end{matrix} \right\} = -r. \quad (\text{B.4-17b})$$

All the other elements are identically zero. To simplify notation, the physical components will not have a tilde over them: instead, any subscript or superscript of  $r$ ,  $\varphi$ , or  $z$  will indicate physical components. The equations of linear elasticity in cylindrical coordinates can now be written with the aid of the expressions above; the displacement gradients will have the form:

$$u^i_{,j} = \frac{\partial u^i}{\partial x^j} + \left\{ \begin{matrix} i \\ jk \end{matrix} \right\} u^k, \quad (\text{B.4-18})$$

which from equations (B.4-17a) and (B.4-17b) will have three special components. The first is:

$$u_{\cdot,2}^2 = \frac{\partial u^2}{\partial x^2} + \left\{ \begin{matrix} 2 \\ 21 \end{matrix} \right\} u^1$$

$$= \frac{\partial \frac{1}{r} u_\varphi}{\partial \varphi} + \frac{u_r}{r}. \quad (\text{B.4-19a})$$

Recall that the physical components are related to the tensor components by:

$$u_{\cdot,\varphi}^\varphi = \sqrt{g_{22}g^{22}} u_{\cdot,2}^2 = \sqrt{r^2 \frac{1}{r^2}} u_{\cdot,2}^2 = u_{\cdot,2}^2. \quad (\text{B.4-19b})$$

Therefore, the physical components of equation (B.4-19a) will be:

$$u_{\cdot,\varphi}^\varphi = \frac{1}{r} \frac{\partial u_\varphi}{\partial \varphi} + \frac{u_r}{r}. \quad (\text{B.4-19c})$$

The second special component is:

$$u_{\cdot,1}^2 = \frac{\partial u^2}{\partial x^1} + \left\{ \begin{matrix} 2 \\ 12 \end{matrix} \right\} u^2, \quad (\text{B.4-20a})$$

which has physical components related to its tensor components in the fashion:

$$u^\varphi = \sqrt{g_{22}g^{11}} u_{\cdot,1}^2 = \sqrt{r^2} u_{\cdot,1}^2 = r u_{\cdot,1}^2. \quad (\text{B.4-20b})$$

This means that the physical form of equation (B.4-20a) will be:

$$u_{\cdot,r}^\varphi = \frac{\partial u_\varphi}{\partial r} + \frac{u_r}{r}; \quad (\text{B.4-20c})$$

and the last special component is:

$$u^{1,2} = \frac{\partial u^1}{\partial x^2} + \left\{ \begin{matrix} 1 \\ 22 \end{matrix} \right\} u^2, \quad (\text{B.4-21a})$$

which has the following physical representation:

$$u^{r,\varphi} = \frac{1}{r} \left[ \frac{\partial u_r}{\partial \varphi} - u_\varphi \right]. \quad (\text{B.4-21c})$$

All the rest of the components will reduce to partial derivatives of the form:

$$u^{i,j} = \frac{\partial u^i}{\partial x^j}, \quad (\text{B.4-22a})$$

with physical representations:

$$\tilde{u}^{\alpha}_{,\beta} = \sqrt{g^{\beta\beta} g_{\alpha\alpha}} u^{\alpha}_{,\beta} = \sqrt{g^{\beta\beta} g_{\alpha\alpha}} \frac{\partial u^\alpha}{\partial x^\beta}. \quad (\text{B.4-22c})$$

The contravariant components of the linear strain are:

$$e^{ij} = \frac{1}{2} (g^{jl} u^i_{,l} + g^{il} u^j_{,i}); \quad (\text{B.4-23})$$

and some specific sample components have the form:

$$\begin{aligned} e^{13} &= \frac{1}{2} (g^{33} u^1_{,3} + g^{11} u^3_{,1}), \\ &= \frac{1}{2} (u^1_{,3} + u^3_{,1}) \end{aligned} \quad (\text{B.4-24a})$$

with physical-component representation:

$$e^{rz} = \frac{1}{2} \left( \frac{\partial u_r}{\partial z} + \frac{\partial u_z}{\partial r} \right). \quad (\text{B.4-24b})$$

Also,

$$\begin{aligned} e^{23} &= \frac{1}{2} (g^{33}u_{,3}^2 + g^{22}u_{,2}^3) \\ &= \frac{1}{2} \left( \frac{\partial u^2}{\partial x^3} + \frac{1}{r^2} \frac{\partial u^3}{\partial x^2} \right), \end{aligned} \quad (\text{B.4-25a})$$

and its physical component is given by:

$$e^{\varphi z} = \frac{1}{2} \left( \frac{\partial u_\varphi}{\partial z} + \frac{1}{r} \frac{\partial u_z}{\partial \varphi} \right). \quad (\text{B.4-25b})$$

The last sample component is:

$$e^{33} = \frac{\partial u^3}{\partial x^3}, \quad (\text{B.4-26a})$$

which is its own physical component, therefore:

$$e^{zz} = \frac{\partial u_z}{\partial z}. \quad (\text{B.4-26b})$$

Before leaving stress, the following contraction will be considered:

$$\begin{aligned} \Delta &= e^k_{,k} = u^k_{,k} = \frac{\partial u^k}{\partial x^k} + \left\{ \begin{matrix} 2 \\ 12 \end{matrix} \right\} u^1 \\ &= \frac{\partial u_r}{\partial r} + \frac{u_r}{r} + \frac{1}{r} \frac{\partial u_\varphi}{\partial \varphi} + \frac{\partial u_z}{\partial z}, \end{aligned} \quad (\text{B.4-27})$$

which, being a scalar, is invariant and is its own physical representation. Now consider the constitutive relationship:

$$\begin{aligned}
 \sigma^{ij} &= c^{ij}_{kl} e^{kl} \\
 &= [\lambda \delta^{ij} \delta_{kl} + \mu (\delta^i_k \delta^j_l + \delta^i_l \delta^j_k)] e^{kl} \\
 &= \lambda \delta^{ij} \Delta + \mu e^{ij} .
 \end{aligned} \tag{B.4-28}$$

Some of the physical components of equation (B.4-28) are:

$$\sigma^{rz} = 2\mu e^{rz} = \mu \left( \frac{\partial u_r}{\partial z} + \frac{\partial u_z}{\partial r} \right), \tag{B.4-29}$$

$$\sigma^{\varphi z} = 2\mu e^{\varphi z} = \mu \left( \frac{\partial u_\varphi}{\partial z} + \frac{1}{r} \frac{\partial u_z}{\partial \varphi} \right), \tag{B.4-30}$$

and

$$\sigma^{zz} = \lambda \Delta + 2\mu e^{zz} = \lambda \Delta + 2\mu \frac{\partial u_z}{\partial z}. \tag{B.4-31}$$

Finally, the two forms of the equation of motion will be:

$$\ddot{u}^i \rho = (\lambda + \mu) g^{ij} u^l{}_{,lj} + \mu g^{jl} u^i{}_{,jl} + f^i \rho \tag{B.4-32}$$

and

$$\begin{aligned}
 \ddot{u}^i \rho &= (\lambda + 2\mu) g^{ij} u^l{}_{,lj} - \mu \epsilon^{ijk} \epsilon_{klm} g^{ln} u^m{}_{,nj} + f^i \rho \\
 &= (\lambda + 2\mu) g^{ij} \Delta_{,j} - \mu \epsilon^{ijk} \omega_{k,j} + f^i \rho ,
 \end{aligned} \tag{B.4-33}$$

where equation (B.4-27) has been substituted and the definition:

$$\omega_k = \varepsilon_{klm} g^{ln} u_{,n}^m, \quad (\text{B.4-34})$$

was used. The physical representations of equation (B.4-34), also called the curl of the displacement, can be found. For this purpose it is easier to work with the contravariant components, so equation (B.4-34) will be cast in its contravariant form as:

$$\omega^i = \varepsilon^{ijk} g_{jl} u_{,k}^l = \varepsilon^{ijk} u_{l,k}^l. \quad (\text{B.4-35})$$

Before proceeding further, the following useful identity will be derived:

**Box II:**

$$u_{i,j} - u_{j,i} = \left[ \frac{\partial u_i}{\partial x^j} - \left\{ \begin{matrix} k \\ ij \end{matrix} \right\} u_k \right] - \left[ \frac{\partial u_j}{\partial x^i} - \left\{ \begin{matrix} k \\ ji \end{matrix} \right\} u_k \right], \quad (\text{B.4-II-i})$$

since:

$$\left\{ \begin{matrix} k \\ ij \end{matrix} \right\} = \left\{ \begin{matrix} k \\ ji \end{matrix} \right\},$$

then:

$$u_{i,j} - u_{j,i} = \frac{\partial u_i}{\partial x^j} - \frac{\partial u_j}{\partial x^i} = u_{i,j} - u_{j,i}. \quad (\text{B.4-II-ii})$$

The first component of equation (B.4-35) is:

$$\begin{aligned} \omega^1 &= \varepsilon^{1jk} u_{j,k} = \frac{1}{\sqrt{g}} e^{1jk} u_{j,k} \\ &= \frac{1}{r} [e^{123} u_{2,3} + e^{132} u_{3,2}] \quad (\text{expansion of permutation symbol}) \\ &= \frac{1}{r} [u_{2,3} - u_{3,2}] = \frac{1}{r} \left[ \frac{\partial u_2}{\partial x^3} - \frac{\partial u_3}{\partial x^2} \right] \quad (\text{by equation B.4-II-ii}) \end{aligned}$$

$$= \frac{1}{r} \left[ \frac{\partial r u_\phi}{\partial z} - \frac{\partial u_z}{\partial \phi} \right] \quad (\text{substitution of physical components}). \quad (\text{B.4-36})$$

Since:

$$\omega_r = \bar{\omega}^1 = \sqrt{g_{11}} \omega^1 = \omega^1,$$

the first physical component of the curl of the displacement in cylindrical coordinates will be:

$$\omega_r = \frac{\partial u_\phi}{\partial z} - \frac{1}{r} \frac{\partial u_z}{\partial \phi}. \quad (\text{B.4-37a})$$

The second and third physical components of the curl of the displacement can be found in a similar fashion to be:

$$\omega_\phi = \frac{\partial u_z}{\partial r} - \frac{\partial u_r}{\partial z}, \quad (\text{B.4-37b})$$

and:

$$\omega_z = \frac{1}{r} \left[ \frac{\partial u_r}{\partial \phi} - \frac{\partial r u_\phi}{\partial r} \right]. \quad (\text{B.4-37c})$$

By the same procedure as above, the physical components of the equation of motion (B.4-33) can also be derived by:

$$\begin{aligned} \ddot{u}^1 \rho &= (\lambda + 2\mu) g^{11} \Delta_{,1} - \frac{\mu}{\sqrt{g}} e^{1jk} \omega_{k,j} + f^1 \rho \\ &= (\lambda + 2\mu) g^{11} \frac{\partial \Delta}{\partial x^1} - \frac{\mu}{r} [e^{123} \omega_{2,3} + e^{132} \omega_{3,2}] + f^1 \rho \end{aligned}$$

$$\ddot{u}^1 \rho = (\lambda + 2\mu) \frac{\partial \Delta}{\partial x^1} - \frac{\mu}{r} \left[ \frac{\partial \omega_2}{\partial x^3} - \frac{\partial \omega_3}{\partial x^2} \right] + f^1 \rho. \quad (\text{B.4-38})$$

Substituting the physical components:

$$u_r = \tilde{u}^1 = \sqrt{g_{11}} u^1 = u^1,$$

$$\omega_\varphi = \tilde{\omega}_2 = \sqrt{g^{22}} \omega_2 = \frac{\omega_2}{r},$$

$$\omega = \tilde{\omega}_3 = \sqrt{g^{33}} \omega_3 = \omega_3,$$

into equation (B.4-38) gives the first physical-component form of the equation of motion:

$$\ddot{u}_r \rho = (\lambda + 2\mu) \frac{\partial \Delta}{\partial r} - \frac{\mu}{r} \left[ r \frac{\partial \omega_\varphi}{\partial z} - \frac{\partial \omega_z}{\partial \varphi} \right] + f_r \rho. \quad (\text{B.4-39a})$$

By using the same method as above, the second and third physical components are:

$$\ddot{u}_\varphi \rho = (\lambda + 2\mu) \frac{\partial \Delta}{\partial \varphi} - \mu \left[ \frac{\partial \omega_z}{\partial r} - \frac{\partial \omega_r}{\partial z} \right] + f_\varphi \rho, \quad (\text{B.4-39b})$$

and:

$$\ddot{u}_z \rho = (\lambda + 2\mu) \frac{\partial \Delta}{\partial z} - \frac{\mu}{r} \left[ \frac{\partial \omega_r}{\partial \varphi} - \frac{\partial r \omega_\varphi}{\partial r} \right] + f_z \rho. \quad (\text{B.4-39c})$$

The tensor equations previously derived for linear elasticity have been translated to the physical components of two particular coordinate systems, the rectangular and cylindrical coordinate systems. This is just an example, of course, since the tensor equations are true in any curvilinear coordinate system. Since physical laws should not depend on the coordinate system in which they are formulated it is prudent to cast the physical laws in some coordinate-independent form. Tensor component formulations provide one such platform; vector notation is another. The tensor route, however, does provide more information than the vector notation and rules of transformations are more

apparent in tensor form. The disadvantage is that tensor component formulas tend to be more complex in appearance and require some time to become comfortable with.

## **C: Cosserat media**

### **C.1: Introduction**

This note represents basically a review of a portion of Mindlin and Tiersten's (1962) paper. I will put the work in Einstein notation, which seems to be clearer. An attempt will be made to keep the development in general curvilinear coordinates (which does not necessarily add to the clarity). The sections of concern are the development of the Cosserat equations, which govern the behavior of continua where couple-stresses are included alongside the more familiar force-stresses, the development of constitutive relations (Toupin, 1962) which in the present analysis concerns the response of a Cosserat medium to deformation, the linearization of these relations, and the analysis of wave propagation through such a medium with emphasis on plane waves.

### **C.2: Force and Couple Stresses in Elasticity (Cosserat Equations)**

It can be shown that any system of forces acting on a rigid body can be broken down into a single force which acts on an arbitrary point of the body plus an appropriate couple (Symon, 1971). A couple, by definition, is a system of forces whose vector sum is zero, and which forces can be reduced to a system of two forces that are equal in magnitude but opposite in direction and do not act directly against each other (i.e., they do not have the same line of action). Otherwise, one could just as well replace these two forces by a force with magnitude zero, which is not very informative in any way. Couples provide a twisting or torquing effect to a mechanical system.

In continuum mechanics, the assumption has been made that a similar scheme can be used to describe the forces acting on a material volume  $V$  centered about the point  $P$ , enclosed by an orientable closed surface  $S'$ , as shown in figure C.2-1.

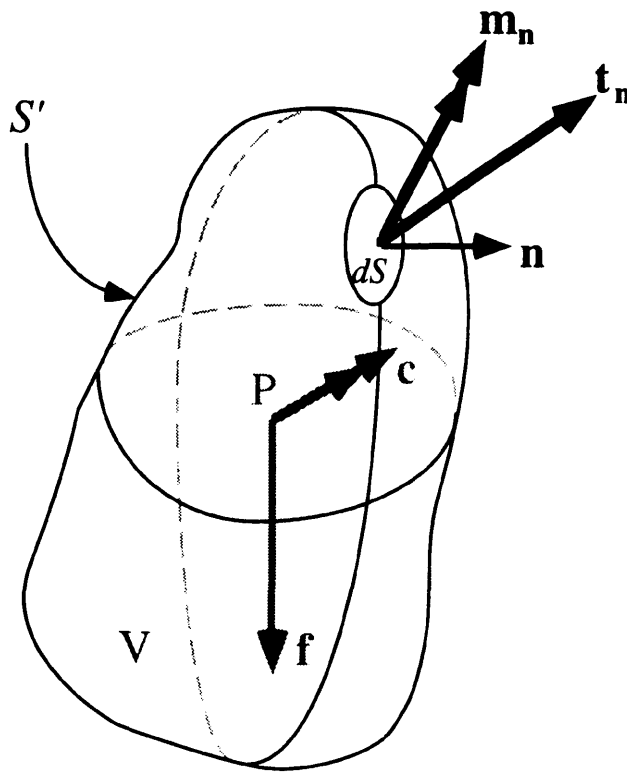


**Fig. C.2-1.** Forces and couples acting on a volume of material.

The material outside of  $V$  exerts forces on the material inside  $V$  through the surface  $S'$ . If we concentrate on a small region of the surface, as outlined by the oval in figure C.2-1, the net influence of the material in the direction of the outward unit normal vector,  $\mathbf{n}$ , consists of a force per unit area,  $\mathbf{t}_n$ , and a couple per unit area,  $\mathbf{m}_n$ . In the interior of  $S'$  action-at-a-distance type forces can influence the material in  $V$ . These forces will be assumed to be proportional to the mass acted upon; again, we will simplify these forces at each point in  $V$  into the now familiar force per unit mass,  $\mathbf{f}$ , and a couple per unit mass,  $\mathbf{c}$ . This is represented in figure C.2-1, where forces are illustrated as line segments ending in a single arrowhead and couples are portrayed with two arrowheads.

We shall now consider the motion of the material in the reference volume,  $V$ , due to these forces and couples. The motion will be governed by the equations of conservation of mass, balance of momentum and moment of momentum, and conservation of mechanical energy. The equations in index notation of these properties are respectively:

$$\frac{d}{dt} \int_V \rho \, dV = 0, \quad (\text{C.2-1})$$

$$\frac{d}{dt} \int_V v^i \rho \, dV = \int_S t_n^i \, dS + \int_V f^i \rho \, dV, \quad (\text{C.2-2})$$

$$\frac{d}{dt} \int_V \epsilon_{ijk}^i x^j v^k \rho \, dV = \int_S (\epsilon_{ijk}^i x^j t_n^k + m_n^i) \, dS + \int_V (\epsilon_{ijk}^i x^j f^k + c^i) \rho \, dV, \quad (\text{C.2-3})$$

and

$$\begin{aligned} \frac{d}{dt} \int_V \left( \frac{1}{2} g_{ij} v^i v^j + U \right) \rho \, dV &= \int_S \left( g_{ij} t_n^i v^j + \frac{1}{2} m_n^i \epsilon_{ijk} g^{lk} v_{,l}^j \right) \, dS \\ &+ \int_V \left( g_{ij} v^i f^j + \frac{1}{2} c^i \epsilon_{ijk} g^{lk} v_{,l}^j \right) \rho \, dV, \end{aligned} \quad (\text{C.2-4})$$

where

$$\frac{d}{dt} \equiv \text{material time derivative,}$$

$$\rho \equiv \text{mass density,}$$

$\mathbf{n} \equiv$  outward normal of surface  $S'$ ,

$x^i \equiv$  position vector component,

$g_{ij} \equiv$  metric tensor,

$\varepsilon_{ijk} = \sqrt{g} e_{ijk} \equiv$  permutation tensor,

such that  $g = \det[g^{lk}] = |g^{lk}|$  and  $e_{ijk} \equiv$  permutation symbols,

$v^i \equiv \frac{d}{dt}x^i = \dot{x}^i \equiv$  material velocity,

and  $U \equiv$  internal energy per unit mass.

We are using the material (Lagrangian) frame of reference, which means the material time derivative can be taken within the integral sign. One direct consequence of this is that equation (C.2-1) can be written as:

$$\frac{d}{dt} \int_{\mathcal{V}} \rho \, dV = \int_{\mathcal{V}} \frac{d\rho}{dt} \, dV = 0 = \dot{\rho} . \quad (\text{C.2-1a})$$

By the tetrahedron argument, as summarized in appendix E, we can recast the force per unit area and couple per unit area, respectively, in the following form:

$$t_{\mathbf{n}}^i = t^{ij} n_j, \quad (\text{C.2-5})$$

and

$$m_{\mathbf{n}}^i = m^{ij} n_j. \quad (\text{C.2-6})$$

The surface integral in equation (C.2-2) can be transformed by use of equation (C.2-5) and the divergence theorem in the following manner:

$$\int_s t_{\mathbf{n}}^i dS = \int_s t^{ij} n_j dS = \int_v t^{ij}_{,j} dV, \quad (\text{C.2-7})$$

where

$$\begin{aligned} t^{ij}_{,j} &= \frac{\partial t^{ij}}{\partial x^j} + \left\{ \begin{matrix} i \\ rj \end{matrix} \right\} t^{rj} + \left\{ \begin{matrix} j \\ rj \end{matrix} \right\} t^{ir} \\ &= \frac{1}{\sqrt{g}} \frac{\partial}{\partial x^r} [\sqrt{g} t^{ir}] + \left\{ \begin{matrix} i \\ rj \end{matrix} \right\} t^{rj} \end{aligned}$$

is a covariant derivative,

$$\left\{ \begin{matrix} l \\ ij \end{matrix} \right\} = g^{lk} [ij, k],$$

and

$$[ij, k] = \frac{1}{2} \left( \frac{\partial g_{ik}}{\partial x^j} + \frac{\partial g_{jk}}{\partial x^i} - \frac{\partial g_{ij}}{\partial x^k} \right).$$

Substituting equation (C.2-7) into equation (C.2-2) and using equation (C.2-1) results in the following, after rearrangement of terms:

$$\int_v t^{ij}_{,j} + f^i \rho - \dot{v}^i \rho dV = 0.$$

Since the volume is arbitrary, we have the result:

$$t^{ij}_{,j} + f^i \rho - \dot{v}^i \rho = 0, \quad (\text{C.2-8})$$

or 
$$t^{ij}_{,j} + f^i \rho = \dot{v}^i \rho$$

which is the usual force-stress equation of motion. In the same spirit of casting the integral equation (C.2-2) into its differential form (C.2-8) we shall do the same for the rest of the equations. First we shall concentrate on the separate parts of equation (C.2-3) as follows:

$$\begin{aligned} \frac{d}{dt} \int_{\mathbf{v}} \epsilon_{jk}^i x^j v^k \rho \, dV &= \int_{\mathbf{v}} \epsilon_{jk}^i (v^j v^k \dot{\rho} + x^j \dot{v}^k \rho + x^j v^k \dot{\rho}) \, dV \\ &= \int_{\mathbf{v}} \epsilon_{jk}^i x^j \dot{v}^k \rho \, dV. \end{aligned} \quad (\text{C.2-3a})$$

The last equality is due to the antisymmetric nature of the permutation tensor and equation (C.2-1a); also,

$$\begin{aligned} \int_{\mathbf{s}} \epsilon_{jk}^i x^j t_{\mathbf{n}}^k \, dS &= \int_{\mathbf{s}} \epsilon_{jk}^i x^j t^{kl} n_l \, dS = \int_{\mathbf{v}} (\epsilon_{jk}^i x^j t^{kl} n_l)_{,l} \, dV \\ &= \int_{\mathbf{v}} \epsilon_{jk}^i (x^j t^{kl}_{,l} + x^j_{,l} t^{kl}) \, dV = \int_{\mathbf{v}} \epsilon_{jk}^i x^j t^{kl}_{,l} + \epsilon_{jk}^i x^j_{,l} t^{kl} \, dV. \end{aligned} \quad (\text{C.2-3b})$$

The first equality uses equation (C.2-5), the second uses the divergence theorem, and finally

$$\int_{\mathbf{s}} m_{\mathbf{n}}^i \, dS = \int_{\mathbf{s}} m^{ij} n_j \, dS = \int_{\mathbf{v}} m^{ij}_{,j} \, dV, \quad (\text{C.2-3c})$$

where equation (C.2-6) and the divergence theorem is used respectively. Substitution of equations (C.2-3a-c) into the conservation of momentum equation (C.2-3) yields:

$$\int_V \epsilon_{jk}^i x^j (t_{,l}^{kl} + f^k - v^k \rho) dV + \int_V \epsilon_{jk}^i x^j t^{kl} + c^i \rho + m_{,j}^{ij} dV = 0,$$

the first integral of which is identically zero, as can be verified by direct comparison with equation (C.2-8). Since again the volume is arbitrary, the integrand of the second integral must equal zero. This results in the equation:

$$\epsilon_{jk}^i x^j t^{kl} + c^i \rho + m_{,j}^{ij} = 0,$$

or

$$\epsilon_{jk}^i t^{kj} + c^i \rho + m_{,j}^{ij} = 0. \quad (\text{C.2-9})$$

Equation (C.2-9) is the couple-stress equation of motion, and it provides an alternative expression for the antisymmetric part of the force-stress tensor as:

$$t^{[ij]} = -\frac{1}{2} \epsilon_{de}^i x^{j,d} (\epsilon_{fg}^e t^{gf}) = \frac{1}{2} \epsilon_{de}^i x^{j,d} (c^e \rho + m_{,f}^{ef}). \quad (\text{C.2-10})$$

The proof that equation (C.2-10) actually furnishes the antisymmetric part of a tensor is given box C.2-1.

**Box C.2-1:** Antisymmetric part of a second-order tensor.

The following development shows that equation (C.2-10) actually furnishes the antisymmetric part of a second-order tensor.

$$t^{[ij]} = -\frac{1}{2} \epsilon_{de}^i x^{j,d} (\epsilon_{fg}^e t^{gf})$$

$$= -\frac{1}{2} g^{il} \epsilon_{lde} g^{dm} x_{,m}^j g^{en} \epsilon_{efg} t^{gf} \quad (\text{raising and lowering indices})$$

$$= -\frac{1}{2} (g^{il} g^{dm} g^{en} \epsilon_{lde}) x_{,m}^j \epsilon_{nfg} t^{gf} \quad (\text{grouping terms})$$

$$= -\frac{1}{2} \epsilon^{imn} \epsilon_{nfg} x_{,m}^j t^{gf} \quad (\text{raising indices})$$

$$= -\frac{1}{2} \delta_{fg}^{im} x_{,m}^j t^{gf} \quad (\text{see B.3-I-i, generalized Kronecker delta})$$

$$= -\frac{1}{2} (\delta_f^j \delta_g^m - \delta_g^j \delta_f^m) x_{,m}^j t^{gf} \quad (\text{expanding Kronecker delta})$$

$$= -\frac{1}{2} (x_{,m}^j t^{mi} - x_{,m}^j t^{im}) \quad (\text{definition of Kronecker delta})$$

$$= \frac{1}{2} (t^{ij} - t^{ji}). \quad (\text{coordinate transform})$$

This completes our demonstration.

Note, the antisymmetric part of the force-stress tensor is identically zero if both the body couple and divergence of couple-stress are zero; therefore, under this condition, the force-stress tensor is totally symmetric. The total tensor can be expressed as the sum of symmetric and antisymmetric parts as follows:

$$t^{ij} = t^{(ij)} + t^{[ij]}, \quad (\text{C.2-11})$$

where the term with superscripts in round brackets is the symmetric part of the tensor. Substitution of equation (C.2-10) into equation (C.2-11), and subsequently into the equation of motion (C.2-8), results in the alternative form of the equation of motion:

$$t^{(ij)}_{;j} + \frac{1}{2} \varepsilon^{ij} m^{ef}_{;ff} + f^i \rho + \frac{1}{2} \varepsilon^{ij} c^e_{;j} \rho = \dot{v}^i \rho. \quad (\text{C.2-12})$$

Note, in equation (C.2-12), that if the body-couple and couple-stress terms are zero, we revert to the standard equation of motion, which is the start of most analysis. A further reduction can be achieved in equation (C.2-12) by considering the scalar of the couple stress given by:

$$\tilde{m} = m^{ij} x_{ij}, \quad (\text{C.2-12a})$$

and the deviator of the couple stress of the form:

$$m^{(ij)} = m^{ij} - \frac{1}{3} \tilde{m} x^{ij}. \quad (\text{C.2-12b})$$

We will now show that equation (C.2-12a) makes no contribution to equation (C.2-12); thus only the deviator given by equation (C.2-12b) will have any effect in equation (C.2-12). Consider the expression:

$$\begin{aligned} \varepsilon^{ij}_{;e} [\tilde{m} x^{ef}]_{;ff} &= \varepsilon^{ij}_{;e} [\tilde{m}_{;f} x^{ef} + \tilde{m} x^{ef}_{;f}]_{;j} \\ &= \varepsilon^{ij}_{;e} [\tilde{m}_{;e}]_{;j} \\ &= \varepsilon^{ije} \tilde{m}_{;ej} = 0, \end{aligned}$$

where the last equality is due to the fact that covariant differentiation of invariants (scalars) is commutative; in other words, we have the following symmetry property:

$$\tilde{m}^{ej} = \tilde{m}^{je}.$$

We can thus substitute equation (C.2-12b) into equation (C.2-12) to arrive at a form which more truly represents the independent parameters constrained by this equation. Equation (C.2-12) becomes:

$$t^{(ij)}_{,j} + \frac{1}{2} \varepsilon^{ij}_e m^{(ef)}_{,fj} + f^i \rho + \frac{1}{2} \varepsilon^{ij}_e c^e_{,j} \rho = \dot{v}^i \rho. \quad (\text{C.2-13})$$

We will now cast the equation of conservation of mechanical energy (C.2-4) into its differential form. To achieve this end we shall manipulate separate terms in the equation independently and then recombine them into our desired form. Start by considering:

$$\frac{d}{dt} \int_{\mathcal{V}} \left( \frac{1}{2} g_{ij} v^i v^j + U \right) \rho \, dV = \int_{\mathcal{V}} (g_{ij} v^i \dot{v}^j + \dot{U}) \rho \, dV, \quad (\text{C.2-4a})$$

where the dots represent material time derivatives. Secondly:

$$\begin{aligned} \int_s g_{ij} t^i_{,n} v^j \, dS &= \int_s (t^{ij} n_j) v_i \, dS \\ &= \int_{\mathcal{V}} (t^{ij} v_i)_{,j} \, dV \\ &= \int_{\mathcal{V}} t^{ij}_{,j} v_i + t^{ij} v_{i,j} \, dV. \end{aligned} \quad (\text{C.2-4b})$$

The first equality is from equation (C.2-6); the second is just the divergence theorem and the last is just the distributive law of covariant differentiation. Finally we consider:

$$\begin{aligned}
\int_S \frac{1}{2} m_n^i \epsilon_{ijk} g^{lk} v_{,l}^j dS &= \int_S \frac{1}{2} m^{ir} n_r \epsilon_{ijk} g^{lk} v_{,l}^j dS \\
&= \int_V \frac{1}{2} (m^{ir} \epsilon_{ijk} g^{lk} v_{,l}^j)_{,r} dV \\
&= \int_V \frac{1}{2} (\epsilon_{ijk} m^{ir}_{,r} v^{j,k} + \epsilon_{ijk} m^{ir} v_{,r}^{j,k}) dV .
\end{aligned} \tag{C.2-4c}$$

The steps taken above are almost identical to the previous and will not be elaborated upon. We can now incorporate equations (C.2-4a) - (C.2-4c) into equation (C.2-4) and upon rearrangement we get:

$$\int_V \dot{U} \rho dV = \int_V \left\{ (t^{ij}_{,j} + \rho f^i - \rho \dot{v}^i) v_i + \epsilon_{ijk} \left( \frac{1}{2} m^{ir}_{,r} + \rho c^i \right) v^{j,k} + t^{ij} v_{j,i} + \frac{1}{2} \epsilon_{ijk} m^{ir} v_{,r}^{j,k} \right\} dV ,$$

which, upon comparison with equations (C.2-8) and (C.2-9), simplifies to:

$$\int_V \dot{U} \rho dV = \int_V \left\{ t^{ij} v_{j,i} - \frac{1}{2} \epsilon_{ijk} (\epsilon^i_{rs} x^r_{,l} t^{sl}) v^{j,k} + \frac{1}{2} \epsilon_{ijk} m^{ir} v_{,r}^{j,k} \right\} dV ,$$

we make further note that:

$$\begin{aligned}
\frac{1}{2} \epsilon_{ijk} \epsilon^i_{rs} x^r_{,l} t^{sl} v^{j,k} &= \left( \frac{1}{2} \epsilon_i^{jk} \epsilon_{ls} t^{sl} \right) v_{j,k} \\
&= t^{[jk]} v_{j,k} .
\end{aligned}$$

The last equality can be seen by direct comparison with equation (C.2-10), hence:

$$\begin{aligned} \int_v \dot{U} \rho \, dV &= \int_v \left\{ (t^{ij} - t^{[ij]}) v_{j,i} + \frac{1}{2} \varepsilon_{ijk} m^{ir} v_{,r}^{j,k} \right\} dV \\ &= \int_v \left\{ t^{(ij)} v_{j,i} + \frac{1}{2} \varepsilon_{ijk} m^{ir} v_{,r}^{j,k} \right\} dV, \end{aligned}$$

or in differential form:

$$\dot{U} \rho = t^{(ij)} v_{j,i} + \frac{1}{2} \varepsilon_{ijk} m^{ir} v_{,r}^{j,k}. \quad (\text{C.2-14})$$

Note:

$$x_{,r}^i \varepsilon_{ijk} v^{j,kr} = \varepsilon_{ijk} v^{j,ki} = 0,$$

which is a trivial consequence in rectangular Cartesian coordinates. This means that the scalar of the couple-stress again has no effect in equation (C.2-14), a result which can be seen by substitution of (C.2-12b) into equation (C.2-14). Therefore, we can rewrite (C.2-14) in the following more informative way:

$$\dot{U} \rho = t^{(ij)} v_{j,i} + \frac{1}{2} \varepsilon_{ijk} m^{\{ir\}} v_{,r}^{j,k}. \quad (\text{C.2-15})$$

Equations (C.2-9), (C.2-13) and (C.2-15), the Cosserat equations, leave the antisymmetric part of the force-stress and the scalar of the couple-stress indeterminate. This means the number of independent variables controlled by these equations is  $(9-3)=6$  from the symmetric part of the force-stress and  $(9-1)=8$  from the deviator of the couple-stress, for a total of 14 independent variables. This becomes important when we try to relate the response of such a medium to deformation in the next section.

### C.3: Toupin's constitutive relations

Constitutive relations here will be concerned with the response of a Cosserat medium to deformation, which mean that other effects such as temperature and temperature gradient will not be considered. The deformation will be described with respect to some initial reference configuration called the material frame. The material frame position will be designated by the capital letter  $X$  and all references to that frame in terms of subscripts and superscripts will also be in capital letters. The arc distance in the spatial and material (Eulerian and Lagrangian) frames are respectively:

$$(ds)^2 = g_{kl} dx^k dx^l \quad (\text{C.3-1a})$$

and

$$(dS)^2 = G_{KL} dX^K dX^L \quad (\text{C.3-1b})$$

where the metric tensors are self-defining in each of the equations (frames). Now consider an infinitesimal directed line segment in the material frame and its image in the spatial frame, they will be related by the following formula:

$$dx^k = x^k_{;K} dX^K \quad (\text{C.3-2a})$$

or

$$dX^K = X^K_{;k} dx^k, \quad (\text{C.3-2b})$$

where the semicolon designates ordinary partial differentiation. Taking the inner product of equations (C.3-2a) and (C.3-2b) we arrive at:

$$(ds)^2 = g_{kl} X^k_{;K} X^l_{;L} dX^K dX^L \quad (\text{C.3-3a})$$

and

$$(dS)^2 = G_{KL} X^K_{;k} X^L_{;l} dx^k dx^l. \quad (C.3-3b)$$

The difference between the squared length of line elements containing the same material points in the deformed and undeformed bodies gives a measure of length change due to deformation. This can then be used as a variable to determine the amount of energy stored during deformation (I will not be considering systems which generate energy during deformation). With this in mind we write the following formula:

$$\begin{aligned} (ds)^2 - (dS)^2 &= (g_{kl} X^k_{;K} X^l_{;L} - G_{KL}) dX^K dX^L \\ &= (g_{kl} - G_{KL} X^K_{;k} X^L_{;l}) dx^k dx^l. \end{aligned} \quad (C.3-4)$$

The terms in parenthesis after the two equal signs provide a measure of length change in the material and spatial frames respectively. We shall give these quantities (Lagrangian and Eulerian strain tensors) special symbols, as defined below:

$$2E_{KL} = 2E_{LK} = g_{kl} x^k_{;K} x^l_{;L} - G_{KL} \quad (C.3-5a)$$

and

$$2e_{kl} = 2e_{lk} = g_{kl} - G_{KL} X^K_{;k} X^L_{;l}. \quad (C.3-5b)$$

The symmetry is obvious due to the symmetry of the metric tensor. When couple-stress is not taken into account, the strain tensors as defined by equations (C.3-5a) and (C.3-5b) are sufficient to describe the specific energy during deformation. However, as can be seen, this provides only 6 independent components while we have seen in the case when couple-stresses are considered there exists 14 degrees of freedom. R.E. Toupin (1962) has shown that an appropriate second variable is:

$$K_{JJ} = -\epsilon_J^{KL} E_{JKL}, \quad (C.3-6)$$

the scalar of which is zero, giving a total of 8 independent components. The 8 independent components from equation (C.3-6) and the 6 independent components from

equation (C.3-5a) are sufficient for our purpose. We now assume that the specific energy can be expressed as a function of these two tensors as:

$$U = U(E_{IJ}, K_{rs}), \quad (\text{C.3-7})$$

which implies:

$$\rho \dot{U} = \rho \frac{\partial U}{\partial E_{IJ}} \dot{E}_{IJ} + \rho \frac{\partial U}{\partial K_{RS}} \dot{K}_{RS}. \quad (\text{C.3-8})$$

The object is to put the conservation of energy equation (C.2-15) into the same double inner product form. After some troublesome manipulations this can be done giving rise to:

$$\rho \dot{U} = \phi^{IJ} \dot{E}_{IJ} + \psi^{RS} \dot{K}_{RS}, \quad (\text{C.3-9})$$

where

$$\psi_{IJ} = \left| X^I_{,i} \right| X_{I,i} m^{(ij)} X_{J,j}, \quad (\text{C.3-9a})$$

and

$$\phi_{IJ} = X_{I,i} t^{(ij)} X_{J,j} - \left| X^I_{,i} \right| A_{(IJ)}, \quad (\text{C.3-9b})$$

such that

$$A_{IJ} = \epsilon_{IKL} X^K_{,k} m^{(kr)} X^R_{,r} X^L_{,j} x^j_{,RJ}. \quad (\text{C.3-9c})$$

Before proceeding we have to note that:

$$\alpha X^{I,J} \dot{K}_{IJ} = 0, \quad (\text{C.3-10})$$

where  $\alpha$  is an arbitrary constant, this is due again to the fact that the scalar of  $\mathbf{K}$  is zero and therefore not all nine components are independent. We can therefore add equation

(C.3-10) to equation (C.3-8) without changing anything then subtract the result from equation (C.3-9) to get:

$$\left[ \phi^{IJ} - \rho \frac{\partial U}{\partial E_{IJ}} \right] \dot{E}_{IJ} + \left[ \psi^{RS} - \rho \frac{\partial U}{\partial K_{RS}} - \alpha X^{R,S} \right] \dot{K}_{RS} = 0. \quad (\text{C.3-11})$$

If we assume all terms within the square brackets of equation (C.3-11) are independent of the terms they are dot-multiplied with, then we can write:

$$\phi^{IJ} = \rho \frac{\partial U}{\partial E_{IJ}}, \quad (\text{C.3-12a})$$

and

$$\psi^{RS} = \rho \frac{\partial U}{\partial K_{RS}} + \alpha X^{R,S}. \quad (\text{C.3-12b})$$

By noting that all terms in equation (C.3-12b) have zero scalars, we can now finally set the constant  $\alpha$  to zero. Now we can solve for the symmetric part of the force-stress tensor and the deviator of the couple-stress tensor from equations (C.3-12a) and (C.3-12b), giving:

$$t^{(ij)} = \rho x^i_{,I} \frac{\partial U}{\partial E_{IJ}} x^j_{,J} + \rho G_{NL} \varepsilon^{INM} \frac{\partial U}{\partial K_{JL}} x^{(i}_{,I} x^{j)}_{,JM}, \quad (\text{C.3-13a})$$

and

$$m^{(ij)} = \rho |x^i_{,I}| x^i_{,I} \frac{\partial U}{\partial K_{IJ}} x^j_{,J}. \quad (\text{C.3-13b})$$

Equations (C.3-13a) and (C.3-13b) are one form of Toupin's constitutive equations.

#### C.4: Linearization

We will now linearize the equations previously developed. This linearized set will form the basis from which all future development will stem. We shall begin by assuming the specific energy can be expressed in terms of a Taylor's series in powers of  $E$  and  $K$  and also allowing the undeformed state to be one of zero stress and density with subscript 0:

$$\rho_0 U = \frac{1}{2} a^{QRST} K_{QR} K_{ST} + b^{QRST} E_{QR} K_{ST} + c^{QRST} E_{QR} E_{ST} + \dots, \quad (\text{C.4-1})$$

where  $\mathbf{a}$ ,  $\mathbf{b}$  and  $\mathbf{c}$  are constant material tetradics and the higher-order terms are understood to have higher-order polyadics for coefficients. The linear terms are zero from our zero-stress assumption above. We will define the material displacement as:

$$\mathbf{u} = \mathbf{x} - \mathbf{X}, \quad (\text{C.4-2})$$

which we will constrain to have a small material gradient in the following sense:

$$|\mathbf{u}_{,K}| \ll 1.$$

This implies that the material gradients and spatial gradients can be taken as approximately equal and the density remains approximately constant. The distinction between material and spatial frame can then be ignored. In this regime we can use the following approximation for the material strain dyadic:

$$E_{ij} \approx \frac{1}{2} (u_{i,j} + u_{j,i}) = \epsilon_{ij}, \quad (\text{C.4-3a})$$

which in turn gives the approximation for:

$$K_{ij} \approx -\epsilon_i^{lm} \epsilon_{lj,m} = -\frac{1}{2} (\epsilon_i^{lm} u_{l,jm} + \epsilon_i^{lm} u_{j,lm})$$

$$= \frac{1}{2} \varepsilon_i^{lm} u_{m,jl} = \chi_{ij}. \quad (\text{C.4-3b})$$

Substitution of approximations in equation (C.4-3a) and (C.4-3b) into equation (C.4-1) yields:

$$\rho_0 U = W \approx \frac{1}{2} a^{qrst} \chi_{qr} \chi_{st} + b^{qrst} \varepsilon_{qr} \chi_{st} + \frac{1}{2} c^{qrst} \varepsilon_{qr} \varepsilon_{st} + \dots, \quad (\text{C.4-4})$$

which can be used with the general constitutive equations (C.3-13a) and (C.3-13b) to give:

$$m^{(ij)} \approx \frac{\partial W}{\partial \chi_{ij}} \quad (\text{C.4-5a})$$

and

$$t^{(ij)} \approx \frac{\partial W}{\partial \varepsilon_{ij}} + \varepsilon_{mn}^i \frac{\partial W}{\partial \chi_{lm}} u_1^{nj},$$

which, upon the further assumption that  $u_1^{nj}$  is negligible, can be written as:

$$t^{(ij)} \approx \frac{\partial W}{\partial \varepsilon_{ij}}. \quad (\text{C.4-5b})$$

By ignoring all terms of higher order, we can write the following set of linearized equations:

$$W = \frac{1}{2} a^{qrst} \chi_{qr} \chi_{st} + b^{qrst} \varepsilon_{qr} \chi_{st} + \frac{1}{2} c^{qrst} \varepsilon_{qr} \varepsilon_{st}, \quad (\text{C.4-6a})$$

$$t^{(ij)} = \frac{\partial W}{\partial \varepsilon_{ij}} = c^{ijst} \varepsilon_{st} + b^{ijst} \chi_{st}, \quad (\text{C.4-6b})$$

and

$$m^{(ij)} = \frac{\partial W}{\partial \chi_{ij}} = a^{ijst} \chi_{st} + b^{qrij} \epsilon_{qr}. \quad (\text{C.4-6c})$$

Equations (C.4-6a),(C.4-6b) and (C.4-6c) are the general linearized constitutive equations. If one considers all the symmetries imposed on the material tetrads we will find that **a** has 36 independent components, **b** has 48 and **c** has the usual 21 independent components. If we now restrict the material to be centrosymmetric-isotropic we wind up with the following much simpler system of equations:

$$W = 2\eta \chi^{ij} \chi_{ij} + 2\eta' \chi^{ij} \chi_{ji} + \lambda (\epsilon_{ii})^2 + \mu \epsilon^{ij} \epsilon_{ij}, \quad (\text{C.4-7a})$$

$$t^{(ij)} = \frac{\partial W}{\partial \epsilon_{ij}} = \lambda \epsilon_{kk} g^{ij} + 2\mu \epsilon^{ij}, \quad (\text{C.4-7b})$$

and

$$m^{(ij)} = \frac{\partial W}{\partial \mu_{ij}} = 4\eta \chi^{ij} + 4\eta' \chi^{ji}, \quad (\text{C.4-7c})$$

where  $\lambda$  and  $\mu$  are the familiar Lamé constants while  $\eta$  and  $\eta'$  are new constants due to the introduction of couple-stresses. If we now substitute equations (C.4-3a) and (C.4-3b) into equations (C.4-7b) and (C.4-7c) we arrive at:

$$t^{(ij)} = \lambda u^{k,k} g^{ij} + 2\mu (u^{ij} + u^{ji}), \quad (\text{C.4-8a})$$

and

$$m^{(ij)} = 4\eta \epsilon_i^{lm} u_{m,jl} + 4\eta' \epsilon_i^{lm} u_{m,jl}. \quad (\text{C.4-8b})$$

Now we can substitute equations (C.4-3a),(C.4-3b),(C.4-8a) and (C.4-8b) into the equation of motion (C.2-13) which takes on the form:

$$\mu u^{i,j}_{\cdot j} + (\lambda + \mu) u^j_{\cdot ji} + \eta \epsilon^i_{jk} \epsilon^j_{lm} u^{l,mks} + \rho f^i + \frac{1}{2} \epsilon^i_{jk} c^k_{\cdot j} \rho = \rho \ddot{u}^i \quad (\text{C.4-9})$$

This equation will be the starting point for further analysis.

### C.5: Wave motion

The equation of motion (C.4-9) in the absence of body forces and body couples has the form:

$$\mu u_{..j}^{i,j} + (\lambda + \mu) u_{.ji}^j + \eta \varepsilon_{jk}^i \varepsilon_{.lm}^j u_{.....s}^{l,mks} = \rho \ddot{u}^i. \quad (\text{C.5-1})$$

We now proceed in the usual manner by taking divergence and curl of the equation of motion (C.5-1), resulting in:

$$c_1^2 \varphi_{.jj} = \ddot{\varphi}, \quad (\text{C.5-2})$$

and

$$c_2^2 \psi_{.jj}^i - c_2^2 \rho^2 \psi_{.jj}^i = \ddot{\psi}^i, \quad (\text{C.5-3})$$

where

$$\varphi = u_{.j}^i, \quad \psi^i = \varepsilon^{ijk} u_{.j,k},$$

$$c_1^2 = \frac{\eta}{\mu}, \quad c_1^2 = \frac{(\lambda + 2\mu)}{\rho} \quad \text{and} \quad c_2^2 = \frac{\mu}{\rho}.$$

As can be seen, the dilatational wave given by equation (C.5-2) is identical to the couple-stress-free case, while the rotational case is quite different. If  $\eta = 0$ , we would recover the usual rotational-wave equation. To examine the effects of this extra term on wave propagation, consider a plane rotational wave of the form:

$$\psi^i = d^i A \exp[i k (n_i x^i - c t)] = d^i A \exp[i(k_i x^i - \omega t)], \quad (\text{C.5-4})$$

where

$d^i \equiv$  unit vector,

$A \equiv$  scalar amplitude,

$k \equiv$  wave number,

$n_i \equiv$  unit wave normal,

$c \equiv$  phase velocity,

and  $\omega \equiv$  angular frequency.

Substitution of (C.5-4) into (C.5-3) results in the following two equations:

$$\omega^2 = c_2^2 k^2 (1 - \iota^2 k^2) \quad \text{and} \quad c^2 = c_2^2 (1 - \iota^2 k^2); \quad (\text{C.5-5})$$

which we can use to solve for  $k^2$ , giving us two roots, which we will denote as:

$$k_1^2 = \frac{1}{2} \iota^{-2} \left[ \sqrt{1 + \frac{4 \iota^2 \omega^2}{c_2^2}} - 1 \right], \quad (\text{C.5-6a})$$

and

$$k_2^2 = -\frac{1}{2} \iota^{-2} \left[ \sqrt{1 + \frac{4 \iota^2 \omega^2}{c_2^2}} + 1 \right]. \quad (\text{C.5-6b})$$

Since  $\iota$  is real we can see that  $k_1$  is real while  $k_2$  is purely imaginary. This means there are two rotational plane waves one propagating and the other nonpropagating, and both are dispersive. The propagating wave will have a group velocity given as

$$\frac{d\omega}{dk_1} = c_2 \frac{1 + 2\iota^2 k_1^2}{\sqrt{1 + \iota^2 k_1^2}}. \quad (\text{C.5-7})$$

Formula (C.5-7) shows the group velocity as a monotonically increasing function of  $\iota k_1$ . The preceding discussion has shown us some of the similarities and differences of a Cosserat continuum, as compared with an ordinary elastic continuum. Regardless of whether or not couples have a strong effect in real systems, we should be aware of the possibility of differences in observations and mindful of the models which we may employ to explain these differences.

## D: Method of Steepest Descent

### D.1: Introduction

The method discussed here is used to obtain an approximate solution to definite integrals of the form:

$$I = \int_A^B \chi(z) e^{t f(z)} dz , \quad (\text{D.1-1})$$

where  $t$  is assumed to be real, positive and large and  $f(z)$  is an analytic function. To find this approximation we need an intermediate result which gives the asymptotic expansion of the integral:

$$J = \int_0^Z e^{-t z} z^m f(z) dz , \quad (\text{D.1-2a})$$

such that the conditions of the corresponding variables and functions are met, that  $f(z)$  is not zero at  $z=0$ , and that  $Z$  is not a function of  $t$ . The asymptotic expansion of the integral  $J$  is given by one form of a lemma due to G. N. Watson. The actual integral we are interested in does not have the form of equation (D.1-2a) but rather that of the special case

$$K = \int_{-A}^B e^{-1/2 t^2 z^2} f(z) dz. \quad (\text{D.1-2b})$$

Generally I will be following the development of Watson's lemma from Jefferys and Jeffreys (1980, p. 501-502) and the approximate solution of equation (D.1-1) from Bâth (1968, p. 51-54), but I will borrow freely from other sources as well as adding my own two bits. The method of obtaining an approximate solution to (D.1-1) is known as the method of steepest descent or saddle-point method.

## D.2: Watson's lemma

### D.2.a: Case 1 ( Equation (D.1-2a) )

Since we have assumed  $f(z)$  to be analytic on the integration path we can, within the circle of convergence, expand  $f(z)$  in a Taylor's series (Churchill, Brown and Verhey, 1976, p. 145-147) as:

$$f(z) = \sum_{i=0}^{n-1} a_i z^i + R_n(z), \quad (\text{D.2.a-1})$$

where

$$R_n(z) = \frac{z^n}{2\pi i} \oint_C \frac{f(s)}{(s-z)s^n} ds, \quad (\text{D.2.a-2})$$

is the remainder and  $C$  is a closed path around the area of convergence. Since  $f(s)$  in equation (D.2.a-2) is analytic on and within  $C$ , it must be bounded within this region. Let the upper bound to its modulus be  $m$ . Then

$$g(z) = \left[ f(z) - \sum_{j=1}^{n-1} a_j z^j \right] z^{-n} = \frac{R_n(z)}{z^n} = \frac{1}{2\pi i} \oint_C \frac{f(s)}{(s-z)s^n} ds, \quad (\text{D.2.a-3})$$

will also be bounded. To see this, let  $|z| = r$  and  $|s| = r_c$ , where  $r_c$  is the radius of the circle of convergence, then:

$$|s - z| < |s| - |z| = r_c - r,$$

This allows us to transform equation (D.2.a-3) into the inequality:

$$\left| \frac{R_n(z)}{z^n} \right| = \frac{1}{2\pi} \left| \oint_C \frac{f(s)}{(s-z)s^n} ds \right| < \frac{m}{2\pi} \left| \oint_C \frac{ds}{(s-z)s^n} \right|,$$

so that

$$\left| \frac{R_n(z)}{z^n} \right| < \frac{m}{2\pi(r_c - r)r_c^n} \left| \oint_C ds \right| = \frac{m r_c}{(r_c - r)} < m = U. \quad (\text{D.2.a-4})$$

Now that an upper bound,  $U$ , of  $\left| \frac{R_n(z)}{z^n} \right|$  has been shown to exist in equation (D.2.a-4), we can use this information to rewrite the remainder as:

$$R_n(z) = z^n \Theta U e^{i\phi} \quad (\text{D.2.a-5})$$

where the new scalars are defined by:  $0 < \Theta < 1$ ,

$$\Theta U = |R_n(z)|, \quad (\text{D.2.a-6a})$$

and

$$\phi = \arg[R_n(z)]. \quad (\text{D.2.a-6b})$$

This means that  $\frac{R_n(z)}{z^n}$  approaches a finite limit as  $z$  approaches zero. We will put equation (D.2.a-5) into a more concise form

$$\frac{R_n(z)}{z^n} = \Theta M, \quad (\text{D.2.a-7})$$

such that  $M = \Theta U$  and  $\theta = e^{i\phi}$ . Now we proceed to break up integral (D.1-2a) into two parts by identifying a point where  $z = A$  within the circle of convergence  $C$  and expressing the integral as:

$$I = I_A + I_B = \left[ \int_0^A + \int_A^Z \right] e^{-tz} z^m f(z) dz, \quad (\text{D.2.a-8a})$$

where I have defined:

$$I_A = \int_0^A e^{-tz} z^m f(z) dz \quad (\text{D.2.a-8b})$$

and

$$I_B = \int_A^Z e^{-tz} z^m f(z) dz. \quad (\text{D.2.a-8c})$$

Using the Taylor expansion (D.2.a-1) and the expression given by equation (D.2.a-7) the first of the two integrals in equation (D.2.a-8b) can be expressed as:

$$I_A = \int_0^A e^{-tz} z^m f(z) dz$$

$$= \left[ \sum_{j=0}^{n-1} \int_0^A e^{-tz} z^m a_j z^j dz \right] + \left[ \int_0^A e^{-tz} z^m \Theta M z^n dz \right]. \quad (\text{D.2.a-9})$$

This was accomplished by substitution of equation (D.2.a-7) into equation (D.2.a-1) and subsequently into the first integral of equation (D.2.a-8). It is important to note that the integration is over a real line segment  $(0,A)$ , therefore  $\theta = e^{i\phi}$  is equal to 1, and the factor

$\theta M$  can be treated as constant and taken outside the integration. This means that both integrals in equation (D.2.a-9) are of the form:

$$J = \int_0^A e^{-tz} z^p dz. \quad (\text{D.2.a-10})$$

This equation can be solved by the repeated application of integration by parts. The result is:

$$J = e^{-tA} \left[ \sum_{n=0}^p \frac{A^{(p-n)} p!}{-t^{(n+1)} (p-n)!} \right] + \frac{p!}{t^{(p+1)}}, \quad (\text{D.2.a-11a})$$

or

$$J = \frac{p!}{t^{(p+1)}} + O(e^{-tA}), \quad (\text{D.2.a-11b})$$

where  $O(\cdot)$  means of the order of the argument. Equation (D.2.a-11b) allows equation (D.2.a-9) to be written in the form:

$$I_A = \left[ \sum_{j=0}^{n-1} a_j \frac{(m+j)!}{t^{(m+j+1)}} \right] + \left[ \theta M \frac{(m+n)!}{t^{(m+n+1)}} \right] + O(e^{-tA}). \quad (\text{D.2.a-12})$$

Now we turn our attention to the second integral in equation (D.2.a-8) given by:

$$I_B = \int_A^Z e^{-tz} z^m f(z) dz. \quad (\text{D.2.a-13})$$

In order to examine the behavior of  $I_B$ , we need Abel's theorem for integrals, which states:

if  $v(x)$  is a non-negative and non-increasing function in the interval,  $a < z < b$  and we can find numbers  $h$  and  $H$  such that:

$$h \leq |F(\xi)| = \left| \int_a^{\xi} f(z) dz \right| \leq H, \quad a < \xi < b, \quad (\text{D.2.a-14})$$

then

$$h |v(a)| \leq \left| \int_a^b f(z) v(z) dz \right| \leq H |v(a)|. \quad (\text{D.2.a-15})$$

A proof of this theorem can be found in **Box D.2.a-1**.

**Box D.2.a-1:** Proof of Abel's theorem for integrals.

Integration by parts allows us to write the integral in equation (D.2.a-15) as:

$$\int_a^b f(z) v(z) dz = \int_a^b v(z) dF(z) = [F(z) v(z)]_a^b - \int_a^b F(z) dv(z), \quad (\text{D.2.a-16a})$$

where  $F(z)$  is self-defined in equation (D.2.a-16a). Since by its definition  $F(a) = 0$  we have:

$$\int_a^b f(x) v(x) dx = F(b) v(b) - \int_a^b F(x) dv(x). \quad (\text{D.2.a-16b})$$

Substitution of the bounds given in equation (D.2.a-14) into equation (D.2.a-16b) results in:

$$h \left| v(b) - \int_a^b dv(z) \right| \leq \left| \int_a^b f(z) v(z) dz \right| \leq H \left| v(b) - \int_a^b dv(z) \right|,$$

which simplifies to equation (D.2.a-15), completing our proof.

If we assume the integral  $\int_A^\xi e^{-tz} z^m f(z) dz$  exists for some  $t = \alpha$  and  $\xi \in (A, Z)$ , then an upper bound  $N$  for the integral must exist giving:

$$\left| \int_A^\xi e^{-\alpha z} z^m f(z) dz \right| \leq N. \quad (\text{D.2.a-17})$$

Therefore, if we make the following associations:

$$\left| F(\xi) = \int_A^\xi e^{-\alpha z} z^m f(z) dz \right| \leq N, \quad (\text{D.2.a-18a})$$

$$v(z) = e^{-(t-\alpha)z}, \quad (\text{D.2.a-18b})$$

then using Abel's lemma, as indicated in equations (D.2.a-14) and (D.2.a-15), we can cast the integral (D.2.a-13) in the form of an inequality:

$$\left| \int_A^Z e^{-tz} z^m f(z) dz \right| \leq N e^{-(t-\alpha)A}, \quad (\text{D.2.a-19a})$$

or

$$|I_B| \leq N e^{-(t-\alpha)A}. \quad (\text{D.2.a-19b})$$

Combining the results from equation (D.2.a-19b) and equation (D.2.a-12) back into equation (D.2.a-8) we arrive at the result:

$$\left| I - \left[ \sum_{j=0}^{n-1} a_j \frac{(m+j)!}{t^{(m+j+1)}} \right] \right| \leq \left[ M \frac{(m+n)!}{t^{(m+n+1)}} \right] + K e^{-tA}. \quad (\text{D.2.a-20})$$

If we multiply equation (D.2.a-20) by  $t^{m+n}$ , the right hand side tends to zero as  $t \rightarrow \infty$ .

Thus by Poincaré's definition of an asymptotic expansion (Jeffreys and Jeffreys, 1980, p. 499) we have the asymptotic expansion of the integral  $I$  or:

$$I = \int_0^Z e^{-tz} z^m f(z) dz \sim \left[ \sum_{j=0}^{n-1} a_j \frac{(m+j)!}{t^{(m+j+1)}} \right], \quad (\text{D.2.a-21})$$

which is one form of Watson's lemma. This is not the exact form we are after. The related integral given by equation (D.1-2b) is the one which will allow us to find an approximate solution for equation (D.1-1).

### D.2.b: Case 2 ( Equation (D.1-2b) )

The integral given by equation (D.1-2b) and reproduced here as

$$K = \int_{-A}^B e^{-1/2 t^2 z^2} f(z) dz, \quad (\text{D.2.b-1})$$

is the actual form that we will be using. Therefore it is worthwhile to see how its asymptotic expansion is derived. The development here is similar in many ways to the development in the previous section. I will refer back to the previous section for reference but will reproduce similar results so as to minimize flipping back and forth between sections, not all steps, however, will be reproduced. Since  $A$  and  $B$  are positive numbers we can recast equation (D.2.b-1) in the form:

$$K = \frac{1}{2} \int_0^A e^{-1/2 t^2 z^2} f(-z) dz + \frac{1}{2} \int_0^B e^{-1/2 t^2 z^2} f(z) dz. \quad (\text{D.2.b-2})$$

We still assume that  $f(z)$  is analytic on the path of integration and therefore, within the circle of convergence, it's Taylor series exists (refer to equation (D.2.a-1) and (D.2.a-2)). The Taylor series and remainder of  $f(z)$  will have the form:

$$f(z) = \sum_{i=0}^{n-1} a_i z^i + R_n(z), \quad (\text{D.2.b-3a})$$

where the remainder is defined by:

$$R_n(z) = \frac{z^n}{2\pi i} \oint_C \frac{f(s)}{(s-z) s^n} ds. \quad (\text{D.2.b-3b})$$

Now, let the point  $\alpha$  be such that it is within the circle of convergence of the expansion given by equation (D.2.b-3a) and rewrite equation (D.2.b-2) as:

$$\begin{aligned} K &= \int_0^\alpha e^{-1/2 t^2 z^2} \frac{f(-z) + f(z)}{2} dz + \\ &+ \frac{1}{2} \int_\alpha^A e^{-1/2 t^2 z^2} f(-z) dz + \frac{1}{2} \int_\alpha^B e^{-1/2 t^2 z^2} f(z) dz \\ &= K_\alpha + K_A + K_B. \end{aligned} \quad (\text{D.2.b-4})$$

We will now deal with the three separate integrals  $K_\alpha$ ,  $K_A$  and  $K_B$  defined in equation (D.2.b-4). Integrals  $K_A$  and  $K_B$  are very similar and will be dealt with together. For the integral  $K_\alpha$ , we begin by using the Taylor expansion given by equation (D.2.b-3a) to express

$$\frac{f(-z) + f(z)}{2} = \left[ \sum_{i=0}^{n/2} a_{2i} z^{2i} \right] + \frac{R_n(-z) + R_n(z)}{2}, \quad (\text{D.2.b-5})$$

where, without loss of generality, I have assumed  $n$  to be even. Substitution of equation (D.2.b-5) into integral  $K_\alpha$  in equation (D.2.b-4) gives

$$K_\alpha = \left[ \sum_{i=0}^{n/2} a_{2i} \int_0^\alpha z^{2i} e^{-1/2 t^2 z^2} dz \right] + \int_0^\alpha \frac{R_n(-z) + R_n(z)}{2} e^{-1/2 t^2 z^2} dz = J_\alpha + R_\alpha. \quad (\text{D.2.b-6})$$

We can substitute equation (D.2.a-7) into the second integral,  $R_\alpha$ , in equation (D.2.b-6) to get:

$$R_\alpha = \int_0^\alpha \theta M z^n e^{-1/2 t^2 z^2} dz. \quad (\text{D.2.b-7})$$

By using the substitution  $\zeta = z^2$  we can transform equation (D.2.b-7) into

$$R_\alpha = \frac{\theta M}{2} \int_0^{\alpha^2} \zeta^{(n-1)/2} e^{-1/2 t^2 \zeta} d\zeta. \quad (\text{D.2.b-8})$$

By using the method of integration by parts, similar to the derivation of equation (D.2-11a),  $R_\alpha$  above can be reduced to the form:

$$\begin{aligned}
 R_\alpha = & -\theta M e^{-1/2 t^2 \alpha^2} \sum_{j=1}^{n/2} \left[ \frac{\prod_{k=1}^{j-1} [n - (2k - 1)]}{t^{2j}} \alpha^{n - (2j - 1)} \right] \\
 & + \frac{\theta M \prod_{k=1}^{n/2} [n - (2k - 1)]}{2t^n} \int_0^{\alpha^2} \zeta^{-1/2} e^{-1/2 t^2 \zeta} d\zeta,
 \end{aligned} \tag{D.2.b-9a}$$

where the assumption of  $n$  being even still holds and we have made the definition

$$\prod_{k=1}^0 [\bullet] = 1. \tag{D.2.b-9b}$$

Now we will deal with the last integral in equation (D.2.b-9a). As a first step we will make the reverse substitution  $z = \sqrt{\zeta}$  so that

$$\begin{aligned}
 I &= \int_0^{\alpha^2} \zeta^{-1/2} e^{-1/2 t^2 \zeta} d\zeta \\
 &= 2 \int_0^{\alpha} e^{-1/2 t^2 z^2} dz \\
 &= 2 \left[ \int_0^{\infty} e^{-1/2 t^2 z^2} dz - \int_{\alpha}^{\infty} e^{-1/2 t^2 z^2} dz \right] \\
 &= 2[I_0 - I_\alpha].
 \end{aligned} \tag{D.2.b-10}$$

The first integral,  $I_0$ , defined in the last line of equation (D.2.b-10), has the solution:

$$I_0 = \frac{\sqrt{2\pi}}{2t}. \tag{D.2.b-11}$$

The second integral  $I_\alpha$ , defined in the last line of equation (D.2.b-10), will be dealt with using Abel's lemma. Prior to applying Abel's lemma we have to show that  $2I_\alpha$  is bounded. The bound is simply found: since the integrand is a positive real function on the interval  $[0, \infty)$ , we can write:

$$|2I_\alpha| = \left| 2 \int_\alpha^\infty e^{-(t^2 z^2)/2} dz \right| < \left| 2 \int_0^\infty e^{-(t^2 z^2)/2} dz \right| = |2I_0|, \quad (\text{D.2.b-12a})$$

and we have the solution given by:

$$|2I_\alpha| < \frac{\sqrt{2\pi}}{t} = H, \quad (\text{D.2.b-12b})$$

which provides us with the bound which we need. Now we can apply Abel's lemma and write:

$$|2I_\alpha| \leq H |e^{-(\alpha^2 t^2)/2}| = O(e^{-(\alpha^2 t^2)/2}). \quad (\text{D.2.b-13})$$

If we now substitute equations (D.2.b-11) and (D.2.b-12b) into equation (D.2.b-10) which we in turn substitute into equation (D.2.b-9a), we get the result:

$$R_\alpha = \frac{M'}{t^{n+1}} - O(e^{-(\alpha^2 t^2)/2}), \quad (\text{D.2.b-14a})$$

where I have grouped all terms of the order  $e^{-(\alpha^2 t^2)/2}$ , and where:

$$M' = \frac{\sqrt{2\pi} \theta M \prod_{k=1}^{n/2} [n - (2k - 1)]}{2}. \quad (\text{D.2.b-14b})$$

Now we will deal with the second integral  $J_\alpha$  in equation (D.2.b-6), reproduced here as

$$J_\alpha = \sum_{i=0}^{n/2} a_{2i} J_i, \quad (\text{D.2.b-15a})$$

where

$$J_i = \int_0^\alpha z^{2i} e^{-1/2 t^2 z^2} dz. \quad (\text{D.2.b-15b})$$

We again apply the substitution  $\zeta = z^2$  to equation (D.2.b-15b), followed by integration by parts, to get

$$J_i = \frac{\prod_{l=1}^i (2i - 2l + 1)}{2 t^{2i}} \int_0^{\alpha^2} e^{-(t^2\zeta)/2} \zeta^{-1/2} d\zeta - O(e^{-(t^2\alpha^2)/2}). \quad (\text{D.2.b-16})$$

The integral in equation (D.2.b-16) can be dealt with in the same manner as that which we went through to get equation (D.2.b-13). This would transform equation (D.2.b-16) into the form:

$$J_i = \sqrt{2\pi} \frac{\prod_{l=1}^i (2i - 2l + 1)}{2 t^{2i+1}} + O(e^{-(t^2\alpha^2)/2}). \quad (\text{D.2.b-17})$$

Substitution of equation (D.2.b-17) into equation (D.2.b-15a) gives

$$J_\alpha = \sum_{i=0}^{n/2} \left[ a_{2i} \sqrt{2\pi} \frac{\prod_{l=1}^i (2i - 2l + 1)}{2 t^{2i+1}} \right] + O(e^{-(t^2\alpha^2)/2}). \quad (\text{D.2.b-18})$$

Finally we need to deal with the last two integrals  $K_A$  and  $K_B$  defined in equation (D.2.b-4). These integrals can be dealt with in the same manner used to obtain equation (D.2.a-19b). From this procedure, which is again a simple application of Abel's lemma, we find

$$K_A = O(e^{-(t^2\alpha^2)/2}), \quad (\text{D.2.b-19a})$$

and

$$K_B = O(e^{-(t^2\alpha^2)/2}). \quad (\text{D.2.b-19b})$$

Now we can collect all the terms comprising the integral  $K$ , that is,

$$K = K_\alpha + K_A + K_B = J_\alpha + R_\alpha + K_A + K_B, \quad (\text{D.2.b-20})$$

as defined in equations (D.2.b-4) and (D.2.b-6). The individual terms have been defined in equations (D.2.b-19a), (D.2.b-19b), (D.2.b-18) and (D.2.b-14a). Collecting these terms and rearranging yields:

$$\left| K - \sum_{i=0}^{n/2} \left[ a_{2i} \sqrt{2\pi} \frac{\prod_{l=1}^i (2i - 2l + 1)}{2 t^{2i+1}} \right] \right| = \left| \frac{M'}{t^{n+1}} + O(e^{-(t^2\alpha^2)/2}) \right|. \quad (\text{D.2.b-21})$$

By direct examination of equation (D.2.b-21) we can see that the right-hand side, when multiplied by  $t^n$ , tends to zero as  $t$  tends to infinity; therefore, by Poincaré's definition of an asymptotic expansion, we have shown the asymptotic expansion of the integral  $K$  to be:

$$K \sim \sum_{i=0}^{n/2} \left[ a_{2i} \sqrt{2\pi} \frac{\prod_{l=1}^i (2i - 2l + 1)}{2 t^{2i+1}} \right], \quad (\text{D.2.b-22})$$

which seems to differ from the classical formula by a factor of one half. I have not been able to track the discrepancy so far. The following development will proceed with the classical formula (Jeffreys and Jeffreys, 1980, p. 503). We now go on to see how this expansion is used in the method of steepest descent or saddle-point method.

### D.3: Steepest-descent or saddle-point method

Watson's lemma will be used to find an approximate solution of:

$$I = \int_A^B \chi(z) e^{t f(z)} dz, \quad (\text{D.3-1})$$

which is just equation (D.1-1). The technique is alternately known as the method of steepest descent or saddle-point method, which according to Jeffreys and Jeffreys (1980, p. 503) is due to Debye.

We can always write:

$$f(z) = \varphi(x,y) + i\psi(x,y), \quad (\text{D.3-2})$$

separating its real and imaginary parts, where the complex variable  $z$  is related to real variables  $x$  and  $y$  in the following manner:

$$z = x + iy. \quad (\text{D.3-3})$$

Since  $f(z)$  is assumed to be analytic, its real and imaginary parts obey the Cauchy-Riemann relations

$$\frac{\partial \varphi}{\partial x} = \frac{\partial \psi}{\partial y}, \quad (\text{D.3-4a})$$

and

$$\frac{\partial \varphi}{\partial y} = -\frac{\partial \psi}{\partial x}. \quad (\text{D.3-4b})$$

If we now take the appropriate partial derivatives of equations (D.3-4a) and (D.3-4b) we find the relations

$$\nabla^2 \varphi = \frac{\partial^2 \varphi}{\partial x^2} + \frac{\partial^2 \varphi}{\partial y^2} = 0, \quad (\text{D.3-5a})$$

and

$$\nabla^2 \psi = \frac{\partial^2 \psi}{\partial x^2} + \frac{\partial^2 \psi}{\partial y^2} = 0. \quad (\text{D.3-5b})$$

Therefore, the real and imaginary parts of  $f$  obey Laplace's equation, which in turn means that, where  $f$  is analytic,  $\varphi$  and  $\psi$  cannot have either minima or maxima. This also means that, at points where  $d\varphi = 0$ ,  $\varphi$  will there exhibit the behavior of local saddle points. This situation is graphically demonstrated in figure (D.3-1). These points are crucial in the following development.

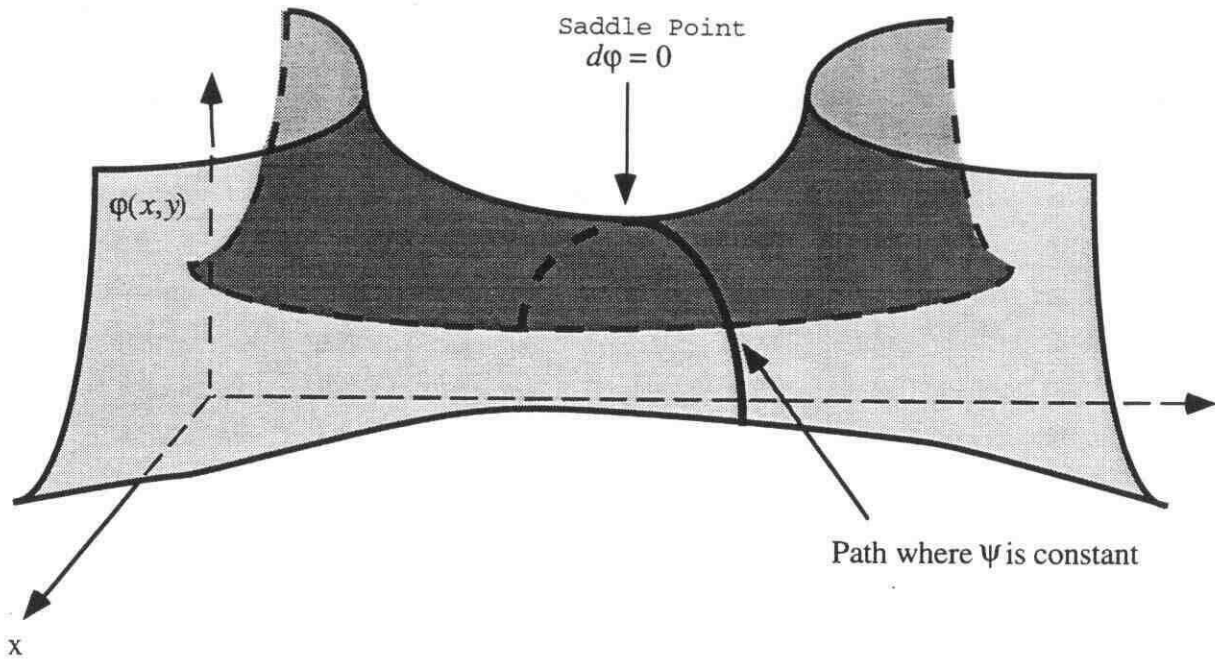


**Fig. D.3-1.** Surface of  $\phi(x, y)$  around a saddle point where  $d\phi = 0$ .

If we examine the integrand in equation (D.3-1) we will notice it can be written as:

$$\chi(z) e^{t f(z)} = \chi(z) e^{t \phi} e^{i t \psi}, \quad (\text{D.3-6})$$

which will be large when  $\phi$  is algebraically large. This means, if we choose a path of integration which passes through points where  $\phi$  is large and then quickly drops off away from these points, an approximation can be made by summing the contributions from these points only. This is basically the procedure we will develop here.

The points we seek are exactly the previously mentioned saddle points, one of which is pictorially represented in figure (D.3-1). Since we can not have local minima or maxima on  $\phi(x, y)$ , the only choice left is to use saddle points, which suits our purpose just fine. A saddle point, say at point  $z_0 = x_0 + i y_0$ , corresponds to a local flat spot on the  $\phi(x, y)$  surface, which means

$$d\phi(x_0, y_0) = \left[ \frac{\partial \phi(x, y)}{\partial x} \right]_{(x_0, y_0)} dx + \left[ \frac{\partial \phi(x, y)}{\partial y} \right]_{(x_0, y_0)} dy = 0. \quad (\text{D.3-7})$$

Since  $dx$  and  $dy$  are arbitrary differentials, equation (D.3-7) can be true only if

$$\left[ \frac{\partial \varphi(x,y)}{\partial x} \right]_{(x_0,y_0)} = 0 \quad \text{and} \quad \left[ \frac{\partial \varphi(x,y)}{\partial y} \right]_{(x_0,y_0)} = 0. \quad (\text{D.3-8})$$

Now that we have characterized the behavior of  $\varphi(x,y)$  at a saddle point  $z_0 = x_0 + i y_0$ , we shall proceed to find the associated local path of steepest descent away from this point. This, as discussed previously, is the second step towards our approximate solution of integral equation (D.3-1). From elementary calculus (Kaplan, 1973, p 204-205), we know that the gradient of a function points in the direction of the function's steepest ascent; therefore, the negative of the gradient must point in the direction of steepest descent. This is exactly the direction in which we want to place our path away from the saddle point. There is one problem: since we have just determined that  $-\nabla\varphi(x_0,y_0) = 0$  from equation (D.3-8) we cannot directly determine the path from the gradient. However, even though the magnitude of the gradient vector is zero at the saddle point its direction is a well defined quantity at all points where  $f(z)$  is analytic. This direction can be represented by an angle  $\theta$  with respect to the  $x$  axis as shown in figure (D.3-2) and relationally represented by:

$$\tan \theta = \frac{dy}{dx} = \frac{\frac{\partial \varphi}{\partial y}}{\frac{\partial \varphi}{\partial x}} = - \frac{\frac{\partial \psi}{\partial x}}{\frac{\partial \psi}{\partial y}}, \quad (\text{D.3-9})$$

where we have used the Cauchy-Riemann relations to get the last equality. This ratio is well defined even at the saddle point. This means that on the path, not necessarily at the saddle point, we will have the condition  $-\frac{\partial \psi}{\partial x} dx = \frac{\partial \psi}{\partial y} dy$  or

$$d\psi = \frac{\partial \psi}{\partial x} dx + \frac{\partial \psi}{\partial y} dy = 0. \quad (\text{D.3-10})$$

Equation (D.3-10) means that  $\psi$  must be constant along this path.

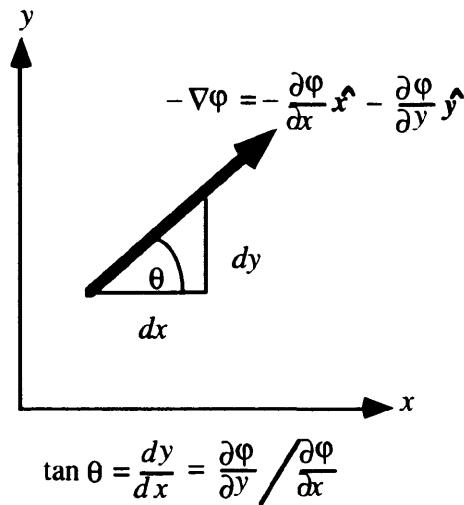


**Fig. D.3-2.** Direction of the path of steepest descent.

To examine the behavior of the surface  $\varphi$  around the saddle point  $z_0$  more rigorously, we can expand  $\varphi(x,y)$  as a Taylor series around  $z_0$ . This results in:

$$\begin{aligned} \varphi(z) = & \varphi(z_0) + \left[ \frac{\partial\varphi}{\partial x} \right]_{x_0} (x - x_0) + \left[ \frac{\partial\varphi}{\partial y} \right]_{y_0} (y - y_0) + \\ & + \frac{1}{2} \left\{ \left[ \frac{\partial^2\varphi}{\partial x^2} \right]_{x_0} (x - x_0)^2 + 2 \left[ \frac{\partial^2\varphi}{\partial x \partial y} \right]_{x_0} (x - x_0)(y - y_0) + \left[ \frac{\partial^2\varphi}{\partial y^2} \right]_{x_0} (y - y_0)^2 \right\} + \dots \end{aligned} \quad (\text{D.3-11})$$

Letting

$$A = \left[ \frac{\partial^2\varphi}{\partial x^2} \right]_{x_0}, \quad B = \left[ \frac{\partial^2\varphi}{\partial x \partial y} \right]_{x_0}, \quad C = \left[ \frac{\partial^2\varphi}{\partial y^2} \right]_{x_0}, \quad X = (x - x_0), \quad Y = (y - y_0), \quad (\text{D.3-12a})$$

and noting at the saddle point that

$$\left[ \frac{\partial\varphi}{\partial x} \right]_{x_0} = \left[ \frac{\partial\varphi}{\partial y} \right]_{y_0} = 0, \quad (\text{D.3-12b})$$

then equation (D.3-11) can locally be cast in the form

$$2[\varphi(z) - \varphi(z_0)] = A X^2 + 2B XY + C Y^2. \quad (\text{D.3-13})$$

Note, the term *locally* means that  $X$  and  $Y$  are small enough that all terms higher than quadratic are assumed to be negligible. We can write equation (D.3-13) in matrix form

$$\Phi = \tilde{X}^T \tilde{\phi} \tilde{X} \quad (\text{D.3-14})$$

where

$$\Phi = 2 [\varphi(z) - \varphi(z_0)],$$

$$\tilde{\phi} = \begin{bmatrix} A & C \\ C & B \end{bmatrix},$$

$$\tilde{X} = \begin{bmatrix} X \\ Y \end{bmatrix}$$

and  $\tilde{X}^T$  is the transpose of  $\tilde{X}$ . Since  $\tilde{\phi}$  is a symmetric matrix we can diagonalize it (Kolman, 1970, p.154). The first step is to form the characteristic polynomial

$$\det[\tilde{\phi} - \lambda \tilde{I}] = \begin{vmatrix} A - \lambda & B \\ B & C - \lambda \end{vmatrix} = \lambda^2 - (A + C)\lambda + (AC - B^2) = 0. \quad (\text{D.3-15})$$

Equation (D.3-15), being a quadratic equation, has the following solutions for the eigenvalues:

$$\lambda_1 = \frac{(A + C) + \sqrt{(A + C)^2 - 4(AC - B^2)}}{2} \quad (\text{D.3-16a})$$

and

$$\lambda_2 = \frac{(A + C) - \sqrt{(A + C)^2 - 4(AC - B^2)}}{2}. \quad (\text{D.3-16b})$$

We can now express  $\tilde{\phi}$  as

$$\tilde{\phi} = \tilde{O}^T \tilde{D} \tilde{O}, \quad (\text{D.3-17})$$

where

$$\tilde{D} = \begin{bmatrix} \lambda_1 & 0 \\ 0 & \lambda_2 \end{bmatrix}$$

and  $\tilde{O}$  is the associated orthogonal matrix which is composed of the eigenvectors of the eigenvalues in  $\tilde{D}$ . We can now express equation (D.3-14) as

$$\Phi = [\tilde{O}\tilde{X}]^T \tilde{D} [\tilde{O}\tilde{X}] = \xi^T \tilde{D} \xi, \quad (\text{D.3-18a})$$

where  $\xi = \tilde{O}\tilde{X} = \begin{bmatrix} \xi \\ \eta \end{bmatrix}$  are the new transformed coordinate variables. In algebraic notation

$$\Phi = \lambda_1 \xi^2 + \lambda_2 \eta^2. \quad (\text{D.3-18b})$$

There are three general cases that represent the surface described by equation (D.3-18b) and they all depend on the factor  $AC - B^2$  in equations (D.3-16a) and (D.3-16b).

(Case I.) If  $AC - B^2 = 0$ , then at least one of  $\lambda_1$  or  $\lambda_2$  is zero,

giving rise to equations of the form  $\Phi = \lambda_1 \xi^2$  or  $\Phi = \lambda_2 \eta^2$ .

These are parabolic equations (see figure D.3-3a).

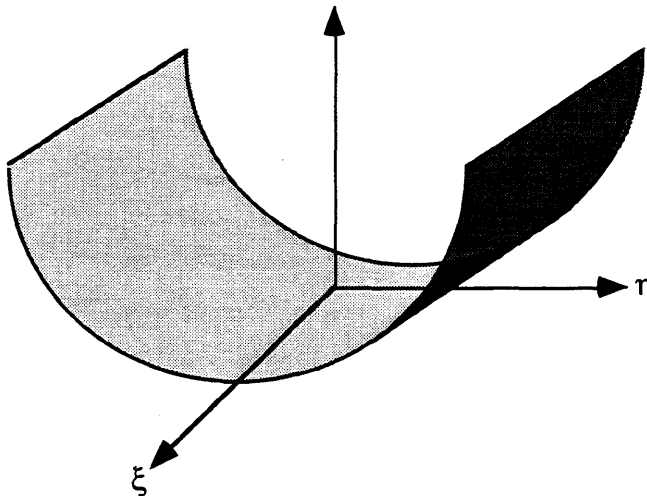


**Fig. D.3-3a.** A paraboloid.

(Case II.) If  $AC - B^2 > 0$ , then both eigenvalues  $\lambda_1$  and  $\lambda_2$  will be positive,

giving rise to equations of the form  $\Phi = |\lambda_1|\xi^2 + |\lambda_2|\eta^2$ .

This is the equation of an ellipsoid (see figure D.3-3b).

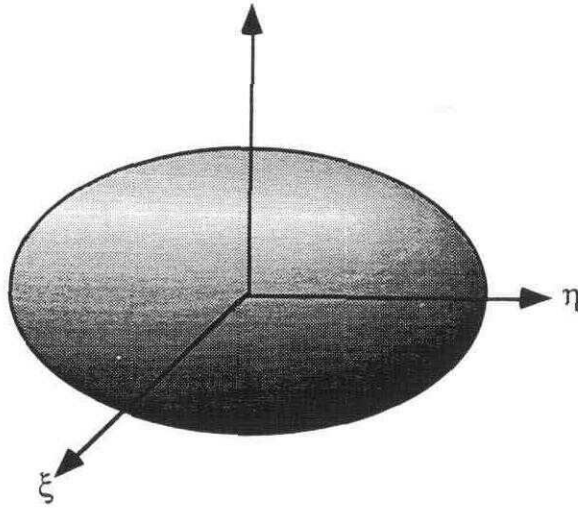


**Fig. D.3-3b.** An ellipsoid.

(Case III.) If  $AC - B^2 < 0$ , then the eigenvalues  $\lambda_1$  and  $\lambda_2$  will be of opposite sign,

giving rise to equations of the form  $\Phi = |\lambda_2|\eta^2 - |\lambda_1|\xi^2$ .

This is the equation of a saddle (see figure D.3-3c).

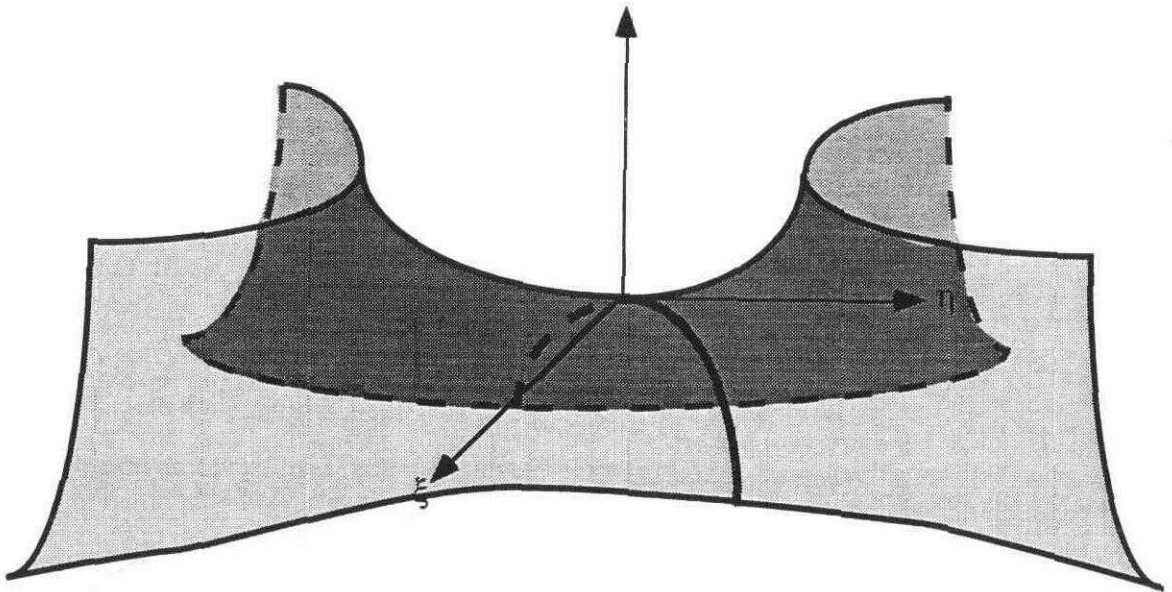


**Fig. D.3-3.** A saddle.

If we examine the Cauchy-Riemann relations, equation (D.3-4a) and (D.3-4b), we will find that

$$AC - B^2 = \frac{\partial^2 \varphi}{\partial x^2} \frac{\partial^2 \varphi}{\partial y^2} - \frac{\partial^2 \varphi}{\partial x \partial y} = - \left( \frac{\partial^2 \psi}{\partial x \partial y} + \frac{\partial^2 \varphi}{\partial x \partial y} \right) < 0; \quad (\text{D.3-19})$$

therefore, we will always satisfy the conditions in case III. This means, we will always have a saddle, as stated previously.

Yet another way to visualize what happens around the saddle point is to look at the curvature along the path of steepest descent and then compare it to the curvature at right angles to this path. I am using the word curvature in the same sense as Båth (1968, p. 52), I believe the quantity,  $d^2\varphi$ , would be more correctly called concavity since curvature is a well defined geometric term different from the current usage, but to maintain consistency with Båth we will keep the same terminology. Along any fixed direction, where  $\tan \theta = \frac{dy}{dx}$  is constant, the curvature is

$$\begin{aligned} d^2\varphi &= \frac{\partial}{\partial x} \left[ \frac{\partial \varphi}{\partial x} dx + \frac{\partial \varphi}{\partial y} dy \right] dx + \frac{\partial}{\partial y} \left[ \frac{\partial \varphi}{\partial x} dx + \frac{\partial \varphi}{\partial y} dy \right] dy \\ &= \frac{\partial^2 \varphi}{\partial x^2} d^2x + 2 \frac{\partial^2 \varphi}{\partial x \partial y} dx dy + \frac{\partial^2 \varphi}{\partial y^2} d^2y. \end{aligned} \quad (\text{D.3-20})$$

The direction perpendicular to the path will be typified by the condition:

$$\tan\left(\theta + \frac{\pi}{2}\right) = \cot \theta = -\frac{dx}{dy}, \quad (\text{D.3-21})$$

and will have curvature

$$d^2\varphi_{\perp} = \frac{\partial^2 \varphi}{\partial x^2} d^2x - 2 \frac{\partial^2 \varphi}{\partial x \partial y} dx dy + \frac{\partial^2 \varphi}{\partial y^2} d^2y. \quad (\text{D.3-22})$$

If we now add the curvatures in the two perpendicular directions, as given by equations (D.3-22) and (D.3-20), the result will be:

$$d^2\varphi_{\perp} + d^2\varphi = \left( \frac{\partial^2\varphi}{\partial x^2} + \frac{\partial^2\varphi}{\partial y^2} \right) (d^2x + d^2y) = 0. \quad (\text{D.3-23})$$

The last equality in equation (D.3-23) is a direct consequence of the Cauchy-Reimann equations as given by equation (D.3-5a). Equation (D.3-23) shows that the curvatures in the two orthogonal directions are of the same magnitude but of opposite sign; this is just the condition that is satisfied at a saddle point. Now that we have seen the geometric behavior around a saddle point, we can proceed to the next stage of finding an approximate solution of equation (D.1-1).

The next stage begins by expanding the analytic function  $f(z)$  as a Taylor's series around the saddle point  $z_0$ , where we have shown, with equations (D.3-7) and (D.3-10), that  $\frac{df}{dz} = 0$ . Therefore, the Taylor's series of  $f(z)$  will have the form:

$$f(z) = f(z_0) + \frac{1}{2} (z - z_0)^2 \left[ \frac{d^2f}{dz^2} \right]_{z_0} + \dots \quad (\text{D.3-24})$$

We will now define a new variable

$$\zeta = -\sqrt{(z - z_0)^2 \left[ \frac{d^2f}{dz^2} \right]_{z_0} + \dots}, \quad (\text{D.3-25a})$$

which has the approximation

$$\zeta = -(z - z_0) \sqrt{\left[ \frac{d^2f}{dz^2} \right]_{z_0}}, \quad (\text{D.3-25b})$$

when  $z$  is close to the saddle point  $z_0$ . Using the new variable  $\zeta$  we can rewrite equation (D.3-24) as:

$$f(z) - f(z_0) = -\frac{1}{2} \zeta^2. \quad (\text{D.3-26})$$

Since from equation (D.3-10) we know that  $\psi$  is constant along the path of steepest descent, and that  $\varphi$  reaches a maximum along the path at the saddle point, we then, from equation (D.3-2), can say that

$$d^2 f = d^2 \phi + i 0 \quad (\text{D.3-27})$$

must be real and negative along this path, which also means that  $(z - z_0)^2 \left. \frac{d^2 f}{dz^2} \right|_{z_0}$  is real and negative along the path. We can then use our new variable, as defined in equation (D.3-25a), to recast equation (D.1-1) in the form:

$$\begin{aligned} I &= \int_A^B \chi(z) e^{t f(z)} dz = e^{t f(z_0)} \int_A^B \chi(z) e^{-(1/2)t \zeta^2} dz \\ &= e^{t f(z_0)} \int_A^B e^{-(1/2)t \zeta^2} \chi(z) \frac{dz}{d\zeta} d\zeta. \end{aligned} \quad (\text{D.3-28})$$

This formula is in exactly the same form as equation (D.2.b-1); therefore, we can use Watson's lemma to get an approximation. Before we proceed, we will cast some of the variables in a more useful form. Using polar notation, we can write:

$$z - z_0 = r e^{i\alpha}, \quad (\text{D.3-29a})$$

where  $r$  is the distance between the points  $z$  and  $z_0$  and  $\alpha$  is the angle subtended by the line segment between  $z$  and  $z_0$  and the real axis on the complex plane; this is also the direction subtended by the cord between the saddle point and a point on the path of steepest descent and the  $x$ -axis. Part of the geometry can be seen in figure (D.3-1). It is also equal to the angle  $\theta$ , as defined in equation (D.3-9) and shown graphically in figure (D.3-2), at the saddle point. The approximation given by equation (D.3-25b) allows us to write our new variable as

$$\zeta^2 = - \left[ \frac{d^2 f}{dz^2} \right]_{z_0} r^2 e^{i2\alpha} = r^2 \left[ \left[ \frac{d^2 f}{dz^2} \right]_{z_0} \right] e^{i2\alpha}, \quad (\text{D.3-29b})$$

where we have used the fact that  $(z - z_0)^2 \left[ \frac{d^2 f}{dz^2} \right]_{z_0}$  is real and negative along the path, as discussed previously, to arrive at the last equality. Furthermore, since  $|e^{i2\alpha}| = 1$ , then

$$\zeta = \pm r \sqrt{\left| \frac{d^2 f}{dz^2} \right|_{z_0}}, \quad (\text{D.3-29c})$$

and

$$\frac{d\zeta}{dz} = \pm e^{-i\alpha} \sqrt{\left| \frac{d^2 f}{dz^2} \right|_{z_0}}. \quad (\text{D.3-29d})$$

The positive sign will be used in the formulas above to determine the direction that the path will take. There are two directions the path could take given by values of  $\alpha$  differing by  $\pi$ . Now, we will use Watson's lemma, as given by equation (D.2.a-21), to get the final form of our approximation. We will only use the first term of the asymptotic expansion.

The correspondence, or mapping, of terms is:

$$a_0 \rightarrow \chi(z_0) \frac{e^{i\alpha}}{\sqrt{\left| \frac{d^2 f}{dz^2} \right|_{z_0}}}, \quad (\text{D.3-30a})$$

and

$$t \rightarrow \sqrt{t}. \quad (\text{D.3-30b})$$

With the substitutions given by relations (D.3-30a) and (D.3-30b), the approximate solution from the saddle point method as shown in equation (D.2.b-22) will be:

$$I \sim \frac{\sqrt{2\pi} \chi(z_0) e^{t f(z_0)} e^{i\alpha}}{\sqrt{t \left| \frac{d^2 f}{dz^2} \right|_{z_0}}}. \quad (\text{D.3-31})$$

This is the approximate solution we have been looking for. It should be noted again that the equation (D.2.b-22) differs from the classical formula, as given by Jeffreys and Jeffreys (1980, p. 503, equation 13), by a factor of one half.

## E: The Cauchy Tetrahedron Argument

The result of the following reasoning is to show that if an arbitrary function  $\varphi$  is dependent only on the position  $x^i$  of the surface  $S'$  on which it is defined and the normal to that surface  $\mathbf{n}$ , then this function can be recast in terms of an inner product between a tensor defined from  $\varphi$  and the unit normal. The function could also be dependent on time. Note that this will not hold in many instances, such as when  $\varphi$  is dependent on the curvature of the surface as well. The quantity of concern is not the value of  $\varphi$ , but rather it is the differential  $\varphi ds$ , which can be approximated by the average value of  $\varphi$  in a small area  $\Delta S$  multiplied by the area; we will write this as  $\tilde{\varphi} \Delta S$ .

We shall now construct a tetrahedron by first introducing locally an orthogonal right-handed system,  $x^i$ , with origin  $O$ , such that the area  $\Delta S$  consists of the region defined by the plane normal to  $\mathbf{n}$  and the intersection of this plane with the orthogonal axis. The points of intersection are labeled  $A^i$ . The altitude from the origin  $O$  to the point  $P$  is of length  $h$ . Each of the surfaces bounded on two sides by the axes and the third by the plane normal  $\mathbf{n}$  are labeled as  $\Delta S^i$ , where the superscript  $i$  determines the axis to which the plane surface is perpendicular. This is shown in figure E-1.

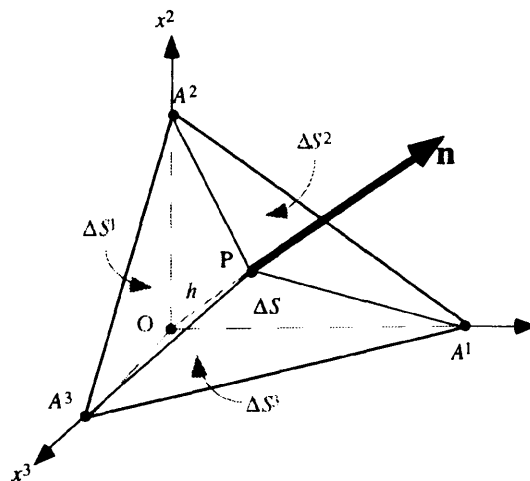


**Fig. E-1.** Cauchy's elemental tetrahedron.

The components of  $\mathbf{n}$  in this local coordinate system are just the direction cosines given by:

$$n^i = \cos(\angle A^i OP) \quad (\text{E-1})$$

The altitude  $h$  is given by:

$$h = \overline{OA^{(i)}} n_i. \quad (\text{E-2})$$

(no summation implied, as indicated by parenthesis)

The volume of the tetrahedron can be written as:

$$\Delta V = \frac{1}{3} h \Delta s = \frac{1}{3} \overline{OA^{(i)}} \Delta s^i. \quad (\text{E-3})$$

Substitution of equation (E-2) into (E-3) and simplifying results in:

$$\Delta s^i = n_i \Delta s. \quad (\text{E-4})$$

We can approximate

$$\psi = \oint_S \varphi dS, \quad (\text{E-5a})$$

the integral of  $\varphi$  around the close surface of the tetrahedron, by the sum of average values it takes at each plane face multiplied by the area of the face (note, the direction of the unit normal is crucial and determines the sign of the sum). This can be written as:

$$\psi \approx \tilde{\varphi}(\mathbf{n}) \Delta s - \tilde{\varphi}(\hat{\mathbf{x}}^1) \Delta s^1 - \tilde{\varphi}(\hat{\mathbf{x}}^2) \Delta s^2 - \tilde{\varphi}(\hat{\mathbf{x}}^3) \Delta s^3, \quad (\text{E-5b})$$

where  $\hat{\mathbf{x}}^i$  is a unit vector in the direction of coordinate axis  $x^i$  and we can assume this average is placed at the centroid of its corresponding face. This sum becomes exact as the volume goes to zero. Substitution of equation (E-4) into equation (E-5b) results in:

$$\psi \approx \left[ \tilde{\varphi}(\mathbf{n}) - \tilde{\varphi}(\hat{\mathbf{x}}^1) n_1 - \tilde{\varphi}(\hat{\mathbf{x}}^2) n_2 - \tilde{\varphi}(\hat{\mathbf{x}}^3) n_3 \right] \Delta s. \quad (\text{E-6})$$

In many instances we can show that the integral  $\psi$  is also dependent on the volume enclosed by the surface. A particular case is if  $\psi$  is proportional to the volume  $\Delta V$ , or

$$\psi = C \Delta V, \quad (\text{E-7})$$

where  $C$  is the constant of proportionality. One way to see this is to use the divergence theorem and write:

$$\psi = \oint_S \varphi \, dS = \int_V \nabla \varphi \, dV$$

Then it is not difficult to see that if  $\nabla \varphi$  is well behaved, then there should exist a constant that will make equation (E-7) true. This is always true where tractions and couples per unit area are concerned. Combining equations (E-6) and (E-7) then substituting in equation (E-3) yields:

$$\left[ \tilde{\varphi}(\mathbf{n}) - \tilde{\varphi}(\hat{\mathbf{x}}^1) n_1 - \tilde{\varphi}(\hat{\mathbf{x}}^2) n_2 - \tilde{\varphi}(\hat{\mathbf{x}}^3) n_3 \right] \Delta s = C \Delta V = C \frac{1}{3} h \Delta s,$$

upon division by  $\Delta s$  we get:

$$\left[ \tilde{\varphi}(\mathbf{n}) - \tilde{\varphi}(\hat{\mathbf{x}}^1) n_1 - \tilde{\varphi}(\hat{\mathbf{x}}^2) n_2 - \tilde{\varphi}(\hat{\mathbf{x}}^3) n_3 \right] \approx C \frac{1}{3} h. \quad (\text{E-8})$$

In the limit as  $h$  approaches zero the formula becomes exact and the left-hand side goes to zero, which results in:

$$\varphi(\mathbf{n}) = \varphi(\hat{\mathbf{x}}^1) n_1 + \varphi(\hat{\mathbf{x}}^2) n_2 + \varphi(\hat{\mathbf{x}}^3) n_3. \quad (\text{E-9})$$

If we now define  $\varphi^i = \varphi(\hat{\mathbf{x}}^i)$ , then we can rewrite equation (E-9) as:

$$\varphi(\mathbf{n}) = \varphi^i n_i, \quad (\text{E-10})$$

which is our desired conclusion.

## **Bibliography**

- Achenbach, J.D., (1980), "Wave Propagation in Elastic Solids", North Holland Publishing Company.
- Alford, R.M., (1986), "Shear Data in the Presence of Azimutal Anisotropy", Dilly, Texas, 56th Annual International Meeting of the Society of Exploration Geophysics, Expanded Abstracts, 476-479
- Aminzadeh, F. and Mendel, J.M., (1980), "On the Bremmer Series Decomposition: Equivalence Between two Different Approaches", Geophysical Prospecting, 28, 71-84.
- Aminzadeh, F. and Mendel, J.M., (1982), "Non-normal Incidence State-Space Model and Line Source Synthetic Seismograms", Geophysical Prospecting, 30, 541-568.
- Aminzadeh, F. and Mendel, J.M., (1983), "Normal Incidence Layered System State-Space Models which Include Absorption Effects", Geophysics, 48, #3, 259-271.
- Aki, K. and Richards, P.G., (1980), "Quantitative Seismology", W.H. Freeman and Company.
- Backus, G.E., (1962), "Long-Wave Elastic Anisotropy Produced by Horizontal Layering", Journal of Geophysical Research, 67, #11, 4427-4440
- Backus, G.E., (1970), "A Geometric Picture of Anisotropic Elastic Tensors", Reviews of Geophysics and Space Physics, 8, #3, 633-671
- Baerheim, R., (1993), "Harmonic Decomposition of the Anisotropic Elasticity Tensors", Quaterly Journal of Mechanics and Applied Mathematics, 46, 391-418.
- Báth, M., (1968), "Mathematical Aspects of Seismology", Developments in Solid Earth Geophysics 4, Elsevier Publishing Co., Amsterdam.
- Bedford, A., (1985), "Hamilton's Principle in Continuum Mechanics", Research Notes in Mathematics, 139, Pitman Pub. Inc..
- Biot, M.A., (1956), "Theory of Propagation of Elastic Waves in a Fluid-Saturated Porous Solid - I. Low Frequency Range", Journal of the Acoustical Society of America, 28, 168-178.
- Cherry, J.T., (1962), "The Azimuthal and Polar Radiation Patterns Obtained From a Horizontal Stress Applied at the Surface of an Elastic Half-space", Bulletin of the Seismological Society of America, 52, 27-36.

- Cherry, J.T. and Waters, K.H., (1968), "Shear-wave Recording using Continuous Signal Methods - Part I - Early Development", *Geophysics*, 33, 229-239.
- Christensen, R.M., (1979), "Mechanics of Composite Materials", John Wiley and Sons, N.Y..
- Churchill, R.V., Brown, J.W., Verhey, R.F., (1976), "Complex Variables and Applications", McGraw-Hill Book Co., N.Y..
- Coburn, N., (1970), "Vector and Tensor Analysis", Dover Publications, Inc., N.Y..
- Dankbaar, J.W.M., (1983), "The Wave-Field Generated by Two Vertical Vibrators in Phase and in Counterphase", *Geophysical Prospecting*, 31, 873-887.
- Easley, D.T., (1992a), "Alternate Description of the Wavefield Generated by Two Vertical Vibrators in Counterphase", *CREWES Research Report*, 4, 2, 1-10.
- Easley, D.T., (1992b), "Composite Media as Generalized Continua", *CREWES Research Report*, 4, 18, 1-6.
- Easley, D.T., (1993a), "Mixed-phase Coupled Vibrators", *CREWES Research Report*, 5, 17, 1-16.
- Easley, D.T., (1993b), "Numerical Trial of a Statistical Method to Find the Preferred Frames of Reference of Elastic Tensors", *CREWES Research Report*, 5, 18, 1-4.
- Easley, D.T. and Brown, R.J., (1992), "Elastic Tensors and their Preferred Frames of Reference", *CREWES Research Report*, 4, 24, 1-4.
- Easley, D.T. and Foltinek, D.S., (1993), "Synthetic Seismograms for P and S Waves Using the Goupillaud Model", *CREWES Research Report*, 5, 14, 1-6.
- Edelmann, H.A.K., (1981), "SHOVER, Shear-Wave Generation by Vibration Orthogonal to the Polarization", *Geophysical Prospecting*, 29, 541-549.
- Encyclopaedia Britannica, (1981), "China, History of", *Macropaedia*, 4, 315, Encyclopaedia Britannica Inc..
- Erickson, E.L., Miller, D.G. and Waters, K.H., (1968), "Shear-Wave Recording using Continuous Signal Methods - Part II - Later Experimentation", *Geophysics*, 33, 240-254.
- Eringen, A.C., (1968), "Mechanics of Micromorphic Continua" Kroner, E., Ed., *IUTAM Symposium, Mechanics of Generalized Continua*, 18-35.
- Eringen, A.C., Ed., (1971), "Mathematics", *Continuum Physics*, 1, Academic Press, N.Y. and London.
- Eringen, A.C., Ed., (1975), "Continuum Mechanics of Single-Substance Bodies", *Continuum Physics*, 2, Academic Press, N.Y. and London.

- Horton, C.W., (1943), "Secondary Arrivals in a Well Velocity Survey", *Geophysics*, 8, 290-296.
- Hubral, P., Treitel, S. and Gutowski, P.R., (1980), "A Sum Autoregressive Formula for the Reflection Response", *Geophysics*, 45, 1697-1705.
- Hudson, J.A., (1980), "The Excitation and Propagation of Elastic Waves", Cambridge University Press, Cambridge.
- Jeffreys, H. and Jeffreys, B.S., (1980), "Methods of Mathematical Physics", Cambridge University Press, Cambridge.
- Johnston, D.H., (1986), "VSP Detection of Fracture-Induced Velocity Anisotropy", 56th Annual International Meeting of the Society of Exploration Geophysics, Expanded Abstracts, 464-466.
- Jolly, R.N., (1956), "Investigation of Shear Waves", *Geophysics*, 21, 905-938.
- Kaplan, W., (1973), "Advanced Calculus", 2nd Ed., Addison-Wesley Publishing Co., Reading, Massachusetts.
- Kolman, B., (1970), "Elementary Linear Algebra", Macmillan Publishing Co., N.Y. and London.
- Mendel, J.M., Nahi, N.E. and Chan, M., (1979), "Synthetic Seismograms using the State-Space Approach", *Geophysics*, 44, 880-895.
- Miller, G.F. and Pursey, H., (1953), "The Field and Radiation Impedance of Mechanical Radiators on the Surface of a Semi-infinite Isotropic Solid", *Proceedings of the Royal Society*, A223, 512-541.
- Mindlin, R.D. and Tiersten, H.F., (1962), "Effects of Couple-stresses in Linear Elasticity", *Archives of Rational Mechanics and Analysis*, 11, 415-448.
- Pipes, L.A. and Harvill, L.R., (1970), "Applied Mathematics for Engineers and Physicists", McGraw-Hill Book Co., N.Y..
- Press, F. and Dobrin, M.B., (1956), "Seismic Studies Over Surface Layers", *Geophysics*, 21, 285-298.
- Press, W.H., Flannery, B.P., Teukolsky, S.A. and Vetterling, W.T., (1988), "Numerical Recipes in C: The Art of Scientific Computing", Cambridge University Press, Cambridge.
- Rivlin, R.S., (1968), "Generalized mechanics of continuous media", Kroner, E., Ed., IUTAM Symposium, *Mechanics of Generalized Continua*, 1-17.
- Schoenberg, M. and Muir, F., (1989), "A Calculus for Finely Layered Anisotropic Media", *Geophysics*, 54, 581-589.
- Spain, B., (1965), "Tensor Calculus", Oliver and Boyd, Edinburg and London.

- Spiegel, M.R., (1968), "Mathematical Handbook of Formulas and Tables", Schaum's Outline Series, McGraw-Hill Book Co., N.Y..
- Stakgold, I., (1979), "Green's Functions and Boundary Value Problems", John Wiley and Sons Incorporated, New York.
- Sun, Z. and Jones, M.J., (1993), "Seismic wavefields recorded at near-vertical incidence from a counterphase source", The CREWES Research Report, 5, (7-1) - (7-12).
- Symon, K.R., (1971), "Mechanics", Addison-Wesley Publishing Company, Reading, Massachusetts.
- Tan, T.H., (1985), "The Elastodynamic Field of N Interacting Vibrators (Two-Dimensional Theory)", Geophysics, 50, 1229-1252.
- Tatham, R.H. and McCormack, M.D., (1991), "Multicomponent Seismology in Petroleum Exploration", Investigations in Geophysics: No.6, Society of Exploration Geophysicists, Tulsa, Oklahoma.
- Tatham, R.H. and Stoffa, P.L., (1984), " $V_p/V_s$  - A Potential Hydrocarbon Indicator", Geophysics, 41, 837-849.
- Tatham, R.H. and Goolsbee, D.V., (1976), "Separation of S-wave and P-wave Reflections, Offshore Western Florida", Geophysics, 49, 493-508.
- Tatham, R.H., Goolsbee, D.V., Massell, W.F. and Nelson, H.R., (1983), "Seismic Shear-Wave Observations in a Physical Model Experiment", Geophysics, 48, 837-849.
- Toupin, R.A., (1962), "Elastic Materials with Couple-Stresses", Archives of Rational Mechanics and Analysis, 11, 385-414.
- Vestrum, R.W., Brown, R.J. and Easley, D.T., (1996), "From Group or Phase Velocities to the General Anisotropic Stiffness Tensor", Proceedings of the 6th Intentional Workshop on Seismic Anisotropy (Trondheim), Society of Exploration Geophysicists (in press).
- White, J.R., Heaps, S.N. and Lawrence, A.L., (1956), "Seismic Waves from a Horizontal Force", Geophysics, 21, 715-723.